Faculty of Engineering

MICROWAVE ENHANCED PROCESSING OF ORES

Joseph Kobusheshe, BSC Eng (Hons), MSC Eng

Thesis submitted to the University of Nottingham for the degree of

Doctor of Philosophy

June 2010

ABSTRACT

Recent research developments have suggested that microwave assisted comminution and liberation could provide a step change in ore processing. The principle exploited in this technology is based on the fact that microwaves selectively heat absorbent phases within a multi-mineral ore and induce internal stresses that create fracture. It has been suggested by several authors that microwave pre-treatment of ores with a mixture of microwave absorbing semiconducting minerals (most sulphides and oxides) well disseminated in microwave transparent gangue (most silicates) can significantly reduce the required comminution or breakage energy and also achieve improved mineral liberation through grain boundary fracture.

A detailed review of existing literature revealed that little or no information is available which relates and examines the influence of hydrated minerals on microwave assisted fracture. This is despite the fact that most important ores are associated with phyllosilicates, the vast majority of which are hydrated. Water in any form significantly affects the dielectric properties of a material, which in turn dictates its microwave absorbing properties. A study was carried out on two Kimberlite diamond ores containing significant hydrated minerals but devoid of any semiconducting minerals which are known to be good microwave heaters, so as to investigate the influence of hydrated minerals on microwave induced fracture. The results confirmed that in this type of ore, microwave induced fracture relies on certain mineral phases within the ore undergoing dehydration. It was concluded that presence of minerals containing interlayer adsorbed water induces significant micro and macro fractures after microwave treatment. The magnitude of induced damage was

quantified by point load testing and ultrasonic pulse velocity (UPV) measurement methods. The results showed significant reductions in the Point Load Index (I_s) and Relative Ultrasonic Pulse Velocity (UPV). It was however noted that significantly higher energy inputs are required in treatment of hydrated ores compared to those used in treatment of metalliferous ores because longer treatment times are required for dehydration to take place.

The significance of microwave induced fracture on beneficiation was investigated by conducting liberation and flotation tests on two porphyry copper ores. It was demonstrated that microwave pre-treatment improves beneficiation at sizes suitable for flotation. Significant improvements in liberation of up to 20% were achieved in particles treated using a single mode cavity at modest energy inputs of less than 2 kWh/t. It was further observed that higher improvements in degree of liberation are attained in coarser particle sizes between 212 and 425 μm. Flotation tests also demonstrated that microwave pre-treatment has potential for real economic benefits in terms of value proposition and also results into more efficient resource utilization. The results showed an increase of 8-10% in copper sulphides recovery from coarse sized particles (-400+200 μm) and an overall increase in grade/recovery of between 1-2%. The results also showed that microwave pre-treatment enhances selective mineral recovery as the grade-recovery of iron sulphides decreased in all but one microwave treated samples.

The major drawback to further developments towards industrial scale application was found to be the lack of an effective continuous processing microwave applicator. It was shown that the conveyor tunnel applicator used in this study did not perform according to the design specifications. It was

observed that power spreads in the transverse direction within the tunnel which causes a deviation from the ideal localised hot spots that are required for more efficient treatment. It was concluded that the rate of power density increase is as important as the ultimate power density and that any future applicator designs must be able to ensure localised hot spots and confinement of all the microwave energy.

ACKNOWLEDGEMENTS

I would like to express my sincere gratitude to various people and organisations without whose support this work would have been impossible to accomplish.

Foremost I would like to thank my supervisor Prof Sam Kingman for his guidance and invaluable kind support throughout the course of this work.

I also wish to thank The University of Nottingham International Office who sponsored my tuition and the sponsors of AMIRA project P879a (Rio Tinto, BHP Billiton, Outotec and Anglo American) for providing materials and funding for this research work.

I would also like to acknowledge the support I have received from various people working with the National Centre for Industrial Microwave Processing. Special thanks go to Dr Steven Plint for his help with MLA work, Dr Aled Jones for his assistance while carrying out microwave treatments, Andrew Batchelor for his help with flotation testing and Dr. Georgios Dimitrakis for his assistance with electric field simulations.

Finally to my wife Irene, family and friends for your motivation and support.

DEDICATION

I dedicate this thesis to my son Kagaba Jonathan Kobusheshe whose entire childhood I have missed while carrying out this work. I love you more than words can express.

CONTENTS

LIST OF FIGURES

LIST OF TABLES

CHAPTER ONE

1 INTRODUCTION AND OBJECTIVES

All valuable minerals are found embedded in rocks within the earth's crust. After the mineral bearing rock is extracted, the valuable minerals need to be 'liberated' from the parent rock to be concentrated into a product of economic value. This process is known as comminution and may involve blasting, crushing and grinding. Comminution processes are highly energy intensive and are said to account for approximately 3% of the global electrical energy consumption (Schwechten and Milburn, 1990). In countries such as South Africa, Canada and Australia where mining forms a larger proportion of the industrial sector, comminution processes may account for as high as over 6% of total electrical energy consumption (IEA, 2009). In the US, annual energy consumption within the mining industry is estimated at over 1 quadrillion Btu (10^{15} Btu) and costs between US$ 3-5 billion, which represents 15-25% of all supplies to the industry.

In 2003, an analysis carried out by the US Department of Energy demonstrated that the largest opportunities for energy savings within the mining industry lay in materials handling, beneficiation and processing and extraction. Comminution processes accounted for approximately 80% of the total energy required for beneficiation and processing (DoE, 2004). This is very significant both in terms of financial costs and also more worrying in terms of environmental effects and sustainability at a global scale.

According to publications from *World Energy Outlook* over the last decade, the world's energy demands continue to rise to sustain economic growth and development thus putting energy resources under pressure (IEA, 2009). There is growing anxiety about the effects of human activities on the environment. There are worrying concerns of climate change due to greenhouse gases generated by burning fossil fuels used to generate electricity and to provide power for manufacturing industries and transportation sector. Under the UN Framework Convention on Climate Change (UNFCCC) Kyoto Protocol, which came into force in February 2005, member countries agreed to reduce green house gas emissions by between 5-10% within a specified time frame (UN, 1998). More recently, the world's most industrialised countries (The G8) have committed to reduce carbon emissions by 80% by 2050 and to help developing countries achieve a 50% reduction within the same time frame (G8, 2009).

The Intergovernmental Panel on Climate Change (IPCC) which is a scientific body that was constituted by the UN to review and assess information relevant to the understanding of climate change has emphasised the use of energy efficient technologies as one of the major requirements to combat climate change (IPCC, 2007). In the US, the mining industry set targets of a 30% increase in energy efficiency and 20% reduction in carbon emissions by 2020 (DoE, 2004). In the EU, the Integrated Pollution Prevention and Control directive 96/61/EC requires operators of specified industries to demonstrate use of "best applicable techniques" when applying for permits (EC, 1996). There is strict environmental legislation in most other countries that requires industrial installations to improve process efficiency, lower energy consumption and lessen carbon emissions. There are also fears that the global

energy sources are fast being depleted and could run out in the foreseeable future. The above, coupled with the insecure supply and unpredictable prices of oil and gas and political instability of the main oil producing countries in the Middle East offers additional motivation to industries for more sustainable industrial processes.

The conventional comminution process flow sheet consisting of crushing and grinding stages is believed to be highly energy inefficient. Whereas crushers and High Pressure Grinding Rolls (HPGRs) operate with modest efficiency of up to 70% (Gerrard et al., 2004), the traditional grinding mills remain highly inefficient. For example, it is reported that less than 1% of the total energy input in a ball mill is utilized to generate new surfaces ready for large-scale separation techniques such as gravity or froth flotation (Rhodes, 1998). As a result, significant research work has been devoted to improving grinding processes (Fuerstenau and Abouzeid, 2002, Fuerstenau and Kapur, 1995, Fuerstenau et al., 1999, Gutsche and Fuerstenau, 2004, Kapur and Fuerstenau, 1987, Zeng and Forssberg, 1991, Zeng and Forssberg, 1992). Most of this work involved the development of innovative grinding technologies such as the use of grinding aids and also optimisation of existing grinding equipment such as the development of Autogenous (AG) and Semi-Autogenous (SAG) mills. The above work has, however, only achieved modest energy savings and the concept of a perfect grinding machine still seems farfetched.

Microwave assisted comminution is a subject that has generated a significant amount of research interest in recent years due to its potential for significant process benefits. Research over the last decade has shown that microwave

pre-treatment of ores has the potential to reduce the overall required crushing and grinding energy by over 60% and also significantly increase mineral liberation (Kingman et al., 1999, Kingman et al., 2004, Al-Harahsheh and Kingman, 2004, Jones, 2005, Jones et al., 2005, Salsman et al., 1996, Groves, 2007, Amankwah et al., 2005). The principle exploited in microwave assisted comminution is based on the fact that microwaves selectively heat absorbent phases within an ore, thereby inducing internal stresses that fracture the material. Although some progress has been made in this area, various associated scientific and engineering aspects still need to be investigated further. Based on microwave induced fracture mechanisms, ore mineralogy plays an important role in inducing fracture. However, the exact mechanisms involved and more importantly how the induced fracture can be enhanced to benefit mineral liberation is not fully understood. In particular, the influence of hydrated minerals has not been investigated at all and yet water in any form significantly affects the dielectric properties of a material which influence its microwave susceptibility.

Numerical models have shown that greater fracture is induced if the temperature gradient between the heated mineral grains and gangue material is maximized (Salsman et al., 1996). All the research work that has been carried out so far has been conducted at power levels in the range of 500 W to 15 kW. Computer simulations conducted by Jones et al (2005) and Wang et al (2008) have suggested that inter-granular micro fractures (which are preferred to macro fracturing) are maximized at a power density in the range of 1×10^{10} and 1×10^{12} W/m^3 with exposure times of between 0.2 and 0.002 seconds. Most existing microwave heating systems were not capable of operating at such specifications and hence these claims have not been

validated. In addition, all previous work has been conducted using batch treatment processes in either multimode or single mode microwave heating cavities. Any realistic industrial microwave treatment process necessitates development of a continuous treatment process.

Conventional comminution techniques do not control the manner in which fracture occurs. Complete liberation and separation of valuable minerals from the host material (gangue) is virtually impossible. As a result, significant amounts of valuable minerals are lost in the gangue. It is reported that up to half of the total mineral content of an ore may be lost in this manner (Wills, 2006). Microwave induced fractures are said to propagate predominantly along the grain-gangue interfaces (Jones et al., 2005, Kingman et al., 1999, Kingman et al., 2004). This intergranular fracturing pattern has potential to increase the degree of mineral liberation because mineral grains may be released from the host ore as full grains.

The overall aim of this research is to investigate the effectiveness of microwave pre-treatment of ores with respect to enhancement of comminution, mineral liberation and grade/recovery. An investigation into the influence of hydrated minerals on microwave induced fracture will be carried out to fill the gap in knowledge that currently exists. A batch single mode applicator and a specially designed continuous microwave treatment system will be used to treat different ores. The effect of microwave pre-treatment on mineral liberation and grade/recovery will be quantified in order to assess the benefits of microwave pre-treatment with respect to value proposition. The advantages of using highly selective pulse microwave heating systems will also be examined.

CHAPTER TWO

2 FUNDAMENTALS OF MICROWAVES AND MICROWAVE HEATING

2.1 Introduction

To the majority of ordinary people, microwaves are synonymous with the kitchen microwave which is a familiar domestic appliance found in most homes. In reality, microwaves are a form of electromagnetic energy with a wide range of scientific and industrial applications. For example, microwaves are used transmit signals that broadcast live programmes on radios and televisions or to diagnose disease in hospitals or for industrial heating. However, this research work will only be limited to the industrial heating applications of microwaves and this chapter presents the scientific basics of microwaves and how microwaves interact with and heat materials.

2.2 The Electromagnetic Spectrum

It is important to first understand electromagnetic waves and the electromagnetic spectrum because microwaves are in fact electromagnetic waves. Electromagnetic waves are self propagating waves characterised by electric (E) and magnetic (H) field components oscillating in phase and perpendicular with each other and also perpendicular to the direction of propagation (Metaxas and Meredith, 1983), as shown in Figure 2.1. Electromagnetic waves can propagate in vacuum or in matter and possess similar characteristics to common waves viz reflection, refraction, diffraction, interference, absorption, etc.

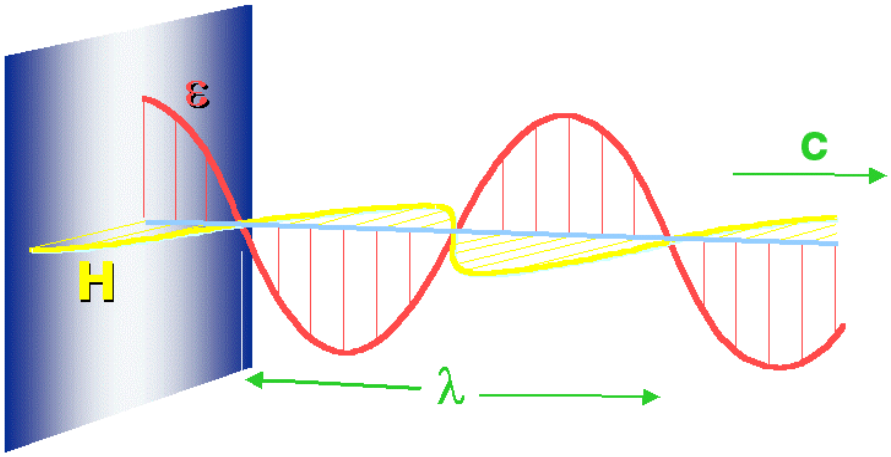

Figure 2.1 Electromagnetic wave components (Whittaker, 1997)

Electromagnetic waves obey the general wave formula given by Equation 2.1 (Metaxas and Meredith, 1983).

$$c = \lambda \cdot f \qquad (2.1)$$

Where c = speed of light (3.0×10^8 m/s)

λ = wavelength in free space (m)

f = frequency (Hz)

Electromagnetic waves are classified according to wavelength into radio waves, microwaves, infrared, light waves (which is the visible region we perceive as light), ultraviolet, X-rays and gamma rays. The full range of the electromagnetic spectrum is shown in Figure 2.2.

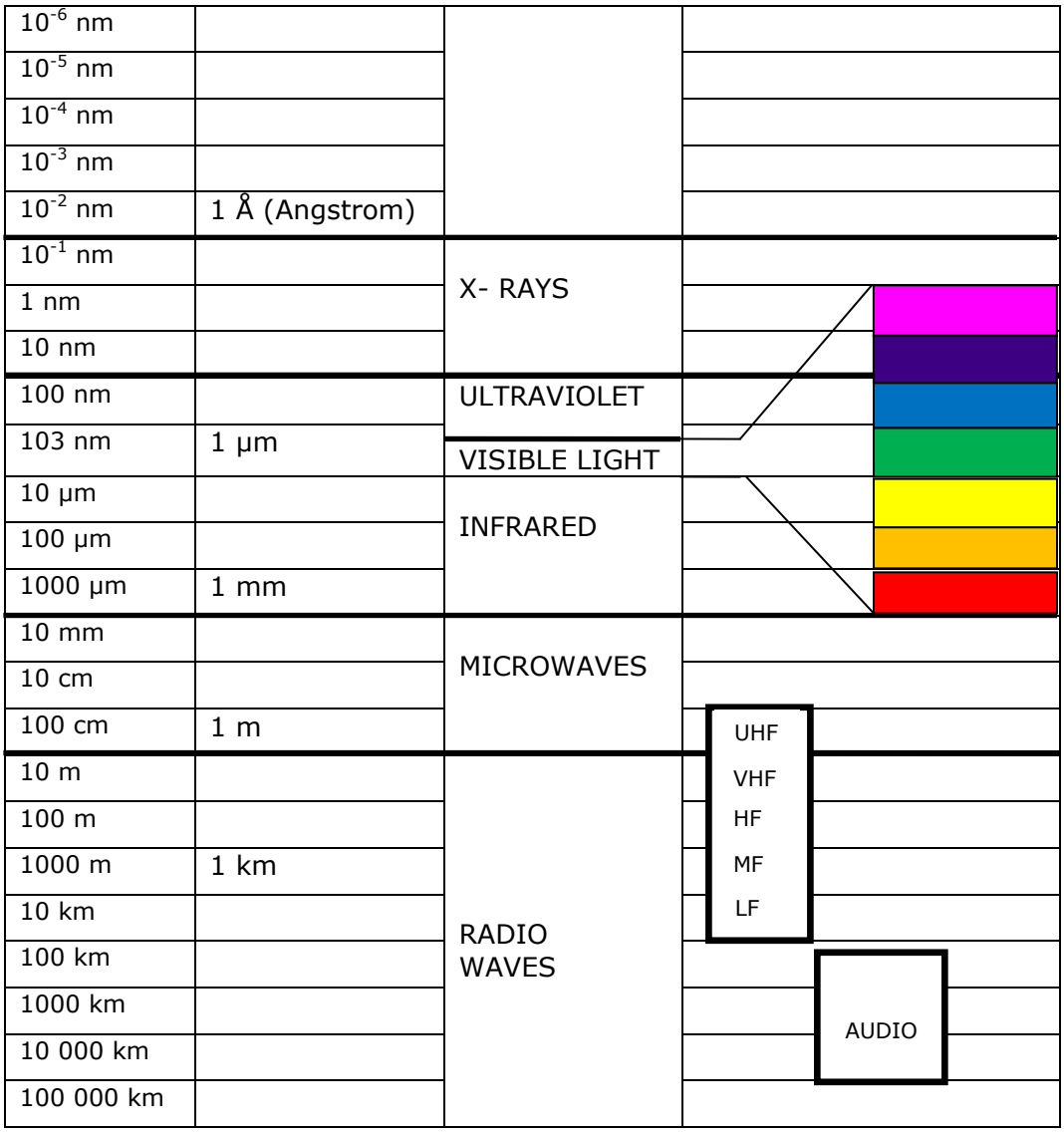

Figure 2.2 The electromagnetic spectrum showing the position of microwaves (Sutton, 1989)

As shown in Figure 2.2 above, microwaves lie between the infrared and radio waves in the electromagnetic spectrum with a typical wavelength in the range of 1mm – 1m. By substituting the typical values of the wave length in Equation 2.1, microwaves have a frequency band of between 300 MHz and 300 GHz. Because microwaves have a wide range of applications, specific frequencies are allocated for different purposes to avoid disturbances that may be caused by interferences. The majority of the microwave frequency

band is used for communication purposes and only certain specific regions have been allocated for non communications purposes, known as the industrial, scientific and medical (ISM) applications. In the UK, frequencies of 896 MHz and 2.45 GHz are exclusively used for ISM applications such as industrial heating and domestic ovens (Meredith, 1998).

2.3 Heating Mechanisms of Microwaves

Essentially, any material can be heated using high frequency electromagnetic waves provided that the material is neither a perfect electrical conductor nor a perfect insulator. The list therefore extends from metals to dielectric materials which could be considered good insulators. Electromagnetic heating of dielectrics originates from either the ability of the electric field to polarise charges in the material and the inability of this polarisation to follow extremely rapid reversals of the electric field or through direct conduction effects (Metaxas and Meredith, 1983). At microwave frequencies, the heating rate varies in each material and generally there is inadequate microwave energy penetration in bulk materials with significant ionic or metallic conductivity. There are primarily two major microwave heating mechanisms, ionic conduction and dielectric polarisation (Metaxas and Meredith, 1983). Dielectric polarisation mechanism is further divided into dielectric, electronic, atomic, dipolar and interfacial polarisation (Botsco and McMaster, 1986, Von Hippel, 1954).

2.3.1 Electronic Polarisation

Atoms which are the basic units of matter consist of a dense positively charged central nucleus surrounded by a cloud of negatively charged electrons

bound to the nucleus by an electromagnetic force. Electronic polarization occurs in neutral atoms when an electric field displaces the nucleus with respect to the electrons that surround it resulting into dipole moments which respond to the applied field (Von Hippel, 1954, Botsco and McMaster, 1986).

Figure 2.3 Electronic polarisation in a stable atom after nucleus is displaced with respect to surrounding electrons (Botsco and McMaster, 1986)

2.3.2 Atomic Polarisation

Atoms may combine to form more stable compounds by sharing their electrons. When this takes place, the electron clouds are more likely to be displaced towards the stronger binding atoms and therefore atoms acquire slight charges of opposite polarity (Von Hippel, 1954). When an electric field is applied, it tends to change the equilibrium state of the atoms themselves. Unlike electronic polarisation, atomic polarisation is therefore as a result of nuclei displacement of different atoms in a molecule.

Figure 2.4 Atomic polarisation as result of nuclei displacement of different atoms (Botsco and McMaster, 1986)

Electronic and atomic polarisations are less significant at microwave frequencies because the time scale is far too long to contribute to dielectric heating (Mingos and Baghurst, 1991).

2.3.3 Orientation Polarisation

Orientation polarisation (sometimes referred to as dipolar polarisation) is the most significant heating mechanism at microwave frequencies (Metaxas and Meredith, 1983). It occurs in dielectrics containing permanent dipoles which are present even in the absence of an external electric field. Permanent dipoles arise from an imbalance in charge distribution in molecules such as water, alcohols and acids. The dipole moments are oriented in a random manner in the absence of an electric field so that no polarisation exists. When an external field is applied, a torque is induced on the dipoles and they rotate to align with the electric field causing polarisation. If the field changes direction, the torque will also change. At low frequencies, the molecules will be polarised uniformly but at higher frequencies, molecules cannot cope with phase change and the alternating motion generates heat due to frictional losses (Whittaker, 1997, Von Hippel, 1954, Meredith, 1998).

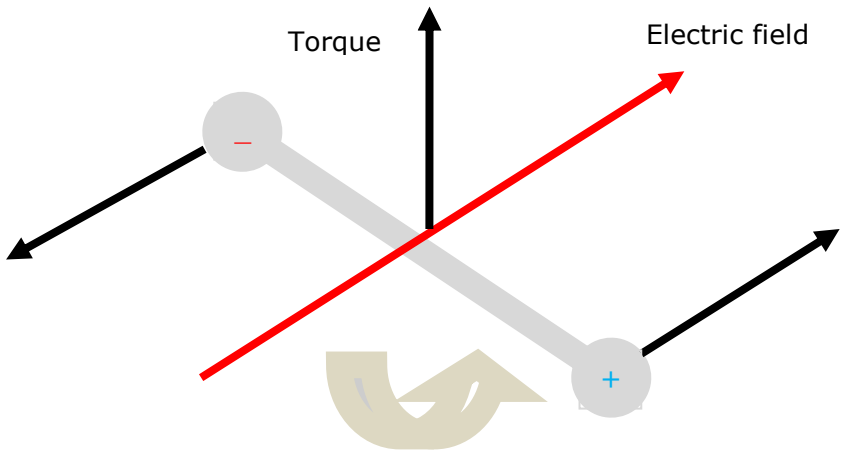

Figure 2.5 Dipole rotations in an alternating electric field

2.3.4 Interfacial Polarisation

Electronic, atomic and dipolar polarisation all occur when charges are locally bound in atoms, molecules or structures of solids or liquids. However, charge carriers also exist that can migrate over a distance through the material and polarisation occurs when this motion is impeded. Interfacial polarisation or space charge polarisation arises from charge build up at an interface between components in heterogeneous materials composed of small conducting particles inter-dispersed within a non-conducting medium (Metaxas and Meredith, 1983, Whittaker, 1997). The heating mechanism is considered to be a combination of conduction and dipolar effects. Within the structure of such heterogeneous materials, charge carriers can migrate a limited distance through the load. When these charge carriers can move no further, either because they are trapped in the material or cannot be freely discharged, a space-charge distortion occurs that results in polarisation (Von Hippel, 1954).

2.3.5 Ionic Conduction

When microwaves interact with an electrical conductor, charge carriers experience a force and move under the influence of the electric field resulting into polarisation. The induced current causes heating due to electrical resistance (Von Hippel, 1954). This heating mechanism is significant in conducting solid materials and ionic solutions. But as stated before, in high conducting materials such as metals, there is inadequate microwave penetration; rather microwaves are reflected at the surface which may lead to arcing (Whittaker, 1997). In liquids, ionic conduction heating may dominate dipolar heating as the conductivity of the liquid is increased either by addition of ions or increase in temperature (Al-Harahsheh and Kingman, 2004).

2.4 Advantages of Microwave Heating

In conventional heating, heat energy transferred to a material must pass through its surface and pass across a temperature gradient from one part of a material to the other by conduction, convection or radiation. The rate of heat flow within is therefore limited by the temperature at the interface and thermal diffusivity. Clearly this results in uneven temperature distributions in the work piece, difficulty in heat control as well as being inherently slow. It also results in energy being wasted in heating the whole sample if selective heating is required. In microwave heating, energy is absorbed volumetrically, thus rapid heating is possible leading to greater time savings (Stuerga and Gaillard, 1996, Sumnu et al., 2005). Microwave heating systems are therefore capable of operating with a high degree of efficiency. In large industrial microwave ovens, the microwave efficiency is defined as the percentage of the applied microwave energy which is dissipated as heat in the workload and can be in the region of 95% (Meredith, 1998). Table 2.1 shows the major differences between microwave heating and conventional heating.

Microwave Heating	Conventional Heating
Energy transfer	Heat transfer
Non contact heating	Conduction or radiation heating
Rapid heating possible	Heating rate limited by thermal diffusion
Material selective heating	Selective heating not possible
Volumetric heating	Surface heating
Energy may be transported to material through hollow wave guide	Heat must be transmitted by medium to material causing heat loses

Table 2.1 Comparison between microwave and conventional heating

2.5 Dielectric Properties

A dielectric material has ability to absorb and store energy through polarisation when an external electric field is applied. The extent to which energy may be absorbed and dissipated in a material depends on its dielectric properties which include permittivity, permeability, conductivity and resistivity. The dielectric properties of a material vary with molecular structure, density, moisture content, temperature, frequency and orientation of the material. Since many heating applications involve the removal of moisture from the workload, this makes the variations an important aspect in the design of microwave heating devices. Dielectric data also enables quantification of power density and microwave penetration depth in materials (Ryynänen, 1995).

2.5.1 Permittivity

Permittivity is the most important property that defines the interaction of electromagnetic waves with materials and is defined as the ratio of electric displacement to electric field strength (F/m). The permittivity of a material is composed of a real part and an imaginary part. The real part is known as the dielectric constant (ε') and is a measure of the ability of a material to be polarised and store energy. The imaginary part (ε'') is a measure of the ability of the material to dissipate stored energy into heat (Metaxas and Meredith, 1983). The two are related by the expression:

$$\varepsilon^* = \varepsilon' - j\varepsilon'' \qquad (2.2)$$

Where ε^* = Permittivity

ε' = Dielectric constant

ε'' = Loss factor

j = $\sqrt{-1}$

In practice it is difficult to separate the heat loss contribution from the different heating mechanisms described in Section 2.2. Instead, the Effective Loss Factor, ε''_{eff} which includes loses arising from both conduction and polarisation is used. Equation 2.2 above is then adjusted as follows.

$$\varepsilon^* = \varepsilon_0\left(\varepsilon'_r - j\varepsilon''_{eff}\right) \qquad (2.3)$$

Where ε_0 = Permittivity of free space (8.86×10^{-12} F/m)

ε'_r = Relative dielectric constant

ε''_{eff} = Effective relative dielectric loss factor

The ratio of the effective loss factor to that of the dielectric constant is called the effective loss tangent (Equation 2.4) and measures how well a material absorbs electromagnetic energy and dissipates it as heat (Chan and Reader, 2000).

$$tan\delta = \frac{\varepsilon''_{eff}}{\varepsilon'} \qquad (2.4)$$

2.5.2 Dielectric Property Variation with Frequency

The dielectric properties of a material are frequency and temperature dependent and also vary considerably with density and moisture content (Meredith, 1998, Nelson and Bartley, 2002, Pickles et al., 2005, Von Hippel, 1954). The variation in dielectric properties with frequency largely depends on the heating mechanism although this may not always be the case (Salsman, 1989b, Atwater and Wheeler, 2003, Pickles et al., 2005). In materials where dipolar heating mechanism dominates, the dielectric constant and loss factor increase with increasing frequency unless the dipoles cannot cope with the frequency change leading to a phase lag which reduces the effectiveness of heating (Von Hippel, 1954). This effect is described by the relaxation time of the material which is the time taken for dipoles to return to their equilibrium position when the externally applied electric field is removed within the alternating field (Atwater and Wheeler, 2004, Sugimoto and Norimoto, 2004). Industrial microwave applications use specified frequencies of 896MHz and 2.45GHz (for UK) and therefore the variation of material dielectric properties with frequency is not as crucial as other factors such as temperature and moisture content which are discussed in the next section.

Table 2.2 gives the dielectric constants and loss factors of selected common materials at different frequencies. It can be seen that water which heats by dipolar re-orientation mechanism shows an increase in both ε' and ε'' with increasing frequency. However, aqueous sodium chloride (NaCl) which heats predominantly by ionic conduction shows a decrease in both ε' and ε'' with increasing frequency.

Material	Temp (°C)	ε'			ε''		
		30 MHz	1 GHz	2.5 GHz	30 MHz	1 GHz	2.5 GHz
Water, ice	-12	3.8	3	3.2	0.7	0.004	0.003
Snow	-20	1.2	1.2	1.2	0.01	0.001	0.0001
Distilled Water	25	78	77	77	0.4	5.2	13
Distilled Water	85	58	56	56	0.3	1	3
Ethyl Alcohol	25	23	12	7	3	3	6.5
NaCl (0.1M)	25	76	76	76	480	30	20
Alumina Ceramic	25	8.9	8.9	8.9	0.0013	0.008	0.009
Fused Quartz	25	3.78	3.78	3.78	<0.001	<0.001	<0.001
Bakelite	24	4.6	3.8	3.7	0.34	0.26	0.23

Table 2.2 Dielectric Properties of selected materials at different frequencies (Metaxas and Meredith, 1988)

2.5.3 Dielectric Property Variation with Temperature

The variation of material dielectric properties with temperature is of great significance in industrial microwave heating because materials may exhibit physical and chemical changes that alter the interaction of microwaves with the material (Meredith, 1998). Generally, the variation of both ε' and ε'' in a material subjected to microwave heating is related to the heating mechanism in the material (Atwater and Wheeler, 2004). For example, in polar liquids, the nature of temperature dependence is a function of the dielectric relaxation processes. Dielectric relaxation is the time taken for dipoles to return to random orientation when the electric field is removed (Sebastian, 2008). An increase in temperature increases both ε' and ε'' because the dipoles can flip faster due to a decrease in relaxation time (Bottcher, 1973, Hairetdinov et al., 1998, Hall et al., 1998). Dielectric property variation with temperature of pure materials such as water whose composition is precisely known may be predicted but this is not always the case with most other materials. This is because as the temperature changes, the heating mechanism may change as

well, making predictions difficult. Due to this fact, the dielectric properties of materials are usually measured over the range of temperature that is of interest. Figures 2.6 and 2.7 show how complex such variations may be. These results were obtained from investigations conducted by Cumbane (2003) on the variation of ε' and ε'' with temperature for five minerals measured at 2.216GHz. The results show that the dielectric properties of galena (PbS) and sphalerite (ZnS) exhibited little variation with temperature, whilst pyrite (FeS), chalcocite (Cu_2S) and chalcopyrite ($CuFeS_2$) showed significant variability related to phase transformations (in this case oxidation processes) that take place within specific temperature regions.

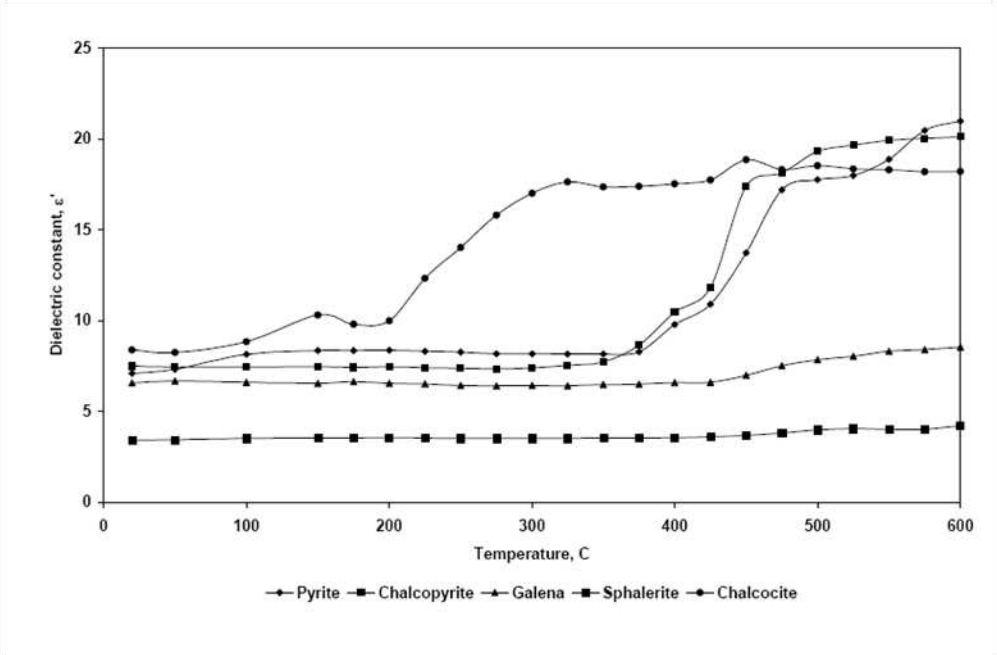

Figure 2.6 Variation of dielectric constant with temperature for selected minerals (Cumbane, 2002)

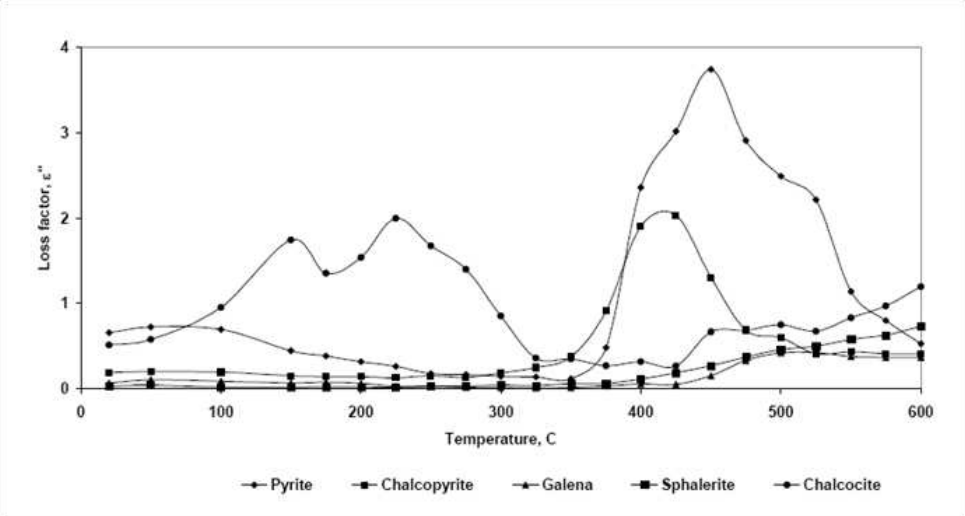

Figure 2.7 Variation of loss factor with temperature for selected minerals (Cumbane, 2002)

The variation of ε' and ε'' can be measured with relative ease using specialised techniques which are discussed later in this chapter. There is a wealth of published data on the dielectric properties of different materials at different temperatures because of the importance of understanding the dielectric properties - temperature variation. The variation of material dielectric properties with frequency is less significant in industrial microwave heating because only specific frequencies are used in microwave heating systems.

2.5.4 Other Factors that affect Dielectric Properties

The variation of dielectric properties with density has been reported by several authors (Landau et al., 1984, Nelson, 1988, Salsman, 1991, Trabelsi et al., 1999, Trabelsi et al., 2001). With respect to microwave heating, density variation is said to be relevant to powders where increase in packing density increases both ε' and ε''. The powder behaves as a two phase mixture with

air, and as the packing density increases, the voids are reduced and both ε' and ε'' increase. The relationship between conductivity and dielectric loss factor is given by the following relationship (Hamon, 1952):

$$\varepsilon'' = \frac{\sigma}{\varepsilon_0 f} \qquad (2.5)$$

Where f = Frequency (Hz)

σ = Electrical conductivity of the material (S/m)

ε_0 = Permittivity of free space (8.85×10^{-12} F/m)

The variation of dielectric properties with moisture content is of great importance to industrial microwave heating because most heating applications vary the moisture content in the work load. The nature of absorbed water in a material has a marked effect upon its dielectric properties (Metaxas and Meredith, 1988). This will be discussed in detail in the next chapter.

2.5.5 Dielectric Property Measurement Techniques

The principle techniques used to characterise the dielectric properties of materials rely on sending an electromagnetic wave to a material and analysing the reflected or transmitted signals. Analysis may be based on different observations such as impedance or resonance depending on the type of material, frequency, temperature, etc. Different specialized techniques have been developed and are extensively discussed by other authors (Altschuler et al., 1963, Hutcheon et al., 1992a, Hutcheon et al., 1992b, Ikeda et al., 2003, Salsman, 1989a, Salsman, 1991, Venkatesh and Raghavan, 1999a, Von

Hippel, 1954, Wu et al., 2000, Salsman, 1989b, Venkatesh and Raghavan, 1999b).

The major difference in all the methods lies in the technique used to determine the attenuation constant (α), phase constant (β) and propagation constant (γ) of the characteristic wave signals. At microwave frequencies, measurements using the coaxial line or resonant cylindrical cavity techniques are considered to be the most suitable (Metaxas and Meredith, 1983) and will be discussed in more detail in the next sections. Below microwave frequencies, Q-meter methods are employed while above 10 GHz, free space methods are used (Scaife, 1989, Sebastian, 2008).

2.5.5.1 Coaxial line

The coaxial line / probe method is sometimes also referred to as the Roberts Von Hippel method and is commonly used to accurately determine the dielectric properties of high-loss materials (Batt et al., 1995, Meredith, 1998). The technique involves the examination of standing waves in a transmission line or wave guide in which the dielectric under investigation is incorporated at the far end. A typical apparatus set-up is shown in Figure 2.8.

The Vector Network Analyser (VNA) generates microwaves, which are transmitted by the coaxial line through a slotted line to the section containing the dielectric. The far end of the dielectric is short-circuited giving rise to a standing wave pattern. Characterisation of the standing wave enables data on dielectric properties of the material under investigation to be obtained.

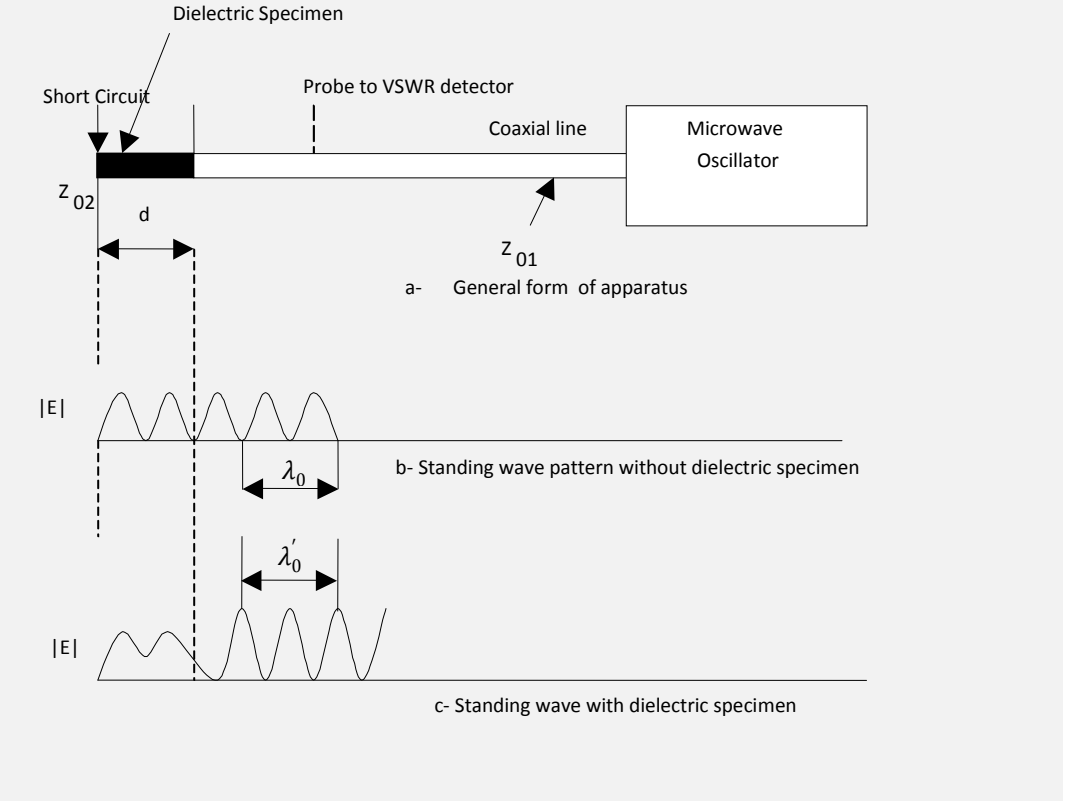

Figure 2.8 The coaxial line method for dielectric property measurement (Metaxas and Meredith, 1983)

The characteristic impedances of the dielectric filled line and the impedance of the line without the dielectric are measured by a *Network Analyser*. The parameters which are measured are illustrated in Figure 2.8 above and they are:

X_o = Shift distance (m)

S = Voltage Standing Wave Ratio (VSWR)

d = Dielectric specimen length (m)

λ_o = Wave length in empty coaxial line (m)

Different mathematical approaches are used to solve for ε' and ε'' from measurement of the above parameters and are discussed in detail by other authors (Arai, 1995, Arai et al., 1993, Metaxas and Meredith, 1983, Roberts

and Von Hippel, 1946, Wu et al., 2000). Nowadays computers are programmed to measure the above parameters and automatically compute ε' and ε'' values negating the need for tedious mathematical computations which may also lead to errors.

2.5.5.2 Cavity perturbation

The cavity perturbation method for dielectric property measurement is based on the perturbation theory, which assumes that the change in the stored energy in a cavity with or without a dielectric material is negligible and hence the electromagnetic fields in the cavity with and without a dielectric material are approximately equal (Metaxas and Meredith, 1983). This technique is widely used for measuring the dielectric properties of low loss solid (or powder) materials although the method can also be used for liquid measurement. Cavity perturbation techniques are also more adaptable for high temperature dielectric property measurement and for multiple discrete frequencies when compared to the coaxial line technique (Hutcheon et al., 1992a, Holderfield and Salsman, 1992, Tinga, 1992, Hutcheon et al., 1992b).

To understand how this method works, it is important to define the key terms used in this technique. Microwave cavities are discussed in detail later in this chapter but basically a cavity is dielectric region of any shape completely surrounded by conducting walls. A resonant cavity is one where the stored electrical energy is equal to the stored magnetic energy (Meredith, 1998). This phenomenon occurs at specific frequencies known as the resonant frequency modes. When a cavity resonates, energy is dissipated in the walls of the cavity. The ratio of the total energy stored in the cavity to the energy dissipated in the walls per cycle is known as the quality factor (Q) of the

cavity and it provides a direct measurement of the "lossiness" of the cavity (Dressel et al., 1993).

The cavity perturbation technique is based on measurement of shift in resonance frequency and change in quality factor when a dielectric material is placed in a resonance cavity. A cylindrical cavity is normally used and its dimensions must be sufficiently larger than the sample so as to cause only a small frequency shift thereby ensuring validity of the perturbation theory (Altschuler et al., 1963). In addition, the unperturbed field in the sample region must be uniform. This is ensured if a rod shaped sample is positioned along the central axis because according to (Donovan et al., 1993), for a large flat cylindrical cavity resonating in the TM_{0n0} mode, the electric field is parallel to the direction of propagation, which results in the maximum electric field strength being along the central axis and diminishing radially to a value of zero at the wall. In contrast the magnetic field is at its maximum at the cavity wall and diminishes to zero along the central axis in a TM_{0n0} cavity, so the sample can be considered as being in a pure electric field.

A typical set-up of the cavity perturbation apparatus is shown in Figure 2.9. The cavity is mounted beneath a furnace and insulated from it so as to enable measurements to be taken at elevated temperatures without affecting the cavity. A holder made of material such as quartz which is transparent to microwaves may be used to hold the sample. The robotic arm is attached to the sample holder and is programmed to move the sample downwards into the cavity or upwards into the furnace.

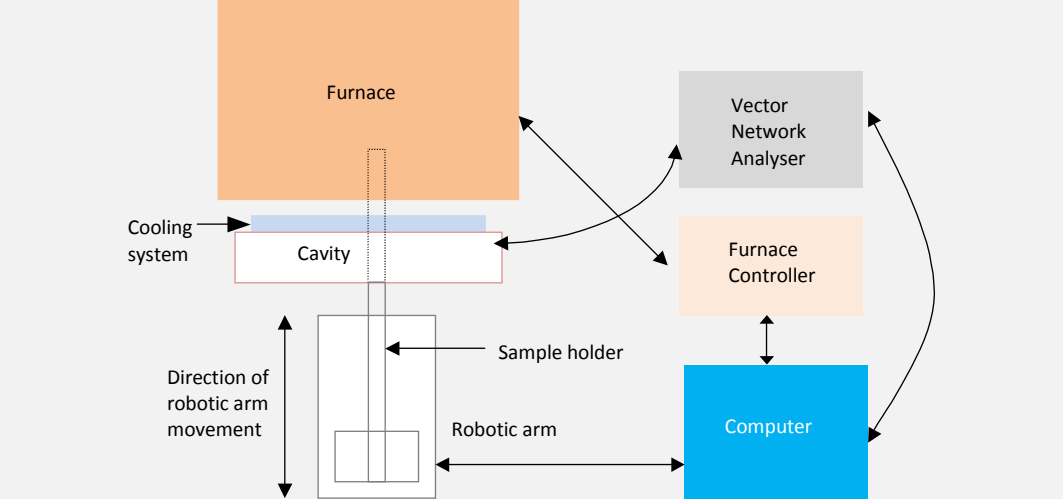

Figure 2.9 Typical apparatus set up for the cavity perturbation technique for measurement of dielectric properties of materials

The values of the dielectric constant ε', and the loss factor ε'', are computed using Maxwell's Equations 2.6 and 2.7 which have been derived from perturbation theory. As stated before, computers are commonly used to solve the equations instead of manual computations.

$$\varepsilon' = 1 + 2 * J_1^2 * \left(X_{l,m}\right) * \frac{V_c}{V_s} * \frac{f_0 - f_s}{f_0} \qquad (2.6)$$

$$\varepsilon'' = J_1^2 * \left(X_{l,m}\right) * \frac{V_c}{V_s} * \left(\frac{1}{Q_s} - \frac{1}{Q_0}\right) \qquad (2.7)$$

Where: V_c = Cavity volume (m^3)

V_s = Volume of sample (m^3)

f_0 = Resonant frequency of cavity without sample (Hz)

f_s = Resonant frequency of cavity with sample (Hz)

J_1 = First order Bessel function

Q_0 = Quality factor of cavity

Q_s = Quality factor of cavity with dielectric material

2.6 Microwave Power Dissipation

Microwave heating is a result of conversion of electromagnetic energy into heat. The former is generated by some source and transported through space or any other medium in form of an electromagnetic wave. The dielectric properties of a material and characteristics of the wave (in particular field intensity and associated power flux density) influence the extent to which microwave energy gets absorbed (Metaxas and Meredith, 1983). Power absorption by a dielectric material is often expressed as a power density (W/m^3) and is given by Equation 2.8 (Meredith, 1998).

$$P_d = 2\pi f \varepsilon_0 \varepsilon'' E^2 \qquad (2.8)$$

Where: P_d = Power density (W/m^3)

E = Root mean square (r.m.s) electric field strength inside the material (V/m)

ε_0 = Permittivity of free space (8.86×10^{-12} F/m)

Equation 2.8 shows that the power density varies linearly with frequency, loss factor and square of electric field strength. Therefore changes in electric field strength will affect power dissipation more significantly compared to frequency or lossiness of the material. For example if the electric field strength is tripled, the power density increases nine fold.

The heating rate of a dielectric material subjected to microwave energy is given by Equation 2.9 (Mingos and Baghurst, 1991). This equation assumes uniform electric field strength throughout the material being heated and also

assumes that there is no temperature drop due to heat losses from the surface of the material.

$$\frac{dT}{dt} = \frac{K.\varepsilon''.f.E^2}{\rho.C} \qquad (2.9)$$

Where: $\frac{dT}{dt}$ = Heating rate of the material (^{0}C /s)

K = Constant

C = Specific heat capacity of the material (J/Kg ^{0}C)

ρ = Density of the material (Kg/m^3)

The energy loss (and thus decrease in temperature due to radiation from the surface) can be taken into account by modifying Equation 2.9 (Mingos and Baghurst, 1991):

$$\frac{dT}{dt} = \frac{-e.\alpha.A_s}{\rho.C.V_s}.T^4 \qquad (2.10)$$

Where e = Sample emissivity ratio

α = Stefan-Boltzmann constant

A_s = Surface area of the sample (m^2)

V_s = Volume of the sample (m^3)

T = Sample temperature (^{0}C)

Equations 2.9 and 2.10 show that at constant frequency, temperature change depends on the loss factor of the material and the electric field strength. It is

very difficult to predict the magnitude of the electric field developed in the material because its introduction in the cavity or applicator alters the absolute value of the field (Greenacre, 1996b, Greenacre, 1996a). Computer simulations are used to predict the field distribution inside a cavity.

2.7 Microwave Power Penetration

When microwave energy is absorbed by materials, the amplitude of the wave decreases gradually as the wave propagates into the material. If any internally reflected waves are neglected, the power density (and therefore power absorbed) falls exponentially with depth. The microwave penetration depth, D_p is defined as the distance into the material at which the power flux falls to 1/e = 0.368 of its surface value (Metaxas and Meredith, 1983). The penetration depth is given by Equation 2.11.

$$D_p = \frac{\lambda_0}{2\pi\sqrt{2\varepsilon'}} \times \frac{1}{\sqrt{\left[\left(1+\left(\frac{\varepsilon''}{\varepsilon'}\right)^2\right)^{0.5}-1\right]}} \qquad (2.11)$$

Where λ_0 = Wavelength of incident radiation

The above equation shows that penetration depth increases with an increase in the wavelength (or a decrease in frequency). The penetration depth also increases with a decrease in values of ε' and ε''. In the microwave frequency range, penetration depth may be smaller than the depth of material interacting with microwave energy particularly when the material is very wet. This presents a problem of unacceptable uniformities in temperature

distribution. Surface heating tends to occur in materials with very high values of ε' and ε'' (Clark et al., 2000, Thostenson and Chou, 1999)

2.8 Engineering Aspects of Microwave Heating Systems

2.8.1 Introduction

The previous sections of this chapter have focused on the interaction of microwaves with dielectric materials. Before microwaves can interact with materials, they have to be generated by some source and need to be delivered to an applicator to interact with the material. The material to be heated is placed in an applicator where it interacts with the microwave energy. There are a wide range of considerations in the design of industrial microwave heating systems. The heating requirements, material type, throughput and economic factors all influence the design of industrial microwave heating systems. This section highlights only the major system components and the basic considerations in the design of microwave heating systems. The devices used to generate microwaves and how microwaves are guided to interact with materials is discussed. The major considerations in applicator design are also presented.

2.8.2 Microwave Power Sources

Microwaves are generated by controlling the movement of electrons generated by electron tube devices. In theory, a wide range of solid and non solid state electronic devices such as amplitrons, diodes, triodes, klystrons, transistors and magnetrons may be used to generate microwaves (Meredith, 1998, Saltiel et al., 1999). In practice, there are technical and economic considerations which make most of the above devices unsuitable for use in industrial microwave heating appliances. The

major economic consideration is the capital cost and operating cost. The major technical considerations are power output, frequency band and conversion efficiency. Most industrial heating processes require high power output and this makes solid state devices such as diodes and transistors unsuitable for use in industrial heating systems. The maximum power that solid state devices can generate is only about 500 W (Porch and Gough, 1997). Most industrial heating systems demand power in excess of 10 kW, often extending into the range of 100 kW to 1 MW (Meredith, 1998). There are stringent international restrictions to operate within the prescribed frequency band in order to avoid interference with communication devices. High conversion efficiency of incoming power to useable microwave energy is also needed in order to keep the operational costs to a minimum. These factors have meant that magnetrons are almost exclusively used to generate microwaves in all domestic and industrial microwave appliances because of their higher power output and efficiency, frequency stability and lower capital cost (Metaxas and Meredith, 1983). The klystron offers better frequency band control but this is outweighed by its capital and operating costs and may only be used where restrictions on band width is less than 2%. The development of the magnetron has had a major impact on the industrial application of microwaves because of its high efficiency enabling "cheaper" microwave heating of some materials.

2.8.3 Propagation of Microwaves

Most of the microwave properties that have been discussed so far relate to heating. But microwaves possess other properties similar to those of light. For example, microwaves propagate through unbounded space at the speed of light (3×10^8 m/s) and may also be reflected or refracted at a dielectric interface and can be focused by parabolic reflectors or horn antennas (Smith, 1995). The reflection property of

microwaves enables them to be guided through corners from one point to another with minimal loses. Specially designed hollow rectangular pipes with highly conducting surfaces are generally used to guide microwaves from the magnetron to the cavity with minimum loss. In industrial microwave heating devices, coaxial cables are not used for transmission due to unacceptable energy losses (Metaxas and Meredith, 1983).

In Section 2.1, it was stated that microwaves are composed of a magnetic field and an electric field propagating in planes perpendicular to each other. If a perfectly conducting plane lies in the path of a plane wave, then the electric field intensity tangential to the surface of the conducting plane is zero since the conducting plane offers no resistance. However the electric field component normal to the surface is not zero (i.e. has a finite value) and the converse applies for the magnetic field. From this principle, there exist certain wave guide geometry combinations that allow propagation of a single wave between parallel conducting surfaces. They are usually classed as either TE (transverse electric, or H) mode or TM (transverse magnetic or E) mode. When in TE mode, the electric field vector is normal to the direction of propagation. Conversely, when in TM mode, the magnetic field vector is normal to the direction of propagation (Meredith, 1998).

2.8.4 Microwave Heating Applicators

A microwave applicator is a device in which the material to be heated is placed to interact with the microwave energy. A familiar applicator is the metallic box inside the domestic microwave where food to be heated is placed. Applicators are classified by the type of field pattern that exists inside them. The domestic microwave oven is a multimode applicator because it supports a large number of resonant high-order waveguide type modes simultaneously which add

vectorialy in space and time to give a resultant field pattern (Meredith, 1998). Other common microwave applicators include travelling wave applicators and single mode cavities. Choice of applicator depends on many factors, such as size, shape and properties of the material to be processed as well as the heating rate required (Saltiel et al., 1999).

2.8.4.1 Multimode Applicators

Multimode cavities are the most commonly used microwave heating cavities. An example of a multimode applicator is the domestic microwave oven. As stated in the last section, multimode applicators are capable of sustaining a number of high order modes simultaneously. They essentially consist of a metal box of at least several half wavelengths long in at least two dimensions so as to be able to support a large number of resonant modes at a given frequency range (Metaxas and Meredith, 1983). The walls of the cavity are made of highly conducting material such as aluminium or copper in order to reflect microwaves with minimal loss. A complex electric field pattern exists inside a multimode cavity, with different electric field intensities and therefore material location within the cavity affects the heating uniformity and efficiency (Mehdizadeh, 2009a). For this reason, stirrers and turntables are used to randomly change the material position and improve on heating uniformity. A typical field pattern inside a multimode cavity is shown in Figure 2.10.

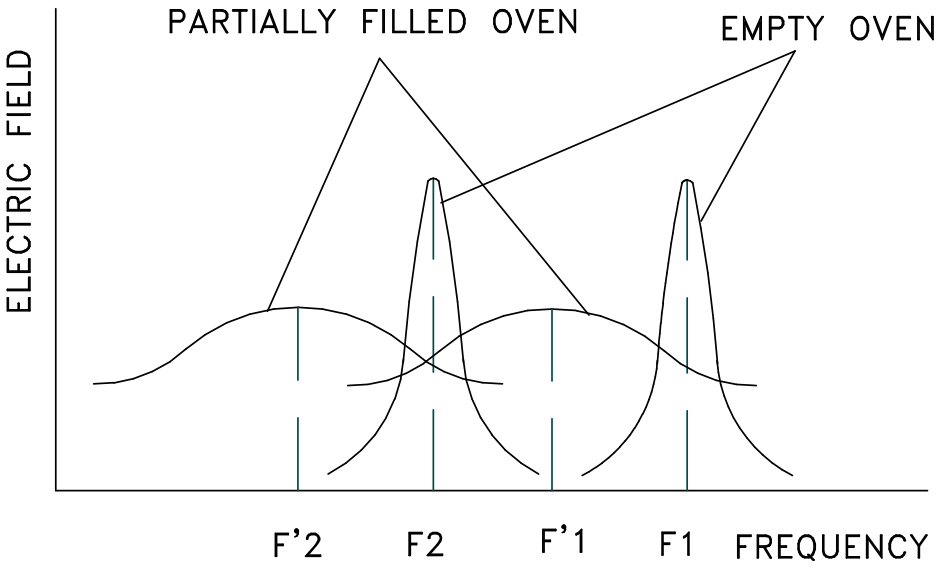

Figure 2.10 Frequency shift and damping of mode patterns due to the loading effect of the dielectric in a multimode cavity (Metaxas and Meredith, 1983)

Multimode cavities can be used to process a wide range of materials but are not suited for high temperature heating requirements because the energy is dissipated through a relatively large volume and this reduces the power density induced within the material. An important design parameter of multimode cavities is the power volume density (kW/m^3) at which it operates. Excessive power volume densities cause breakdown of air inside the cavity or destructive damage to the material being processed. Theoretically, increasing the dimensions of the cavity causes an increase in the number of modes within the cavity and also improves uniformity. Complete uniformity of field strength throughout the cavity is achieved if its longest dimension is approximately 100 times the wavelength of the operating frequency. However, this is not always practical due to limitations on the overall size of the cavity. For example, a domestic microwave oven operating at a frequency

of 2.45 GHz (wave length is approximately 0.12 m) would need to be at least 12 m long to achieve uniformity.

2.8.4.2 Single Mode Applicator

Single mode applicators support only one well defined electric field pattern inside the cavity. The single mode pattern is established by the superposition of the forward and reflected waves, which gives rise to a standing wave with maximum field intensity (Mehdizadeh, 2009b). The field pattern in a single mode cavity is therefore easier to predict and describe than in a multimode cavity. This is achieved by solving Maxwell's equations with known boundary conditions and the geometry of the cavity. The material to be heated is placed in a position of maximum field strength for optimum transfer of the electromagnetic energy. The size of the standing wave dictates the size of the cavity and consequently the size of a single mode cavity is in the order of one wavelength across (e.g 12.2 cm at 2.45 GHz). For the same power applied, a single mode cavity will establish higher electric field strength than other applicator types. Single mode cavities are therefore preferred where high heating rates are required and are also suitable for low loss material processing.

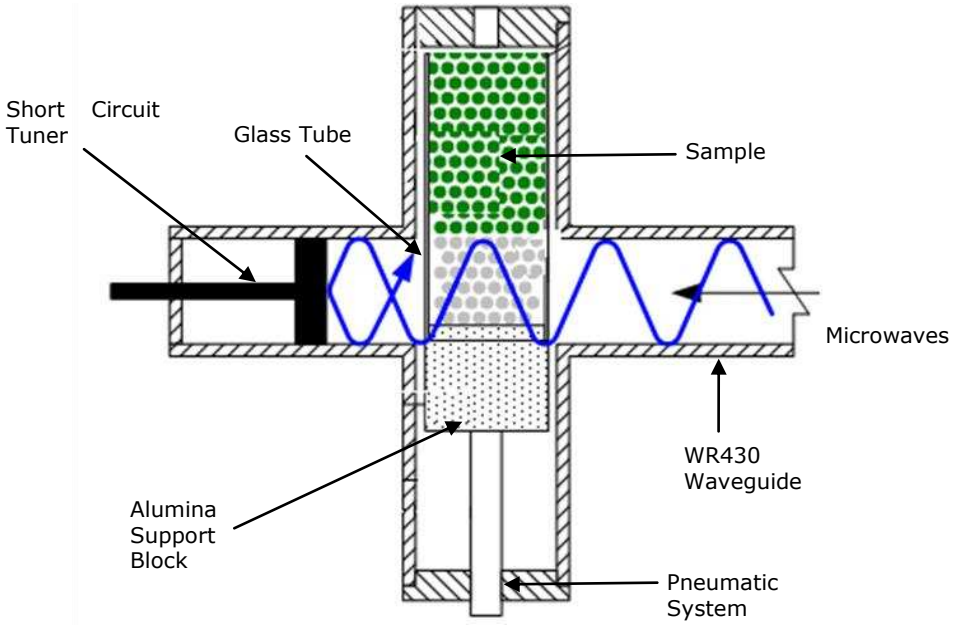

Figure 2.11 Schematic of a single mode cavity

2.8.4.3 Travelling Wave Applicators

In a travelling wave applicator, power is fed into a chamber and is absorbed by the workload with the residue being dissipated into a terminating load (Metaxas and Meredith, 1983). Travelling wave applicators are suitable for continuous flow processing with a conveyor belt but are not suitable for low loss materials. The heating efficiency depends on the permittivity and loss factor of the material to be heated and the cross sectional area of the applicator. In principle, all travelling wave applicators behave like single mode cavities if the terminal load is replaced by an adjustable short circuit and an aperture plate is fitted at the generator end.

2.8.5 Other Components of Microwave Heating Systems

Industrial microwave heating systems usually have controls that allow impedance matching. This ensures that most of the available energy from the power input unit is dissipated within the cavity. Theoretically, this is achieved when losses in the

dielectric material and walls are equal to the characteristic impedance of the wave guide (Metaxas and Meredith, 1983). In practice this is difficult to achieve because changing conditions inside the cavity due to spatial, temperature, chemical or phase changes alter the impedance of the heating system. A terminating load to absorb residual power (reflected microwaves) that is not absorbed by the material to be heated is provided. A water bath is usually used due to its abundance and high loss factor. Modern microwave heating systems are designed with automatic tuners to keep the reflected power to very low levels. If reflected power is not safely absorbed, this can cause damage to the magnetron. Knowledge of the reflected power together with forward power is valuable for impedance matching and efficiency of the heating system.

2.9 Conclusions

Microwaves are a form of electromagnetic energy which in theory can be used to heat any material as long as the material is neither a perfect conductor nor a perfect insulator. The ability of a material to heat when it interacts with microwave energy is characterised by the dielectric properties of the material and is proportional to a factor $\tan\delta$ (read tan delta) which is a ratio of the loss factor to the dielectric constant. The dielectric properties of a material vary with frequency, temperature and moisture content. Microwave heating systems operate at fixed specified frequencies. Dielectric property variation of a material can be measured with relative ease using specialized techniques such as the coaxial/probe line and resonance cavity perturbation techniques.

Industrial microwave heating systems often require high power output and are designed to ensure efficient conversion of power supply to useable microwave

energy. Magnetrons are widely used for this purpose. The generated microwaves are guided by hollow highly conducting rectangular tubes (ensuring minimal loss of energy) to the applicator where the material to be heated is positioned. Multimode cavities are widely used in many microwave heating appliances. However, single mode cavities have potential for higher and well defined electric field patterns compared to multimode cavities. This implies that uniform and faster heating rates may be achieved using single mode cavities compared to multimode cavities.

CHAPTER THREE

3 REVIEW OF MICROWAVE HEATING APPLICATIONS IN MINERAL PROCESSING

3.1 Introduction

The mining industry is a major supplier of raw materials to other sectors such as manufacturing, power plants, infrastructure etc and each year, millions of tons of ore are mined. The ores must first be processed in order to extract the targeted valuable minerals, a process known as mineral processing. The cost of energy in mineral processing represents a significant proportion of the overall cost of production. For example, it is estimated that the energy cost in copper production is about 35% of the selling price of the metal (Dahlstrom, 1986). Vast amounts of energy are expended in crushers and grinding mills for size reduction of ores in order to expose mineral grains from the host rock so that they can be concentrated. Other significant energy requirements are ore handling and metal extraction (Billiton, 2009). Energy consumption in mineral processing is therefore a key aspect of the economic feasibility of an ore. Lowering energy consumption in mineral processing does not only lower the carbon footprint but could also enable processing of low grade ores.

An energy analysis conducted by the US Mining Industry demonstrated that the largest opportunities for energy savings in mining are in materials handling, beneficiation and processing and extraction (DoE, 2004). Approximately 87% of energy in materials handling is used in diesel

technologies in machines and trucks used to move ore and waste. Comminution activities are the largest energy consumers in beneficiation and processing accounting for 75% and slurry pumping consumes the most energy in extraction at 41%. It has been observed that conventional comminution techniques are highly energy inefficient and extraction techniques such as smelting are not only energy intensive but also environmentally damaging. There is, therefore, a need to improve existing process techniques or develop novel technologies that are more efficient, clean, reliable and affordable.

Grinding is the most energy intensive and inefficient stage in comminution. Grinding technologies have therefore generated more research interest than crushing which is considered to be relatively efficient. Some authors have suggested that grinding is inherently inefficient while others have blamed conventional grinding equipment such as the ball mill for being highly energy inefficient (Austin and Bagga, 1979, Fuerstenau et al., 1990, Fuerstenau and Abouzeid, 2002, Rhodes, 1998, Schonert, 1972, Lowrison, 1974, Schoenert, 1972). More recent studies based on the concept of maximum theoretical grinding energy efficiency have shown that there is room for improvement of grinding efficiency (Tromans, 2008). As discussed later in this chapter, some process benefits have been reported by using High Pressure Grinding Rolls (HPGRs) and Semi-Autogeneous (SAG) mill based circuits instead of the traditional ball mills (Gerrard et al., 2004, Gupta and Yan, 2006). Other work has involved use of so called "assisted techniques" such as grinding aids and thermal pre-treatment (Wang and Forssberg, 2007).

Thermally assisted comminution of ores has been investigated since the early twentieth century (Yates, 1919). Previous work demonstrated that heat pre-

treatment of rocks improves grindability but is not economically feasible due to the vast required energy input (Fitzgibbon and Veasey, 1990). Recent studies have shown the potential use of microwave heating technologies to improve the efficiency of various mineral processing unit operations at economies that favour the overall process. The potential for microwave applications has been identified in leaching, refractory gold ore treatment, grindability and liberation. This chapter examines the challenges and opportunities for efficient comminution technologies. The potential of microwave heating as an "assisted technique" for improved comminution efficiency is discussed in detail.

3.2 Comminution in Ore Processing

3.2.1 Introduction

Valuable minerals are almost always associated with or embedded in other rock minerals in very low proportions compared to the host rock. For example, typical mineral to gangue ratios in copper ores are usually in the range of 0.5-2% and may be as low as 0.01 ppm in precious metal ores such as diamonds and gold (Wills, 2006). The objective of mineral processing is to separate valuable minerals from each other and/or from the host rock material (gangue) and then concentrate all the valuable minerals into a saleable product. Therefore, to produce one kilogram of a pure copper ore concentrate would typically require processing between 50-200 kgs of material and one gram of diamond would require processing about 10 tons of ore.

The process by which a mineral grain is released from the host rock matrix is known as liberation. The only practical way to achieve liberation is to crush

and grind the rock material to expose the mineral grains either wholly or at least partially. The process of size reduction to achieve mineral liberation is known as comminution. The degree of liberation refers to the percentage of the mineral occurring as free particles in the ore in relation to the total ore content (Wills, 2006). Figure 3.1 below illustrates the degree of liberation achieved by three fracture planes through a mineral grain.

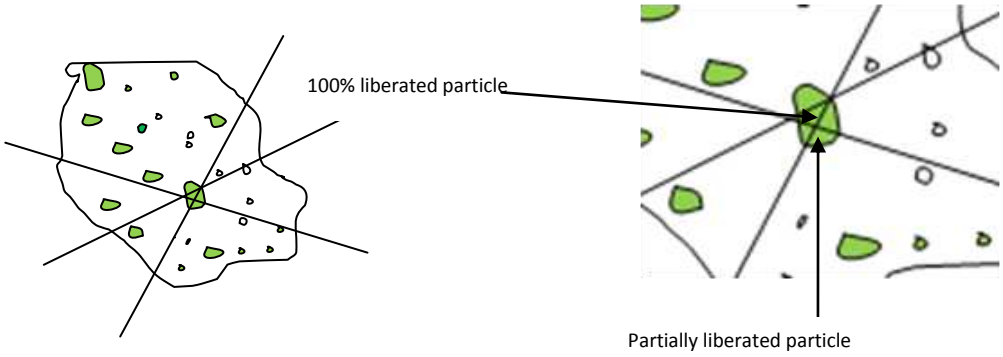

Figure 3.1 Liberation of mineral grains in ore comminution

3.2.2 Significance of Comminution in Ore Processing

A typical ore process flow sheet consists of crushing and grinding stages followed by separation and recovery stages. Theoretically, if the size of the ore is reduced to below the size of the smallest mineral grain, 100% liberation is achieved. Above this size, some minerals will remain either partially or completely locked with the host rock. The portion of material after separation, which is rich in the targeted valuable minerals, is known as the "concentrate". The unwanted material which is disposed of is referred to as "tailings". Practically it is extremely difficult and also not economically attractive to achieve 100% liberation as this would consume a vast amount of energy and time. As a result of this (but also depending on the efficiency of the separation

method) there will always be some fraction of mineral that is lost in the tailings and conversely, a small proportion of unwanted material (gangue) will be in the concentrate. The grade of the concentrate is a measure of amount of targeted minerals relative to the bulk of the concentrate (Wills, 2006). Comminution is therefore always a trade-off between an acceptable degree of liberation, the recoverable mineral and the cost of crushing or grinding to the required size.

The degree of liberation significantly affects the amount of recoverable mineral. A high degree of liberation is required in processes such as froth flotation where as much of the surface area as is possible is desirable (Feng and Aldrich, 1999). In this case the higher the degree of liberation, the higher the efficiency of the separation process. In other processes such as leaching where only a small surface of mineral may be sufficient for extraction, the required degree of liberation for efficient separation may be considerably lower (Al-Harahsheh and Kingman, 2004).

3.2.3 Mechanism of Brittle Fracture

It is generally agreed that rocks are brittle materials although the degree of "brittleness" is a subject of debate mainly because rocks are anisotropic and their composition varies greatly. The mechanism of brittle fracture was first explained in a paper published by Griffith in 1920 (Lawn and Wilshaw, 1975). It was observed that the magnitude of stress required to fracture a material is proportional to the length of a flaw inside the material. The property of fracture toughness, which is defined as the ability to resist propagation of existing cracks in a material, is now used to characterise fracture in brittle materials (Ayatollahi and Aliha, 2007). Fracture initiates either at the tips of

pre-existing open or closed cracks which act as stress concentrators, intensifying the stress field at their tips (Lawn and Wilshaw, 1975). Largest favourably oriented cracks experience the greatest crack-tip stress. The fracture toughness of a material represents the critical level of the stress intensity factor above which catastrophic crack extension will lead to breakage (Bearman et al., 1997). If the remote stress at a critical crack tip is increased until the stress intensity on the critical flaw exceeds the fracture toughness index (K_c) of the material, the cracks will grow in the plane perpendicular to the maximum tensile stress direction until the sample is fractured (Lawn and Wilshaw, 1975).

Three different theories based on Linear Elastic Fracture Mechanics (LEFM) have been put forward to explain the different modes of fracture propagation. These are discussed in detail by Fett and Munz (2003). Essentially, Mode I is associated with tensile fracture (crack opening). Mode II and III fracture mechanisms are both associated with crack shear either in same direction with the crack plane (sliding) or anti-plane (tearing) as shown in Figure 3.2.

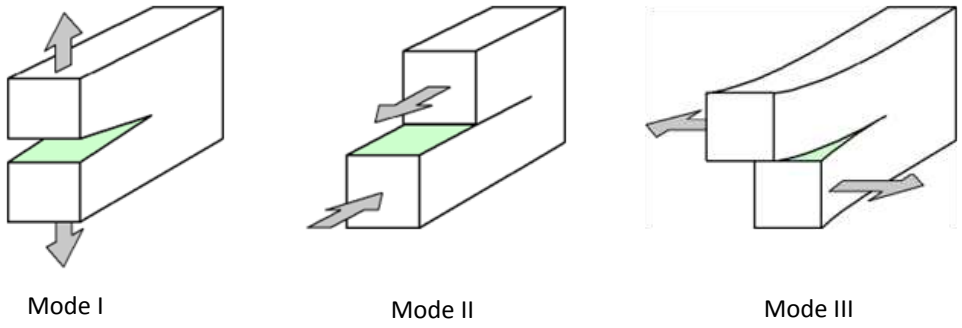

Figure 3.2 Modes of fracture propagation in brittle materials (Fett and Munz, 2003)

(Bearman, 1991) carried out a study to examine strength tests which could be used to characterise rocks with respect to resistance to crushing. Twelve

different rock types were crushed using a jaw and a cone crusher. The throughput, power consumption and product size for a range of crusher settings and feed sizes was analysed. The results showed that the strength parameters closely related to crusher performance are those involving tensile based properties. It was concluded that Mode I fracture toughness and Point Load tests best model the type of failure that occurs during comminution. Fracture of rocks is therefore associated with tensile failure even with compressive loading conditions typical in most comminution machines.

Fracture during comminution is propagated depending on the orientation of the cracks inside the particle with respect to the loading conditions. If the weak grain boundaries can act as stress concentrators, then fracture propagation will mainly follow grain boundaries i.e. fracture will be predominantly intergranular as shown in Figure 3.3.

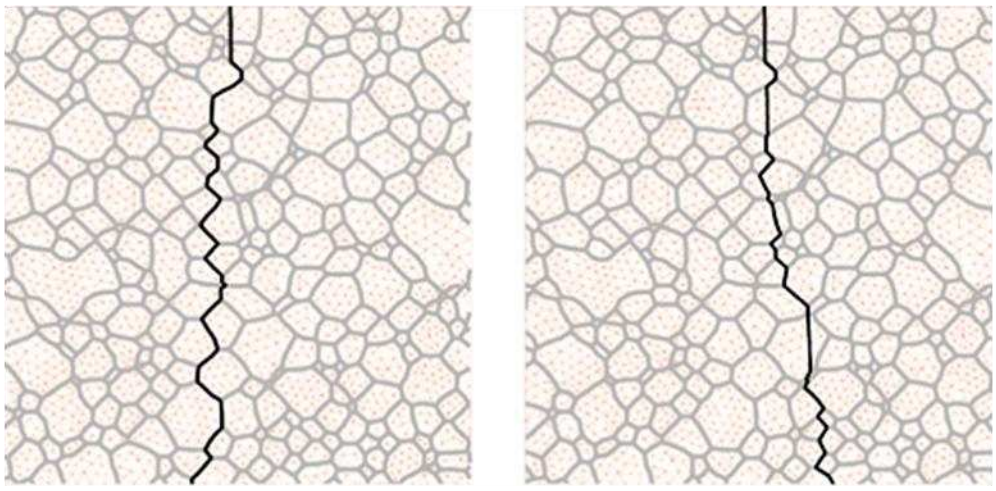

Figure 3.3 Fracture propagation in ores (Left) Perfect intergranular fracture (Right) Intergranular and transgranular fracture typical in comminuted particles (Sukumar and Srolovitz, 2004)

From the mineral processing point of view, intergranular fracture is desirable because liberation is achieved at approximately the same size as the grain

(higher degree of liberation) and therefore less valuable minerals are lost in tailings. In practice, transgranular fracturing is dominant in most conventional comminution machines due to random orientation of particles and complex loading conditions and particle interaction during comminution (Kelly and Spottiswood, 1982). However, recent developments in comminution technology have suggested that intergranular fracture may be enhanced by using by using High Pressure Grinding Rolls (HPGR) and assisted techniques such as heat pre-treatment. These are discussed in detail later.

3.2.4 Conventional Comminution Techniques

3.2.4.1 Crushing

Crushing is the first stage in the process of comminution and is usually conducted in two to three stages depending on the size of the run-of–mine ore and grinding machine. Typical reduction ratios in the crushing circuit are in the range of 40 to 100. Blast rock of a size in the range of 200-500 mm is crushed down to p_{80} of 5-6 mm (Lindqvist, 2008). The p_{80} is the particle size that is larger than 80% by mass and is commonly used as a characteristic particle size of feed or product material in mineral processing (Wills, 2006). The mechanical stress required for ore breakage is delivered predominantly by two mechanisms depending on the type of crusher used. Jaw crushers and cone crushers generally operate by applying compressive pressure to the material passing in between 'jaws' while impact crushers rely on impact as the major mechanism for breakage (Bearman, 1991). As the costs associated with grinding greatly outweigh those associated with crushing, the latter is considered relatively efficient and most research and developments have focused on grinding circuit optimization. Considerable energy savings in grinding have been reported by using Impact crushers and High Pressure

Grinding Rolls (HPGR) due to production of more fine material than the conventional Jaw crushers (Lindqvist, 2008). The HPGR is discussed in more detail in the next section.

3.2.4.2 Grinding

Grinding is the last stage in the process of comminution where particles are reduced in size by a combination of impact and abrasion, either dry or in suspension in water. It is often performed in rotating cylindrical steel vessels which contain a charge of loose crushing bodies (grinding medium) which is free to move inside the mill, thus comminuting the ore particles. Grinding mills are generally classified according to the ways by which motion is imparted to the charge into two types namely tumbling mills and stirred mills (Wills, 2006). In tumbling mills, the mill shell is rotated and motion is imparted to the charge via the mill shell. Stainless steel balls or rods are commonly used as grinding medium. SAG mills are similar to ball/rod mills but are characterised by a lower ball/rod charge typically 6-15%. Grinding is achieved via impact with the large chunks of the ore itself in addition to the grinding medium. Tumbling mills are typically employed in the mineral industry for coarse-grinding processes, in which particles between 5 and 250 mm are reduced in size to between 40 and 300 μm (Wills, 2006). In stirred mills, the mill shell is stationary and either horizontally or vertically orientated. Motion is imparted to the charge by the movement of an internal stirrer. Fine grinding media inside the mill are agitated or rotated by a stirrer, which typically comprises a central shaft to which are attached pins or discs of various designs. Stirred mills find application in very fine (15–40 μm) and ultra-fine (<15 μm) grinding and therefore have little application in mineral processing as it is often not necessary or not cost effective to grind ores to this size.

Typical reduction ratios for grinding in mineral processing are usually in the in range of 25-100.

Despite having considerably lower reduction ratios than crushing, the cost and energy consumption associated with grinding is significantly higher than that associated with crushing (Eloranta, 1997). Different authors have put forward several explanations for this. The first claim is that the amount of energy consumed during grinding is a monotonic function of surface area i.e. Rittinger's law is obeyed. In earlier years, comminution efficiency was often defined as the ratio of the energy of the new surface created during size reduction to the mechanical energy supplied to the machine performing the size reduction. In terms of this concept, the energy efficiency of the tumbling mill is as low as 1% or less. For example, it is reported that for a ball mill, the theoretical energy for size reduction (the free energy of the new surface produced during grinding) is in the range of 0.1-1% of the total energy supplied to the mill set-up (Lowrison, 1974, Ocepec et al., 1986, Rhodes, 1998). Taking a slightly different approach, another school of thought is that breakage occurs at micro defects in the rock particles and that as the particles get smaller, these defects are "consumed" and the remaining particles become relatively more and more difficult to break (Lindqvist, 2008). These claims seem to suggest that grinding is inherently energy inefficient because as the particle size is reduced, the specific surface area increases. As the particle size approaches zero, the number of particles and the specific surface area of all those particles approaches infinity and the defects in the particles diminish and therefore vast amount of energy is required to create new surfaces. Fuerstenau and Abouzeid (2002) proposed that assessing ball mill efficiency be in terms of the energy required to produce new surface area by

compression loading or impact loading of single specimens and on this basis, ball mill efficiency was found to be about 15%.

Other researchers have disputed the above methods of assessment and argued that any useful assessment of energy efficiency should be based on the minimum energy required in breaking the particles and not on the surface area produced. Schoenert (1972) simply considered that the upper limit of energy utilization in size reduction processes is that required for the mechanical breakage of single-particles and that the maximum utilization of energy is only obtained when inter-particle friction and inter-particle energy transfer is absent. Tavares and King (1998) proposed that the specific fracture energy is a better method of assessing comminution efficiency but this method also gives an efficiency of less than 8%. Tromans (2008) suggested that the maximum limiting energy efficiency E_{Limit} of compression loading comminution processes is dependent upon Poisson's ratio and lies in the range of approximately 7.5±2.5% when based on the energy required to generate new fracture surface area relative to the mechanical strain energy input. Estimates of actual energy efficiency values (E_B), based on surface area generated relative to the work input using the standard Bond Work Index, were found to be in the range of 0 to 2%. By comparing the actual efficiency with the limiting efficiency via the ratio E_B/E_{Limit}, the resulting relative efficiency of comminution was found to be in the range of 3–26%.

Despite various claims as to the best option for assessing grinding energy efficiency, there seems to be a general consensus that impact conditions in grinding mills do not provide the best technology for efficient size reduction and that there is potential for increase in efficiency. For example, it is claimed

that the best conditions for energy efficiency occur when energy is applied under low intensity of say 1 J/g or less and yet the specific impact energy in a ball mill is about 15-20 J/g (Tavares and King, 1998). This produces an excess of elastic energy in the load, an important part of which is finally dissipated as heat.

3.2.5 Challenges in Comminution

Based on the criteria of increase in surface area per unit energy, developed by Schoenert (1972) or that by Tavares and King (1998) which is based on fracture energy, a perfect comminution machine can be described as one which fulfils the following conditions:

- All the energy input is used to fracture the material to create new surfaces
- Only the minimum energy required to cause fracture is utilized
- Size reduction only to achieve targeted degree of liberation i.e. no excessive grinding

Unfortunately no perfect comminution machine is known to exist and there are no reports of any being developed in the near future. In current comminution equipment, more energy is used to cause fracture than is theoretically required and a significant amount of energy is wasted in unnecessary grinding. Although the dream of a perfect comminution machine is still farfetched, the following specific research issues have been identified as some of the key areas pertinent to energy efficiency in comminution (DoE, 2004).

- Developing comminution schemes that take advantage of natural weakness in rock. Such technology could include pre-treatment of

rocks or breakage of rocks in tension rather than in compression since the tensile strength of rocks is weaker than the compressive strength

- Developing new ways to deliver impact energy to ores
- Developing technology to improve grinding
- Developing accurate models of fracture which can be used to predict the behaviour of ores during comminution
- Optimizing comminution circuits to eliminate over grinding

Although some progress (which is discussed in the next section) has been made in addressing some of the above issues, this has only led to modest process benefits. It is clear that more research and development work needs to be carried out. This study is aimed at developing a novel microwave assisted comminution technique that enhances intergranular fracture in order to increase mineral liberation and recovery and possibly lower grinding energy requirement.

3.3 Recent Developments in Comminution Technology

3.3.1 Introduction

The last two decades have been marked by a sharp increase in global environmental awareness. As a result, many industries are concerned about efficiency and sustainability. In broad terms, efficiency is measure of input savings that can be realised with technological development without necessarily compromising output. Opportunities for improved efficiency in comminution cut across a range of scientific and engineering aspects. In recent years, research and developments from different professional bodies have expanded the wealth of knowledge in the field of comminution.

Mathematical models and computer simulations can now be used to provide an insight of what takes place inside comminution machines. Engineering developments have enabled improvements of conventional comminution equipment. Process developments have provided more accurate methods of measuring and characterising control parameters such as particle size distribution to reduce unnecessary grinding. It is anticipated that a multidisciplinary approach of scientists and engineers with different expertise provides the best hope for a lasting solution to the challenges in comminution.

3.3.2 High Pressure Grinding Rolls (HPGR)

It was suggested that the most energy efficient method of comminuting particles is to compress them between two plates (Schoenert, 1979). Compressing a particle bed between two counter rotating rolls was achieved by the invention of the high pressure grinding rolls (HPGR). Comminution in the HPGR is as a result of high inter particle stresses generated when a bed of solids is compressed as it moves down a gap between two pressured rolls (Wills, 2006). Such inter particle stresses result in a greater proportion of fines in comparison to conventional crushing. The HPGR has achieved considerable interest over the last two decades due to its potential for significant benefits in comminution circuits. Process benefits such as increases in liberation, reduction in untreatable fines, reduction in grinding energy and increase in grade and recovery have been reported (Aydogan et al., 2006, Clarke and Wills, 1989, Fuerstenau and Kapur, 1995, Norgate and Weller, 1994). It has also been claimed that the Bond Work Index of the HPGR product is significantly lower than the product of conventional crushers due to creation of micro cracks (Clarke and Wills, 1989).

The extent of the weakening caused by HPGR is dependent on the specific energy input (grinding pressure) and is greater for coarser sized particles but becomes insignificant for particles less than 1.5 mm (Tavares, 2005). Successful application of the HPGR has been reported at the Argyle Diamond Mine (ADM) in Australia where they have been used for tertiary crushing of material with p_{80} of 75 mm since the early nineties and more recently for re-crush of material with size range 6-15 mm. The total cost of operating a HPGR was about 14% less than that of operating a cone crusher. The Relative Comminution Efficiency (RCE) of the HPGR was between 51-75% higher than for the Cone crusher depending on the size fraction (Gerrard et al., 2004).

The main advantages of HPGRs are summarised as follows (Kellerwessel, 1993):

- Less specific energy consumption and consequently less wear in downstream ball milling
- Increased capacity of existing plants with comparatively small investment
- Better liberation of valuable constituents
- More intense attack by leach liquor
- Comparatively low space requirement depending on the selected flow sheet

The HPGR seems to be the most energy efficient comminution device currently available to the mineral processing plant designer. The focus therefore should be on the development of both the machine and flow sheet to maximize the proportion of total comminution performed by the HPGR. Properly designed HPGR-based circuits offer potential of significant savings in comminution

energy requirements, increased liberation and overall operating costs when compared to ball or SAG-mill based circuits.

3.3.3 Grinding Technologies

Until the 1970s, almost all grinding in mineral processing was carried out using rod and ball mills. Arguably, no novel grinding technologies that significantly differ from the tumbling technology have dominated mineral processing to date. However, subsequent technological developments have resulted in "improved versions" of the traditional ball/rod mill. The SAG mills have come to dominate comminution in mineral processing. The efficiency of SAG mills, in terms of energy consumption, has been disputed by some authors. It is claimed that "critical size particles" can build up in the SAG mill charge, limiting mill throughput and increasing unit power consumption (Johnson et al., 1993). However, it has generally been agreed that removing the critical size particles from the mill, crushing them, and returning them to the circuit, can significantly improve the power efficiency of the circuit and result in substantial increases in circuit throughput and efficiency (Apelt and Thornhill, 2009, Napier-Munn et al., 1996). There have also been reports of reduced capital cost as a result of ability to eliminate at least one grinding step, less resistance to lining wear and grinding media capital requirement although these are not very significant when compared to the cost of energy (Johnson et al., 1993).

A plethora of other equipment such as IsaMill, stirred mill and tower mills have also come into use for ultra fine grinding (Wang and Forssberg, 2007), although these have had little application in base metal mineral processing as, often, ultra fine grinding is either not necessary or not cost effective. Shi et al

(2009) conducted a study to compare the performance of a laboratory scale Vertical Impact Stirred mill with a ball mill. It was reported that there had been an indication that on average, 30% energy savings can be expected by using the stirred mill to replace the ball mill for coarse grinding. However, this difference was expected to decrease to some degree when using a larger ball mill and this claim has not been substantiated. In addition, there are reports of other "high efficiency" mills such as the VKE (manufactured by Microgrinding Systems Inc) and The Hicom Mill, that are associated with vibration or eccentric impact and centrifugal actions but likewise these have had little impact in mineral processing due to limitations in capacity and other associated engineering and design problems (Shi et al., 2009).

Due to limited alternatives for grinding technology with respect to mechanical stressing of particles, significant research efforts have been directed towards optimizing performance of existing mills and grinding circuits. Several studies have focused on enhancing performance indicators such as throughput, energy consumption and product quality. Other studies have investigated the effect of variations in mill load, speed, inlet water flow and feed size distribution on performance of mills (Morrell, 2003, Powell et al., 2009, Powell et al., 2001). Improved particle classification systems during processing can save energy, avoid over grinding, improve product quality and increase unit capacity. Laboratory test work has also indicated that the way circuits are operated with respect to classifier performance and recycle load in closed ball mill circuits could save up to 15% of the required grinding energy (Morrell, 2008). The increase in efficiency was said to result not from the view point that more of the energy in the balls is transferred into breaking feed ore, but that the same amount of energy is used to break more of the coarser ore

particles and less of the finer ones, thereby changing the product size distribution. In effect, the increase in recycle load reduces over grinding. Other work has involved developing numerical models and computer simulations that enable analysis of charge motion for improved mill design and operation and to develop a so-called "virtual comminution machine" (Venugopal and Rajamani, 2001, Morrison and Cleary, 2008). Although all these developments have provided a wealth of knowledge about comminution processes and some significant process benefits, they have not provided the breakthrough in grinding efficiency that is required.

3.4 Thermally Assisted Comminution

3.4.1 Introduction

The use of heat to enhance fracture of rocks is a technique believed to have been known since pre-historic times. Archaeological investigations have suggested that rocks were heated before carving tools or sculpture (Guisepi, 2000). The first documented studies about the potential of preheating rocks to enhance breakage date back in the early 20^{th} century (Yates, 1919, Holman, 1926). This early work showed that heating quartz and immediately quenching it in cold water weakened it so much that it could be crushed between finger and thumb and passed through a 500 μm screen. Although these initial findings seemed very promising, to date nearly 100 years later, this technology has not been developed to benefit comminution in mineral processing mainly due the vast energy input requirement. In this section, the scientific aspects of thermally induced fracture in rocks will be examined. A review of research work on challenges and potential of thermally assisted comminution in mineral processing will be presented.

3.4.2 Thermal-Mechanical Properties

3.4.2.1 Introduction

Extensive work has been carried out on the physical and chemical properties of common minerals that constitute most rocks and ores. There is a wealth of data on the mechanical and thermal properties of most important minerals. The bulk ore properties are influenced by the properties of the composite minerals and their association. In order to explain the phenomenon of thermally induced fractures in rocks, there is a need to couple the thermal and mechanical properties of composite minerals.

3.4.2.2 The Point Load Strength Index

Just like other materials, the mechanical strength of rocks is defined with respect to the loading conditions. The International Society for Rock Mechanics (ISRM) describes various standard methods for in situ and laboratory testing of different strength properties of rocks such as hardness, fracture toughness, tensile and shear strength and other physical properties such as density and porosity. As stated in Section 3.2.3, the strength properties of rocks that are of greatest significance to comminution are those related to tensile strength and in particular the mode I fracture toughness.

There are various methods for testing the fracture toughness of a material. The ISRM recommends the Chevron Notched Short Rod (SR) and the Chevron Notch Round Bar in Bending (CB) tests. Despite the standardisation of the fracture toughness test, its use in rock characterisation is not widespread mainly because of lengthy sample preparation and testing procedure. Bearman (1999) provided a correlation between the mode I fracture toughness index (K_{IC}) and the Point Load Index (I_s). The Point Load test was

developed by Broch (1971) and standardized by ISRM in 1985 (ISRM, 1985). It was incorporated into the American Society for Testing and Materials in 1995 (ASTM D5731-95). The test is basically performed by loading a sample between two platens thereby inducing a tensile stress using an external compressive load as shown in Figure 3.4 below.

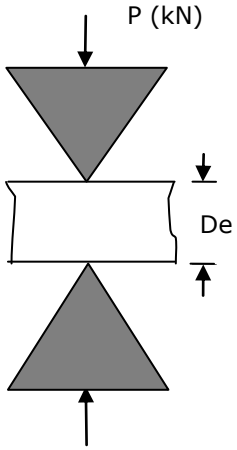

Figure 3.4 Schematic of a sample under Point Load testing

The Point Load Index (I_s) is given by:

$$I_s = \frac{P}{D^2} \qquad (3.1)$$

Where I_s = Point load Index (MPa)

P = Maximum Load (kN)

D = Distance between the loading platens (mm)

I_s varies with geometry of the test specimen and so a corrected value equivalent to I_s of a specimen of 50 mm ($I_{s(50)}$) is used as the standard. In addition, the concept of an equivalent depth D_e, (which is the diameter of an

equivalent circle) is used for irregularly shaped test specimens. Equation 3.2 is generally used to obtain the standardised index for a test specimen of any shape.

$$I_{s(50)} = \left(\frac{D_e}{50}\right)^{0.45} \times \left(\frac{P}{{D_e}^2}\right) \quad (3.2)$$

Where $$D_e = \left(\frac{4WD}{\pi}\right)^{0.5} \quad (3.3)$$

W = Width of the sample (mm)

The relationship between the Point Load Index and Mode I fracture toughness is given by Equations 3.4 and 3.5 (Bearman, 1999). Equation 3.4 is used for diametric testing on cores while Equation 3.5 is used for irregular test pieces or axially tested core samples.

$$K_{IC} = \frac{29.84P}{D^{1.5}} \quad (3.4)$$

$$K_{IC} = \frac{26.56P}{(WD)^{1.5}} \quad (3.5)$$

Where
K_{IC} = Mode I fracture toughness (MN/m$^{3/2}$)
P = Force at failure (kN)
D = Distance between the point load platens (mm)
W = Minimum width of test piece (mm)

The Point Load test is flexible and simple compared to other conventional testing methods. The specimen fails at much lower loads than in compression so no bulky equipment is required (Broch, 1971). The time required to perform the test is much less as no special preparation of specimens is required and the method of loading is simple as well. Due to anisotropy in most rocks, it is recommended that several tests be carried out. Some authors have suggested that ten or more tests are required to be within 96% confidence interval of the mean strength (Yamaguchi, 1970). However, the author's experience, which is discussed in detail in the next chapter, has cited some limitations of this method and also observed that far more particles (possibly in hundreds) need to be tested to obtain a good degree of confidence. Some care should also be taken when selecting particles to be tested.

3.4.2.3 Heat Capacity of Minerals

Different materials usually heat at different rates even when exposed to the same thermal energy. The inherent property of a material that determines its heating and cooling rate is known as the heat capacity of the material. The specific heat capacity of a material is defined as the energy required to raise the temperature of a unit mass (1 kg) of material by one Kelvin (Borgnakke, 2008). The standard units are J / kg K. The specific heat capacity of a material may be measured under constant pressure (c_p) or under constant volume (c_v) but c_p and c_v values at room temperature are equal to within 1% (Cezairliyan, 1981). The specific heat capacity values of common rocks and minerals are quoted in various scientific texts such as (Touloukian et al., 1981).

Mineral	C_p 298 K (J/kg K)	C_p 500 K (J/kg K)	C_p 100 K (J/kg K)	*a* (J/kg K)	*b* (J/kg K^{-2})	*c* (J K/kg) x10^6
Calcite	818.70	1051.00	1238.50	1045.16	0.219	-26
Rutile	688.75	850.75	933.75	916.82	0.038	-21
Sphalerite	467.63	514.85	557.01	507.69	0.054	-5
Quartz	740.50	991.17	1167.17	682.83	0.743	-14
Feldspar	567.23	951.73	1175.83	1857.21	0.418	-45
Fluorspar	860.90	925.51	1248.33	529.38	0.711	11
Barytes	436.65	546.39	591.80	606.94	0	-15
Wolframite	377.46	454.52	527.33	437.04	0.098	-8
Dolomite	843.32	1015.54	-	843.62	0.436	-12
Corrundum	772.84	1057.16	1217.16	1151.83	0.102	-36
Gypsum	579.36	695.23	982.27	408.18	0.574	0
Bauxite	338.21	338.21	-	387.28	0	0
Cassiterite	348.34	450.93	539.34	440.17	0.110	-11
Hematite	654.81	820.31	641.25	614.23	0.486	-9
Ilmenite	654.61	774.41	874.01	767.15	0.120	-13
Chalcopyrite	516.52	597.01	1068.70	-134.38	1.203	0
Pyrite	517.08	600.42	683.83	574.60	0.117	-8
Pyrrhotite	572.61	827.27	693.18	580.05	0.113	0
Chalcocite	477.00	604.19	529.00	529.01	0	0
Magnetite	654.22	829.91	865.65	394.64	0.871	0
Bornite	487.30	740.42	659.94	413.08	0.291	-1
Galena	208.95	215.23	234.94	195.54	0.039	0

Table 3.1 Specific heat capacity (c_p) and coefficients of heat capacity of selected minerals at different temperatures (Knacke and Hesselmann, 1991)

The energy into a material is related to the specific heat capacity of the material by Equation 3.6.

$$Q = mc_p\Delta T \qquad (3.6)$$

Where Q = Energy (J)

m = Mass (Kg)

c_p = Specific heat capacity (J / Kg K)

ΔT = Change in temperature (K)

Equation 3.6 shows that for same energy input, the higher the specific heat capacity, the lower the temperature change. Table 3.1 gives values of c_p of common minerals. It is evident that minerals such as calcite, quartz and fluorspar experience considerably slower heating rates than others such as galena, bauxite and cassiterite. Such differences in heating rates inside a multi mineral ore induce stress as a result of differences in thermal expansion. Specific heat capacity varies with temperature for most solids. The relationship between temperature and c_p is given by Equation 3.7.

$$c_p = \alpha + bT + cT^{-2} \quad (3.7)$$

Where a, b and c are constants known as the coefficient of heat capacity of the material (see Table 3.1)

3.4.2.4 Thermal Conductivity of Minerals

In solids, heat is transmitted mainly by the conduction mechanism. This involves transfer of energy between neighbouring vibrating molecules or free electrons (Borgnakke, 2008). The thermal conductivity of a material is the property that relates to its ability to conduct heat. The general equation for heat flow through a slab of material is derived from Fourier's law of heat conduction and is given by Equation 3.8.

$$\frac{Q}{t} = \frac{kA(\theta_2 - \theta_1)}{l} \qquad (3.8)$$

Where Q = Heat conducted (W)

t = Time (s)

A = Surface area of slab (m^2)

θ_1 = Original temperature (^0C)

θ_2 = Final temperature (^0C)

l = Length of slab (m)

k = Thermal conductivity (W/m K)

Re-arranging Equation 3.8;

$$k = \frac{Q.l}{A.t.(\theta_2 - \theta_1)} \qquad (3.9)$$

Due to the degree of anisotropy of most minerals and rocks, thermal conductivity varies in different directions and values of thermal conductivity are usually measured relative to the mineral's optical axes (a, b or c) or by the diagonal elements of the thermal conductivity tensor k_{11}, k_{22}, or k_{33} (Clauser and Huenges, 1995). Table 3.2 gives values of thermal conductivity (k) of selected minerals.

Mineral	k_{11} W/m K (30^{0}C)	k W/m K (30^{0}C) a-directional
Diamond	545.3	155.0
Graphite	355	-
Ice	1.9	4.0 (-125^{0}C)
Talc	-	6.1
Magnetite	9.7	5.10
Hematite	14.7	11.28
Sphalerite	26.61*	
Pyrite	37.9	19.21
Pyrrhotite	-	4.6
Galena	-	2.28
Gypsum	2.6	-
Calcite	4.2	3.59
Quartz	6.5	7.69

Table 3.2 Variation of thermal conductivity of minerals with temperature(Clauser and Huenges, 1995) *- direction of measurement not specified

From Table 3.2 above, it can be seen that thermal conductivity varies greatly with different minerals. For example, the thermal conductivity of pyrite is approximately five times that of quartz and nearly ten times that of calcite.

The thermal conductivity of a material is related to its specific heat capacity by thermal diffusivity which is the ratio of thermal conductivity to volumetric heat capacity. This relationship is expressed mathematically by Equation 3.10.

$$\alpha = \frac{k}{\rho c_p} \qquad (3.10)$$

Where α = Thermal diffusivity (m^2/s)

k = Thermal conductivity (W/m K)

ρ = Density (kg/m^3)

c_p = Specific heat capacity (J / Kg K)

Equation 3.10 shows that materials with high thermal conductivity easily transmit heat in comparison to heat storage.

3.4.2.5 Thermal Volumetric Expansion

When a material is heated (or cooled), the energy stored in the intermolecular bonds between atoms changes. This change affects the size of the bonds and as a result, all matter generally expands in response to heating and contracts when cooled. This dimensional change is expressed by the coefficient of thermal expansion and may be linear or volumetric. For bulk solids, the dimensional change is often characterised by the volumetric thermal expansion coefficient (α_v) of the material, given by Equation 3.11 (Clark, 1966).

$$\alpha_v = \frac{\delta V}{V_o(\theta_2 - \theta_1)} \qquad (3.11)$$

Where α_v = Volumetric thermal expansion coefficient (K^{-1})

θ_1 = Initial temperature (K)

θ_2 = Final temperature (K)

V_o = Original volume (m^3)

δV = Change in volume (m^3)

By re-arranging Equation 3.11, an expression (Equation 3.12) for the change in volume that occurs when a material is heated or cooled can be obtained. Equation 3.12 shows that thermal expansion (or contraction) of a material is proportional to the change in temperature.

$$\delta V = \alpha_v V_0(\theta_2 - \theta_1) \quad (3.12)$$

Table 3.3 below gives the volumetric thermal expansion coefficient, α_v (10^{-6} m^3/ K) of some common minerals at different temperatures.

Mineral	373 K	473 K	673 K	873 K	1073 K	1273 K
Calcite	13.1	15.8	20.1	24.0	-	-
Rutile	22.7	24.1	25.4	25.8	26.4	13.1
Sphalerite	19.5	24.4	23.6	24.8	25.5	13.1
Quartz	45.0	43.3	49.7	77.9	56.6	13.1
Feldspar	6.1	8.6	15.3	20.4	24.4	13.1
Fluorspar	58.7	62.2	-	-	-	-
Barytes	54.2	56.8	62.6	-	13.1	-
Corrundum	17.8	19.6	22.5	24.1	24.9	13.1
Hematite	25.2	26.9	30.9	-	-	-
Chalcopyrite	52.5	-	-	-	-	-
Pyrite	27.3	29.3	33.9	-	-	-
Pyrrhotite	66.2	-	-	-	-	-
Magnetite	26.5	28.5	34.9	39.3	41.5	43.4
Galena	61.2	61.0	63.2	66.8	-	-

Table 3.3 The variation of volumetric expansion coefficient with temperature for selected common minerals (Clark, 1966)

It is clear from the above table that the thermal expansiveness of common minerals associated with rocks and ores varies greatly. Although all values are in the same order of magnitude, this variation is still significant considering that the thermal expansion of solids is generally low compared to say fluids. Very small changes in volume can induce a significant imbalance in stress equilibrium as will be discussed later.

3.4.3 Microwave Heating of Minerals

The ability of microwaves to heat a wide range of dielectric materials was discussed in the last chapter. The first attempt to heat minerals using microwaves is reported to have started as early as 1967 (Ford and Pei, 1967). Microwaves were used to heat a number of reagent grade metal oxides and sulphides. Between 10-200 g of a powdered sample was heated by microwaves at 50-200W and 2.45 GHz. It was concluded that dark coloured compounds heated rapidly to temperatures of over 1000^0C and the heating rates of dark coloured compounds were much higher than those of light coloured compounds. Although this work was not very comprehensive, it seems to have triggered an interest in microwave heating of ores and possible applications of microwaves in mineral processing.

Subsequent work on microwave heating of minerals was reported by several authors (Chen et al., 1984, Jacobs, 1982, Wong and Brace, 1979). Jacobs (1982) showed that pyrite could be oxidised to pyrrhotite when subjected to microwave radiation. Chen et al (1984) investigated the heating rate of forty minerals individually using microwave energy. Minerals were heated for between 3-5 minutes using microwave power of between 30-150 W at 2.45 GHz. Due to difficulties in measuring temperature, samples were categorized according to qualitative observations. The first group comprised of minerals where little or no heat was generated and the mineral properties remained essentially unchanged. The second group of minerals generated significant heat but remained thermally stable. The last group comprised of minerals that generated significant heat and decomposed/reacted rapidly into a different product. Table 3.4 summarises the full results obtained from this study.

Very little or no heat generated at all	Heat generated but mineral thermally stable	Readily heated and decomposed
•**Carbonates** Aragonite, calcite, dolomite, siderite •**Slicates** Almandine, allanite, anorthite, gadolinite, muscovite, potassium feldspar, quartz, titanite, zircon •**Sulphates** Barite, gypsum •**Oxides** Fergusonite , allanite, columbite, monazite •**Others** Sphalerite (low-Fe), stibnite, tennantite, jarosites	•**Metal oxides** Cassiterite, hematite, magnetite, nickeline/cobaltite •**Uranium Metals** Pitchblende	•**Metal Sulphides** Arsenopyrite, chalcopyrite, galena, pyrite, pyrrhotite, tetrahedrite, bornite covellite*

Table 3.4 Microwave heating of selected minerals according to observations made by Chen et al (1984) *- difficult to heat but sulphur fumes emitted

It was observed that most silicates, carbonates and sulphates which are common gangue minerals in most ores are not readily heated by microwaves. However, the metal semi-conductors such as metal sulphides and oxides were easily heated by microwave energy.

The major test work that followed from above was conducted by the US Bureau of Mines and is reported by (Walkiewicz et al., 1991, Walkiewicz et al., 1988). In this work, a more detailed and qualitative study of microwave heating characteristics of a number of minerals and reagent grade inorganic compounds was carried out. All heating tests were conducted on same mass

of powdered sample of 25 g using a 1 kW power generator at a frequency of 2.45 GHz. The maximum temperature attained was measured accurately using a thermocouple. The test results obtained were similar to those obtained by Chen et al (1984) but this work provided temperatures which were attained after heating. Highest temperatures of over 1000^0C were obtained with carbon and most of the compounds that heated readily as shown in Table 3.4 after just a few seconds to microwave exposure. None of the minerals described as "bad heaters" in Table 3.4 recorded a temperature of above 80^0C after the same duration of heating. This study also revealed rapid heating of ore minerals within a non-heating matrix which generated thermal stresses of sufficient magnitude to create cracks along mineral boundaries. The studies concluded that some indication had been given to potential application of microwave energy in metallic ore processing. Other similar work and results were reported by McGill (1988).

Microwave heating of minerals may be predicted from its dielectric properties. Currently, there are devices designed to measure the dielectric properties of solids and fluids at different frequencies and temperatures with relative ease. It is therefore possible to predict how the heating rate of minerals changes with frequency and temperature. Cumbane (2003) investigated the variation of dielectric properties of five powdered sulphide minerals with frequency and temperature using the cavity perturbation technique. The samples were examined at frequencies of 625 MHz, 1410 MHz and 2210 MHz over a temperature range of 0-650^0C. The dielectric properties of galena (PbS) and sphalerite (ZnS) exhibited little variation with temperature, whilst pyrite (FeS), chalcocite (Cu_2S) and chalcopyrite ($CuFeS_2$) showed significant variation with temperature. These findings were consistent with observations

made by previous work involving the direct heating of minerals which showed that pyrite and chalcopyrite reacted easily to form other products while galena and sphalerite remained thermally stable (see Table 3.4).

3.4.4 Microwave Selective Heating of Ores

Ores essentially consist of discrete multi mineral grains, cementitious materials and voids containing air or fluids usually water. Each of these components typically has different thermal, dielectric and mechanical properties. During microwave heating, energy is absorbed volumetrically and microwaves directly heat each constituent phase of a material individually. Microwave heating is therefore largely independent of surface temperature and thermal diffusivity of the material and because of differences in dielectric properties; it is possible to have different phases in the ore with a very high temperature gradient which is not possible with conventional heating techniques which rely on transfer of heat across a temperature gradient to heat the bulk of the material.

Due to abundance of oxygen and silicon in the earth's crust, most minerals are found associated with compounds of silicon and oxygen (silicates) which do not absorb microwave energy. The valuable minerals usually occur as small grains with different sizes and distribution pattern. Most valuable minerals such as chalcopyrite, pyrite, galena, hematite, magnetite etc are easily heated by microwaves (see Table 3.3). Microwaves are therefore capable of heating the mineral grains to very high temperature without heating the gangue material and with overall low bulk temperature. Inevitably, there will be some conduction between the phases but because microwave heating takes place rapidly, this effect may be minimized.

3.5 Microwave Assisted Comminution of Base Metal Ores

3.5.1 Introduction

Microwave selective heating of ores has been investigated for potential application in thermally assisted liberation. The major economic incentive for microwave selective heating is that energy is not wasted in heating the bulk of the ore and thermal conversion efficiency is very high. Microwave heating is also very rapid and this may lead to very sharp differences in temperature gradient and subsequently differential expansion of the constituent phases. The resultant thermal stresses may be exploited in mineral processing. The next sections of this chapter present a review of recent scientific and engineering research work on microwave assisted comminution.

3.5.2 Initial Investigations into Microwave Assisted Comminution

Early test work regarding the potential for microwave assisted comminution was reported by (Walkiewicz et al., 1991, McGill, 1988, Walkiewicz et al., 1988, Veasey and Fitzgibbon, 1990). All these authors stressed that microwave heating could have future potential applications in mineral processing. For example, it was demonstrated that microwave heating produced thermal stresses of sufficient magnitude to cause both transgranular and intergranular fracturing in some ores with the degree of fracturing increasing as the power density increased. However, it was concluded that the high energy input makes microwave pre-treatment of ores commercially unattractive. All these studies were conducted in kitchen microwave-like equipment with reported powers of between 300 W and 3 kW and heating exposures of between a few seconds to a couple of minutes. It also seems that these initial investigations were mainly based on previous observations by

microwave heating of minerals and lacked a comprehensive understanding of the theoretical and scientific aspects of microwave interactions with materials.

3.5.3 Effect of Microwave Heating on Point Load Index

It was stated in Section 3.2.3 that the point load test provides an effective method of predicting the amenability of ores to comminution. Kingman et al (2004) carried out point load tests on a lead-zinc ore before and after microwave treatment in both single mode and multimode cavities. Unlike previous studies which were carried out using "kitchen- like" microwaves, this study used a specially designed heating system incorporating an E-H plane automatic tuner to match the impedance of the generator and waveguide to that of the applicator and its load, thus ensuring maximum absorbance of microwave energy by the load. Microwaves were generated using a 3-15 kW variable power generator operating at 2.45 GHz and treatments were carried out at 5, 10 and 15 kW for 1, 5 and 10 s. The results showed that significant reductions in strength of up to 55% of original were possible after only 1 s of heating when using a power level of 15 kW. For lower power levels, similar reductions were achievable only after prolonged heating of up to 10 s (See Figure 3.5). There was also evidence that it is possible to induce only a certain amount of thermal damage for a certain applied power level. Samples treated at 15 kW exhibited significant reductions in strength after only 1 s of treatment but showed little further decrease in strength with an increase in exposure time.

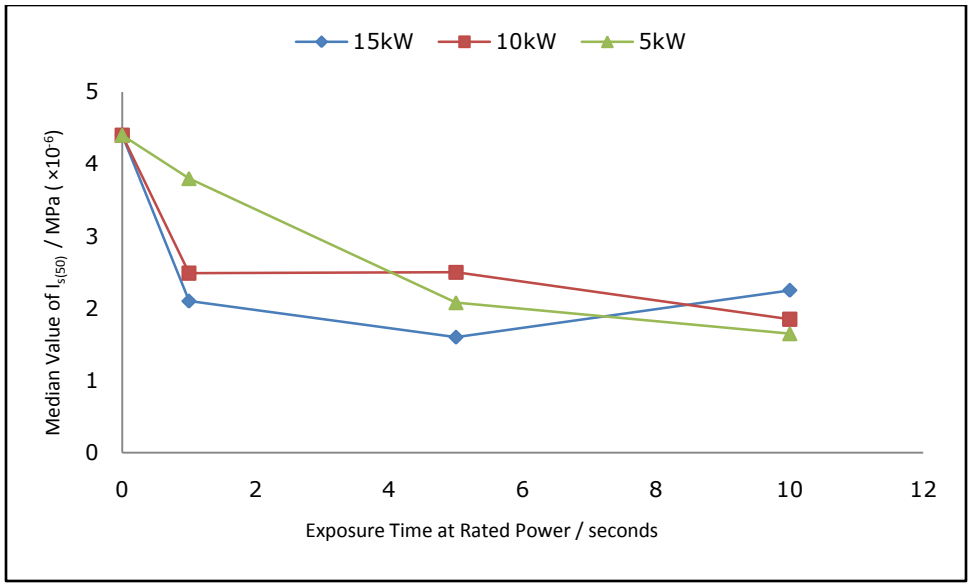

Figure 3.5 Variation of Point Load Index with microwave power and exposure time in multimode cavity (Kingman et al., 2004)

Similar work was carried out on a South African copper carbonatite ore consisting of mainly calcite and dolomite as microwave transparent phases and magnetite as the major microwave absorbing phase but also copper bearing sulphide minerals mainly cubanite, chalcopyrite, bornite and chalcocite. The same microwave system described earlier was used but heating was carried out in a TE_{10n} single mode cavity with reduced exposure times of 0.1, 0.5 and 1 s. Point load test results showed that significant reductions in strength are possible with exposure times as short as 0.1 s (See Figure 3.6). This underlined the importance of the electric field strength and further demonstrated that microwave pre-treatment of ores is effective at much lower energy inputs than previously thought.

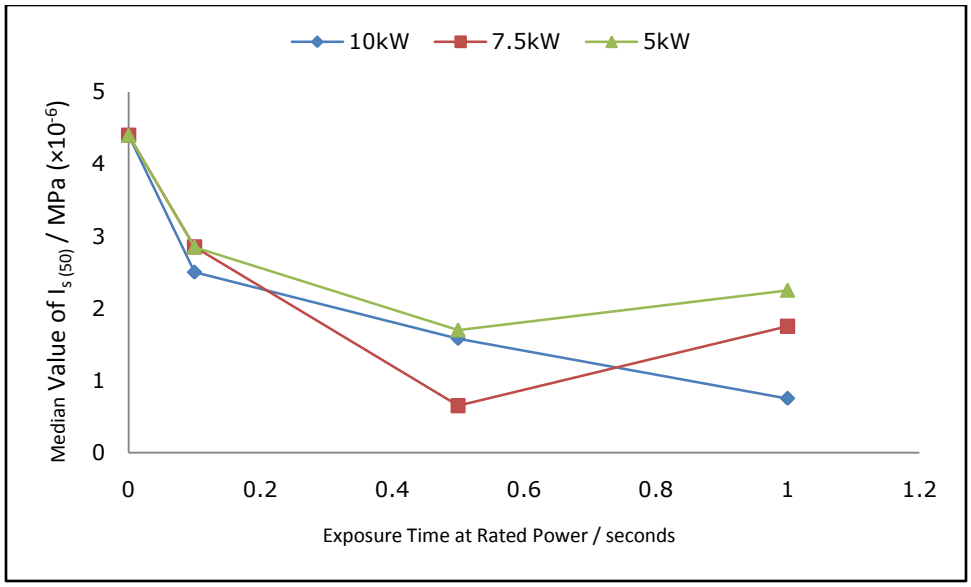

Figure 3.6 Variation of Point load Index with microwave power and exposure time in single cavity (Kingman et al, 2004)

Reports of ore weakening after microwave treatment were also reported by (Olubambi et al., 2007, Scott et al., 2008) although these studies were based on energy inputs that do not make the process cost effective.

3.5.4 Effect of Microwave Heating on Comminution Energy Requirement

From the discussions of the previous section, there is a general consensus amongst different authors that microwave pre-treatment lowers the ore mechanical strength. What is debatable is the effect this has on downstream processing and whether the benefits of microwave treatment can justify the capital and operating costs associated with inclusion of a microwave pre-treatment stage in the process flow sheet. This uncertainty may be partly answered by analysing the effect of microwave pre-treatment on required comminution energy. As was discussed earlier in this chapter, comminution

processes are complex and there is no established technique that can accurately predict comminution energy requirements from laboratory testing.

Kingman et al (1999) investigated the influence of mineralogy on microwave assisted grinding. A massive Norwegian ilmenite ore, a massive sulphide ore from Portugal, a highly refractory gold ore from Papua New Guinea and an open pit carbonatite ore from South Africa described in Section 3.5.3 were irradiated with microwaves for varying time periods at a power level of 2.6 kW and a frequency of 2.45 GHz in a multimode oven. For each ore, the change in Bond Work Index with exposure time was determined using Equations 3.13 and 3.14. The Bond Work Index is defined as the energy input required to reduce the size of feed material from infinite size to d_{80}=100 μm.

$$Wi = \frac{10}{\sqrt{P}} - \frac{10}{\sqrt{F}} \tag{3.13}$$

$$Wi_t = Wi_r \times \frac{\left[\frac{10}{\sqrt{P_r}} - \frac{10}{\sqrt{F_r}}\right]}{\left[\frac{10}{\sqrt{P_t}} - \frac{10}{\sqrt{F_t}}\right]} \tag{3.14}$$

Where Wi = Bond Work Index (kWh/t)

P = d_{80} of product (μm)

F = d_{80} of feed (μm)

Wi_t = Bond Work Index of test material (kWh/t)

Wi_r = Bond Work Index of reference material (kWh/t)

P_r = d_{80} of product of reference material (μm)

F_r = d_{80} of feed of reference material (μm)

P_t = d_{80} of product of test material (μm)

F_t = d_{80} of feed of test material (μm)

The results showed that microwave treatment had a significant effect upon ilmenite and carbonatite ores which contained several good absorbers of microwave energy in a matrix of poor absorbing material. A mineralogical investigation of the ilmenite ores which showed the highest reduction in Bond Work Index revealed that the ore contained coarse grains of magnetite (excellent heater) and ilmenite (good heater) in a plagioclase (poor heater) matrix. Other downstream process benefits like increased magnetic separation and recovery were also reported. The refractory gold ore which did not show significant changes in the Bond Work Index contained finely disseminated pyrite grains in K-feldspar and quartz gangue. It was suggested that for effective microwave treatment, ores should have a consistent mineralogy and a good absorber of microwave radiation in a transparent gangue matrix. The study also concluded that small particles that are finely disseminated in discrete elements respond poorly to microwave treatment in terms of reductions in required grinding energy. It was also stated that use of purpose built and more efficient microwave heaters was required in order to make microwave treatment of ores economically attractive. Similar studies were conducted by Vorster et al (2001) who investigated the effect of microwave treatment on a Neves Corvo copper ore. Samples of the ore weighing approximately 0.5 kg were treated with microwave energy at 2.6 kW and 2.45 GHz for different durations. The samples were then ground to approximately 80% passing the 53 μm sieve. The results showed up to 70% reduction in the Bond Work Index for samples treated for 90 seconds (Vorster et al., 2001).

The pendulum and drop weight tests have been successfully used to predict comminution behaviour of single particles (Groves, 2007). The twin pendulum test relies on the particle being broken between an input pendulum released

from a known height and a rebound pendulum. The drop weight test differs from the pendulum test in that the particles are placed on a hard surface and struck by a falling weight. Both methods are based on energy models (energy input versus product size) but are limited in scope when considering the actual process in comminution machines. This is mainly because of the dynamic nature of interaction of particles during comminution. The methods are however very useful in comparing how different rocks are likely to behave or investigate the influence of microwave pre-treatment on strength.

In the drop weight test, samples of material are crushed as individual particles at a combination of energy inputs and size fractions using a drop weight test apparatus. After each test has been completed, the resulting fragments from each individual drop are collected and sieved to give the complete cumulative product size distribution. The size distributions are then used to determine breakage functions for the material from which the required comminution energy to induce a certain degree of breakage can be calculated using Equation 3.15.

$$t_{10} = A\left[1 - e^{-b.ECS}\right] \qquad (3.15)$$

Where ECS = Specific Comminution Energy Input (kWh/t)

t_{10} = Amount passing 10% the original mean size

A = Breakage parameter (essentially the theoretical maximum value of t_{10})

b = Breakage parameter indicating softness of the material

According to Bearman et al (1997), the parameters **A** and **b** be can be estimated from Equations 3.16 and 3.17 below.

$$b = 2.2465 \times K_{IC}^{-1.6986} \quad (3.16)$$

$$A.b = 126.96 \times K_{IC}^{-1.8463} \quad (3.17)$$

Where K_{IC} = Mode I fracture toughness index that is estimated using Equations 3.4 and 3.5

Kingman et al (2004) conducted drop weight test studies on the South African carbonatite ore which was described in Section 3.5.3 to compare the required breakage energy of microwave treated and untreated samples. A 3-15 kW variable microwave power generator operating at 2.45 GHz was used. For each drop weight test, fifteen samples were tested in five size fractions at three levels of energy input. The results showed an increase in the impact breakage parameter (b-values) for treated material. For example, particles treated at 15 kW for 0.2 s had a *b-value* of 2.35 compared to a value of 1.61 for the untreated material. This indicated an increase in softness of the treated ore samples, which in turn suggests improved grindability after microwave treatment. There was no apparent reduction in *ECS* for the larger size fractions (average size of 41.08 and 57.78 mm) but smaller values of *ECS* were observed for the treated material in the smaller factions. For example, to produce a t_{10} of 10% from particles with an average feed size of 14.53 mm would require a comminution energy input of 0.1 kW h/t for the untreated and 0.06 kW h/t for the treated material indicating a 60% reduction in required breakage energy. As stated earlier, the breakage pattern in drop weight testing is significantly different from that in comminution machines and the

ECS values reported may differ from comminution energy in commercial plants. However, this study demonstrated that there is potential for microwave pre-treatment to reduce comminution energy requirement.

3.5.5 Effect of Microwave Heating on Mineral Separation and Recovery Processes

The efficiency of mineral recovery processes is highly dependent on the efficiency of the separation process. Different techniques are utilized to separate the targeted valuable minerals from each other or from the unwanted gangue material. The choice of the separation process involves both economical and technical considerations. The major technical consideration is the mineralogy of the ore and the physical and chemical properties of the constituent minerals and gangue. For example magnetic separation methods could be used to separate paramagnetics such as ilmenite ($FeTiO_3$) or hematite (Fe_2O_3) from non-magnetic gangue such as quartz. Dense Medium Separation (DMS) techniques are used to separate materials by utilizing the difference in specific gravity of different minerals in response to gravity. Froth flotation is a physico-chemical separation process that utilizes the differences in surface properties of valuable minerals and unwanted gangue material in a three phase agitated mix (Wills, 2006). Other separation processes include leaching (differences in solubility in a solvent) and electrical separation techniques.

Scott et al (2008) conducted studies on the effect on microwave treatment on the liberation spectrum of a rod milled, low grade copper carbonatite ore based on quantitative mineralogical analysis. The ore consisted of approximately 50% microwave absorbing material occurring predominantly as

magnetite with small amount of copper sulphides (less than 0.5%). The non absorbing gangue material consisted mainly of calcite and dolomite. The microwave system used for treatment was similar to that used by Kingman et al (2004) described earlier but treatments were carried out at a power level of 10.5 kW for 0.5 s. Grinding was conducted in a laboratory scale rod mill to produce a product with a d_{80} of 800 μm for both treated and untreated material. Liberation analysis was carried out using a QEMSCAN over particle size ranges from 850 μm to 25 μm. Over the whole rod mill product (i.e. -850+25 μm), the results did not show any significant changes in magnetite or copper mineral liberation for the microwave treated and untreated ores. However, the liberation of all mineral grains at each size class showed that there is a general trend with a displacement of more liberated minerals to the higher size classes. The results suggested a change in the fracture pattern after microwave treatment where the mineral grains have most likely been shielded from fracture by the cracking induced around the microwave susceptible mineral phases (Scott et al., 2008). The implication of these findings in mineral processing was that microwave pre-treatment has potential for increased liberation at coarser sizes hence saving on both time and energy required for finer grinding.

Kingman et al (2004) carried out liberation tests on treated (15 kW, 2.45 GHz, 0.2 s) and untreated samples of the carbonatite ore produced after the drop weight test described in the last section. Tests were conducted on four different size classes viz +500, -500+150, -150+38 and -38 μm. The results showed a significant increase from 31.8% to 69.2% for copper sulphide liberation in the coarser size fraction (+500 μm). No significant changes were observed for the other size fractions. Kingman et al (1999) and Amankwah et

al (2005) also reported an increase in gold recovery of up to 98% and 20% in refractory gold ores from the Lihir gold mine in Papua New Guinea and Ghana, respectively, after treatment with microwave energy. Another claim of increased liberation after microwave treatment was reported by (Wang et al., 2000) who conducted studies on a low grade copper ore.

Kingman et al (1998 and 1999) also investigated the effect of microwave radiation upon the mineralogy and magnetic processing of several minerals. Treatments were carried out for 5 minutes using a 650 W kitchen type microwave. A magnetometer was used to determine the magnetic susceptibility of the minerals before and after microwave treatment. Significant increases in magnetic susceptibility were recorded for chalcopyrite, ilmenite, hematite and wulframite. A reduction in magnetic susceptibility was recorded in bornite, pyrrhotite and magnetite. This reduction was attributed to possible changes within the iron structure after microwave treatment although this claim was not substantiated. The result however highlighted the potential for enhancing magnetic separation processes of certain ore types.

Groves (2007) investigated the magnetic separation enhancement and liberation of a sulphide contaminated ore and a low grade copper ore respectively. The study investigated the opportunities for magnetic separation of iron sulphide impurities from the talc ore by utilizing microwave energy to enhance the magnetic susceptibility of the sulphide phases. A microwave power of 3 kW at 2.45 GHz was used to treat approximately 1 kg batch samples for duration of 120 s. The design of the microwave cavity used for treating the samples allowed for an even electric field whilst the base was fluidized for oxygen or nitrogen during oxidation and desulphurisation

processes respectively. Each sample of treated and untreated material was then screened into different size fractions which were then passed through a magnetic separator. However, the results obtained did not suggest the potential for enhanced magnetic separation. There was a reduction in the content of magnetic sulphides after microwave treatment. The reduction was more significant in the coarser size fractions (>2 mm) and less significant in size fractions less than 1 mm. After further investigations, it was noted that the pyrite impurities in the talc ore may have been, in fact pyrrhotite, in which case exposing the latter to microwave energy may have altered some of its properties and rendered it non-magnetic. Tests conducted on the low grade copper ore after microwave treatment showed a shift from transgranular fracture to predominantly intergranular fracture and also showed an increase in degree of liberation of chalcopyrite.

The literature on effects of microwave heating of ores discussed in this section has demonstrated the potential for microwave heating to enhance comminution and improve mineral liberation. It is noted that most of this work was carried out using high energy inputs which on the face of it do not favour the overall process economics. However, it was also pointed out that significant benefits may be realised using much lower energy inputs than those reported in these studies if further research and development work is carried out. It was stressed that purpose built microwave treatment systems be developed and further research into finding ways of enhancing microwave induced fracture be carried out. It is important to have an in-depth understanding of the scientific and engineering aspects of microwave heating of ores in order to deduce how microwave induced fracture can be enhanced using modest energy inputs. The next section will focus on investigations that

have been carried out in order to understand microwave induced fracture and how it can be enhanced. The engineering aspects of microwave heating are discussed later.

3.6 Understanding Thermal Stresses due to Microwave Selective Heating

Analysis of thermal stresses due to microwave heating is necessary in order to understand how microwave induced fracture occurs in ores and how this can be maximized to benefit downstream processing. Salsman et al (1996) investigated the thermal-mechanical response of a typical ore subjected to microwave heating. This study illustrated the relationship between microwave power density, temperature gradient and induced thermal stresses. The simulation was geometrically simplified by considering only a single spherical pyrite mineral particle surrounded by a larger spherical calcite rock. The temperature and stress profile at power densities of 10^{10}, 10^{12} and 10^{14} Wm^{-3} after heating for 1 s, 40 milliseconds and 40 micro seconds was modelled. The results from the model showed that the temperature gradient between the two phases increases with increase in power density. At a power density of 10^{10} W/m^3 and heating period of 1 s, there was virtually no difference in temperature between the two phases. At a power density of the order of 10^{12} Wm^{-3}, the average temperature in the pyrite phase after 40 milliseconds was about 1000 K while that in the calcite phase gradually dropped to about 750 K over a radial distance of 150 μm. At 10^{14} W/m^3 with an exposure period of 40 μs, the temperature gradient was in excess of 1200 K. These results clearly illustrated that the temperature gradient is increased with an increase in power density. Although the author did not construct a model for same power

density but different heating periods, these results also seem to suggest that the temperature gradient is increased with decrease in heating period, most likely as a result of a reduction in thermal diffusion between the pyrite and calcite phases.

The maximum principal stress profile was computed from the temperature profile by using Hooke's law for thermo-elasticity given by Equation 3.18.

$$\varepsilon_{rr} = \frac{1}{E}[\sigma_{rr} - \nu(\sigma_{\theta\theta} + \sigma_{zz})] + \alpha T \qquad (3.18)$$

Where ε_{rr} = Strain component (m)

σ_{ij} = Stress components (N/m^2)

E = Young's modulus

ν = Poisson's ratio

α = Thermal expansion coefficient

T = Temperature (K)

As the energy deposition rate increased, the compressive stress in the pyrite increased substantially. The stress gradient increased likewise as the stress changed from compressive to tensile across the mineral interface. For the two lower power densities, the peak tensile stresses in the calcite near the material interface were only of the order of 20 to 30 MPa, but at the higher power density of 10^{14} W/m^3, the peak stress was significantly higher at about 360 MPa. It is worthy to note that the tensile stress of most rocks is much less than this and is reported to be in the range of 3 to 10 MPa (Vutukuri et al.,

1974). Thus the thermal stresses obtained from this model would most certainly result into ore fracture.

Further work investigating the effect of microwave power and corresponding induced thermal stresses was reported by Jones (2005) and Whittles et al (2003). The results from these studies agree with those obtained by Salsman et al (1996). It was shown that the theoretical strength of samples treated at a power density of 1×10^{11} W/m^3 reduced from 125 to 60 MPa in 0.05 s (Whittles et al., 2003). The work by Jones et al (2005) showed the gradual development of fractures as a pyrite-calcite sample is heated. The model used a 500 μm circular microwave absorbent heated phase contained within a 2 mm microwave-transparent circular matrix. The model applied a power density of 1 x 10^{11} W/m^3 and using a thermal step of 1 μs, the development of fractures as the composite particle was heated from 1 μs up to 1ms was investigated. Figure 3.7 shows the key stages of fractural development as the particle is heated. The yellow colours correspond to tensile fractures, deep red colours depict shear fractures, and the purple colour corresponds to regions where the material had previously been at yield but receded due to stress redistribution. No fractures were seen to develop before 10 μs (top centre). After 250 μs, tensile plasticity was observed at the edges (top right). Shear plasticity around mineral grain occurred after 300 μs (bottom left). Radial shear cracks developed after 600 μs (bottom centre) and both shear and tensile cracks around the grain boundary developed after about 1 ms (bottom right)

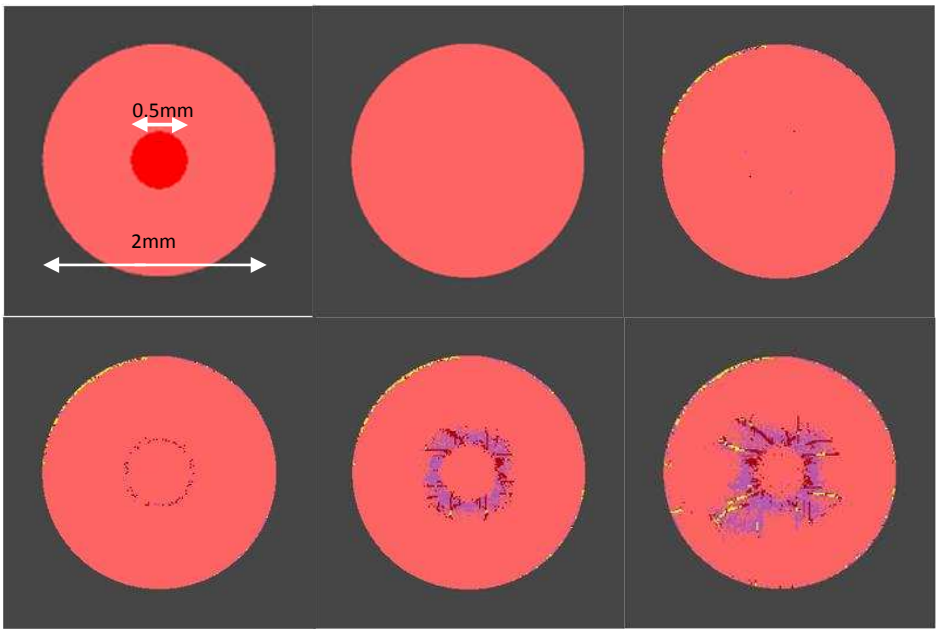

Figure 3.7 Model of development of fractures in a pyrite–calcite composite subjected to microwave heating (Jones et al, 2005)

These results showed that fractures originate at the grain boundary between heated and transparent phases, which once again illustrated the potential for increased liberation in addition to particle weakening. It is also clear from above that there is a specific microwave exposure time which results into "optimal" microwave induced inter-granular fracture and that there may be a power density above which no further reduction in strength is possible.

The effect of mineral grain size on the magnitude of stress (and subsequent fracture) was examined by modeling ten different grain particle diameters of between 50 to 500 μm, which is the typical size range of mineral grains in ores. The results showed that there was a general increase in peak temperature with grain size. For example, for a 50 μm particle and a microwave power density of 10^{11} W/m^3 for 0.01 s, the peak particle temperature was only about 33^0C whilst for a 500 μm particle under the same exposure time and power density, the peak particle temperature was 278^0C.

Therefore, as the size of the heated mineral grain increases, less energy is required to sufficiently raise the temperature such that thermal stresses of a sufficient magnitude to damage the rock are generated. Greater reductions in strength were also observed, for a given total energy input, if the exposure time was decreased. Based on this model, it was suggested that for major breakages leading to economical microwave comminution, power densities of between 1×10^{10} and 1×10^{12} W/m^3 with exposure times of between 0.2 and 0.002 s should be applied.

3.7 Pulse Microwaves or Continuous Microwaves?

The significance of microwave power level on induced fracture has been explained in the previous sections. The results from the work by Kingman et al (2004) showed that the reduction in mechanical strength (reduction in Point Load Index) is higher when the power level is increased. This work was conducted at power levels in the region of 5-15 kW with typical heating times in the range of 1-5 s. Simulations conducted by Salsman et al (1996) and others demonstrated that the magnitude of fracture in metal base ores is increased when the power density is increased and the microwave exposure time is kept to a minimum. The heating times used in the simulation were in the region of 40 μs to 1 s. Simulations conducted by Jones et al (2005) using a power density of 1×10^{11} W/m^3 which was of the same order of magnitude to that used by Salsman et al (1996) demonstrated that significant fracture develops after about one millisecond. These findings suggest that a microwave system operating at high power levels (required to induce a power density of at least 1×10^{11} W/m^3 in the heated phases of the ore) over a very short

period in the order of a thousandth of a second gives the best results, not only in terms of increased fracture, but also the economics of the process.

The above requirement suggests that pulse microwaves are more suited for treatment of base metal ores compared to continuous waves. Pulse microwave systems generate very high power for short periods of time. For example, a power level of 1 MW for 0.001 s is equal to a power output of just 1kWh. Jones et al (2007) simulated the variation of unconfined compressive strength (UCS) of a composite pyrite-calcite matrix, at different values of power density, induced by continuous microwaves and pulse microwaves. Unlike in previous studies that utilized a single microwave absorbing particle surrounded by a microwave transparent phase, the model in this study comprised of several pyrite particles randomly disseminated in a calcite matrix. This study therefore represented ore texture more accurately than previous studies. The mechanical behaviour of the mineral phases in the ore was simulated using two constitutive models which related the stress conditions within the mineral phases to the associated strains. The results obtained are shown in Figures 3.8 and 3.9.

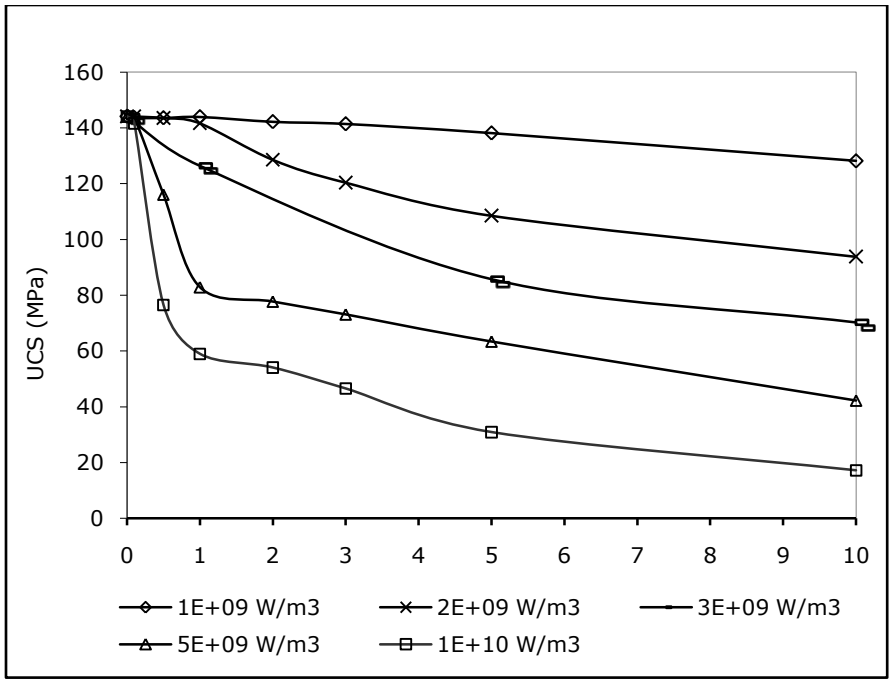

Figure 3.8 Variation of UCS with power density- Continuous microwave applicator (Jones et al., 2007)

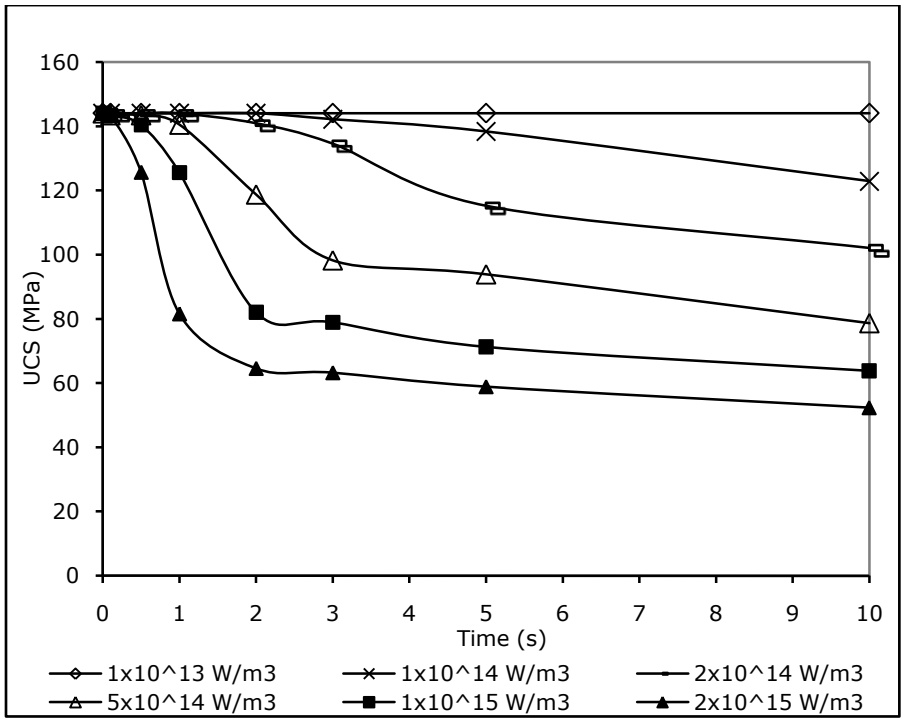

Figure 3.9 Variation of UCS with power density- Pulsed microwave applicator (Jones et al, 2007)

As in previous work which was discussed earlier, higher reductions in UCS were achieved at higher power density. Higher reduction rates were observed generally for heating periods less than 1s. As the exposure time was increased beyond 3-5 s, no further significant strength reductions were achieved. The reduction in strength also diminished as the power density was increased beyond certain values. For example, there was a much greater reduction in strength between 1×10^9 and 1×10^{10} W/m^3 than there was between 1×10^{12} and 1×10^{15} W/m^3 despite the latter being an increase of three orders of magnitude compared to just one in the former. This study recommended that future microwave assisted comminution equipment should be capable of generating power densities of between 1×10^{10} W/m^3 and 1×10^{12} W/m^3 with exposure times of between 0.2 and 0.002 s. Pulse microwave systems are more suited to operate at such conditions.

3.8 Microwave Assisted Leaching of Minerals

Hydrometallurgical metal extraction is highly attractive due to its potential for economic and environmental benefits (Han, 1996). Smelting is highly energy intensive and harmful to the environment due to emission of green house gases, mainly SO_2. Conversely, leaching has potential for low grade ore processing, low temperature processing and low process costs (Al-Harahsheh and Kingman, 2004). Studies on leaching of sulphide minerals have been conducted using different solvents such as ferric sulphate and ferric chloride to dissolve targeted minerals (Young et al., 2008). Although most of these studies showed promising potential for high metal recovery, economic and environmental benefits, they faced a similar problem of extremely slow process kinetics. Other problems reported for individual case studies included

fouling, corrosion and contamination. These problems were compounded by conflicting reports on the process mechanism. Some researchers claimed that diffusion of solvent ions is the rate limiting step (Dutrizac, 1978, Dutrizac et al., 1969) while others suggested that surface chemical reaction (Hirato et al., 1987) or electron transfer (Parker et al., 1981) determine the reaction kinetics. In all studies conducted, however, the leaching kinetics were found to be highly dependent on temperature.

The potential applications of microwaves in leaching of minerals have been reported by several authors. Kruesi and Frahm (1982) carried out several experiments to recover copper from its sulphide and oxide ores. The ores were ground and blended with different solvents before being irradiated with microwaves at 600 W, 2.45 GHz for varying times. The mixtures were then leached in brine solution, attaining between 86-91% copper recoveries (Kruesi and Frahm, 1982). Walkiewicz et al (1988) reported "non-thermal effects" of microwave leaching of a chalcopyrite ore. Two identical ore mixtures were blended with ferric chloride hexahydrate ($FeCl_3.6H_2O$). One was heated by microwaves to 224^0C in 10 minutes and the other in a muffle furnace to 255^0C. The microwave heated mixture gave a higher copper recovery of 30% compared to 22% for the muffle furnace heated mixture. Other early work that investigated microwave heating on leaching was conducted by (Antonucci and Correa, 1995, Worner, 1990). All these studies reported a positive effect on recovery but did not investigate the process kinetics or economic feasibility.

Harrison (1997) investigated the kinetics of treated (2.6 kW, 2.45 GHz) and untreated bornite, chalcocite, chalcopyrite and pyrite leached in a solution of

cupric chloride. The dissolved amount increased with increasing exposure to microwave energy and this was attributed to surface oxidation enhancement by heating. Faster leaching rates were also achieved as the heating time was increased from 10 s to 30 s although the difference was not very significant (Harrison, 1997). Kingman (1998) observed much faster initial reaction rates for a chalcopyrite concentrate leached in a solution of 0.25 M $Fe_2(SO_4)_3$ and 1 M H_2SO_4 after microwave treatment at 2.6 kW, 2.45 GHz. The observed phenomenon was attributed to oxidation of chalcopyrite to bornite which is more amenable to microwave leaching.

3.9 Conclusions

This chapter has provided a review of the state-of-the art of comminution in ore processing. It was stated that the cost of energy in mineral processing represents a significant proportion of the overall cost of production, the most energy intensive stage in comminution being grinding. The current conventional grinding machines such as ball mills and SAG mills, which are almost exclusively used for grinding, were found to be highly energy inefficient and yet they provide arguably the only practical method for fine (below 300 μm) size reduction. It was stated that liberation is key to good ore processing and that the degree of liberation is enhanced by inter-granular fracture. However, current comminution machines have no mechanisms that take advantage of natural weakness in ores to control fracture and to ensure that energy is not wasted in over grinding. The major opportunities for improving comminution were emphasised as follows:

- Developing comminution schemes that take advantage of natural weakness in rock

- Developing new ways to deliver impact energy to ores
- Developing technology to improve grinding
- Developing accurate models of fracture which can be used to predict the behaviour of ores during comminution
- Optimizing comminution circuits to eliminate over grinding

Recent research developments aimed at addressing the above issues were discussed. For example, the integration of High Pressure Grinding Rolls in the traditional process flow sheet was found to offer some benefits such as increases in liberation, reduction in untreatable fines, reduction in grinding energy and increase in grade and recovery but it was observed that all these have only led to modest overall process benefits.

Thermal pre-treatment of ores is another area which has been explored for potential process benefits in ore processing. It was observed that thermal pre-treatment of rocks induces differential expansion which causes ore weakening and also enhances intergranular fracture with potential process benefits of comminution energy savings and increased mineral liberation. The major problem with thermal pre-treatment was found to be the additional energy cost required. Some authors claimed that more energy was actually required to pre-treat the ores compared to the anticipated savings. Most studies in the 80s and early 90s concluded that thermal pre-treatment of ores could only become feasible if a "cheap" energy source was found.

Comprehensive studies involving microwave assisted comminution commenced in the mid nineties. It was observed that the ability of microwaves to selectively heat a multi-mineral ore could be exploited to

provide an economic method of pre-treating ores since energy is not wasted in heating the bulk of the ore and thermal conversion efficiency is very high. Early work showed that a potential for microwave heating to enhance comminution exists. It was shown that significant reductions in strength of up to 55% were possible after only 1 s of heating when using a power level of 15 kW. Significant reductions of up to 70% of Work Bond Index and increases in liberation were also reported. However, it was noted that some of this work was carried out using energy inputs still considered high to favour the overall process economics. Some of the work reported was, however, carried out using kitchen type microwaves or power levels not considered economical. Numerical and computer simulations showed that significant benefits could still be achieved using modest energy inputs only if the right ores are selected for pre-treatment using well developed microwave heating systems. These studies illustrated the relationship between microwave power density, temperature gradient and induced thermal stresses. It was shown that microwave induced fracture is maximized if the temperature gradient between microwave heating and microwave transparent mineral phases is increased and that the temperature gradient increases with an increase in power density within the microwave absorbing mineral phases. These findings illustrated the importance of the electric field intensity and also the importance of ore mineralogy and texture. It was suggested that for effective microwave treatment, ores should have a consistent mineralogy and a good absorber of microwave radiation in a transparent gangue matrix. It was also shown that as the size of a heated mineral grain increases, less energy is required to sufficiently raise the temperature such that thermal stresses of a sufficient magnitude to damage the rock are generated. Greater reductions in strength were also observed, for a given total energy input, if the exposure time is

decreased. It was concluded that for major breakages leading to economical microwave comminution, power densities of between 1×10^{10} and 1×10^{12} W/m^3 with exposure times of between 0.2 and 0.002 s should be applied.

Despite all the above developments, it was observed that there still exists a gap in some of the scientific and engineering aspects needed to drive this technology to industrial scale level. For example very little information was available in the literature that relates to the influence of hydrated minerals on microwave induced fracture and yet water significantly affects material dielectric properties. Also the microwave heating systems that were used were not capable of generating the required power density within the ores. All treatments were also carried out in batch single mode cavities and any realistic industrial microwave treatment system would necessitate development of a continuous treatment system.

CHAPTER FOUR

4 MICROWAVE INDUCED FRACTURE IN HYDRATED MINERALS

4.1 Introduction

The potential benefits of microwave heating in mineral processing were discussed in the last chapter. It was stated that selective heating of ores induces fracture due to differences in thermal behaviour between heated and non heated mineral phases. The induced fracture may render the ore more susceptible to grinding, thereby saving on the required grinding energy. Other process benefits such as increased liberation at coarser grind sizes were also suggested, implying that even less grinding may be required by pre-treated ores to achieve same degree of liberation when using conventional comminution techniques.

Ore mineralogy has been shown to significantly influence the magnitude of fracture induced. Minerals such as quartz were shown to be transparent to microwaves while others such as magnetite heat rapidly. Kingman et al (1999) put forward a theory suggesting that significant fracture occurs only in ores with "a consistent mineralogy and a good absorber of microwave radiation in a transparent gangue matrix and that ores that contain small particles that are finely disseminated in discrete elements respond poorly to microwave treatment in terms of reductions in required grinding energy." The context of "good absorbers" in this study referred to the known good heaters

of microwave energy such as metal oxides and sulphides, but in reality includes all semi conducting mineral phases

Moisture content has a considerable effect on the dielectric properties of materials, particularly for low-loss materials (Metaxas and Meredith, 1983). This is because water has a relatively high value of dielectric constant and loss factor of 77 and 13 respectively at 2.45 GHz and can therefore be classed as an excellent absorber of microwave energy. Studies conducted on coal showed that expansion of moisture within a coal matrix has the potential to cause cracks or breakage when microwave energy is applied (Lester and Kingman, 2004). These developments were seen to provide potential for increased coal grindability after microwave pre-treatment and further work using more efficient microwave delivery means was proposed (Lester et al., 2005). In relation to these findings, it is thought that water yielding species within a given mineral may influence the microwave absorbing properties of the mineral. From the viewpoint of microwave assisted comminution and liberation, it is useful to know which types of "hydrated minerals" heat and yield water on processing with microwave irradiation. A hydrated mineral in this context refers to any mineral that may yield water with sufficient energy input including minerals incorporating structural OH groups. Yielding of steam on microwave irradiation could enhance damage to a material in several ways. Firstly, the microwave absorbing properties of the mineral phases that yield steam could be enhanced and the resulting temperature gradient may result in fracture. Alternatively, the evolved steam could result in internal pressure building within and causing the material to crack. In some compounds, such as gypsum where water forms an essential part of the crystal structure, driving it out causes gypsum to change to a hemihydrate and then to

anhydrite with associated shrinking and cracking (Sipple et al., 2001). Any of these mechanisms decrease the mechanical strength of the ore, implying that less energy may be required for subsequent comminution processes. The grinding time could be reduced hence lowering the overall process time. Other downstream process benefits could include increased concentrate grade and mineral recovery as a result of improved liberation.

Despite the above potential process benefits, microwave processing of ores containing hydrated minerals has not been studied in any depth. Research into microwave assisted comminution and liberation has focused on metallic based ores known to contain semi conductors. This chapter presents an investigation into the influence of water containing minerals on microwave induced breakage. Ores with a range of hydrated minerals were selected for study basing on literature and laboratory mineralogical examination. Thermal analysis of the composite minerals was carried out in order to elucidate the dehydration characteristics of the contained minerals. The dielectric properties of the minerals were measured over a wide temperature range and the microwave heating ability of the minerals assessed. The bulk ore water content and water loss at different temperatures was determined and compared to the theoretical water content as calculated from the mineralogical composition and/or thermal analysis of composite minerals. Samples of each ore were irradiated with microwaves and the influence of microwave heating was assessed both qualitatively and quantitatively. Conclusions were then drawn from the relationships between dehydration characteristics, dielectric properties and the observed effects of microwave heating.

4.2 Ores Used for the Study

Four ores were selected for this study namely:

I. A copper – nickel ore obtained from the Nebo-Babel ore deposit in West Musgrave, Western Australia
II. A copper ore from the Los Bronces mine in Chile
III. A Kimberlite diamond ore (type I) obtained from the Ekati Diamond Mine, Canada
IV. A heavily weathered Kimberlite diamond ore (type II), also from the Ekati Mine but with a distinctively different texture

The choice of the above ores was influenced by:

- Mineralogical composition: Ores I and II above present mineral assemblages with a matrix of known good absorbers of microwave energy in a transparent gangue matrix. Previous studies have described such ores as "good candidates" for microwave pre-treatment (Kingman et al., 1999). On the other hand, the Kimberlite ores contain a significant amount of hydrated minerals. The effect of microwave treatment on the two groups of ores was compared.
- Availability of ore samples in sufficient quantities for the tests required.

4.3 Mineralogical Analysis of Ores

4.3.1 Introduction

The mineralogy of an ore largely determines both the physical and chemical characteristics of the bulk ore. It has also been stated above that ore mineralogy (and texture) influence response to microwave heating. This study therefore required a detailed mineralogical investigation of the ores to be

carried out. It was important not only to identify the minerals present in each ore but also to quantify them and to determine their association and distribution. A JKTech FEI, Quanta 600 Mineral Liberation Analyser (MLA) was used for this purpose. The MLA incorporates similar detectors to those of a standard Scanning Electron Microscope (SEM), including those for Scanning Electron (SE) and Back Scattered Electron (BSE) imaging and Energy Dispersive X-ray spectroscopy (EDS) (JKMRC, 2004). A typical column of an SEM is shown in Figure 4.1.

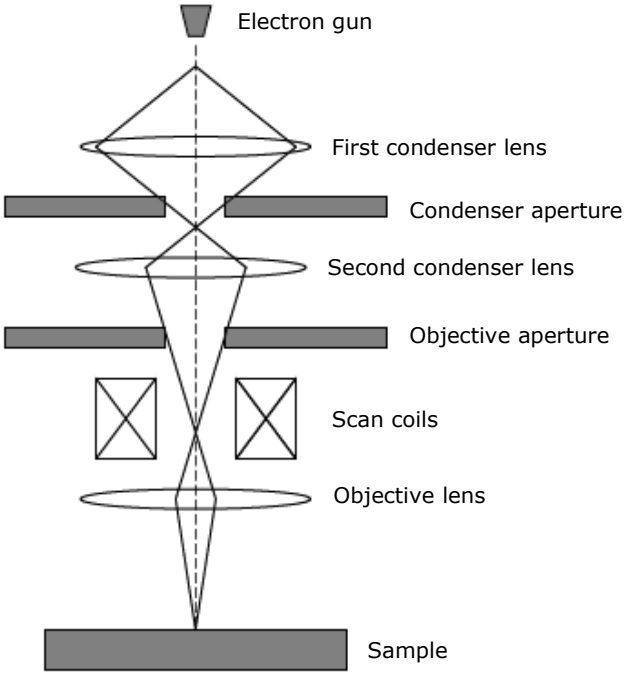

Figure 4.1 An Electron-optical column of the Scanning Electron Microscope (Plint, 2006)

The electron gun produces a beam of monochromatic electrons in vacuum which are then collimated by magnetic condenser lenses and apertures and focused onto a selected region of the sample by the final objective lens (Reed, 1996). When the beam of electrons interacts with the sample surface, the

resulting signals (which may include BSE, X-rays and Secondary Electrons) are measured with various detectors. Back scattered electrons are generated when a primary electron passing close to an atomic nucleus changes its direction with very little energy loss (Wittke, 2003). Those electrons deflected through a very large angle re-emerge from a specimen surface with high energy and are collected for imaging usually by atomic number contrast. Secondary electrons are generated by inelastic scattering of primary electrons resulting in ejection of orbiting shell electrons of the specimen atoms. X-rays are emitted as a result of inelastic scattering processes, producing Continuum X-rays or Brehmstrahlung and characteristic X-rays (Reed, 1996).

4.3.2 Method for MLA Mineralogical and Textural Analysis

The production of high quality polished sections is essential for obtaining accurate results whilst using the MLA system (JKMRC, 2004). A representative sample with randomly oriented particles must be presented to the MLA for accurate measurements. Ores were received in drums weighing between 150 and 250 kgs and containing lumps of ore with size range between 10 and 100 mm. There was a small proportion of fine material and particles less than 10 mm produced as a result of attrition during transportation. The ores were spread out on a floor and allowed to dry under room conditions for 2 days. Large ore lumps were hand sorted out and a *Russell* sieve shaker was used to screen out particles that were less than 10 mm. A Rotary Sample Divider (RSD) shown in Figure 4.2 was then used to obtain a homogeneous mixture of the retained ore type by splitting the bulk ore into quarter fractions and re-combining the fractions obtained three times.

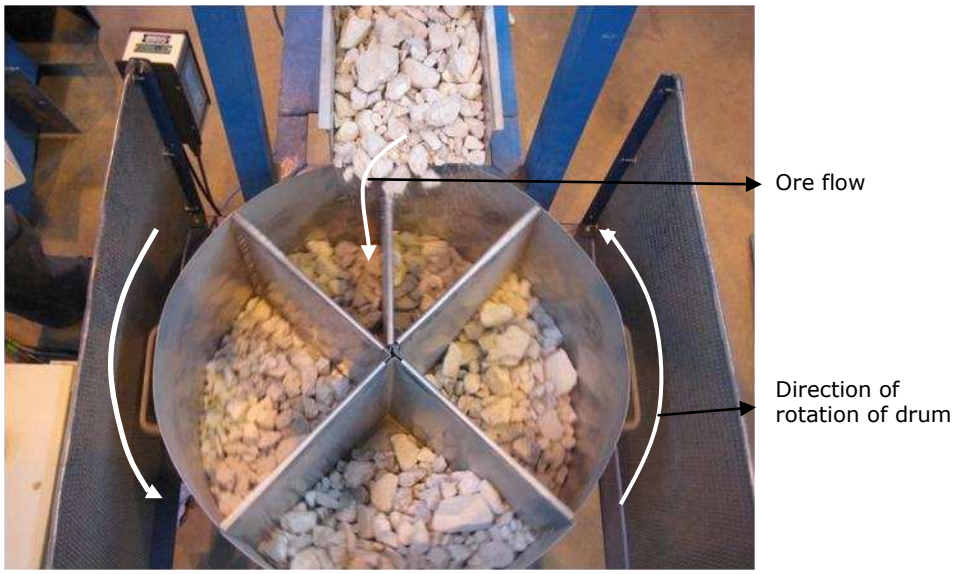

Figure 4.2 Rotary sample divider (RSD) used for ore sampling

The ores were then progressively split using the RSD into eight representative fractions. The large ore lumps (which were hand sorted prior to screening) were distributed between the eight sample fractions on a one on one basis. Each sample fraction, weighing about 14 kgs, was then bagged and labelled. For each ore, a randomly selected bag was carefully examined for any distinct features in texture to ensure that the ore particles selected for MLA examination represented all the textural features of the bulk ore. The selected ore particles were then sawn using a diamond impregnated saw and a section representing all the textural features of the particle cut out and sized into a thin section with a diameter less than 30 mm and a depth less than 20 mm. The surface to be examined was levelled using a grinder.

The procedure followed in preparing the samples for examination was as recommended in the *MLA System User Operating Manual (Module 1)*. Epoxy resin mixed with a hardener in a ratio of 15:2 by weight was used to mount

the specimens for examination. The mounted specimens were then placed in a *Struers Epovac* vacuum pump for about 15 minutes to drive out all the air and ensure that all pores are filled with resin and then left to set overnight. The specimens were then subjected to a series of grinding and polishing stages in successively finer steps to remove material from the surface and attain a polished surface of high quality. Three stages of grinding using *MD-Piano 120, 220* and *1200* plates were carried out and then followed by three stages of polishing with *MD-Plan* (9 µm)*, MD-Dac* (3 µm) and *MD-Dur* (1 µm) polishing cloths. Each grinding and polishing stage was run for between 2 to 5 minutes. The polishing stages all used automatically introduced diamond lubricants. After polishing, samples were then cleaned and allowed to dry in ambient room conditions.

The final stage in the preparation of the samples was to "carbon coat" the surfaces to be examined. This was carried out to prevent charging of the surface which improves the quality of acquired BSE/X-ray signals (JKMRC, 2004). A *JEE-420* carbon evaporator was used for this purpose. Essentially, a mould was placed inside the evaporator with the surface to be examined facing upward. The evaporator was then evacuated and a high electric current passed through carbon rods which evaporated and deposited a very thin layer of carbon, in the order of 20-50 nm on the surface of the material to be examined.

The specimens were then positioned inside the SEM which has a large chamber that allows automated measurement of up to fourteen polished sections, each with a diameter of 30 mm. An EDAX X-ray detector collected a representative spectrum for each mineral phase. The minerals were identified

by matching the collected spectra to standard spectra held in the MLA database. With aid of installed *EDAX Genesis* software (XBSE and GXMAP programs), automated measurements were generated via the following steps:

- Capture of multiple frames with BSE imaging
- On-line segmentation of the images based on BSE contrast. BSE contrast is a function of mean atomic number and the BSE contrast of a multi-mineral ore gives the spatial distribution of all mineral phases
- On-line acquisition of energy dispersive X-ray spectra for each segment. Additional spectra were acquired for those minerals of coincident contrast, so that mineral phase boundaries could be determined
- Classification of each mineral segment was achieved by automatic pattern matching of the measured spectra by EDS with predetermined standard spectra for each mineral in the ore
- Multiple frames were then merged to produce a classified image of the complete particle
- Finally, analysis of the classified image to quantify textural parameters such as mineral weight percentages, grain size distributions and mineral associations was carried out

4.3.3 Results from Ore Mineralogical and Textural Analysis

It was stated earlier in this chapter that mineralogy, texture and "mineral dissemination" influence the magnitude of microwave induced fracture. The following key data was processed from the MLA to enable an assessment of the mineralogical and textural features of each ore to be made:

- The identity of minerals present in each section examined
- The mineral abundance by weight of each mineral phase
- The spatial distribution of each mineral phase
- The grain size distribution of microwave absorbent mineral grains
- The variation of the above in all the 14 specimens that were examined

The full results of all minerals identified in each measured section, which includes the abundance of each mineral by weight and classified images of all measured sections showing the mineral distributions, are given in Appendix I. Tables 4.1 to 4.4 present the combined weight percentages of the minerals in all the specimens examined.

Mineral	Formula	Microwave Heating	Weight Percentage
Pyrrhotite	$Fe_{1-x}S$	readily heated	5.1
Pentlandite	$(Fe,Ni)_9S_8$	readily heated	0.9
Chalcopyrite	$CuFeS_2$	readily heated	0.7
Ilmenite	$FeTiO_3$	readily heated	0.6
Magnetite	Fe_3O_4	readily heated	0.5
Plagioclase	$(Na,Ca)(Si,Al)_4O_8$	does not heat	49.7
Pyroxene	$(Ca,Na)((Mg,Al,Fe,Ti)(Si,Al)_2O_6$	does not heat	38.9
Biotite	$K(Mg,Fe)_3AlSi_3O_{10}(OH,F)_2$	unknown but contains OH	2.1

Table 4.1 The most abundant microwave heating and transparent mineral phases in Nebo Babel Copper Nickel Ore

Mineral	Formula	Microwave Heating	Weight Percentage
Hematite	Fe_2O_3	readily heated	3.1
Chalcopyrite	$CuFeS_2$	readily heated	1.4
Pyrite	FeS_2	readily heated	1.2
Quartz	SiO_2	does not heat	32.4
Muscovite	$KAl_2[(OH)_2AlSi_3O_{10}]$	does not heat	27.4
Orthoclase	$K[AlSi_3O_8]$	does not heat	10.4
Plagioclase	$(Na,Ca)(Si,Al)_4O_8$	does not heat	8.4
Albite	$Na[AlSi_3O_8]$	does not heat	10.0

Table 4.2 The most abundant microwave heating and transparent mineral phases in Los Bronces Copper Ore

Mineral	Formula	Microwave Heating	Weight Percentage
Olivine	$(Mg,Fe)_2[SiO_4]$	does not heat	39.1
Serpentine	$(Mg,Fe)_3\,Si_2O_5\,(OH)_4$	unknown but contains OH	24.2
Monticellite	$CaMg[SiO_4]$	does not heat	13.9
Calcite	$CaCO_3$	does not heat	5.1
Micas	$X_2Y_{4\text{-}6}[(Si,Al)_6O_{20}](OH,F)_4$	unknown but contains OH	6.7
Hydrobiotite	$[K(Mg,Fe)_3\,(Al,Fe)Si_3O_{10}\,(OH,F)_2]\cdot$ $[(Mg,Fe,Al)_3(Si,Al)_4O_{10}(OH)_2\cdot 4(H_2O)]$	unknown but contains OH and interlayer water	4.4

Table 4.3 The most abundant mineral phases in Ekati Kimberlite diamond (type I) ore

Only the most abundant microwave absorbing and microwave transparent mineral phases are shown in Tables 4.1-4.4. Minerals which occurred in smaller proportions or which were not consistently detected in all the measured specimens have been excluded. The "responsiveness" to microwave heating is also shown for those minerals where such data was available in

literature from previous heating studies such as work carried out by (Chen et al., 1984).

Mineral	Formula	Microwave Heating	Weight Percentage
Smectite	$(½Ca,Na)0.33(Mg,Fe)_3(Si,Al)_4O_{10}(OH)_2 \cdot 4H_2O$	unknown but contains OH and interlayer water	50.6
Olivine	$(Mg,Fe)_2[SiO_4]$	does not heat	9.2
Thaumasite	$Ca_3Si(CO_3)(SO_4)(OH)_6 \cdot 12(H_2O)$	contains OH and water of crystallization	7.6
Feldspars	$XAl_{(1-2)}Si_{(3-2)}O_8$ $(X = Na,K,Ca)$	does not heat	7.8
Biotite	$Ca_2(Fe,Al)_3(SiO_4)_3(OH)$	unknown but contains OH	5.4
Talc	$Mg_3Si_4O_{10}(OH)_2$	unknown but contains OH	6.4
Hydrobiotite	$[K(Mg,Fe)_3(Al,Fe)Si_3O_{10}(OH,F)_2] \cdot [(Mg,Fe,Al)_3(Si,Al)_4O_{10}(OH)_2 \cdot 4(H_2O)]$	unknown but contains OH and interlayer water	5.4
Hornblende	$(Ca_2)(X_4Al)_3[(OH)_2lAlSi_7O_{22}]$ X= Mg, Fe	contains OH	2.6

Table 4.4 The most abundant mineral phases in Ekati Kimberlite diamond (type II) ore

The results obtained indicate that the ores were multi-mineralic and varied in composition. The Nebo Babel Cu-Ni ore contained pyroxene, plagioclase and pyrrhotite as the major mineral phases but also contained significant proportions of biotite, pentlandite and chalcopyrite. This ore contained several known good heaters of microwave energy, with a combined weight average of approximately 8%. The MLA specimen images which present the spatial distribution of each mineral phase (see Appendix I), showed that the microwave absorbing minerals are randomly distributed throughout the ore. On the other hand, pyroxene and plagioclase, which were the major gangue minerals, are transparent to microwaves. Examples of classified MLA specimen images of each ore are shown in Figures 4.3 and 4.4.

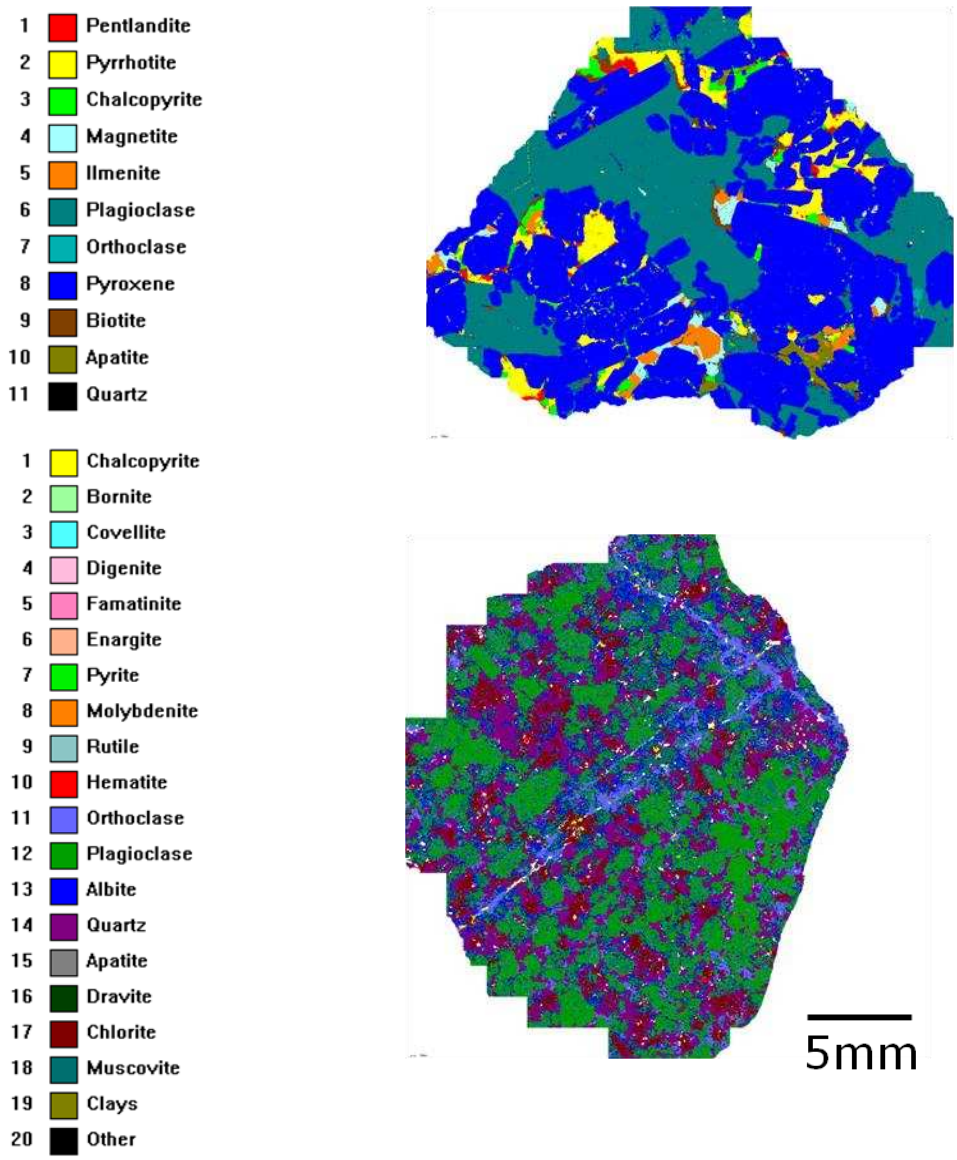

Figure 4.3 Examples of classified MLA specimen images (Top) Nebo Babel Cu-Ni ore (bottom) Los Bronces Copper Ore

The main microwave absorbing minerals within the Los Bronces copper ore were hematite, chalcopyrite and pyrite which were also randomly distributed throughout the specimen. The major gangue minerals, quartz, muscovite and orthoclase, are essentially transparent to microwaves (see Table 4.2 and Figure 4.3).

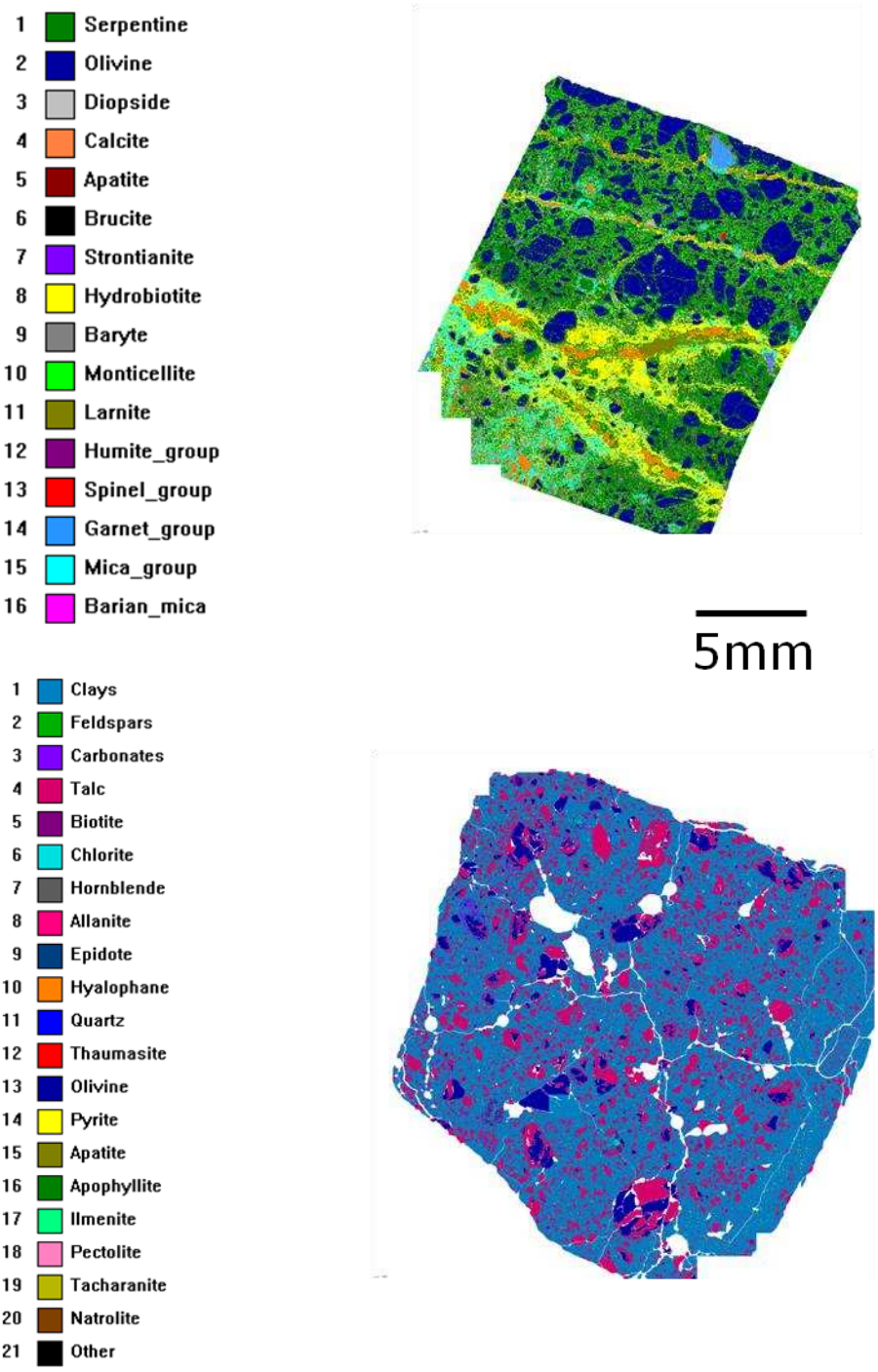

Figure 4.4 Examples of MLA specimen images (Top) Ekati Kimberlite diamond ore - type I (bottom) type – II Kimberlite ore

Both Nebo Babel Cu-Ni and Los Bronces copper ores comprise matrices of microwave transparent minerals with dispersed microwave absorbent

minerals. Based on the findings of Kingman et al (1999) and subsequent work that followed, which was discussed in the previous chapter, it was expected that "weakening" of these ores when treated with microwaves should occur as a result of differences in thermal expansion between heated and non-heating minerals.

Figure 4.5 shows the grain size distribution of combined microwave absorbent mineral grains in the Nebo Babel and Los Bronces ores. For the Nebo Babel ore, this represents the combined grain sizes of pyrrhotite, pentlandite, chalcopyrite, ilmenite and magnetite whereas the combined grain sizes of hematite, chalcopyrite and pyrite have been plotted for the Los Bronces ore. The results show that the grain sizes of microwave absorbent minerals range approximately between 40 μm – 10 mm and 40 μm - 2.5 mm in the Nebo Babel and Los Bronces ores respectively. It is clear that the microwave absorbent mineral grains in the Nebo Babel ore are coarser compared to the Los Bronces ore. Figure 4.5 shows that the d_{80} of the Nebo Babel microwave absorbent grains was approximately 1.5 mm whereas that of the Nebo Babel grains was approximately 100 μm. It can also be seen from Figure 4.5 that approximately 90% of the Nebo Babel grains were coarser than 600 μm, whereas only about 25% of the microwave absorbent mineral grains in Los Bronces ore were coarser than 600 μm.

The Kimberlite ores did not contain any minerals which are known to be good microwave heaters. The results in Table 4.3 and Figure 4.4 show that the Kimberlite II ore consisted of approximately 55% clay minerals (mainly smectites) but also thaumasite and hydrobiotite. The responsiveness of these minerals to microwave heating has not been previously investigated.

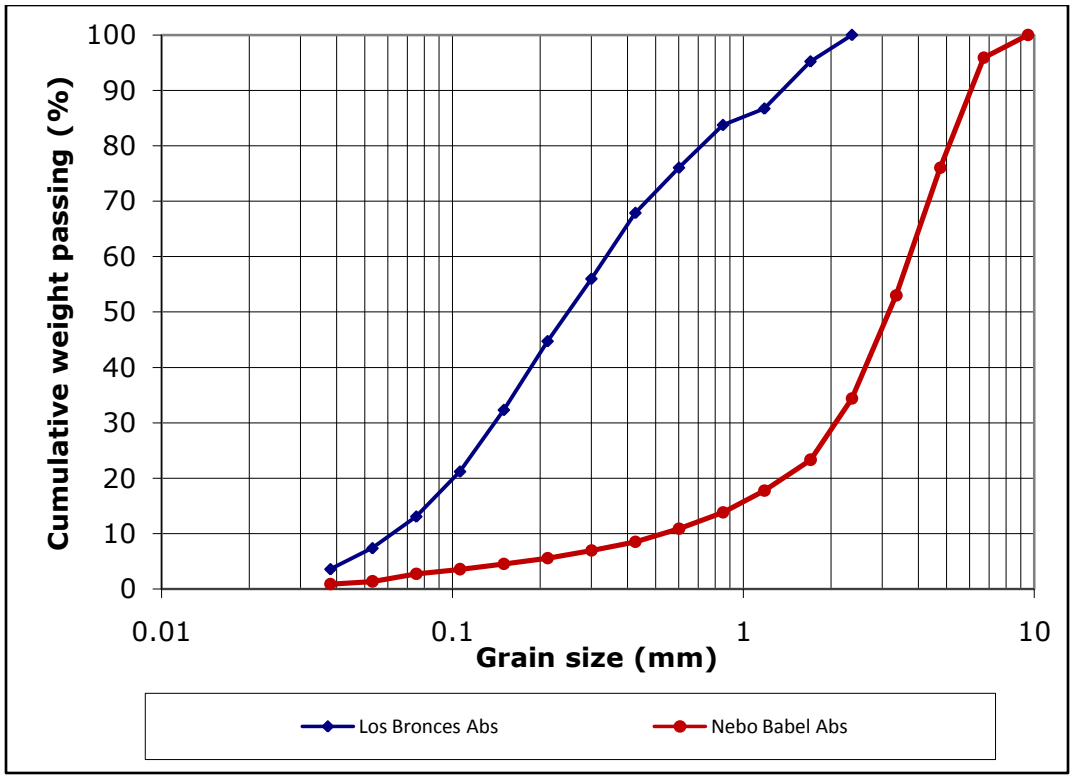

Figure 4.5 Size distribution of microwave absorbent mineral grains in Nebo Babel and Los Bronces ores

Smectite is a "swelling clay" that incorporates interlayer absorbed water (Grim, 1968) and therefore its presence was likely to influence the overall microwave heating characteristics of the Kimberlite II ore. Olivine and feldspars were also present in significant proportions and are transparent to microwaves. The Kimberlite I contained mainly olivine, serpentine and monticellite, which when combined accounted for over 77% by weight, and also contained about 5% hydrobiotite. Again, none of these minerals are known to heat readily when exposed to microwaves. Olivine, serpentine and monticellite incorporate structural OH groups. Hydrobiotite, however contains significant amount of interlayer water (Grim, 1968). Further analytical work carried out on this ore showed that although the quoted average content of hydrobiotite was only 5%, it was actually highly variable and ranged from 0.3

to 17% (see Appendix I). Therefore, even though the Kimberlite I ore also lacked microwave highly absorbent conductive metal phases, the presence of minerals containing OH groups and interlayer adsorbed water was thought to influence its microwave absorbing properties. These hypotheses were investigated in this work.

4.4 X-ray Diffraction (XRD) Mineral Identification

4.4.1 Introduction

XRD analysis is a semi-quantitative technique widely used for identification of minerals and compounds crystallographically. The method relies on the fact that X-rays can be diffracted by crystalline solids which exhibit regularly repeating atomic structures. Figure 4.6 shows the reflection of a parallel beam of X-rays from two successive planes of atoms in a crystal.

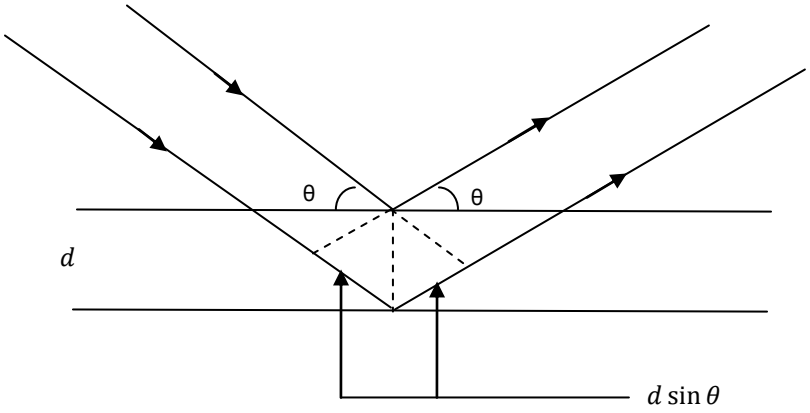

Figure 4.6 The diffraction of coherent X-rays from successive planes of atoms in a crystal

When the path difference (2dsinθ) is a multiple of the wavelength λ, X-rays scattered from a crystalline solid can constructively interfere and produce a diffracted beam. The relationship between the inter-atomic planar spacing (d-

spacing), the angle of diffraction and the wavelength of the incident radiation is given by the Bragg law (Kittel, 1986):

$$n\lambda = 2d\sin\theta \qquad (4.1)$$

Where n = Integer

λ = Wavelength (Å)

θ = Diffraction angle (degrees)

d = d-spacing

If a finely ground crystalline powder is placed in the path of a monochromatic X-ray beam, diffraction occurs from atomic planes in those crystallites which are oriented at the correct angle to satisfy the Bragg condition (Connolly, 2005). X-ray powder diffraction patterns are most commonly measured with a powder diffractometer (Eberhart, 1991). This utilizes a movable X-ray detector to measure the position and intensity of diffracted X-rays. Each crystalline substance exhibits a characteristic powder diffraction pattern which may be used for its identification by comparison with standard patterns published by the Joint Committee on Powder Diffraction Standards (JCPDS). Multi-phase samples can also be analyzed provided that the powder diffraction files for each phase is available. Details about the theory and principles of the XRD technique are available in many publications such as (Dinnebier and Billinge, 2008).

The hydrated minerals which were identified with aid of MLA were sourced from Nottingham University rock store. In cases where there was difficulty obtaining the mineral required, a mineral in the same classification group with

as near similar properties as possible was used instead. Literature sources that were used to relate mineral groups and properties included (Grim, 1968, Todor, 1976) and mineral database website *mindat.com*. The full list of the minerals used in this study and their composition is given in Table 4.5. The minerals were first subjected to XRD examination to confirm their identity. Different tests (which are described later) were then conducted on a sample of each mineral in order to assess their amenability to microwave heating and how this would affect the overall microwave absorbing properties of the ores. The implications for microwave assisted processing of ores containing hydrated minerals were assessed following the results of this study.

4.4.2 Materials and Method for XRD Analysis

Small lumps of "pure" mineral weighing between 3-5 g were obtained. Each mineral sample was ground using a *tema* mill and passed through a 53 μm sieve. Each mineral sample was then divided into three portions using a rotary sample divider. The first portion was used for XRD analysis and the other two portions were reserved for TGA and dielectric property measurements. The portion retained for XRD analysis was further ground in a mortar and pestle to suit XRD sample requirements. The sample to be analysed was then carefully spread out on a slide.

The system used for analysis consisted of a computer controlled Hiltonbrooks generator with a Phillips PW 1050 diffractometer, an automatic divergence slit and a copper anode producing X-rays of wavelength $\lambda = 1.54056$ A^{o}. The diffractometer was operating at 40 kV and 20 mA and automatic routines allowed scanning for values of 2θ between 5^{o} and 95^{o} using a step size of 0.05^{o} and scan speed of 2^{o}/min. Data was processed with aid of Diffraction

Technology *Traces V.3* software with a database of diffraction spectra developed by the *Joint Committee on Powder Diffraction Standards–International Centre for Diffraction Data (JCPDS-ICDD).* Identification of the minerals contained in the sample was achieved by matching the X-ray spectrum obtained with the standard JCPDS spectra.

4.4.3 Results of XRD Mineral Analysis

Table 4.5 shows the composition and classification of the minerals tested. Classification was based on various literature sources such as (Grim, 1968, Sinkankas, 1964, Vaughan and Pattrick, 1995). Talc, Kaolinite, halloysite, sodium montmorillonite and actinolite all belong to the *phyllosilicate* group of minerals. Phyllosilicates are "sheet" or "layer" silicates and form the most important hydrated mineral groups which include serpentines, clays, micas, talc and chlorites. They are built from tetrahedra of silicon in 4-fold coordination with oxygen atoms which extend outward in infinite sheets. Three quarters of the oxygen atoms from each tetrahedra are shared with other tetrahedra, leading to a structural unit of $Si_2O_5^{-2}$ (Sinkankas, 1964). These alternate with sheets of divalent (Mg, Fe) or trivalent (Al, Fe) cations in octahedral oxygen coordination as shown in Figure 4.7.

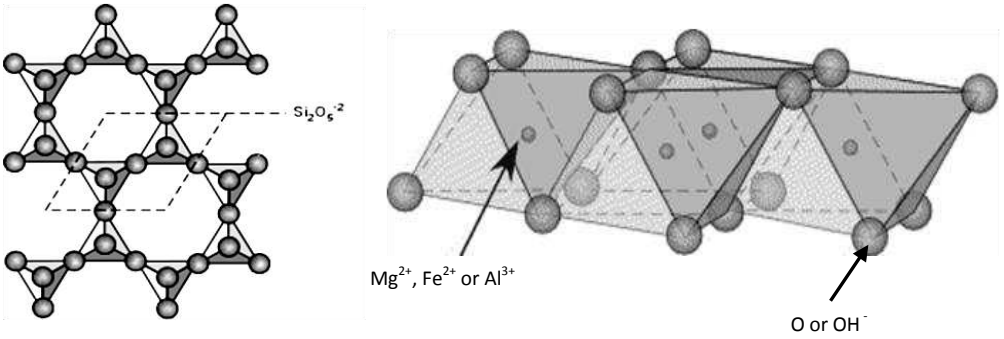

Figure 4.7 The basic tetrahedral building block for phyllosilicate minerals (left). Illustration of phyllosilicate sheet coordination (right) (Nelson, 2008)

Mineral	Composition	Classification	Hydrate Group
Talc	$Mg_3Si_4O_{10}(OH)_2$	2:1 tri-octahedral phyllosilicate	Structural OH
Kaolinite	$Al_2Si_2O_5(OH)_4$	1:1 dioctahedral phyllosilicate clay	Structural OH
Halloysite	$Al_2Si_2O_5(OH)_4.\ 2(H_2O)$	1:1 dioctahedral phyllosilicate clay	Structural OH and Interlayer water
Na-montmorillonite	$(Na)_{0.33}(Al,Mg)_2Si_4O_{10}(OH)_2{\cdot}n(H_2O)$	2:1 dioctahedral phyllosilicate clay	Structural OH and Interlayer water
Actinolite	$Ca_2(Mg,Fe)_5Si_8O_{22}(OH)_2$	Amphibole	Structural OH
Apatite	$Ca_5(PO_4)_3(OH,F.Cl)$	Anhydrous phosphate	Structural OH
Gypsum	$Ca\ [SO_4].\ 2H_2O$	Hydrated sulphate	Water of crystallization
Stichtite	$Mg_6\ Cr_2\ [(OH)_{16}\ CO_3].4H_2O$	Hydrated carbonate (Hydrotalcite group)	Water of crystallization and interlayer water
Biotite	$K(Mg,Fe)_3[AlSi_3O_{10}(OH,F)_2$	2:1 trioctahedral phyllosilicate	Structural OH

Table 4.5 Hydrated minerals indentified by powder diffraction analysis. Classification is based on various literature sources such as (Grim, 1968) and (Vaughan and Pattrick, 1995)

Phyllosilicate structures are classified based on their sequence of tetrahedral and octahedral layers, and exhibit either 1:1 or 2:1 tetrahedral to octahedral (T:O) sequences. They are sub-classified based on whether the octahedrally coordinated cation is divalent or trivalent. This controls the octahedral site occupancy. In trioctahedral sheet silicates, each O or OH ion in the octahedral layer is surrounded by 3 divalent cations, Mg^{+2} or Fe^{+2}. In dioctahedral sheet silicates, each O or OH ion is surrounded by 2 trivalent cations, usually Al^{+3}. The trioctahedral analogue of kaolinite is lizardite $Mg_3Si_20_5(OH)_4$. Likewise, talc $Mg_3Si_40_{10}(OH)_2$ and pyrophyllite $Al_2Si_40_{10}(OH)_2$ are trioctahedral and dioctahedral analogues with a 2:1 T:O:T stacking sequence. Interlayer bonding between adjacent T:O and T:O:T sheets is weak and relies on Van der Waals bonding only, from which arises the characteristic softness and cleavage behaviour of the phyllosilicates (Grim, 1968).

Most phyllosilicate minerals incorporate the hydroxyl ion (OH) which is always strongly bonded to the octahedral coordinated cation within the crystal structure and will yield water and in most cases undergo structural reorganization only with sufficient thermal energy as shown by Equation 4.2 below (Grim, 1968).

$$2OH^- \rightleftharpoons H_2O + O^{2-} \qquad (4.2)$$

Octahedral cation substitution greatly influences the thermal energy required for OH removal and bond strengths are in the order $\mathrm{Fe}-\mathrm{OH} < Al-OH < Mg-OH$. For example, for Fe substitution in the octahedral layers, removal of OH groups occurs between 400 and 550°C whereas with Mg substitution, removal occurs between 800 and 1000°C (Todor, 1976). Because of the structural re-

organizations and substitutions that are associated with silicates, very many mineral compounds with very similar properties are formed.

Smectites are 2:1 phyllosilicates and include montmorillonite (dioctahedral) and vermiculite (trioctahedral). They have the ability for water molecules to be absorbed between the tetrahedral sheets as shown in Figure 4.8. This causes a volume increase when in contact with water. Unlike structural OH, complete elimination of interlayer water may be achieved by low temperature heating and takes place between 100 and 200^{0}C and in most cases is regained readily at ordinary temperatures (Todor, 1976). Halloysite which is a 1:1 dioctahedral also has the ability to incorporate interlayer water.

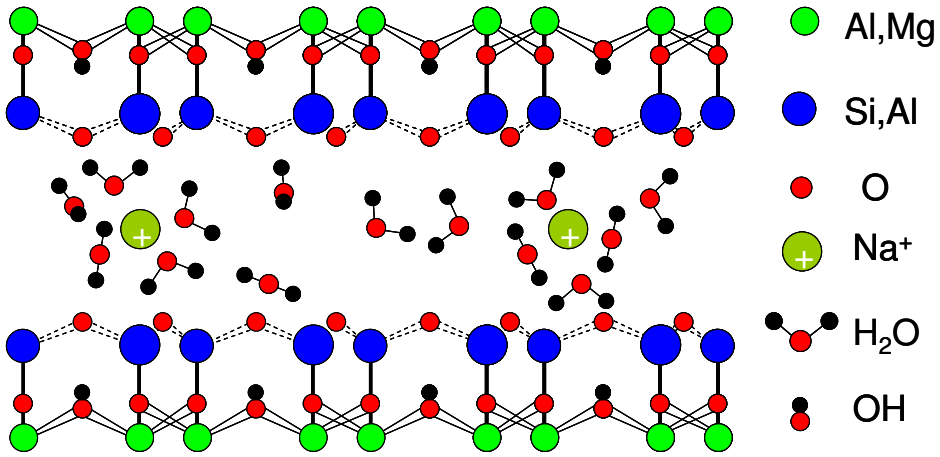

Figure 4.8 Structure of Na-montmorillonite (Sparks, 1995)

Stichtite has a hydrotalcite structure. Hydrotalcites (or layered double hydroxides, LDH, as they are sometimes called) belong to a large class of anionic and basic clays comprising positively charged brucite-like [$Mg(OH)_2$] structures. A trivalent cation such as Al^{3+}, Fe^{3+}, Cr^{3+} substitutes part of the Mg^{2+} and the substitution creates a positive layer charge on the hydroxide

layers which is compensated by interlayer anions or anion complexes and water molecules. Kaolinite does not absorb water and does not expand in contact with water. When well crystallized it presents a horizontal section on the thermal curve up to about 400^0C, except if water is present as moisture (Todor, 1976). Interlayer water species are also present in hydromica minerals such as hydrobiotite, which is a "mixed layer clay" with a 1:1 interstratification of biotite $(K(Mg,Fe)_3(Al,Fe)Si_3O_{10}(OH,F)_2)$ and vermiculite layers $(Mg,Fe,Al)_3(Si,Al)_4O_{10}(OH)_2 \cdot 4(H_2O)$ (Grim, 1968).

4.5 Analysis of Mineral Dehydration Characteristics

4.5.1 Introduction

The different groups of minerals that may yield water with sufficient thermal energy input were discussed in the last section. Water may exist in a mineral assemblage in the form of free surface adsorbed or absorbed water, water of hydration or may be yielded from minerals containing structural hydroxyl (OH) groups (Sinkankas, 1964). Surface absorbed or adsorbed water is weakly bonded with 'H_2O – surface' and H_2O - H_2O hydrogen bonds. Water of crystallisation occurs within the crystal framework of certain minerals where the water molecules are structurally ordered and attached via hydrogen bonds. Often, the mineral cannot be crystallized in the absence of water even though no chemical bond exists between the cation sub-lattice and water molecules. Structural hydroxyl groups are incorporated in many common minerals, most notably the phyllosilicates such as serpentines, talc, micas, chlorites and clays. The oxygen position of the structural OH is fixed by a chemical bond between the oxygen and cation sub-lattice. Some amphiboles, hydroxides and sulphates such as hornblende, goethite and brucite also

incorporate structural OH groups. Thermally driven dehydroxylation of phyllosilicates is generally achieved at temperatures above 400°C (Tudor, 1976).

The dehydration characteristics of minerals are used to determine the nature of the water species present. Dehydration studies are concerned with the amount of water lost, the rate of water loss and the temperature at which this occurs, and the energy involved (Todor, 1976). Thermo-gravimetric analysis (TGA) is commonly used to investigate the dehydration characteristics of minerals. In thermogravimetry, a sample subject to analysis is weighed continuously as it is heated under a controlled environment. By following the variation of mass as a function of temperature, conclusions concerning the transformations which have occurred in the sample under investigation may be drawn. A graph of weight loss (or weight remaining) percentage against temperature is commonly referred to as a dehydration curve and shows the dehydration characteristics of a mineral. The dehydration curves of the hydrated minerals given in Table 4.5 were obtained by TGA analysis.

4.5.2 Method for Thermo-gravimetric Analysis of Minerals

All the minerals listed in Table 4.5 were subjected to thermo-gravimetric analysis. Approximately 1 g of the same sample that was examined by XRD was thoroughly mixed using a rotary sample divider and then split into quarters. About 25 mg of each mineral sample was taken using a spatula and placed in a crucible. A PerkinElmer Pyris 1 TGA, shown in Figure 4.9, was used to perform the analysis. The instrument consisted of a tray of 14 crucibles each of which could be picked by a robotic arm weighing scale and held inside

a furnace. The instrument was automated to accurately take weights of samples at pre-set temperatures during heating or cooling.

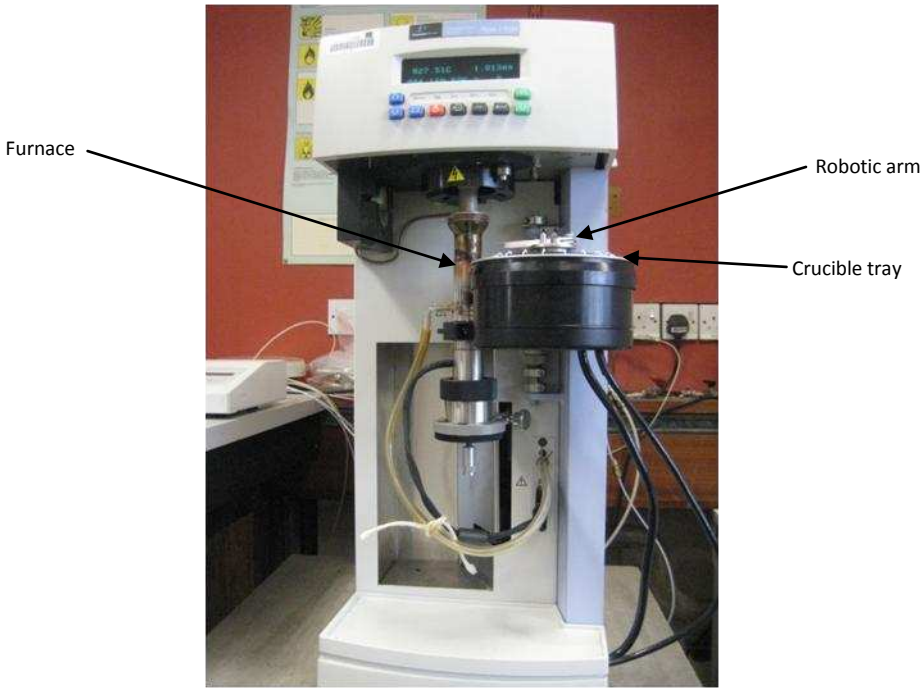

Figure 4.9 PerkinElmer Pyris 1 instrument used for mineral dehydration characterisation

A slow heating rate of to 100^0C/min was chosen to provide a good level of detail of the hydration curves. All samples were heated in nitrogen to prevent any oxidation processes occurring. A constant heating step was set at 75^0C for 10 minutes to allow any moisture present in the sample to dry. Any mass losses after this temperature were assumed to be associated with dehydration involving the loss of adsorbed, interlayer or lattice water or from dehydroxylation of OH groups. The weight loss was automatically recorded every second from 20^0C to 850^0C. Due to the difficulty and uncertainty in obtaining very small samples that are representative, the test was repeated to check the precision of the results.

4.5.3 Results from TGA Analysis of Mineral Samples

Figure 4.10 shows the dehydration curves of the different minerals. It is clear from these results, that there is high variability in thermal characteristics of the different minerals.

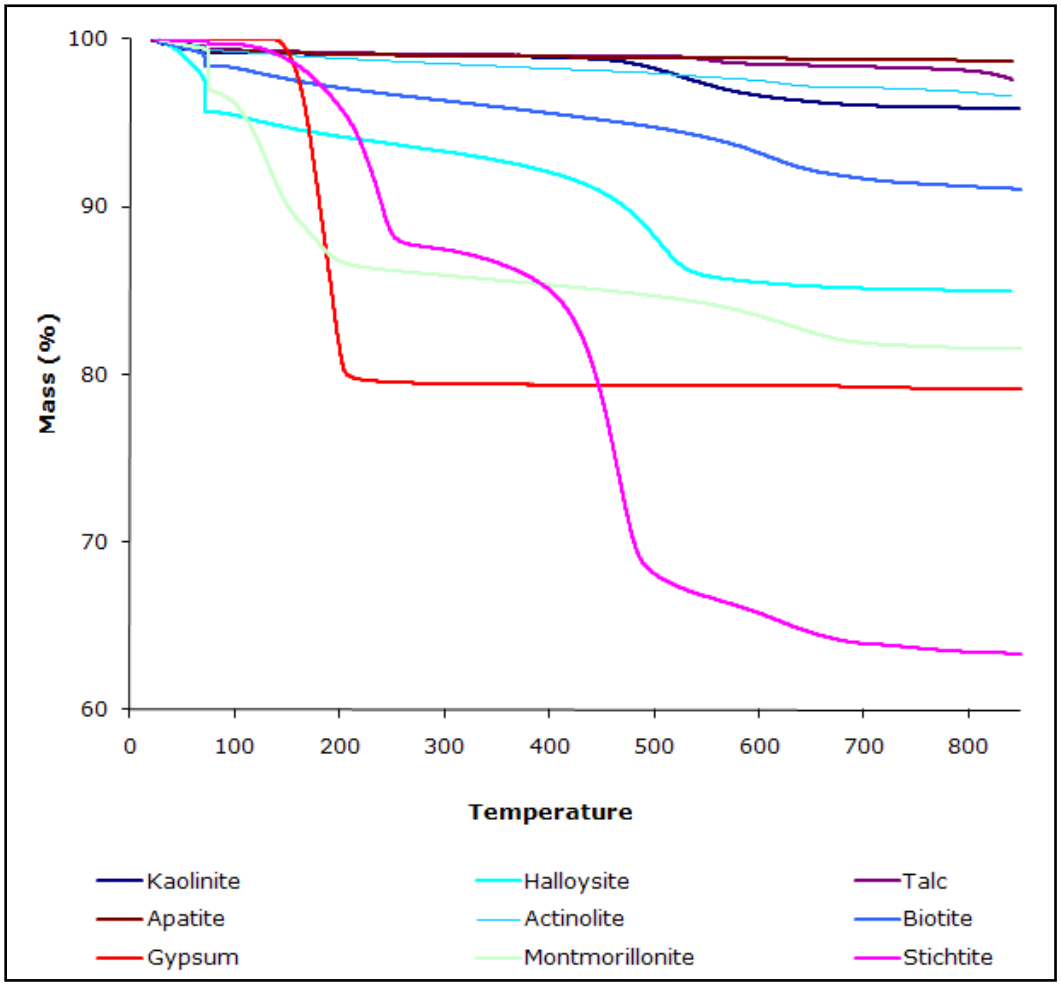

Figure 4.10 Dehydration curves obtained from TGA analysis of selected mineral samples

The dehydration curves can be characterised into three broad groups. The first includes minerals that showed no change in weight, with an overall loss of less than 2% over the whole temperature range. These minerals appeared to remain thermally stable and showed no dehydration characteristics for the

temperature range at which this study was conducted (25-850^{0}C). They are apatite, talc and actinolite. This result agrees with literature sources that, for example, state that dehydration of apatite does not occur until partial melting is achieved between 825^{0}C and 875^{0}C (Tudor, 1976, Grim, 1968).

The second group is comprised of minerals characterized by a slight gradual weight loss up to temperatures of at least 150^{0}C followed by sudden weight loss. In this category, kaolinite showed very little loss of water at low temperature indicating absence of any thermal reactions in the low temperature region. Between 400^{0}C and 600^{0}C, a distinct weight drop of about 2.8% occurred due to dehydroxylation (loss of OH group). Gypsum exhibited a significant weight loss of about 20% between 180^{0}C and 200^{0}C. This weight loss is attributed to removal of water of crystallization and after this transition, no further thermal transformations were recorded up to the highest temperature achieved. Stichtite underwent two distinct weight losses of about 13% and 20% between 100-200^{0}C and 400-500^{0}C respectively. The first stage is attributed to removal of interlayer water and water of crystallisation while the last stage is due to removal of structural OH groups.

The third characteristic dehydration curve pattern is for minerals which exhibited significant low temperature weight loss in addition to one or a combination of the other characteristics described above. Halloysite and biotite showed a gradual loss of weight of about 5-10% from room temperature up to about 450^{0}C (slightly higher for biotite). After this, there was an abrupt weight loss between 450^{0}C and 550^{0}C after which no further changes were recorded. Likewise, montmorillonite exhibited even higher gradual weight loss of about 15% to a temperature of 200^{0}C. Another

significant weight loss was observed between 550^0C and 650^0C. According to Todor (1976), the sudden mass loss at the higher temperatures is a dehydration process most presumably of the type shown in Equation 4.2.

The results therefore suggest that dehydroxylation in all the minerals studied may only take place at temperatures over 450^0C. Water of crystallization in gypsum is removed at lower temperatures in the range of 100-200^0C. As stated previously, removal of interlayer water occurs at the lowest temperatures due to the weak bonding between water molecules and the lattice structure. The minerals that exhibited significant low temperature gradual weight loss i.e halloysite and montmorillonite contain interlayer water.

4.6 Determination of Bulk Ore Water Content and Water Loss

4.6.1 Introduction

The total free water in an ore consists of both surface and absorbed interlayer water. The amount of free water in an ore can be determined by drying a sample in a ventilated oven. A study was carried out to estimate the total free water in each ore and the water loss at different temperatures. The water loss content of the ores at different temperatures, as determined from this study, was compared with water loss as estimated from the mineralogical composition and TGA results discussed in the last section.

4.6.2 Method for Determining Bulk Ore Water Content

The sampling procedure used to get representative test samples was as described earlier in Section 4.3.2. About 2 kg of ore particles, which were sawn off the ore sections used for MLA work, were used in this study. The

particles were then crushed using a Jaw crusher and the material passing through a 150 μm sieve were retained. A rotary sample divider was used to obtain a homogenous mixture of the retained material and thereafter to split the latter into smaller fractions. Three representative test samples, each of approximately 10-20 g, were obtained. The test samples were then placed in a crucible and heated in an open air furnace over night. The mass of the samples was taken at 100^0C, 200^0C and 400^0C, each time after heating for at least 12 hours at the pre-set temperature.

4.6.3 Results of Bulk Ore Water Content

Figure 4.11 shows the average mass loss percentage of the ores at 100^0C, 200^0C and 400^0C.

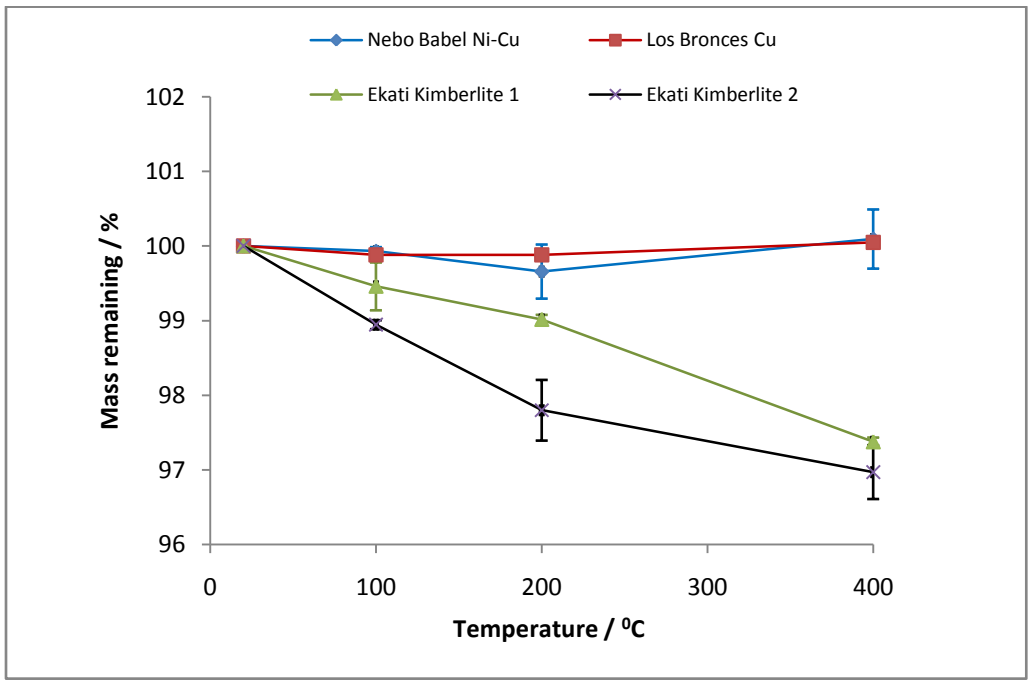

Figure 4.11 The mass loss percentage of ores at different temperatures

The British Standard for determining free unbound water content in aggregates and soils takes the water loss at 110^0C as the amount of free unbound water (moisture) in the material. The results obtained show that the Kimberlite I and II ores contained the highest amount of free water, approximately 0.5% and 1% of the total mass at 100^0C respectively. From the TGA results shown in Figure 4.10, the total water loss at 200^0C includes losses from free surface water and loosely bound interlayer water and water of crystallisation. This is approximately 3% for the Kimberlite II ore and about 2% for the Kimberlite I ore. The Kimberlite ores, with significant proportion of minerals which exhibited low temperature dehydration characteristics, correspondingly showed a higher mass loss than the other two ores. Also, the mass loss exhibited by the Kimberlite II was significantly higher than that of the Kimberlite I ore. These results are in agreement with both TGA and MLA results. The Kimberlite ores contained hydrated minerals with interlayer water and correspondingly showed higher mass loss than the other two ores devoid of minerals containing interlayer water. The theoretical water content of most clay minerals is reported to be in the range of 6-10% by weight (Tudor, 1976). The Kimberlite II ore consisted of about 50% clay minerals and showed a total mass loss of about 4%, which is consistent with predictions of 2-5% from theoretical calculations. Both the Nebo Babel Ni-Cu and Los Bronces Cu ores showed a slight increase in mass after 200^oC which is most likely due to metal oxidation processes, since the heating was conducted in an air ventilated furnace. For example, magnetite is readily oxidized to hematite at temperatures below 350^0C according to the following equation (Forsmo, 2005).

$$4Fe_3O_4 + O_2 \longrightarrow 6Fe_2O_3$$

4.7 Mineral Dielectric Properties

4.7.1 Introduction

The significance of dielectric properties with respect to microwave heating was discussed in chapter one. The ability of a material to be heated by microwave energy can be determined from measurement of dielectric constant and loss factor. The aim of this test work was to investigate the microwave "responsiveness" of constituent minerals in the Kimberlite ores over a wide range of temperature. Knowledge about microwave responsiveness of constituent minerals in an ore enables assessment of the potential for microwave assisted process benefits. It has been stated that microwave absorbing metallic based ores in a non absorbing gangue matrix offer the best opportunity for microwave assisted comminution and liberation due to ore weakening as a result of differential expansion. It is thought that dehydration of hydrated minerals in a microwave field may also offer some downstream process benefits, especially ore weakening due to thermal destabilization of the lattice structure.

4.7.2 Method for Determining Mineral Dielectric Properties

The cavity perturbation technique was used to determine the variation of dielectric constant and loss factor with temperature for each mineral. A representative portion of each mineral used for XRD examination was reserved for this test. Each sample was thoroughly mixed using a rotary sample divider. About 10 g of pulverised mineral was encased into a 4mm quartz tube holder of known mass. To ensure uniform packing density, the material was compressed using a vibrator for a specified number of strokes. The mass of the holder and mineral sample was also taken. The volume of the

sample was computed from the sample length and internal diameter of the holder.

The system used for this work is shown in Figure 4.12. It consisted of four major components i.e. the network analyser, cavity, furnace and computer. The sample holder was carefully inserted into the cavity and fixed to the lever arm system. The lever system was linked and controlled by computer and was able to move upward and downward to three pre set positions. This allowed the sample to be positioned inside the furnace during the heating phase and downward into the cavity when measurements at a specified temperature were to be taken. The furnace temperature was controlled by a computerised thermostat and a water load was used to dissipate the extra heat.

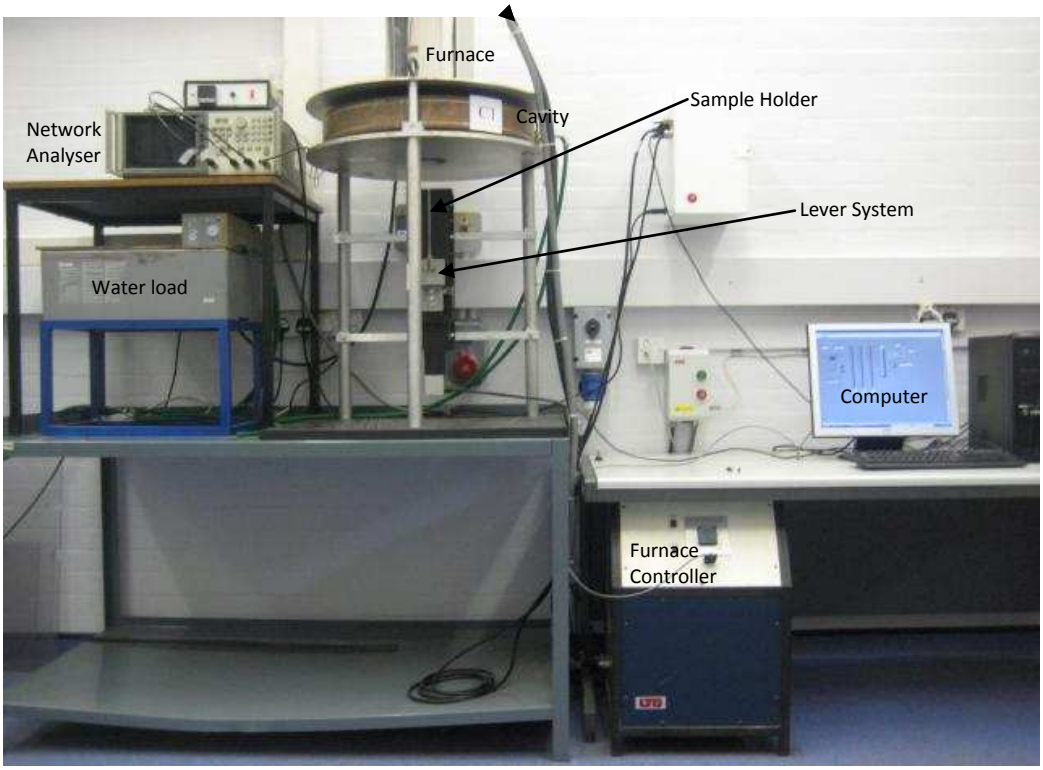

Figure 4.12 Cavity perturbation system used for measurement of dielectric properties of different minerals

Measurements were carried out with aid of *VNA 2ii Version 1.0* program installed on the computer. The network analyser generated and sent a signal to the cavity and the frequency shift (*f*) and quality factor (*Q*) before and after the sample is inserted into the cavity were automatically recorded at resonant frequencies of 2.45GHz and 911MHz, at pre-set temperatures ranging between 20- 850^{o}C. ε'' and ε' were then computed using Maxwell's Equations 2.6 and 2.7. An Excel spreadsheet shown in Appendix II was used to ease the computation.

4.7.3 Results of Mineral Dielectric Properties

The full results of the measured values of the dielectric constant (ε') and the loss factor (ε'') are given in Appendix II. Figures 4.13 and 4.14 show the variation of ε' with temperature.

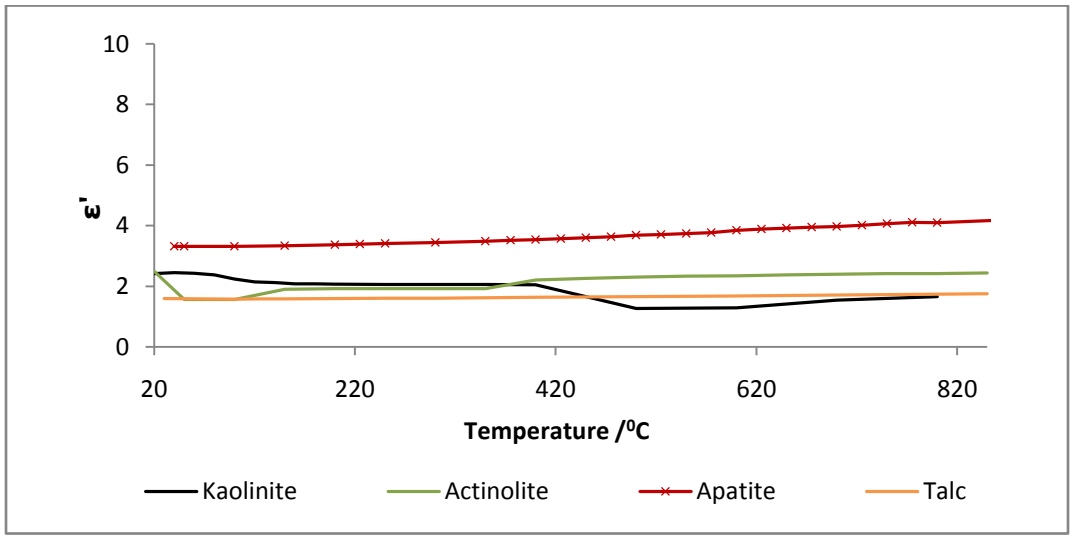

Figure 4.13 Minerals which showed little or no change in ε' values with temperature

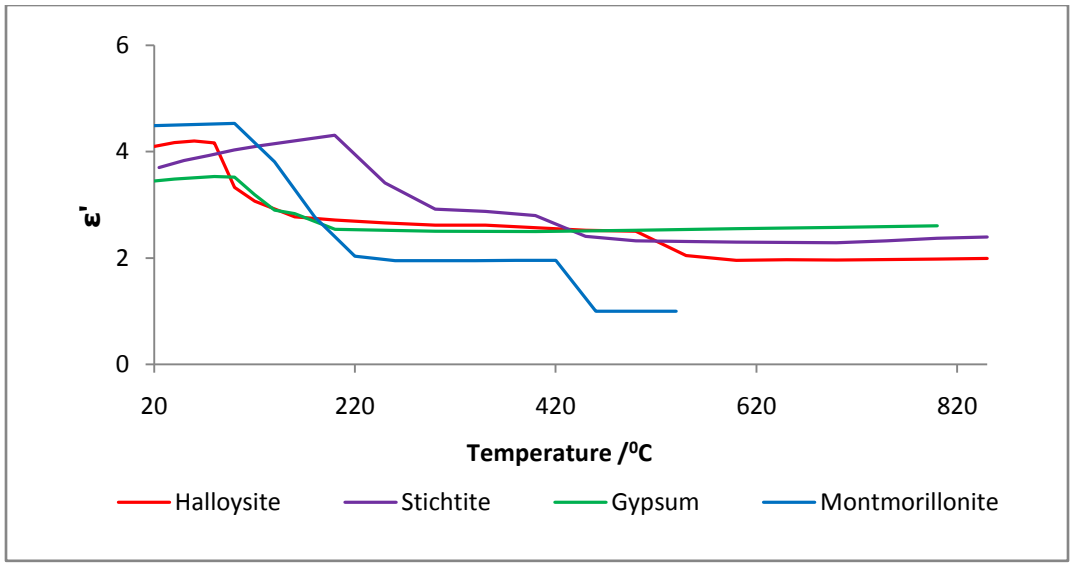

Figure 4.14 Minerals which showed significant change in ε' values moving from the low temperature region between 20-200 ^{0}C

The above results show that, within a certain temperature in the range of 20-200^{0}C, some minerals such as gypsum, stichtite, halloysite and montmorillonite attain peak values which are significantly higher and there is potential for interaction with the applied electromagnetic energy at these temperatures. Other minerals such as talc, actinolite, kaolinite and apatite do not exhibit this trend. The major mechanisms by which energy may be stored by a material irradiated with microwaves are exhibited in the conduction or polarisation properties of the material, as was discussed in Chapter two. The composition (see Table 4.5), structure and properties of the minerals do not suggest any significant conducting or dipolar polarisation potential. The apparent changes in stored energy are therefore most likely related to water associated with these minerals as will be discussed later in this section.

Figure 4.15 and 4.16 show the variation of loss factor, ε'' with temperature. This corresponds to a measure of ability of the minerals to dissipate stored

energy into heat. By comparison with known good heaters of microwave energy, such as water (ε'' =77 at 25°C), the values obtained in this study are low and range just between 0 and 1.

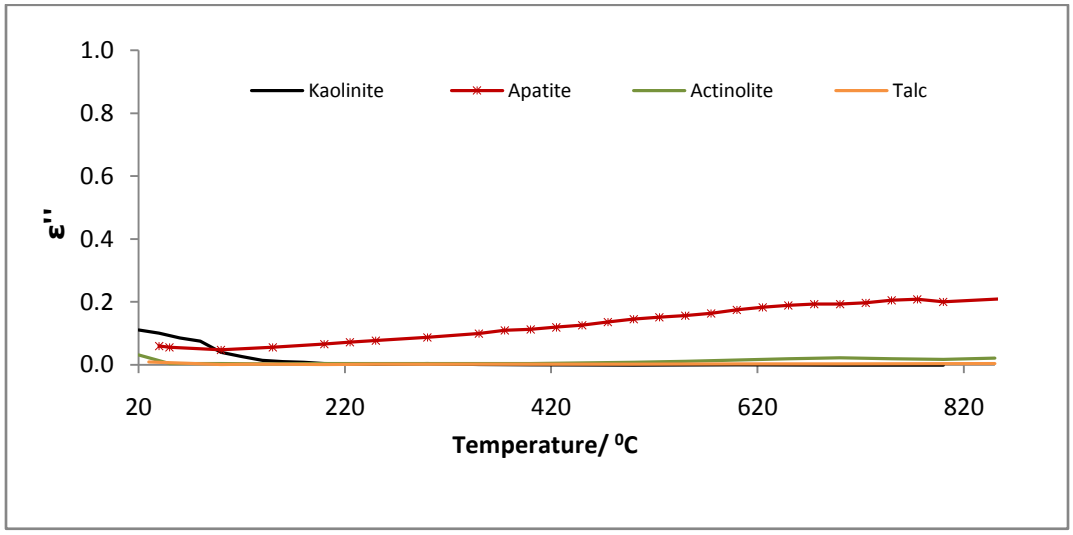

Figure 4.15 The variation of ε'' values with temperature for minerals which showed little or no change in ε' over the whole temperature range

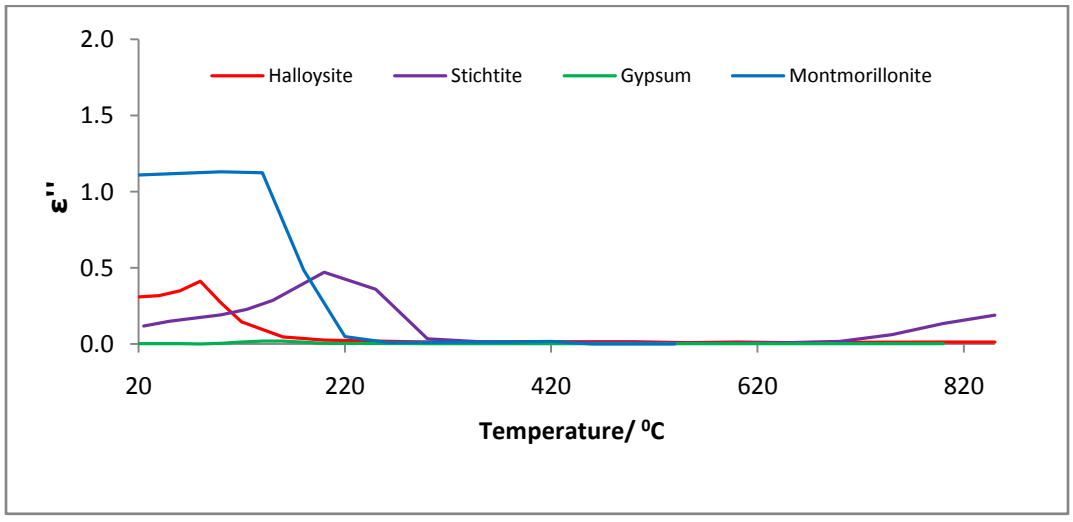

Figure 4.16 The variation of ε'' values with temperature for minerals which showed significant values of ε' in the low temperature range

With exception of gypsum, all other minerals (montmorillonite, halloysite and stichtite), which showed significant higher values of ε' in the low temperature region, exhibit correspondingly higher values of ε'' in the same temperature range. Montmorillonite in particular has a loss factor greater than 1 up to approximately 150^0C. According to Metaxas and Meredith (1983), materials with loss factors greater than 0.02 are deemed to be likely dielectric heaters. Accordingly, in the low temperature region indicated, montmorillonite, stichtite and halloysite may be deemed good heaters of microwave energy.

As stated previously in this chapter, the apparent microwave energy storage and dissipation properties of the minerals studied are likely to be associated with water contained in these minerals. It was stated that water may exist in minerals in different forms and requires varying amounts of thermal energy to be removed. A study of the dehydration properties of the minerals was presented in the last section. Figures 4.17 to 4.20 present a comparison between the dielectric properties and the dehydration characteristics of the minerals.

Talc, actinolite, apatite and kaolinite incorporate water only in the form of hydroxyl ion (OH) which may be removed via a dehydroxylation process. The results shown in Figure 4.10 indicate that dehydroxylation is achieved at temperatures above 400^0C. When this occurs, there is a corresponding decrease in the dielectric constant possibly as result of a decrease in overall polarisability due to loss of OH group.

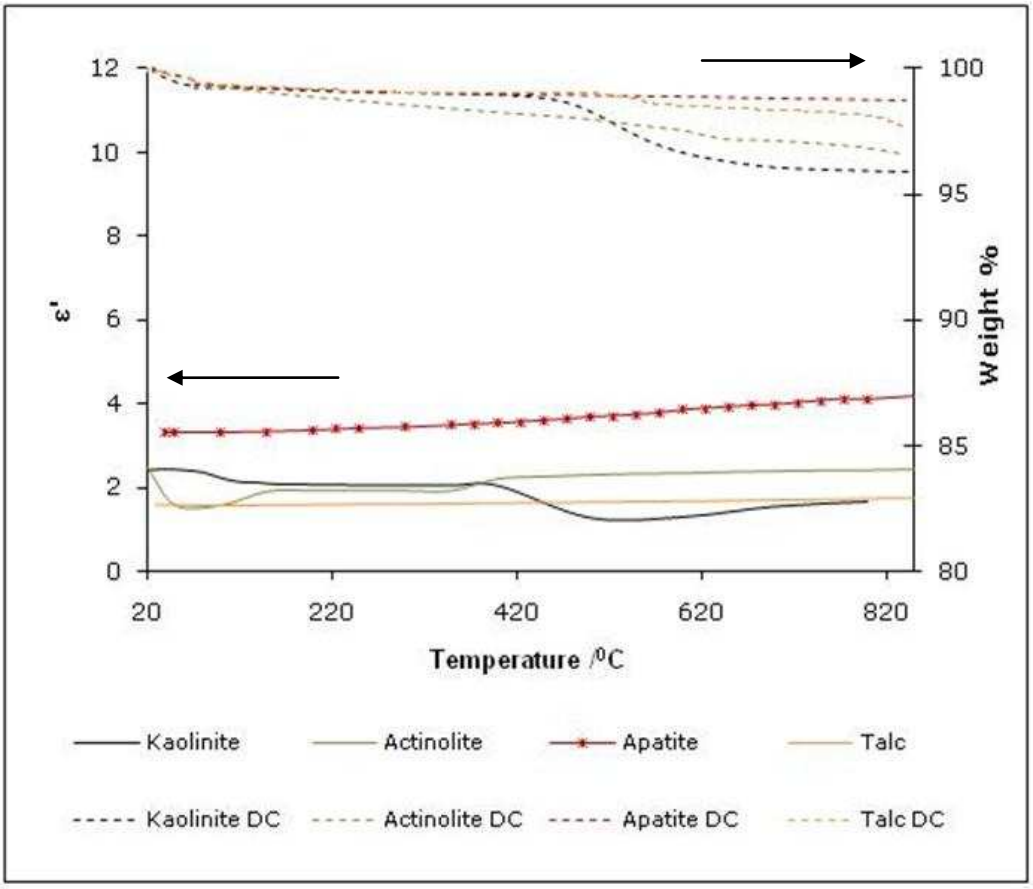

Figure 4.17 Comparison between dielectric constant and dehydration curves of minerals which show little or no change in values of ε' with temperature

Actinolite indicates some decrease in the dielectric constant in the low temperature region (at about 70°C) perhaps as a result of the presence of adsorbed surface water. This temperature is insufficient for dehydration which according to Tudor (1976) occurs at between 800 and 1000°C. The dielectric constant of apatite at ambient temperature is similar to that of the water bearing clays indicating a similar degree of polarisability, although the room temperature loss is much lower.

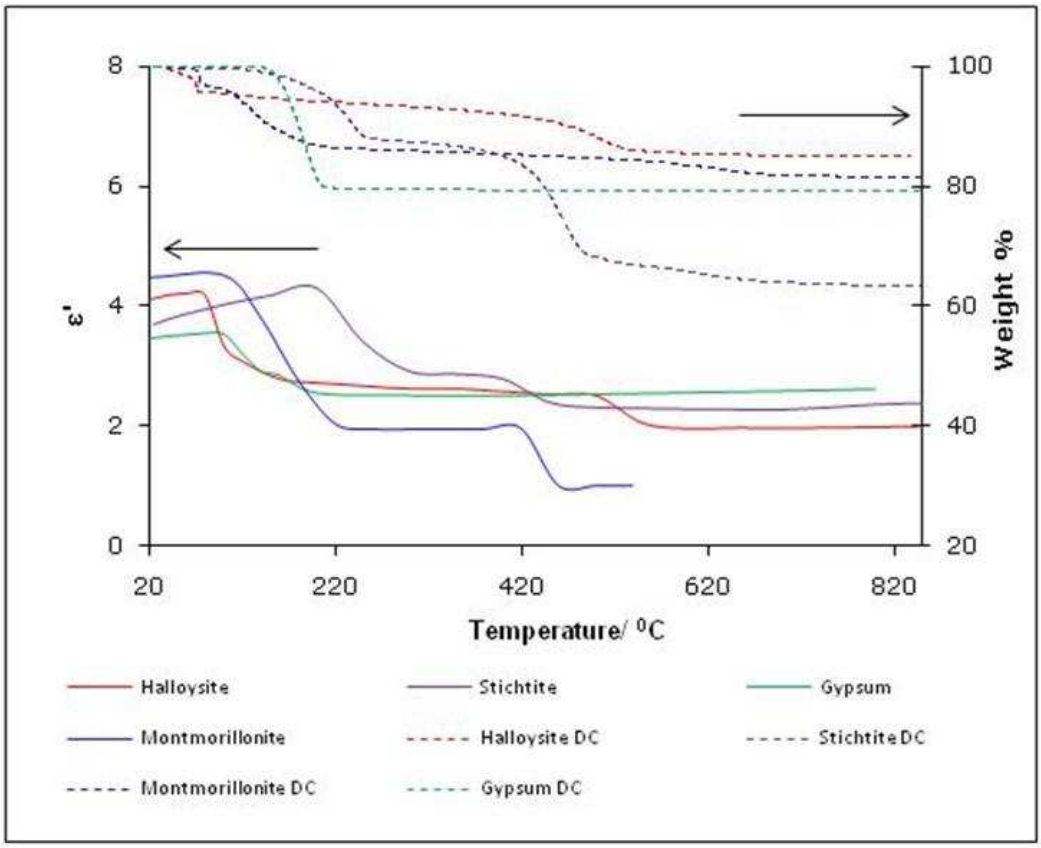

Figure 4.18 Comparison between dielectric constant and dehydration curves of minerals which show significant change in values of ε' with temperature

Gypsum contains both hydroxyl ions and water of crystallisation. Water of crystallization is removed at lower temperatures than those required for OH removal (in the range of 150-200^{0}C). Gypsum shows a decrease in the dielectric constant after dehydration but has very low values of loss factor over the whole temperature range and no noticeable change in loss factor is observed after dehydration.

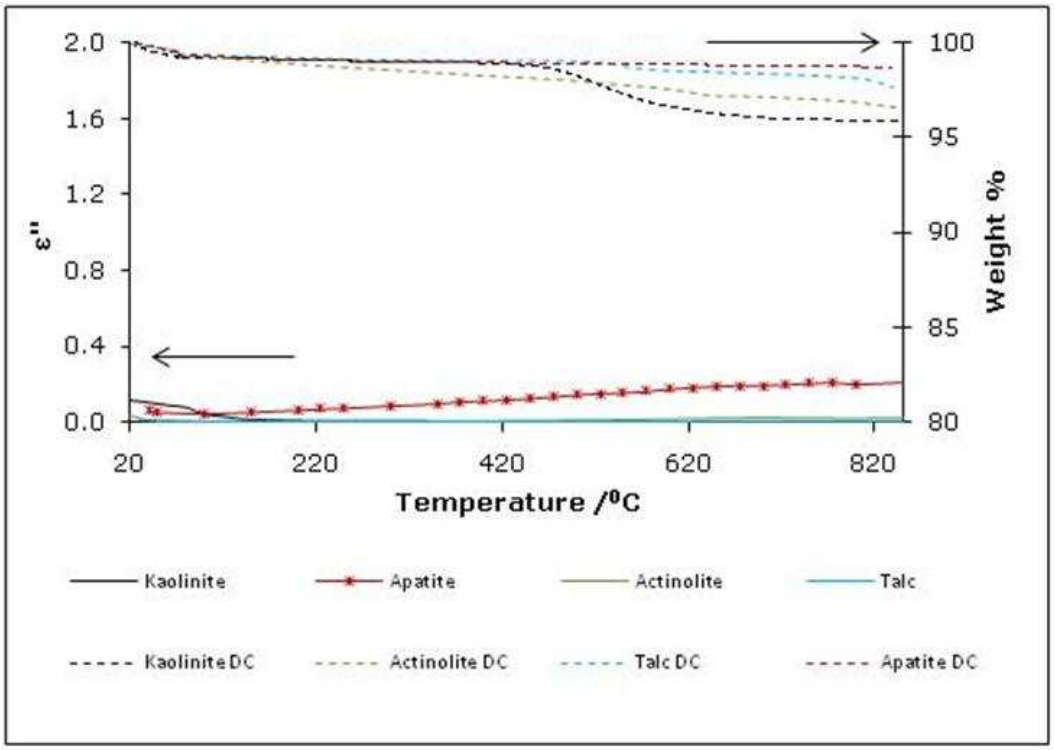

Figure 4.19 Comparison between loss factor and dehydration curves of minerals which showed little or no change in ε'' over the whole temperature range

Montmorillonite and halloysite contain adsorbed interlayer water in addition to structural hydroxyl (OH) groups. Interlayer water is removed at much lower temperatures compared those required for OH removal (in the range 70-150^{0}C). These clays also show significant gradual low temperature weight losses which correspond to the loss of interlayer water. Figures 4.14 and 4.16 show that between ambient temperatures up to about 150^{0}C, montmorillonite and halloysite have values of ε′ and ε′′ high enough to be considered good absorbers of microwave energy. It is also clear that there is a drop in both ε′ and ε′′ after about 100-150^{0}C which corresponds to the low temperature dehydration zone on the TG curves. Interlayer adsorbed water therefore seems to affect the dielectric properties of minerals more significantly than water yielding from dehydroxylation of structural OH. Stichtite also incorporates both interlayer water and structural OH. The weight loss

corresponds to a decrease in the dielectric constant and also a decrease in the "peak" loss factor attained before dehydration, indicating the influence of the interlayer water on microwave absorption.

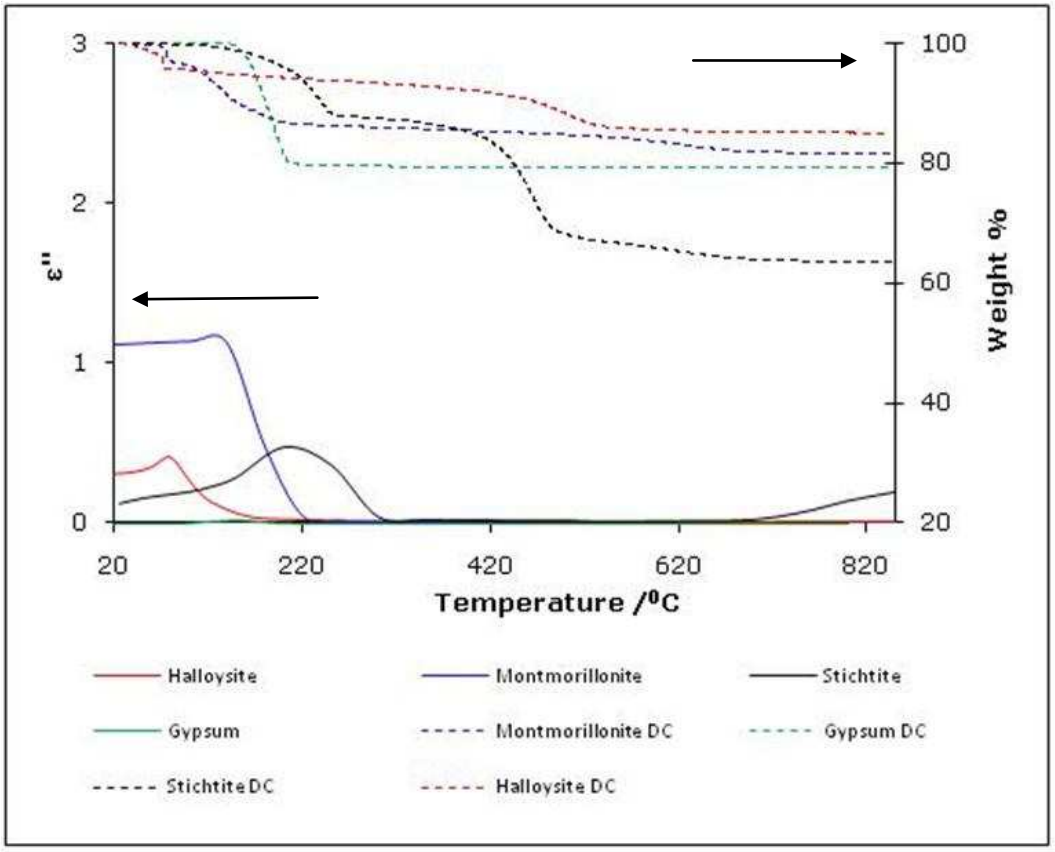

Figure 4.20 Comparison between loss factor and dehydration curves of minerals which showed significant change in ε'' in the low temperature region

It appears that the dielectric properties can be inferred from the thermo-gravimetric curves. TGA analyses provide an indication of the level of intrinsic and extrinsic bonding of the water yielding species and in that sense an indication of the potential for reorientation in an electromagnetic field. The results show that low temperature weight loss is associated with higher values of both the dielectric constant and loss and when dehydration takes place, this is attended by a drop in both ε' and ε''. It is therefore clear that a direct

relationship between dielectric properties and dehydration characteristics exists.

The differences between the measured dielectric properties of the selected minerals can be explained in general terms by the structure of the water yielding species. The clays incorporating interlayer water show significant values of both dielectric constant and dielectric loss at low temperatures and therefore potential exists for dehydration in a microwave field. However, based on the dielectric properties, phyllosilicates not incorporating interlayer water are unlikely to heat rapidly in a microwave field unless external thermal energy is supplied by conduction. These results imply a difference in the microwave behaviour of absorbed water and structural OH which may be explained by considering the relevant mechanisms giving rise to the dielectric effects. It is likely that the loosely bound absorbed water within the interlayer clays behaves in a similar manner to the free water in an electromagnetic field. In this case the dielectric constant arises from alignment of water dipoles to the field. The dielectric loss originates from lag of the dipole behind the field, leading to an energy loss by heating. The hydroxyl groups within the minerals do not impart high dielectric constant or dielectric loss, although there seems to be some increase in the dielectric constant on dehydration. This is in contrast to polar solvents incorporating OH groups such as alcohols, which heat rapidly in a microwave field. The forces opposing dipole OH reorientation in the crystalline solid are profoundly higher than those in the liquid solvent, and may not generate kinetic energy via rotation and molecular friction.

From the preceding discussions, it seems like individual minerals that may heat and yield steam on microwave treatment will be either swelling clays or minerals with water of crystallization where removal occurs at low temperatures, ideally less than 150^0C. The dehydration temperatures required for clays are easily achievable during microwave treatment. The results also suggest that dehydroxylation is unlikely to take place. However, there may be potential that in a multi-mineralic ore with highly absorbent metal oxides or sulphide, additional thermal energy could be provided by association with these phases in which case dehydroxylation may be possible. This is possible since due to the selective heating nature of microwaves very high temperature spots can occur within the ore compared to the overall bulk temperature.

This study has suggested that ores containing hydrated mineral phases may become responsive to microwave heating. From the microwave assisted mineral processing point of view, these results show that potential for microwave treatment of the Kimberlite ores in particular and certain hydrated ores in general exists

4.8 Microwave Treatment of Ores and Minerals

4.8.1 Introduction

Prior to this work, the downstream process benefits of pre-heating ores with microwave energy have been demonstrated only for metallic based ores with a matrix of microwave absorbing and non-absorbing mineral phases. The results obtained in this work, so far, have suggested potential applications for microwave heating in non metallic based ores which contain hydrated minerals. Microwave heating of ores containing hydrated minerals is thought

to cause weakening of the ore through a mechanism associated with dehydration. Several theories that are associated with microwave induced fracture in ores containing hydrated minerals have been proposed in this work. It is thought that fracture may be initiated or enhanced by any or a combination of the following:

- Expansion of certain mineral phases (e.g. swelling clays such as smectite, halloysite and montmorillonite)
- Differential thermal expansion as a result of very high temperature spots within steam yielding mineral phases
- Loss of water of crystallisation leading to lattice structural defects e.g. in gypsum
- Thermal decomposition of certain minerals phases
- Internal pressure resulting from steam yielding minerals

The significance of the above mechanisms was investigated by irradiating samples of ore with microwave energy and using a combination of chemical, optical and strength characterisation techniques to analyse treated ore samples. Microwave treatment was also carried out on minerals shown in Table 4.5, which represent the different categories of hydrated minerals in the ores under investigation. The heating rate of each mineral was investigated. TGA and XRD analysis was then carried out on the treated mineral samples. Other observations like changes in bulk volume, steam evolution and decomposition were also noted during and after microwave heating.

The ores selected for this study also provide a means to compare and understand the different mechanisms of microwave induced fracture in ores. The Los Bronces copper ore and the Nebo Babel nickel-copper ore provide

mineral assemblages with good absorbers of microwave energy in a transparent gangue matrix. It therefore represents ore types previously described as good candidates for microwave pre-treatment. Subjecting the Kimberlite ores to the same treatment conditions provides an excellent method of evaluating the effectiveness of microwave pre-treatment of hydrated ores. The fracture patterns were analysed using electron microscopy and the mechanical strength of treated and untreated ores compared using strength characterisation techniques.

4.8.2 Methodology for Treatment of Ore Samples

The size of the microwave cavity used for this work required that sample particles do not exceed approximately 30 mm so as to allow a reasonable number of particles to be treated per batch. In addition, the samples were required to be suitable for point load and PUNDIT ultrasonic tests (described in Section 4.10) which were conducted on the particles after microwave treatment. The "as received" ores had been screened and sampled prior to MLA test work as was described earlier in this chapter. The lumps of ore from which thin sections were taken for MLA mineralogical analysis were sawn into rectangular blocks. This was done in order to provide smooth parallel contact surfaces for the point load tester platens and PUNDIT coupling. This enables accurate measurement of the distance between the contacts and, in the case of PUNDIT test, it is also necessary to have good contact between the coupling and material. The sized block samples were then split into four groups by distributing a particle to each group on a one by one basis. One group of particles was not treated and the remaining sample batches were irradiated with microwaves under different treatment conditions as shown in Table 4.6.

The system used consisted of a variable microwave generator capable of operating up to a maximum power of 30 kW, connected to a single-mode cavity applicator via an automatic E-H tuner. The tuner matches the impedance of the transmission line to the load, ensuring a minimum amount of reflected power. Microwaves are directed from the magnetron to the applicator by WR430 waveguides. The reflected power is directed to the circulator and absorbed by a re-circulating water load.

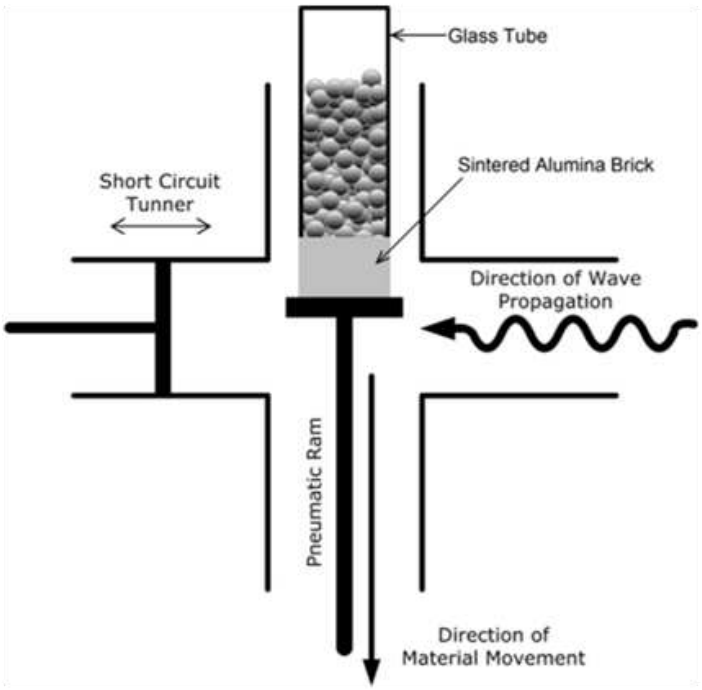

Figure 4.21 Cross section of single mode cavity used for treatment of ore particles (AMIRA, 2006)

The mass, *m* (g) of the batch sample to be treated was taken and the samples were then placed in a cylindrical glass tube. The packing density, *D* (g/m) was calculated after measuring the sample length. The tube was then passed vertically down through the single mode cavity using a pneumatic system as shown in Figure 4.21. The treatment time, *t* (s), which was the time taken for

the sample to fall through the cavity, was recorded. The treatment time was set and varied by adjusting the speed of the pneumatic system. The stroke speed (m/s) was then calculated from the treatment time (t s) and the distance between the top and bottom pneumatic positions.

Samples were treated under three different conditions by either varying the treatment time or by varying the microwave generator power level (Table 4.6). An assumption was made that all the net power output was absorbed by the material. The energy in kilowatt hours per tonne expended in treating the samples was calculated from:

$$Energy\ Expended\ (kWh/t) = Net\ Power\ (kW)/Flow\ Rate\ (t/h)$$

Sample ID	Mass	Packing Density	Time	Stroke Speed	Flow Rate	Forward Power	Reflected Power	Net Power	Energy
	g	g/m	s	m/s	t/h	kW	kW	kW	kWh/t
NB T1	982	5036	0.25	1.00	18.1	15	1.7	13.3	0.73
NB T2	974	4995	0.25	1.00	18.0	20	1.5	18.5	1.03
NB T3	991	5082	1.10	0.23	4.2	23	3.0	20.0	4.81
LB T1	850	4361	0.25	1.00	15.7	20	7.0	13.0	0.83
LB T2	859	4403	1.10	0.23	3.6	21	10.0	11.0	3.05
LB T3	852	4367	2.75	0.09	1.4	20	10.0	10.0	7.00
Ek I T1	1196	21745	7.40	0.03	2.6	22	4.0	18.0	6.81
Ek I T2	1100	20000	12.50	0.02	1.4	25	0.4	24.6	17.08
Ek I T3	1338	24327	17.00	0.02	1.3	26	14.0	12.0	9.32
Ek II T1	922	16769	3.50	0.07	4.3	27	4.0	23.0	5.33
Ek II T2	1020	18553	7.86	0.03	2.1	26	4.0	22.0	10.36
Ek II T3	957	17400	10.00	0.03	1.6	26	4.0	22.0	14.05

Table 4.6 Microwave treatment conditions for the different batch tests conducted

The choice of the treatment conditions in this work was influenced by the following:

- Observations made from heating trials conducted on the ores
- Previous work by other authors who investigated microwave induced fracture in metallic based ores such as Kingman et al (1999 and 2004), Jones et al (2004 and 2006), Olubambi et al (2007) and Scott et al (2007)
- Limitations of the microwave system used. For example it was difficult to maintain similar power levels for different batch tests because the reflected power fluctuated and could not be easily maintained. This is because the reflected power was dependent on other things such as the packing density of the batch sample and the dielectric properties of the ore, all of which vary from one batch sample to another.

Based on previous work which was discussed in the last chapter, the system used did not provide an efficient method of treatment because the power levels used for treatment were too low and therefore much longer heating times were required to compensate for the low power. This study was conducted bearing in mind that the energy expended in treating the samples cannot be used as a basis for assessment of the economic feasibility of microwave pre-treatment. As stated previously, the major objective of this study was to demonstrate the occurrence of microwave induced fracture in ores containing hydrated minerals and investigate the mechanisms under which it occurs. The engineering developments required on the existing equipment and the methods of power delivery that suggest a more efficient treatment method have been discussed by other authors such as Whittles et al (2003), Kingman et al (2004) Jones et al (2005 and 2007) and Wang et al (2008).

4.8.3 Results of Microwave Ore Treatment

Figures 4.22 and 4.23 show the extent of damage observed in some samples after microwave treatment. It can be seen that significant damage was induced in all ore types studied including the Kimberlite ores which did not contain microwave absorbent semi conducting minerals. The observed fracture patterns and severity varied significantly in each ore and also varied in particles of the same ore. Some particles developed a network of visible multiple minor and major cracks while in others only one or two major cracks that completely split the particle into smaller pieces were observed. Only a small proportion of particles did not exhibit any visible cracks.

There was a tendency for greater damage to occur when samples were heated either for longer durations or when a higher power was applied. This observation was more pronounced in the Kimberlite ores than in the other two ores. It appeared that the magnitude of fracture increased with increase in energy input. At this stage, it was unclear whether damage was more associated with duration of heating or the applied power. The fracture patterns also seemed to be influenced by the mineralogy and texture of each particle. There was evidence of very hot spots and arcing around grains of hematite and a tendency for cracks to originate from these spots. These areas are shown highlighted in red in Figure 4.22. No such spots were observed in the Kimberlite ores.

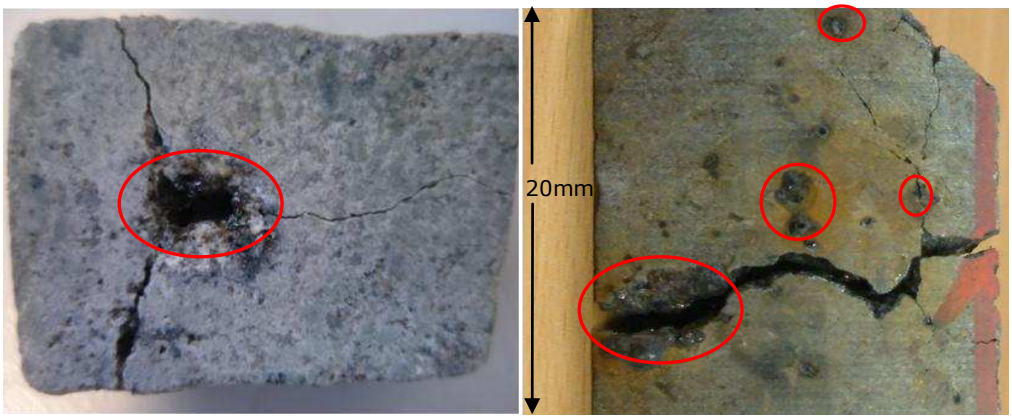

Figure 4.22 Damage to ore sample blocks after microwave treatment. (Left) A Los Bronces Cu ore sample treated at 11 kW for 1.1 s. (Right) A Nebo Babel Cu-Ni sulphide ore treated at 20 kW for 1.1s

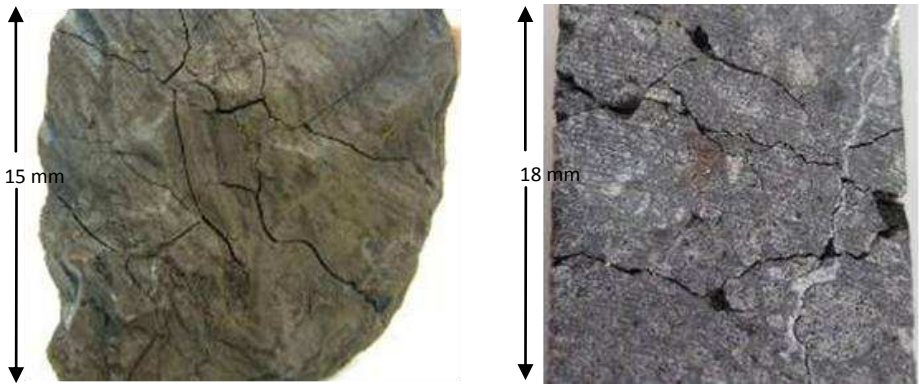

Figure 4.23(Left) A Kimberlite II ore sample treated at 22 kW for 10 s (Right) A Kimberlite I sample treated at 18 kW for 7.5 s

The mechanism of microwave induced fracture in metallic based ores has been investigated extensively by other authors such as Jones et al (2004 and 2005). This study focussed on explaining the fracture patterns observed in the Kimberlite ores and deducing the major mechanism(s) for microwave induced fracture in hydrated minerals. In order to understand the fracture patterns, sections of selected particles were examined microscopically. Figure 4.24 shows a typical BSE image of a section of an untreated Kimberlite I ore.

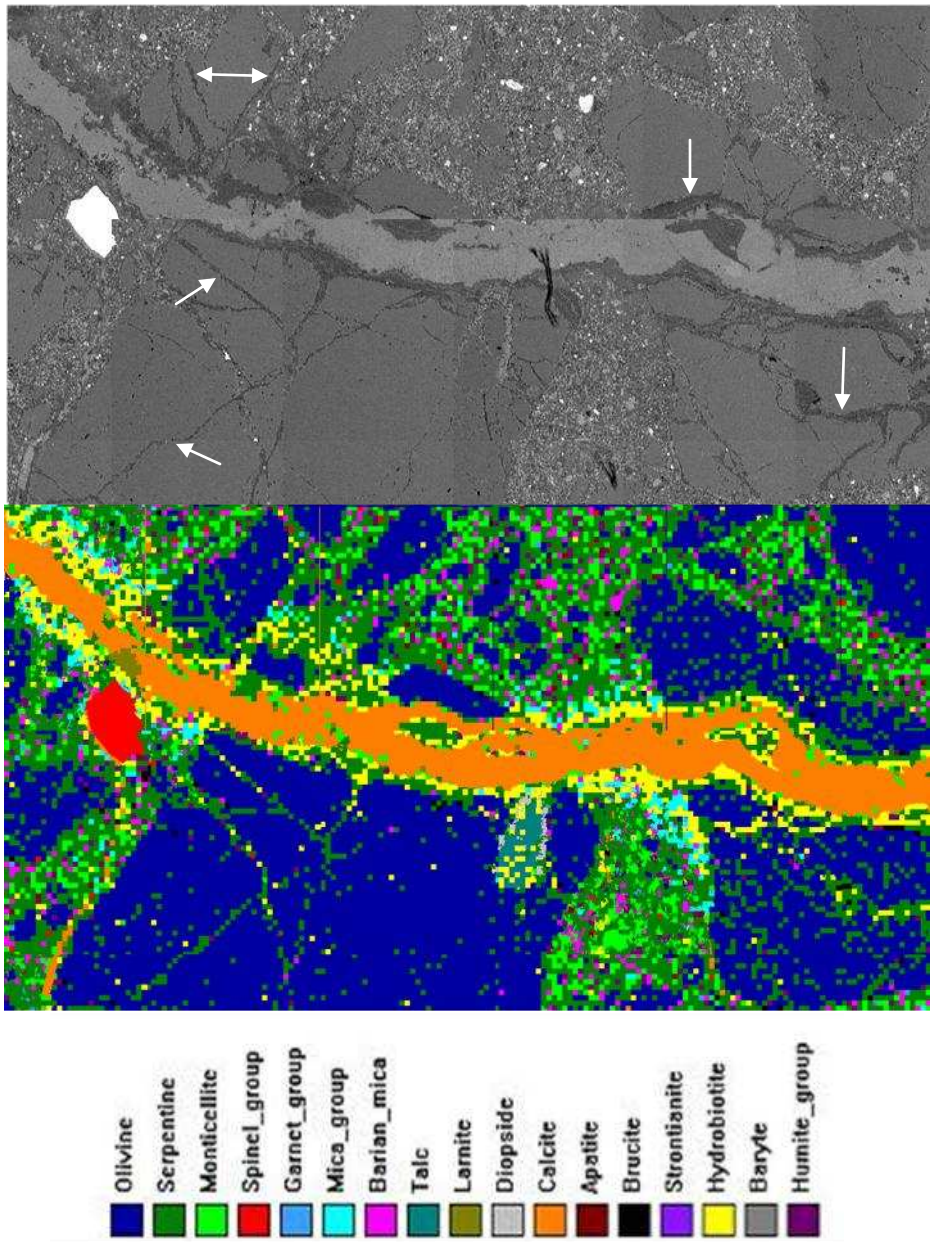

Figure 4.24 BSE image of an untreated Kimberlite I ore showing existing minor, randomly oriented cracks

It was observed that there were existing small, randomly oriented, fractures before microwave treatment, as shown by white arrows in Figure 4.24. These cracks could have been related to geological effects and/or as a result of crushing. However, after microwave treatment, significantly larger fractures were observed to follow light coloured veins and also axially within the calcite

phase. The position of the fractures is indicated by the white arrows in Figure 4.25. The region highlighted in red has been magnified to show the micro cracks clearly.

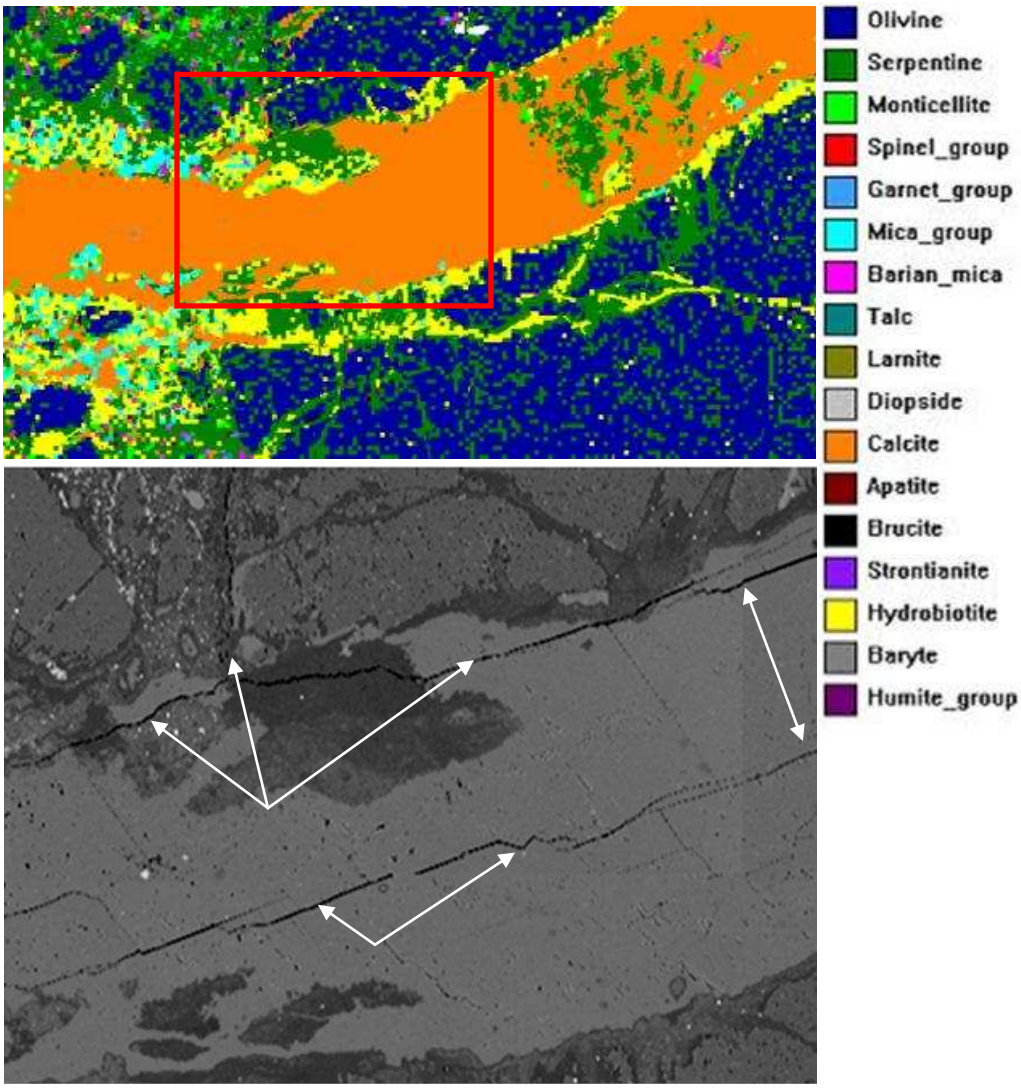

Figure 4.25 BSE image of a treated Kimberlite I ore showing significant microwave induced cracks within the calcite-hydrobiotite phase

The veins dominated by fracture were found to be rich in calcite and hydrobiotite. These observations suggested that the presence of hydrobiotite led to increased likelihood of microwave-induced fracture in the localised area.

It is almost certain that the presence of a mineral phase incorporating interlayer water or with a composition close to hydrobiotite will show similar effects. It is also likely that the calcite is compressed on all sides by the pressure generated from the superheated interlayer water to such a degree that compressive fracture occurs within the calcite veins. Figure 4.26 shows a high magnification image of a region of hydrobiotite adjacent to a crack.

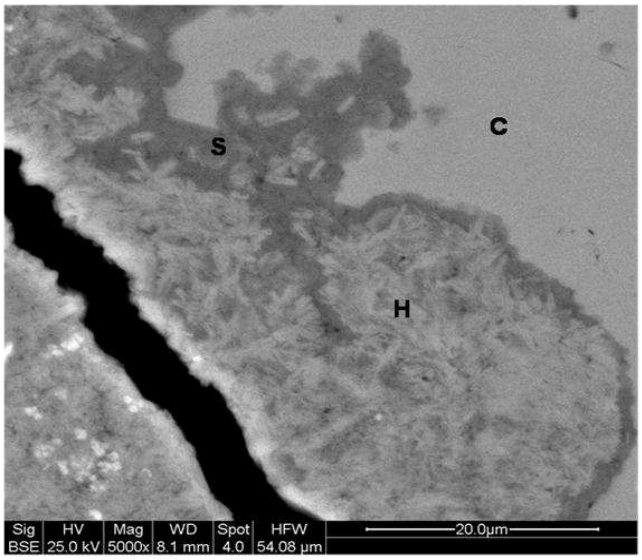

Figure 4.26 BSE image showing a microwave induced crack within the hydrobiotite layer

Microwave fracture in hydrated minerals, therefore, seems to be dependent on the presence of minerals with interlayer water. The dissemination of these minerals within the ore is also likely to affect the severity of damage caused. This perhaps explains why more particles of the heavily weathered Kimberlite II ore were severely fragmented by microwave treatment with some particles effectively turning to dust as shown in Figure 4.27.

Figure 4.27 Kimberlite type II ore before and after microwave treatment

Figure 4.4 and Table 4.4 show that the Kimberlite II ore is almost entirely composed of clays, mainly smectite. The average clay content in the measured specimens was over 50% by weight or area. It is worth noting that not a single particle of the Kimberlite I ore showed similar fragmentation characteristics. It is also possible that particles that showed less or no damage at all after microwave treatment lacked the threshold amount of hydrated minerals to induce fracture as the content of hydrobiotite in the Kimberlite I ore was found to vary greatly. The weight percentages given in Table 4.4 are averages of each mineral in the measured specimens but the content of hydrobiotite in the individual specimens as shown in Appendix I varied between 0-17 percent.

The propagation of the induced fractures was observed to preferentially follow the weaker paths around grain boundaries. This is illustrated in Figure 4.28 in which the crack network follows the olivine phenocryst-calcite interface. Such fracture patterns have potential to increase grade-recovery of minerals by preferentially liberating mineral grains.

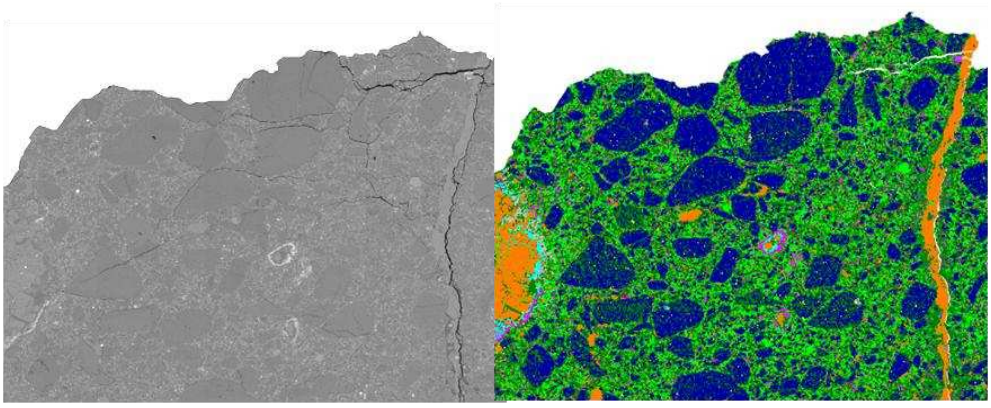

Figure 4.28 Extensive intergranular crack propagation in a microwave treated Kimberlite I ore.

4.8.4 Method for Microwave Treatment of Mineral Samples

Only small amounts (about 1-2 g) of each mineral were available for this test work and therefore a different treatment method from the one described above was designed for this test. The system used consisted of a 1.5 kW variable microwave generator connected to a single mode cavity similar to the one described in the last section but without a pneumatic system. About 0.1-0.5 g of a representative portion of the sample which was used for previous XRD work was obtained using a rotary sample divider. A test run using the mineral to be tested was first used to set the power level to 1 kW by adjusting a short circuit tuner. The real sample which was encased in a quartz tube holder was then lowered and positioned in the central axis position of the cavity. An optic fibre thermocouple was used to monitor the temperature of the sample during heating. The heating time and the maximum temperature attained during heating were recorded. All samples were heated for a maximum of 10 s.

4.8.5 Results from Microwave Heating of Minerals

The maximum temperatures recorded from microwave heating of mineral samples are shown in Table 4.7. Sodium montmorillonite heated very rapidly with temperatures rapidly exceeding the 250^0C temperature limit of the thermocouple with massive evolution of steam. The heating was stopped after only two seconds. Halloysite also heated rapidly to 209^0C after only 4 s. Other minerals such as talc, Kaolinite, actinolite and apatite did not show any significant temperature change after 10 s of exposure to microwaves. Biotite and gypsum recorded a slight increase in temperature.

Mineral	Time (s)	Max Temp (° C)	Comments
Talc	10	40	
Kaolinite	10	56	
Halloysite	4	209	heats rapidly
Na-montmorillonite	2	>250	rapidly heats above 250^0C
Actinolite	10	36	
Apatite	10	32	
Gypsum	10	68	
Stichtite	10	122	gradual temperature rise
Biotite	10	66	

Table 4.7 Results from microwave heating of mineral samples

The results obtained show a heating pattern which agrees with the dehydration curves and dielectric properties of the minerals. Minerals with interlayer adsorbed water which showed low temperature dehydration and high values of ε'' and ε' in the low temperature region heat rapidly and evolve steam when exposed to microwave energy. It is probable that microwaves provide enough thermal energy to cause low temperature dehydration of interlayer water but not enough energy to drive out water of crystallization or

structural OH water. Steam evolution and differential heating of certain mineral phases may therefore contribute to microwave induced fracture in ores containing hydrated minerals. The results show that dehydration of water of crystallization can only take place if enough thermal energy is provided via conduction from superheated phases but not as a result of direct interaction of the mineral with microwave energy. A model of temperature distribution within the different mineral phases can demonstrate whether this is possible but that is outside the scope of this work.

Microwave heating also caused swelling and expansion of halloysite and montmorillonite samples as shown in Figure 4.29. The expansion was more significant in montmorillonite which expanded by nearly twice the original volume.

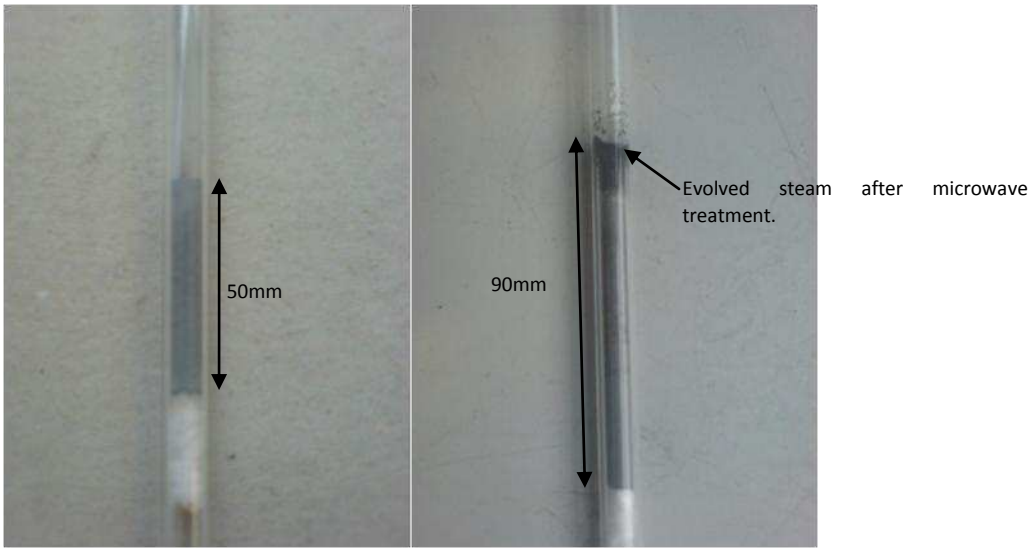

Figure 4.29 Montmorillonite sample before and after microwave heating

Swelling occurs most likely as a result of expansion and steam evolution. Thermal expansion of clay minerals therefore contributes to microwave induced fracture. TGA and XRD analysis of microwave heated mineral samples

revealed that no chemical changes occurred. The dehydration curves obtained for treated minerals matched exactly those obtained for untreated samples which are shown in Figure 4.10. This demonstrates that microwave heating only results in loss of interlayer water, which is reabsorbed on cooling. Thermal decomposition therefore does not seem to contribute to the observed fracture. Microwave induced fracture seems to be triggered by providing sufficient thermal energy to cause dehydration. When the latter occurs, the evolved steam is rapidly heated by microwaves to cause superheated layers which expand resulting into fracture.

4.9 Quantification of Microwave Induced Damage

4.9.1 Introduction

The above results have demonstrated that microwave heating may induce fracture in hydrated minerals of a magnitude comparable to that observed in metallic based ores. The weakening caused is believed to improve comminution and reduce grinding energy. There have also been suggestions of likelihood in increase in liberation and this will be investigated in the next chapter. It is necessary to have a method for characterisation of microwave induced damage in order to:

- Provide a means for quantifying the magnitude of induced damage
- Provide a quick method for predicting how the induced damage relates to process benefits such as comminution energy consumption and mineral liberation
- Provide an opportunity to determine optimum treatment conditions i.e process benefits versus input requirements

- Be able to compare the magnitude of fracture induced in different ores and infer their suitability for microwave treatment

The point load test has been reported to represent more accurately the comminution behaviour of single particles when compared to other strength parameters such as the unconfined compressive strength (UCS) and Young's Modulus (Bearman, 1991). This makes it a potentially useful test for this work. Kingman et al (2004) used the test to investigate the effect of microwave pre-treatment of ore mechanical strength and also as a basis for predicting potential comminution energy savings for microwave treated ores. Its simplicity makes it particularly attractive when compared to other material testing techniques. The point load test was adopted in this study for strength characterisation of treated and untreated ore samples. Because of the extremely varied fracture patterns observed, ultrasonic testing was also used as it is thought to be more sensitive to micro-cracking than point load testing.

4.9.2 Materials and Methods for Point Load Test

Some authors have previously stated that the point load test can be conducted on samples of any shape and that there is no need for any form of sample preparation (Bearman, 1991, Broch, 1971). Personal experiences carrying out this test have however shown that in order to avoid inconsistencies, which can at times be misleading and also affect the statistics of the results, some care needs to be taken when carrying out the test and some form of "sample preparation" may be necessary. Ore anisotropy may result in directional strength characteristics, especially in stratified ores (Amadei, 1995). When conducting the test, significant variations in breakage pressure may be observed depending on the direction of testing. Also any

existing cracks or flaws in the specimens lower the point load index so the particles to be tested need to be chosen carefully. When conducting the point load test to evaluate the effect of microwave treatment on the point load index, these precautions are necessary to be certain that the observed effects are purely as a result of microwave treatment.

The ore sampling methods and the preparation of sample blocks used for this test were described earlier in Section 4.8.2. All samples were carefully inspected for any visible pre-existing cracks in which case these were discarded. The smallest dimension of all samples used for this test was larger than 10 mm so as to eliminate the effects of "edge failure." "Edge failure" is a phenomenon which was observed when testing samples smaller than 10 mm in which case failure occurs preferentially around the corners of the block sample. Under these circumstances, the point load platens tend to knock off the edges of the sample instead of splitting the whole sample.

The apparatus which was used for point load testing is shown in Figure 4.30. It consisted of two cone shaped loading platens between which the specimen to be tested was loaded. The load was applied via the hand lever system and transmitted to the specimen. The maximum pressure, recorded in lb/in^2, at which the specimen failed, was recorded by the gauge.

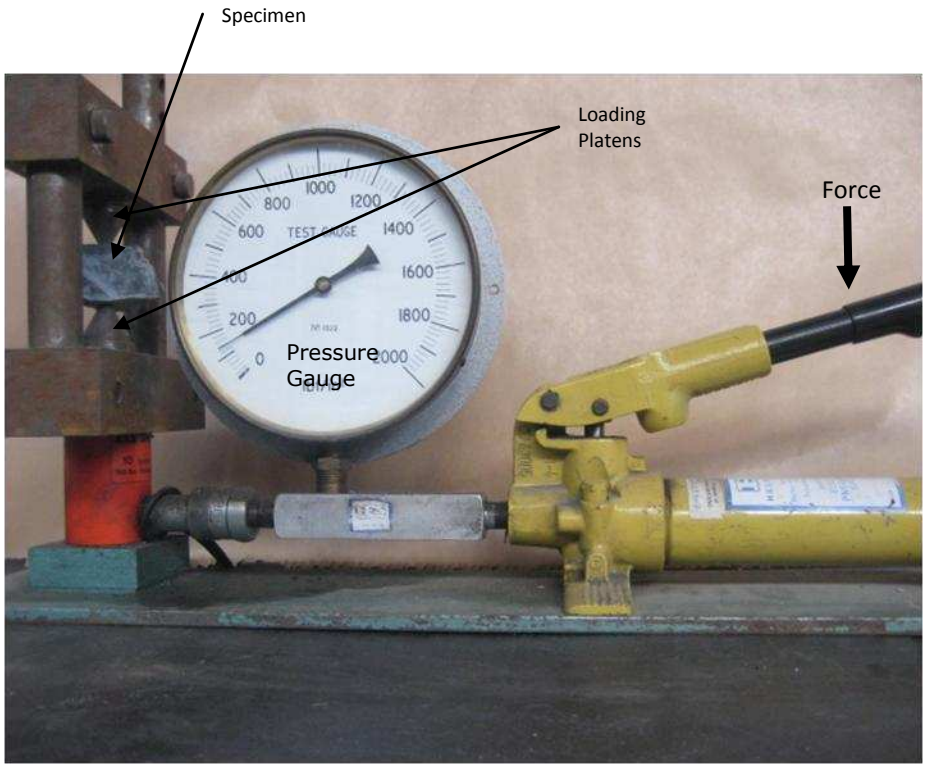

Figure 4.30 The apparatus used for point load testing

A load cell was used to calibrate the point load test gauge in order to convert the recorded breakage pressure in lb/in^2 to an equivalent breakage load (P) in Newtons. The calibration graph is shown in Appendix III. Equation 3.2 was then used to calculate the standardised point load index, $I_{s(50)}$. An Excel spreadsheet was used to ease the computation. Point load tests were conducted on several untreated and specimens treated at different treatment conditions as shown in Table 4.6.

4.9.3 Results of Point Load Tests

The full results of the measured breakage pressure of each individual particle are shown in Appendix III. Figure 4.31 shows the normalised spread of the standardized point load index $I_{s(50)}$ of the Nebo Babel sample particles tested.

Essentially, this is a plot of the measured strength indices of ninety five particles belonging to the same sample batch arranged in ascending order. The results show that the point load index of all particles tested lies between 0 and 16 MPa. The results also show a trend that suggests a reduction in particle strength after microwave treatment. For example, none of the treated particles possesses a strength index higher than 12 MPa. The batch of particles treated at 20 kW for 1.1 s exhibits the highest reduction in strength.

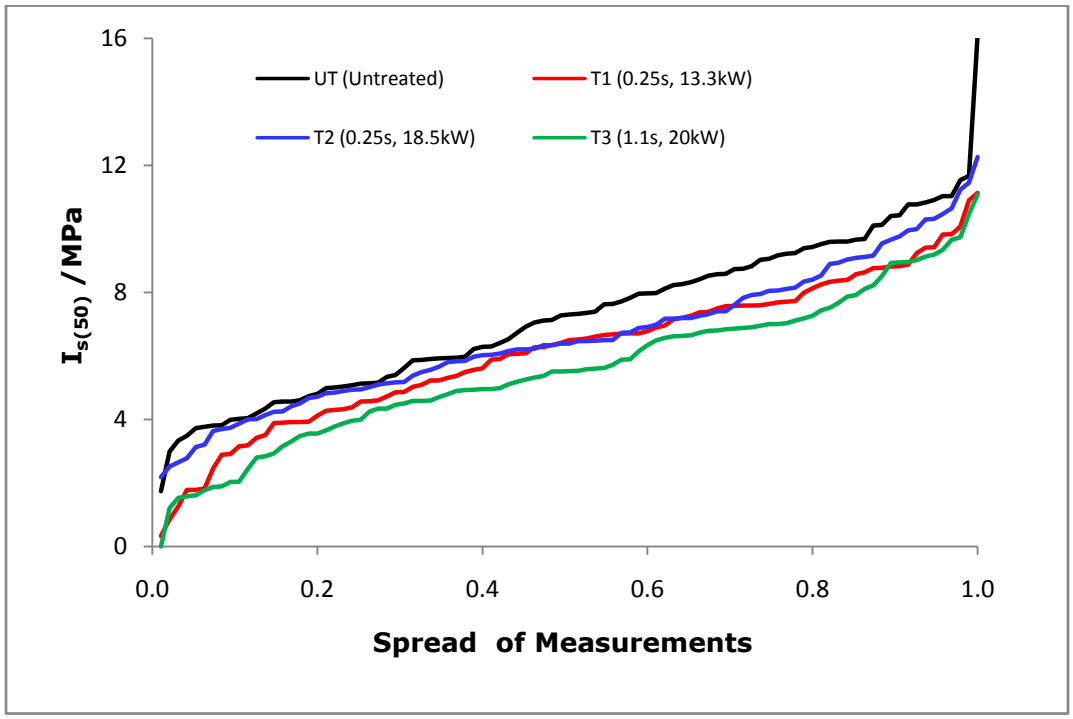

Figure 4.31 Spread of Point load index for treated and untreated Nebo Babel Ni-Cu ore

Figure 4.32 presents a statistical summary of $I_{s(50)}$ values for each treatment condition. It can be seen that there is a reduction in both mean strength and median strength of treated particles. The reduction in median strength signifies a shift in the numbers of particles with reduced strength. In this case, the proportion of particles with reduced strength increases after treatment.

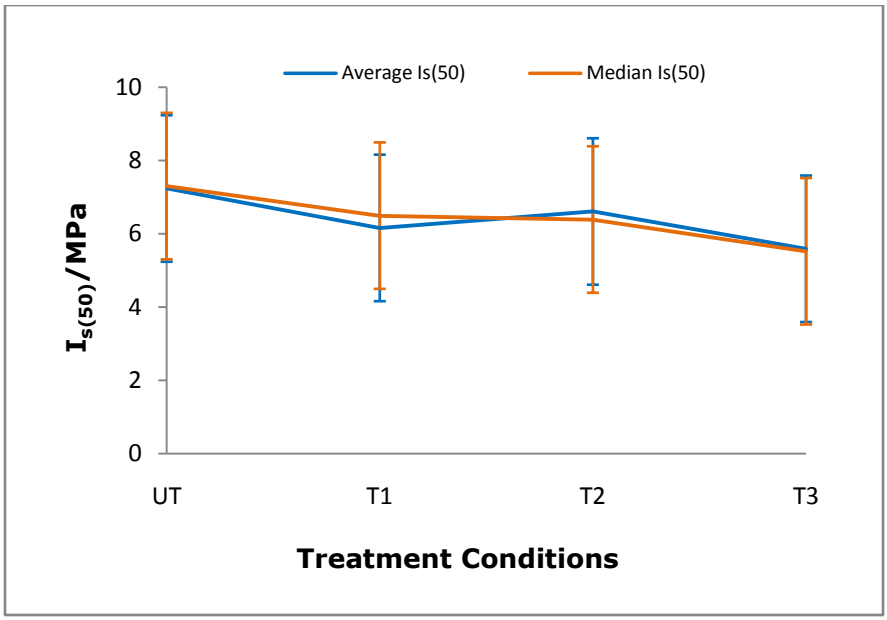

Figure 4.32 Summary of point load test results for Nebo Babel Ni-Cu ore

The results show a very high degree of variability. In theory, a particle in batch T3 (i.e particles treated for 1.1 s at 20 kW), which statistically exhibit the highest reduction in strength has a probability of retaining strength equal to or higher than an untreated particle. The high variability of the results is attributed to:

- Ores are generally highly anisotropic. Their composition is highly variable and also due to the nature of formation of rocks, some ores tend to have directional strength properties.
- Difficulty in reproducing the same loading rate on the particles when conducting the test.
- Unequal distribution of the electric field within the cavity which varies from zero at the walls of the cavity to a maximum around the centre of the cavity.

- It is also likely that as the microwaves interact with the material and energy gets absorbed, the energy intensity decreases in the direction of propagation of the microwaves. Therefore particles closest to the direction of propagation receive more energy than those at the far end.

Figure 4.33 shows the results for Los Bronces Cu ore samples. The strength of this ore is generally lower than that of Nebo Babel ore because $I_{s(50)}$ values of Los Bronces sample particles are between 0 to 8 MPa compared to 0 to 16 MPa for the Nebo Babel samples. The results also suggest that only about 60% of the particles show a reduction in strength after treatment and even then, the reduction is not significant.

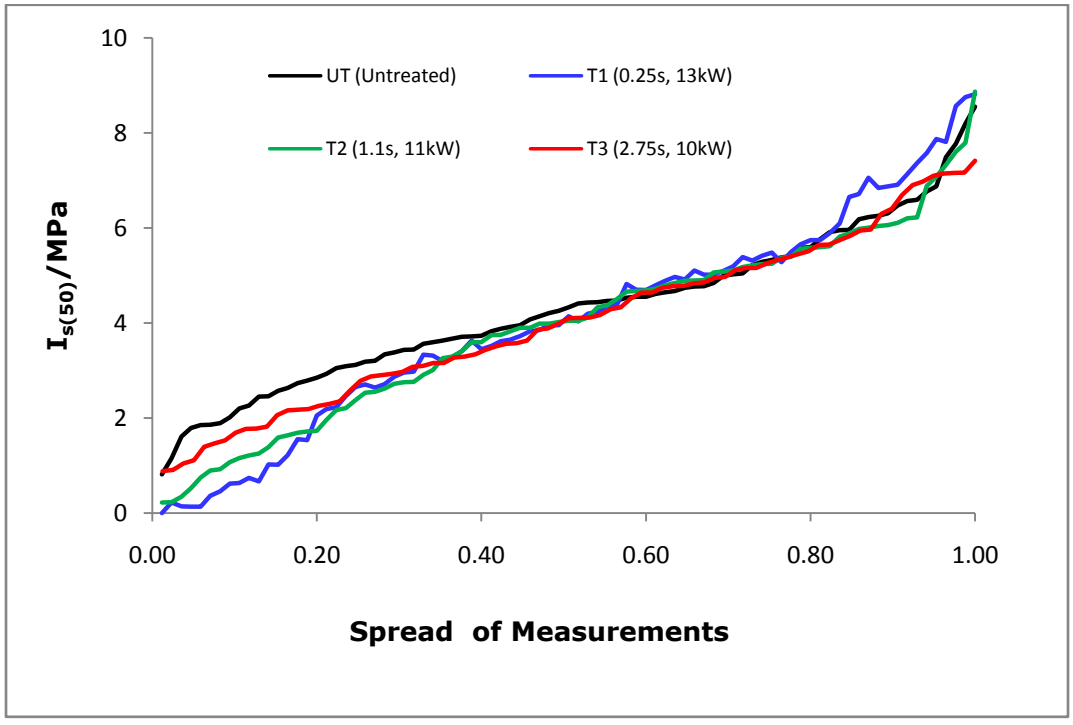

Figure 4.33 Spread of Point load index for treated and untreated Los Bronces Cu ore

Figure 4.34 shows that there is only a marginal decrease in average strength after treatment for 0.25 s at 13 kW (T1) and no apparent changes in strength when samples were heated for longer durations (T2 and T3). This result demonstrates that the magnitude of fracture in metallic based ores is not dependent on the treatment time. This is in agreement with reports by other authors that the magnitude of microwave induced fracture in metallic ores does not necessarily increase with heating duration but is majorly dependent on the temperature gradient between the heated and non heated phases.

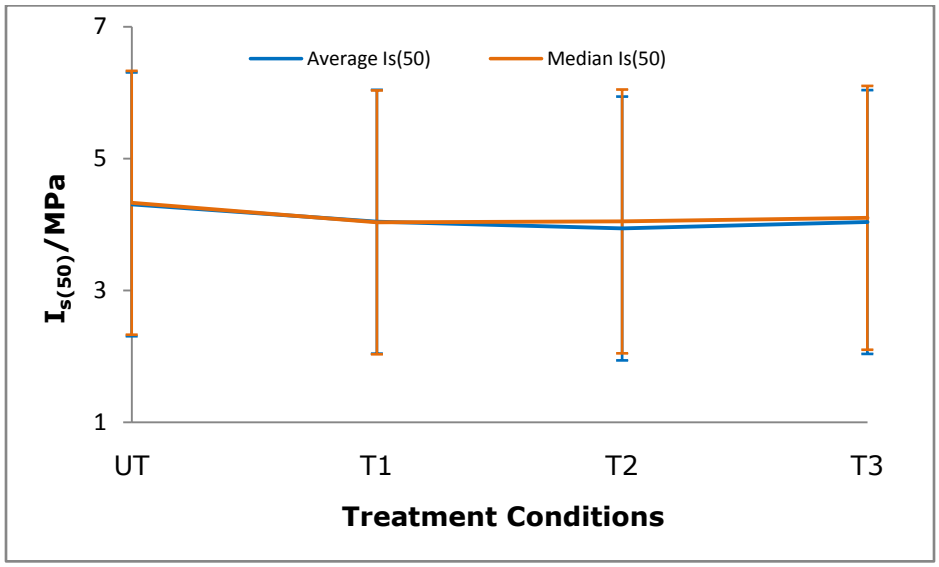

Figure 4.34 Summary of point load test results for Los Bronces Cu ore

Figure 4.35 shows that both mean and median strength decrease with increase in energy input but the relationship is nonlinear. The results suggest that there exists an energy input where the strength reduction per unit energy is maximized. In this case, the optimum energy input seems to be of a value below 1 kWh/t where the gradient is steepest.

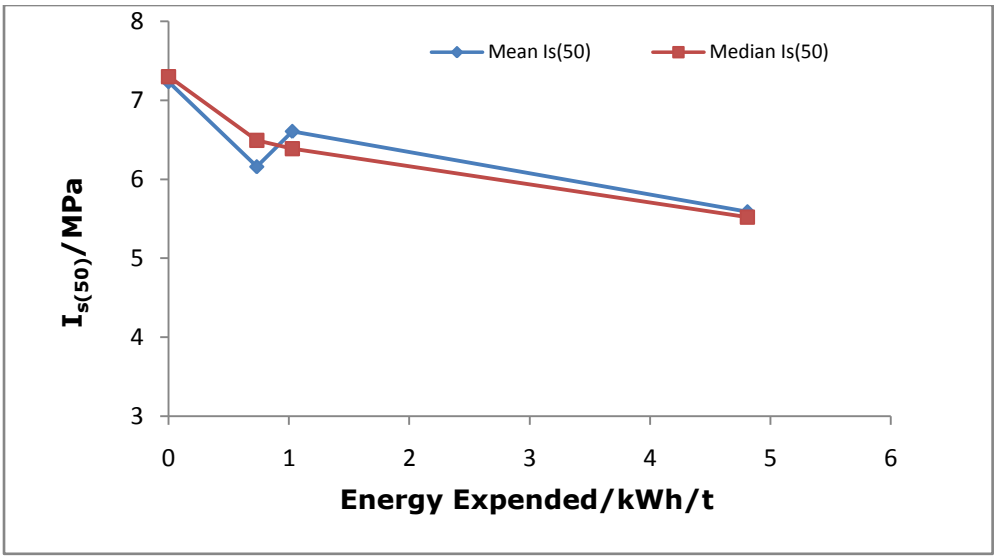

Figure 4.35 Variation of Strength with energy input- Nebo Babel Ni-Cu ore

Figure 4.36 shows a slightly different relationship (from the one above) between strength reduction and energy input.

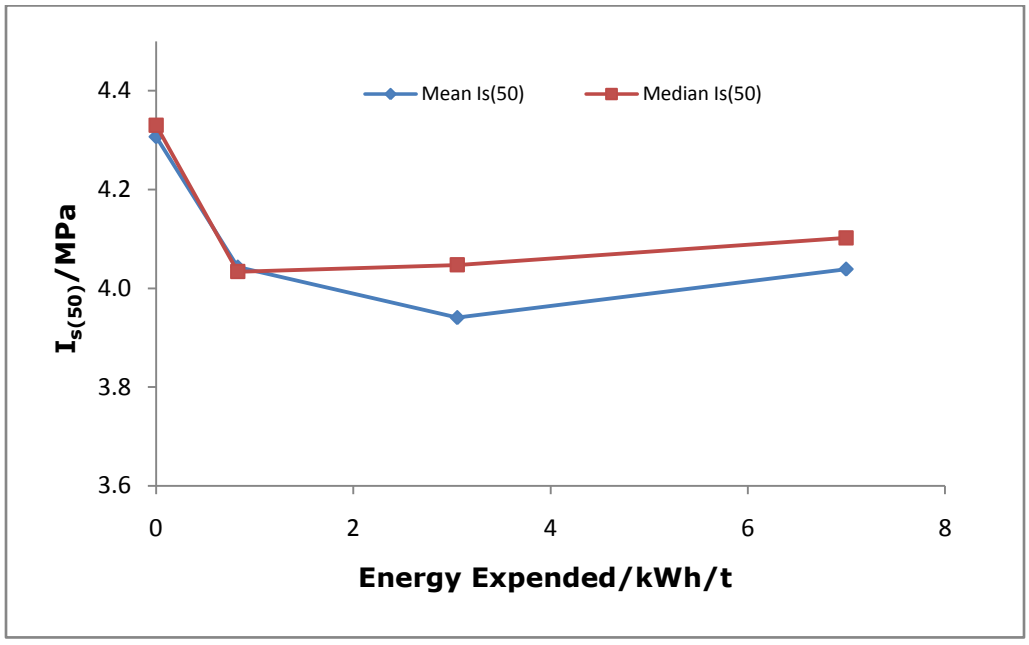

Figure 4.36 Variation of Strength with energy input- Los Bronces Cu ore

There is no apparent change in strength in particles treated at energy inputs higher than 0.8 kWh/t. In fact there is a slight increase in both mean and median strength for particles treated at the highest energy input of approximately 7 kWh/t. This result shows that the magnitude of fracture is not only dependent on the amount of energy "delivered" to the material but also the "delivery method". The magnitude of fracture is limited by the power level (which influences the maximum power density induced in the material). In this case, the power levels used for treatment of Los Bronces Cu ore samples were 13, 11 and 10 kW which do not vary significantly and although the treatment time increases more than tenfold from 0.25 s to 2.7 s, and the energy input increases more than sevenfold from 0.8 to 7 kWh/t, there is actually a slight increase in both mean and median strength because the treatment power level was reduced from 13 to 10 kW. (Note that it was difficult to maintain or reproduce similar power levels for different batch tests because the reflected power fluctuated and could not be easily maintained).

The observed differences between Los Bronces and Nebo Babel ore samples, with regard to fracture, could also be related to the differences in mineral texture. As shown in Figure 4.5, the microwave absorbent mineral grains in Nebo Babel ore are coarser compared to the Los Bronces ore. Approximately 90% of the Nebo Babel microwave absorbent grains are coarser than 600 μm whereas only about 25% of the microwave absorbent mineral grains in Los Bronces ore are coarser than 600 μm. It was stated in the last chapter that as the size of heated mineral grains increases, less energy is required to sufficiently raise the temperature gradient between the microwave absorbent and transparent mineral phases. Therefore, thermal stresses of a sufficient magnitude to damage the rock are more likely to be generated in Nebo Babel

ores with coarse grained microwave absorbent minerals than in Los Bronces with finer microwave absorbent mineral grains.

It seems like there is only a certain magnitude of damage that can be imparted to the ores and irrespective of the energy input, the maximum damage "possible" in a particular ore cannot be exceeded. The maximum damage possible seems to be related to the maximum power density in the microwave absorbent mineral phases and not on the duration of heating. By comparing the magnitude of strength reduction in the Nebo Babel ore and Los Bronces ore, it is logical to conclude that ores with higher initial strength experience greater damage than weaker ores treated under similar conditions.

The spread of results of the point load index obtained from tests carried out on the Kimberlite ores are shown in Figures 4.37 and 4.39. It is clear from the results that there is a significant reduction in strength between the treated and untreated ores. The separation between the curves is narrowest at the top indicating that a small proportion (approximately 5%) of particles retains nearly their original strength after microwave treatment. However, a significant proportion of the treated particles have zero strength indices. These are particles which were either fragmented or were simply too weak to record any readings on the pressure gauge after microwave treatment. The high variability in magnitude of damage caused to particles treated under the same conditions could be due to variation in field intensity within the cavity used. As stated before, some particles in the middle of the cavity receive more energy than those in the sides where the electric field intensity is low. The proportion of particles with zero strength indexes is higher for samples which were treated for longer durations (or at higher energy inputs). For example

about 30% of Kimberlite I samples treated at 12 kW for 12 s have zero strength compared to about 10% for particles heated for 7.5 s.

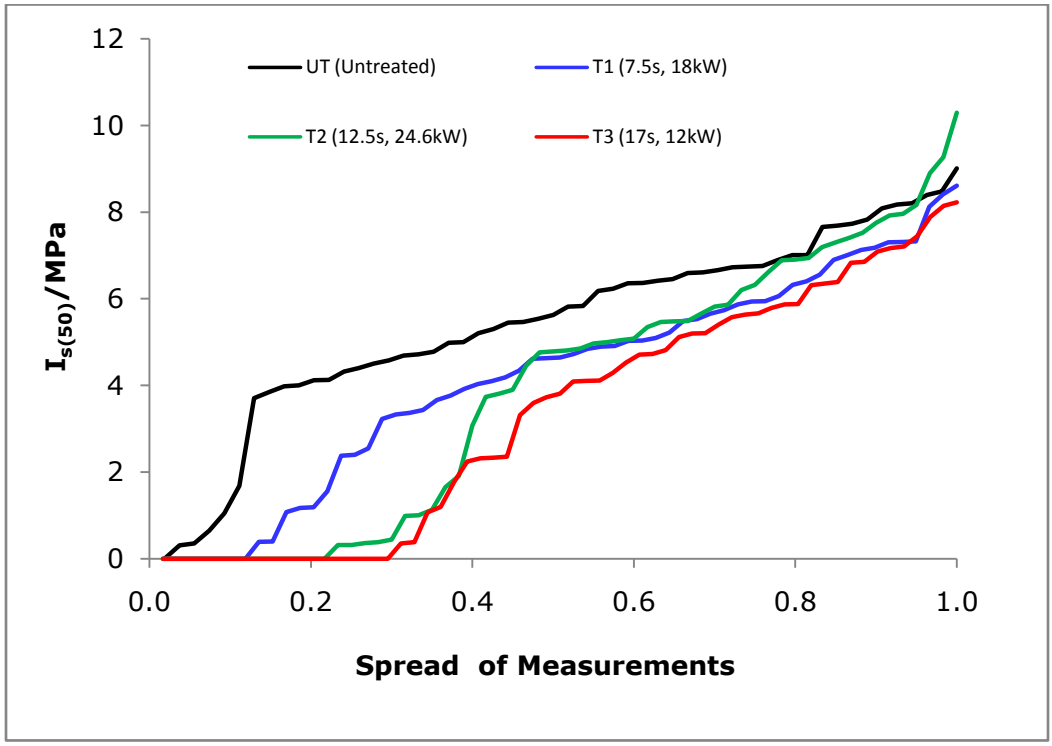

Figure 4.37 Spread of Point load index for treated and untreated Kimberlite I ore

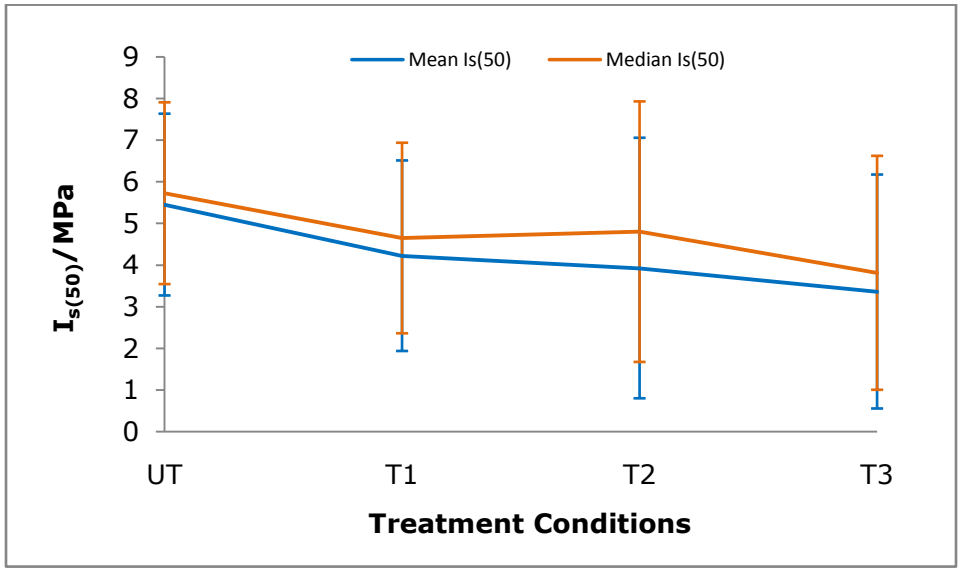

Figure 4.38 Summary of point load test results for Kimberlite I ore

The spread of results of point load index of the Kimberlite II ores does not show a significant reduction in strength except for particles which were treated for longer durations. However, it should be noted that, overall, this ore is "weak". The strength index ranges between about 0.3 to 3 MPa with a mean strength of just about 1.5 MPa compared to a mean strength value of about 5 MPa for the Kimberlite I ore. Higher reductions in strength are achieved in ores with higher original strength. It seems like there is a threshold of strength below which no further significant reductions may be possible irrespective of the duration of heating or the power level. Figure 4.40 shows that there is a significant reduction in the median for particles in batch T2 (i.e particles treated for 7.86 s at 22 kW) although the mean strength is higher at the same treatment conditions. This shows that there a "gap" in the measured strength values with a higher proportion of particles with very low strength on one side and others that retain nearly their original strength of the other side and this increases the mean strength value. As stated before, this could be as a result of uneven heating patterns in the cavity used but could also be as a result of ore anisotropy and non-homogeneity.

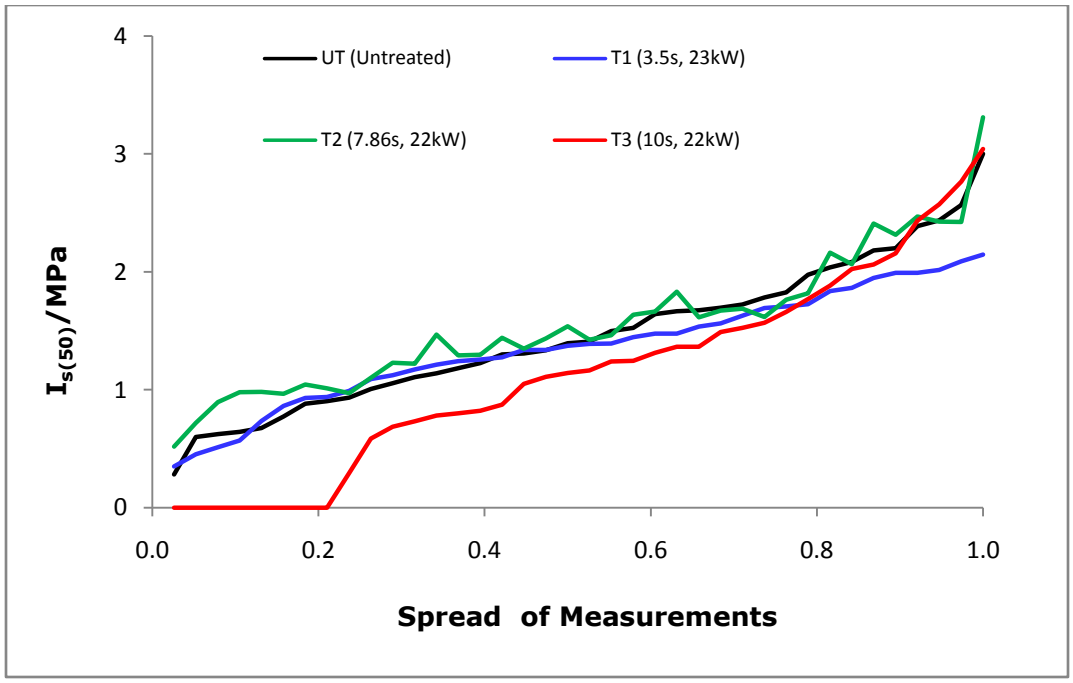

Figure 4.39 Spread of Point load index for treated and untreated Kimberlite II ore

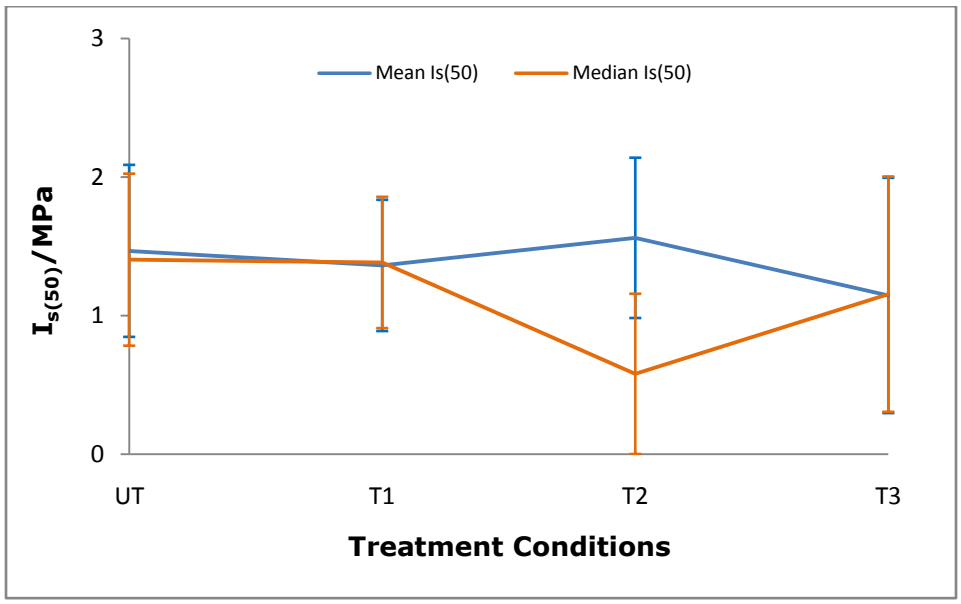

Figure 4.40 Summary of point load test results for Kimberlite II ore

Figures 4.41 and 4.42 show the variation of the mean and median strength with energy expended during the treatment process. The highest strength

reduction of nearly 40% is observed in particles treated at 12 kW for 17 s with a total energy output of about 9 kWh/t. These results again demonstrate the importance of "the method of power delivery" as opposed to "magnitude of power". It can be seen that despite nearly doubling the energy expended, from about 9 to 17 kWh/t, there is no apparent reduction in strength but instead a slight increase is recorded. The treatment conditions for particles that exhibit the greatest strength reduction seem to suggest a different mechanism of breakage in hydrated ores when compared to results from the Nebo Babel and Los Bronces metallic based ores. The highest reduction in strength is achieved in particles treated for the longest duration. Since it has already been proved that microwave induced fracture of ores containing hydrated minerals is due to dehydration, it seems like the kinetics of dehydration influence the magnitude of fracture and this requires further investigation.

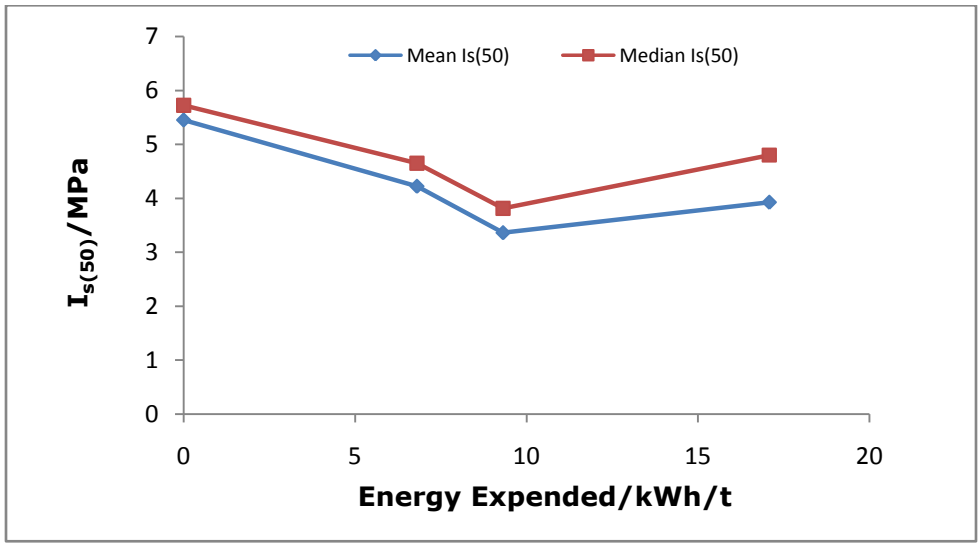

Figure 4.41 Variation of Strength with energy input- Ekati Kimberlite I ore

Figure 4.42 shows the variation of mean and median strength with energy input for the Kimberlite II ores.

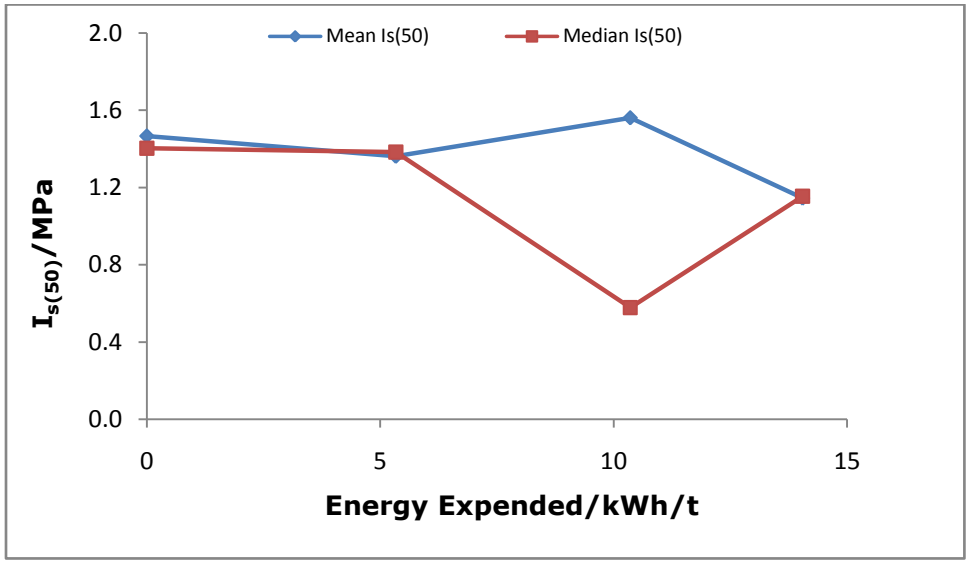

Figure 4.42 Variation of strength with energy input- Ekati Kimberlite II ore

In this case, the results do not show any significant reduction in mean strength for any of the treated particles. There is an apparent reduction in the median for particles treated at 10 kWh/t (22 kW for 7.86 s) but this is offset by the increase in mean. This is again most likely as a result of a few particles with extremely low strength. It appears that the ore is naturally too weak in strength to record significant reductions in strength after treatment.

The results discussed above illustrate some of the limitations and shortcomings of the point load test and in general the method of treatment used in this work. Firstly, the system used did not ensure uniform treatment of particles. It is possible that a combination of factors such as the anisotropic and non-homogeneity nature of the ores, severely weakened particles and particles retaining nearly their original strength, can lead to false

interpretation of the mean strength. The basis of this test is an assumption that each batch of particles has similar strength characteristics before treatment. In practice, this is not the case. For example, Figure 4.31 shows that for the untreated batch of particles, the weakest particle has an original strength index of about 2 MPa while the strongest has an index of about 16 MPa. This is a variation of 700%. This means that a treated particle may experience a significant reduction in strength and still appear to have increased strength because the comparison is based on measurements conducted on a different particle. This observation stresses the importance of a non destructive characterisation technique where measurements are conducted on the same particle. It also shows that it is necessary to conduct tests on many particles (possibly hundreds) to approximate a normal distribution and improve the level of confidence in the results. In this case only between 35-50 and 240-260 particles were tested for the Kimberlite ores and metallic base ores respectively. The effectiveness of the point load test to accurately pinpoint and characterise microwave induced damage also needs to be investigated further. The aim of any comminution process is to reduce the size of feed material. In this case, the point load test does not take into consideration the proportion of particles that were fragmented although clearly this would have a very significant effect on the comminution energy. The method appears to be less effective for testing of "weak" ores which exhibit a level of plasticity.

Despite the above shortcomings, the results from point load testing have further demonstrated that microwave energy can induce fracture in ores containing hydrated minerals and that the magnitude of induced damage is comparable to that observed in metallic based ores. A reduction in mean

strength of more than 15% was observed in Nebo Babel Ni-Cu ore samples when treated for 0.25 s at 18.5 kW with a total energy input of less than 1 kWh/t. A 40% reduction in mean strength was observed in the Ekati Kimberlite I ore treated for 12 s at 24.6 kW with a total energy input of about 9 kWh/t. The total energy input for the Kimberlite ore is very high compared to that used in treatment of Nebo Babel ores because longer heating periods were used. Although the results from Kimberlite ores suggest that the magnitude of fracture is influenced by the kinetics of dehydration, it is possible that the total energy input can be significantly reduced by using more efficient and specialized heating systems and selecting the optimum operating conditions of power level and treatment time.

4.10 Ultrasonic Test Characterisation of Microwave Induced Fracture

4.10.1 Introduction

An ultrasound wave is a pressure wave with a frequency above the upper limit of human hearing (usually regarded as 20 kHz) (Raj et al., 2004). Ultrasound based techniques have traditionally been used in medical equipment to visualize internal organs of humans. Over the last two decades, there has been a growing interest in the use of ultrasound techniques to provide non destructive method of testing or analysing engineering materials. Essentially, all ultrasound based techniques operate by focusing a signal to a material that is to be analysed and the resulting signals are detected and processed to provide the analysis required. The commonest methods are based on either analysis of reflected signals (reflection/echo mode) or attenuation (through transmission) signals (Raj et al., 2004). In the reflection mode, a transducer sends pulsed waves through a coupling on the surface of the material and the

signals reflected are analysed to characterise the material. In the attenuation mode, a transmitter sends an ultrasound through one surface and the signal that travels through the material and is received at another surface is detected and analysed.

Ultrasonic testing has been reported by several authors as a useful and reliable non destructive technique of assessing the mechanical characteristics of existing structures such as the modulus of elasticity and the compressive strength (Sack and Olson, 1995). The ultrasonic pulse velocity (UPV) method has been reported to be effective in testing both homogeneous materials such as steel and heterogeneous materials such as concrete and timber. The following equations that estimate the elastic properties of materials from UPV testing were developed by (Prassianakis, 1977) and are said to be generally applicable to most solid materials.

$$E = \frac{(1+\nu)(1-2\nu)}{(1-\nu)}\rho c_l^2 \qquad (4.2)$$

$$G = \rho c_t^2 \qquad (4.3)$$

$$\nu = \frac{(c_l/c_t)^2-2}{2[(c_l/c_t)^2-1]} \qquad (4.4)$$

Where E = Modulus of elasticity (Pa)

ν = Poisson's ratio

ρ = Density of material (kg/m^3)

c_l, c_t = longitudinal and transverse pulse velocity (m/s)

G = Shear modulus of elasticity (Pa)

The UPV testing method has also been successfully used to detect cracks and internal damage in "in- service" concrete structures. A parameter of internal damage, D where $0 \leq D \leq 1$ is given by (Prassianakis, 1994):

$$D = \frac{A - A_0}{A} \qquad (4.5)$$

Where A = Initial cross sectional area (m^2)

A_0 = Undamaged load transmitting area (m^2)

The value of D is derived from Equation 4.6 (Prassianakis, 1994) and by substituting into Equation 4.5 above, the load transmitting area A_0, is obtained and used to conduct a safety check on the serviceability of the cracked structure.

$$D = 1 - \frac{H_i}{H_0} \qquad (4.6)$$

Where H_0 = Amplitude of reflected ultrasonic wave (unloaded)

H_i = Amplitude of reflected ultrasonic wave (loaded)

Ultrasonic testing of concrete has been investigated extensively but there is limited application of ultrasonic testing methods for other engineering materials such as metals and ceramics and other materials such as rocks. The relationship between UPV and rock strength parameters such as fracture toughness and bulk modulus has not been investigated extensively. Despite the limited application of ultrasonic testing to rocks and ores, this study found

the method attractive in characterising microwave induced fracture in ores mainly due to the "non destructive" nature of ultrasonic pulse testing. Unlike point load testing, UPV tests are conducted on the same specimen before and after microwave treatment. This eliminates errors arising from anisotropy and non-homogeneity.

For the first time ever, an attempt is made in this study to characterise microwave induced fracture using a non destructive ultrasonic based technique. A testing device known as PUNDIT 7 tester, manufactured by CNS Farnell, UK was used. The PUNDIT tester was designed primarily for non destructive concrete testing to detect extremely small flaws, cracks and voids in in-service concrete structures in accordance with British Standards for Concrete Testing BS 1881-203:1986. Essentially, the PUNDIT is an attenuation mode ultrasonic testing device in which a pulse of longitudinal vibrations is generated and traversed through a material. The time, t taken by the generated pulse to travel through the material is accurately measured with aid of a receiver transducer attached on the other side (see Figure 4.43). The receiving transducer detects the arrival of that component of the pulse which arrives earliest. This is generally the leading edge of the longitudinal vibration that traverses the direct path (shown in red, Figure 4.43) between the two transducers. The pulse velocity is then calculated after measuring the length l of the sample.

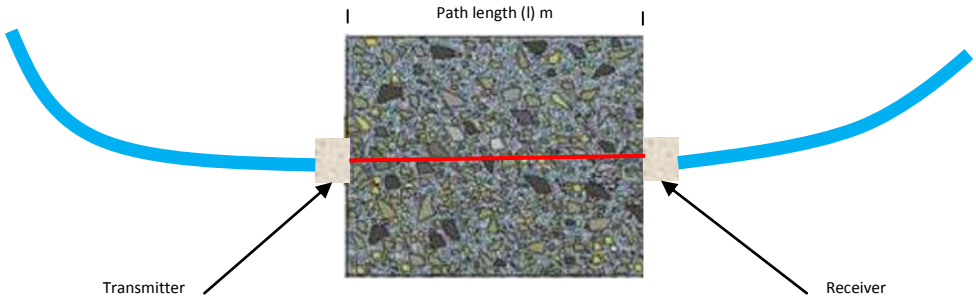

Figure 4.43 Transmission of an ultrasound pulse signal through a concrete material

When a crack or other damage occurs in the region of the path of the longitudinal signals, there is negligible transmission of energy across the interface. The direct ultrasonic beam is obstructed and the detected signal will have been diffracted around the periphery of the defect and the transit time will be longer. The pulse velocity may also be affected due to change of medium (in this case an air void) across the interface since the speed of sound in air is less than that in solids.

4.10.2 Limitations of PUNDIT Testing for this Work

Research into ultrasonic based methods of testing has focused mainly on engineering materials and on concrete in particular. As a result, there was a limited choice of ultrasonic testing devices for this work. In addition, there has been slow progress in scientific research work in ultrasonic testing of rocks. For example, the dispersion and propagation of ultrasound pulse signals inside a severely damaged rock material could not be predicted for this work. UPV methods for concrete testing are concerned with structural cracks, which are of a very high magnitude compared to microwave induced cracks in ores. In addition, structural cracks occur in relatively small numbers compared to

microwave induced cracks which may be exhibited as a web (matrix) of micro/macro fractures inside a material. When using the PUNDIT, only the leading edge signal (lead wave front) that arrives first is recorded and forms the basis for calculation of the pulse velocity. Signal attenuation and propagation through a material is very significant when testing for microwave induced fracture in ores. A typical fracture in a concrete structure is shown in Figure 4.44 (left). It can be seen that in this case, the propagation of the wave front (shown in red), after a crack has developed, is easily defined and therefore the crack formed can be characterised easily.

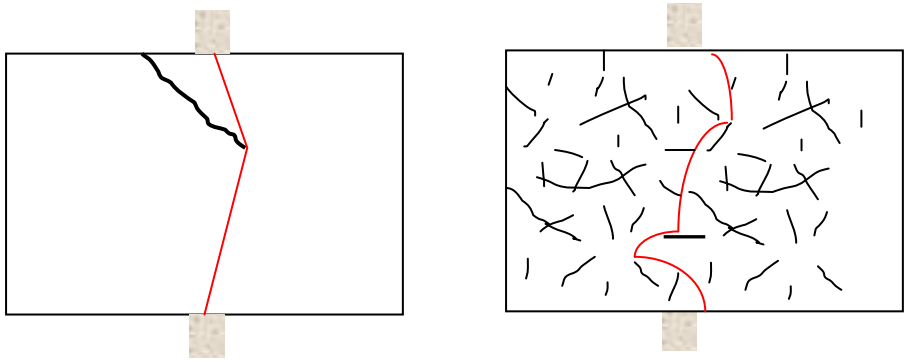

Figure 4.44(Left) Signal propagation around a typical concrete crack (Right) Probable signal manoeuvre through microwave induced cracks

However, with multiple cracks formed inside a microwave treated ore, (Figure 4.44, right) the propagation is not clearly defined. According to the manufacturer's specifications, the PUNDIT is said to be sensitive to "extremely small flaws" in a material (Proceq, 2009) However, the crack width above which a pulse will not traverse and must negotiate its way through a continuous medium is not known. It is likely that the context of "extremely small flaws" is in reference to concrete where cracks below 1mm are not of structural significance. However, with microwave induced fracture, even micro cracking is of great significance and a method of quantifying it would be

very helpful in assessing the full process benefits. Another uncertainty surrounding the PUNDIT tester for this work was lack of a clear knowledge about "the extent of influence" of the pulse wave as it propagates through the material. It is not clear if the damage that occurs in the whole sample is accounted for. As a result, measurements were taken from different points across the sample. However, a device that detects and analyses multiple transmitted signals and signals reflected from imperfections over a wider area of the surface of the material would have been ideal for this work.

Despite the above shortcomings, the PUNDIT was used in this work to provide the first step in non destructive ultrasonic characterisation of microwave induced fracture. In addition, the PUNDIT tester was:

- Easy and quick to use and therefore measurements could be conducted on several particles. This is important when testing rocks due to anisotropy. In addition, it was necessary to conduct multiple tests to get convincing results because of the shortcomings in the method highlighted above.
- It was very sensitive to lapse time. The PUNDIT tester accurately recorded the lapse time to the order of a hundredth of a micro second and was therefore sensitive to changes within a material.

4.10.3 Methodology for Ultrasonic Pulse Velocity Testing

Ore test blocks were sampled and sawn using the same procedure described previously for the point load test. The surfaces were smoothened using a grinder in order to allow good contact between the specimens and the transducer/receiver couplings. The material was tested from multiple points

pre-marked on the specimens in order to increase the region of influence so that the results obtained represented damage over a wider volume of the material. Depending on the size of the sample, three or four points were selected. The points were selected so as not to be so close to each other and also not close to the edges. Ideally the selected points would form the corners of a concentric rectangle or triangle as shown in Figure 4.45.

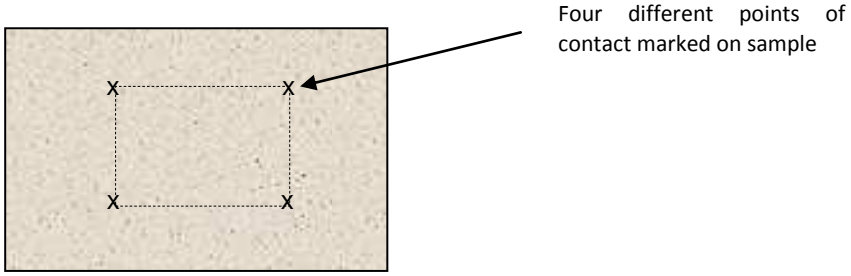

Figure 4.45 The points marked "x" on two parallel faces where measurements were taken

Measurements were taken from corresponding points before and after microwave treatment. The microwave system and treatment procedure were described in Section 4.7.2.

The PUNDIT tester with "extras" fitted specifically to suit this test work is shown in Figure 4.46. The transmitter was welded to a metal frame carrying a light weight attached to its body. This ensured that a uniform pressure was exerted on the sample before and after microwave treatment. The sample was positioned at the pre-marked contact points and held in position by the rigid frame. The lapse time was automatically recorded and displayed on the PUNDIT screen.

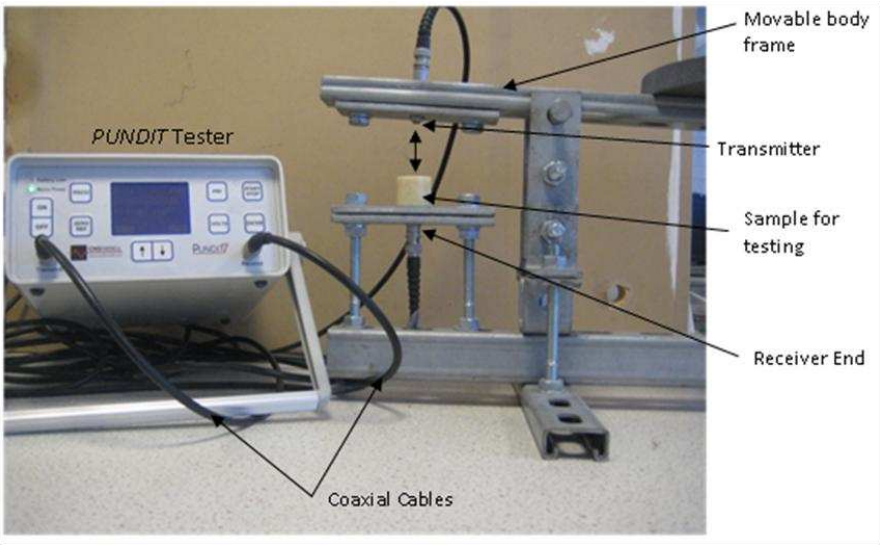

Figure 4.46 The PUNDIT test equipment used for UPV characterisation of microwave induced fracture

If t_1 and l_1 are the lapse time and path length before microwave treatment then:

$$v_1 = \frac{l_1}{t_1} \qquad (4.7)$$

$$v_2 = \frac{l_1+\delta}{t_2} \qquad (4.8)$$

Where v_1, v_2 = pulse velocity before and after microwave treatment (m/s)

t_2 = lapse time after microwave treatment (s)

δ = change in path length due to internal damage (m)

As stated previously l_1 is assumed to be the shortest distance between the contacts which is also equivalent to the length of the sample. When measurements are taken from the same points before and after microwave

treatment, the need to accurately measure the path lengths l_1 is eliminated. An assumption is also made that the change in path length δ, after microwave treatment is too small compared to l_1, hence:

$$\frac{v_2}{v_1} = \frac{t_1}{t_2} \qquad (4.9)$$

Equation 4.9 shows that the ratio of the ultrasonic pulse velocity of microwave treated particles to the pulse velocity of untreated particles (i.e v_2/v_1) is equal to the ratio of initial lapse time to the lapse time after microwave treatment. The ratio (v_2/v_1) is the ultrasonic pulse velocity (UPV) of treated particles relative to the UPV of untreated particles (or simply called the relative UPV of treated particles). Initially $t_1 = t_2$ and therefore for zero microwave induced fracture, the relative UPV is equal to one. After some damage has been induced in the material, $t_2 > t_1$ and the relative UPV is less than one. The apparent reduction in relative UPV, which arises from the difficulty of defining exactly the onset of the pulse, is therefore given by:

$$Reduction\ in\ Relative\ UPV(\%) = 100 - 100\left({}^{t_1}/_{t_2}\right) \qquad (4.10)$$

Equation 4.10 was used in this study to characterise microwave induced fracture. The magnitude of damage induced is proportional to the reduction in relative UPV.

4.10.4 Results of Ultrasonic Pulse Velocity Testing

The full results from measurements conducted on individual particles of each ore sample are shown in Appendix III. Figure 4.47 shows the spread of the

reduction in relative UPV of Nebo Babel particles treated at different energy inputs. The results indicate a reduction in UPV in at least 50% of all treated particles. The trend of results shows the highest reduction in UPV is obtained in particles treated at the highest energy input of 4.83 kWh/t. The general trend of results obtained is similar to those obtained from the point load test shown in Figures 4.31.

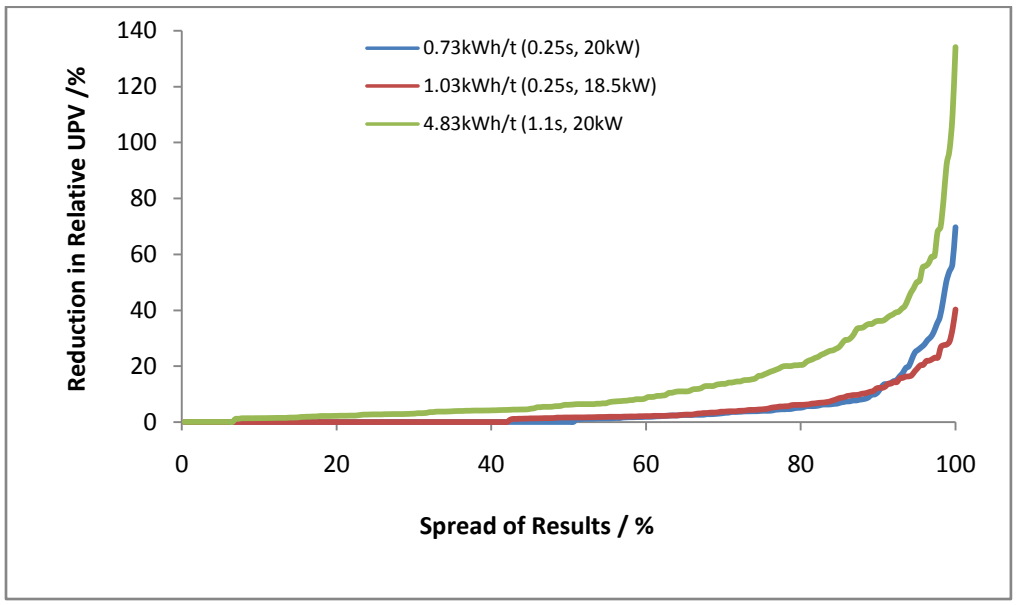

Figure 4.47 Variation of UPV in the treated Nebo Babel ore samples

Figure 4.48 shows the variation of the mean and median relative UPV values with energy expended in treating the samples. The results indicate a reduction in mean UPV values of between 4-14% in all the treated particles. The mean and median values of relative UPV are highest in particles treated at 4.83 kWh/t. This indicates that overall, more damage is induced in these particles after microwave treatment. This observation agrees well with the results from point load testing which showed that the lowest mean point load strength index (mean $I_{s(50)}$) is obtained in particles treated at the same energy input.

The results also show a non linear relationship between UPV reduction and energy input. The logarithmic trend is steepest at energy inputs less than 2 kWh/t suggesting that under the treatment conditions and system used, greater fracture per energy input is achieved at energy inputs less than 2 kWh/t. This result also agrees with that obtained in point load testing as shown in Figure 4.35.

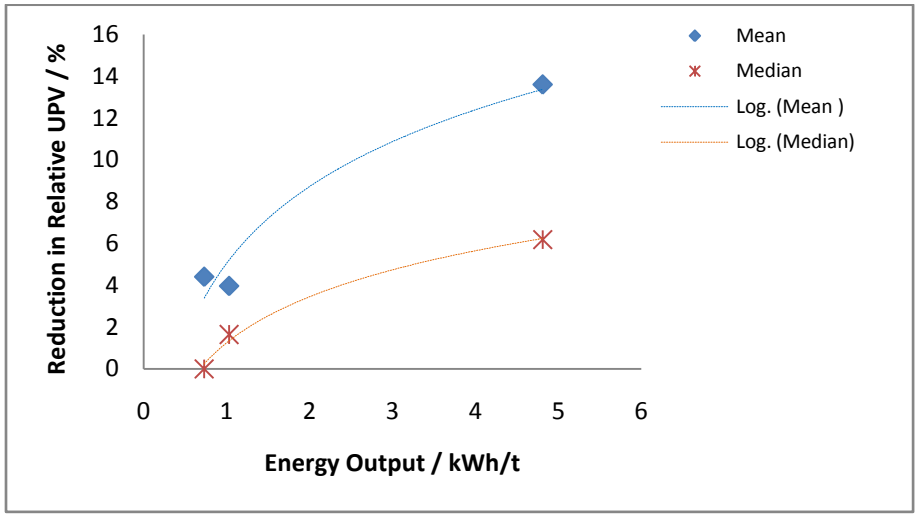

Figure 4.48 Variation of UPV with energy expended in treating Nebo Babel ore samples

The results obtained from Los Bronces test samples are summarised in Figure 4.49. The trends do not show an overall significant reduction in UPV in any of the treated sample batches. The results suggest that significant reduction in UPV is obtained in only less than 3% of the particles treated at the highest energy input of 7 kWh/t. This result again correlates well with the result from point load tests carried out on Los Bronces samples as shown in Figure 4.33.

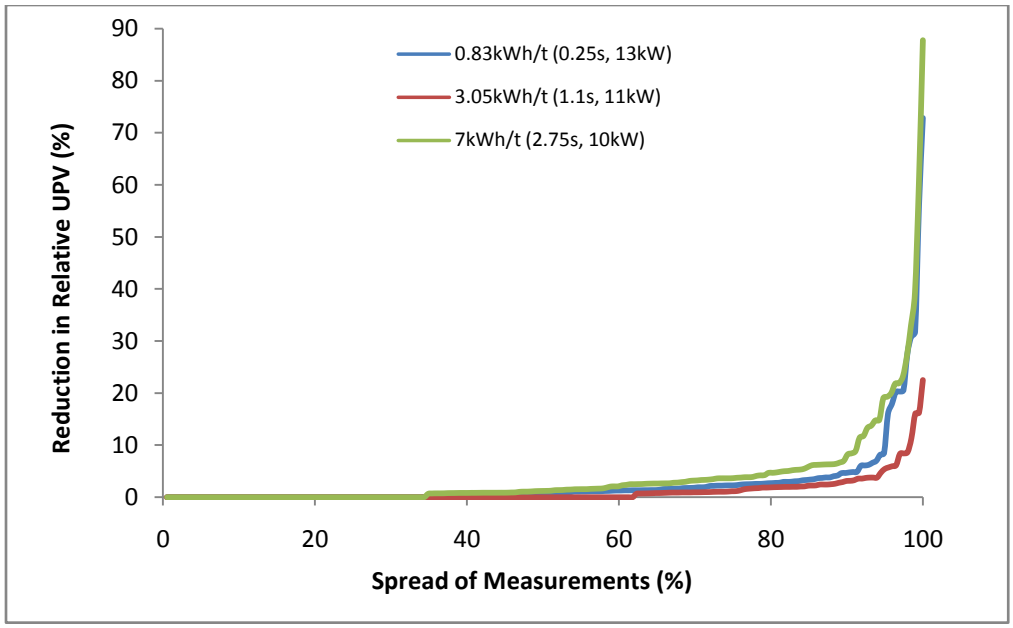

Figure 4.49 Variation of UPV in the treated Los Bronces ore samples

The variation of mean and median values of relative UPV with energy input is shown in Figure 4.50 below. The results show only a marginal reduction in UPV of between 1-4% even at the highest energy input of 7 kWh/t. This result again is in agreement with point load tests (see Figure 4.36) and the explanation for this was stated previously.

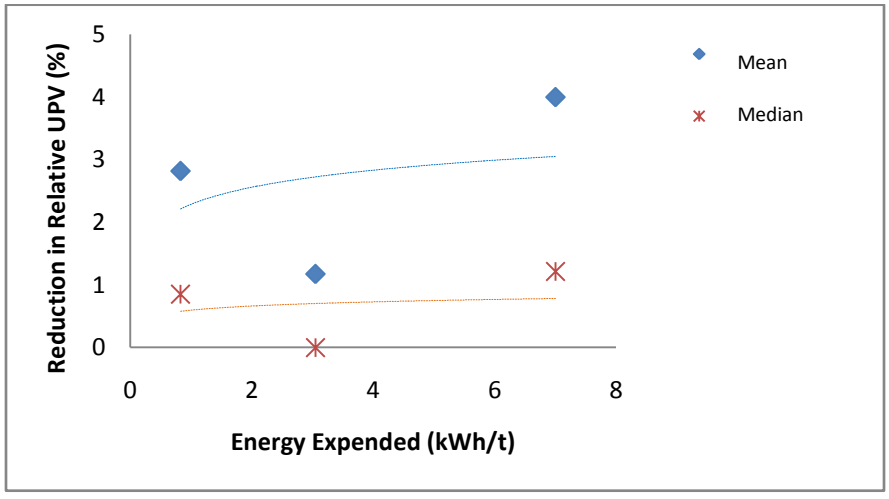

Figure 4. 50 Variation of UPV with energy expended in treating Los Bronces ore samples

Figure 4.51 shows spread of results of relative UPV values obtained from Kimberlite I test samples. Over 50% of the treated particles record a reduction in UPV. The scale of reduction in this case is very significant. For example over 20% of particles treated at 9.32 kWh/t show a reduction in UPV of more than 100%. Overall a higher reduction in UPV is observed in particles treated at 9.32 kWh/t.

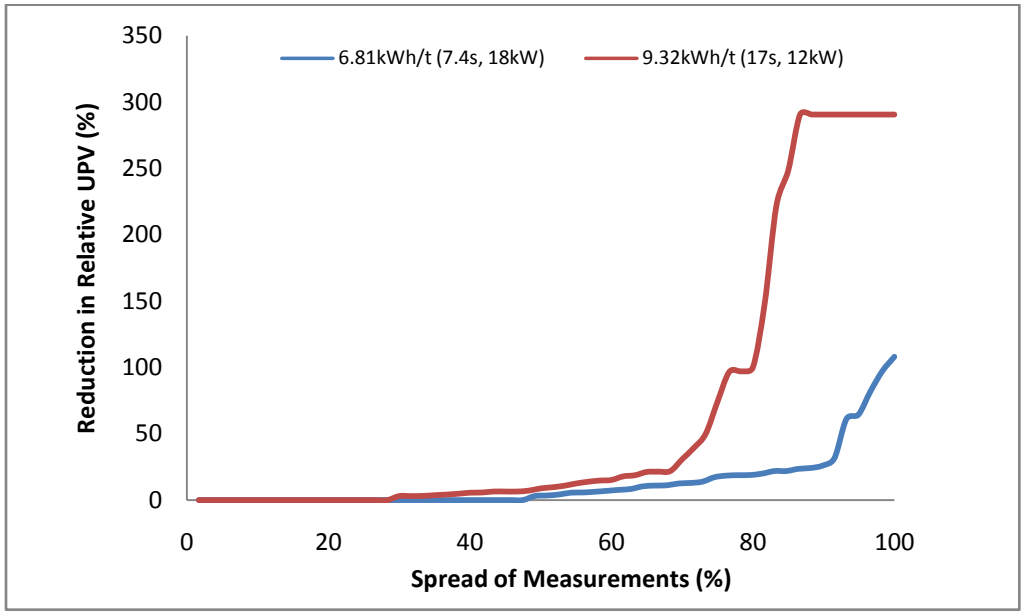

Figure 4.51 Variation of UPV in the treated Kimberlite I ore samples

The variation of mean and median UPV values is shown in Figure 4.52. A reduction in mean UPV of about 10% is achieved in particles treated at 6.81 kWh/t while an even higher reduction of nearly 70% is achieved in particles treated at 9.32 kWh/t.

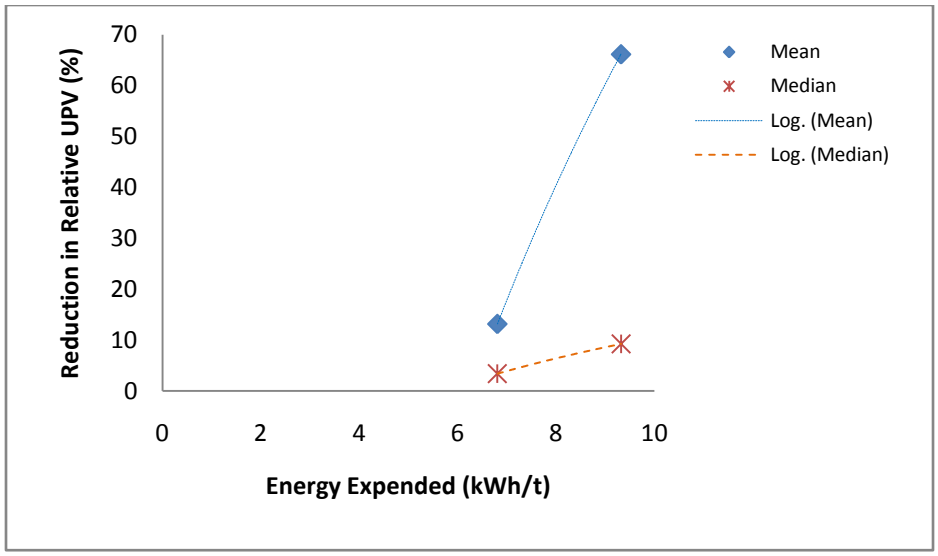

Figure 4.52 Variation of UPV with energy expended in treating Kimberlite I ore samples

The PUNDIT test results have demonstrated that it is possible to characterise microwave induced fracture using non destructive ultrasonic testing techniques. In all the tests conducted, the trends of results obtained agree with those obtained from point load testing.

4.11 Conclusions

This study has demonstrated that significant fracture may be induced in ores containing hydrated minerals after microwave treatment. Significant micro and macro fractures were observed in Kimberlite ores devoid of any known good heaters of microwave energy such as metal oxides and sulphides. It appeared that damage relies on certain mineral phases within the ore undergoing dehydration. The fractures that occur in the Kimberlite I ores seem to be associated with the presence of a mineral phase incorporating interlayer water with a composition close to hydrobiotite. Cracks were observed to form at the edges of caclcite grains throughout the hydrobiotite phase. Fracture propagation through the texture appears to be highly

intergranular and follows mainly the olivine phenocryst- calcite groundmass interfaces. The damage observed in the heavily weathered Kimberlite II ores is most certainly due to dehydration of the abundant smectite minerals. When the interlayer water is heated, steam is evolved and the smectite mineral phases expand. On cooling, cracks are formed due to shrinkage. The internal pressure due to steam evolution contributes towards the explosive fragmentation observed in the Kimberlite II sample particles.

The magnitude of induced damage was quantified by point load testing and ultrasonic pulse velocity (UPV) measurement method. Point load test results suggested that there exists a non linear relationship between strength reduction with increasing microwave energy input. The results obtained from UPV characterisation correlated with those obtained from point load testing. It is believed that there exists a limit on the maximum damage that can be induced in ores containing hydrated minerals and that the limit is related to the content of hydrated minerals and the degree of dehydration. For example, less damage was observed in Kimberlite I ores as there are relatively low amounts of hydrobiotite present (4.35%); it may be that the hydrated portion is rapidly exhausted upon microwave treatment. However the results from both methods showed a high degree of variability although this was partly attributed to the anisotropic nature of rocks.

Significantly higher energy inputs were used in treatment of hydrated ores compared to those used in treatment of the metalliferrous ores because longer treatment times were used. The results indicated that the magnitude of fracture in the Kimberlite ores increases with treatment time unlike in metalliferrous ores where shorter heating times are preferred. Both the

magnitude and kinetics of dehydration seem to influence the damage induced. It must be noted however, that all of the microwave treatments carried out in this work utilized non specialized microwave heating equipment. Any commercial industrial microwave processing installation requires careful design for delivery of microwave power to the optimal applicator geometry based on throughput and processing requirements. This involves accurate dielectric property measurement of all the phases present in isolation, subsequent thermo-mechanical and numerical simulation to ascertain the likely strength reduction, and electromagnetic numerical simulation to determine the optimal microwave operating conditions and applicator geometry for the greatest field intensity, homogeneity and safety respectively. Improvements in matching or tuning the system more accurately to the ore would also dramatically reduce energy consumption. The next chapter will also investigate the highly selective heating of mineral phases by use of pulsed energy delivery. Potentially this is ideal for metallic based ores and the Kimberlite I ore in particular because only a small percentage of the mineral phase is microwave heated. In pulsed systems, very high power levels are created for short periods of time (typically as high as 1 MW in a thousandth of a second). Therefore as long as enough joules are contained within the pulse, significant damage will be possible at significantly lower overall energy inputs.

CHAPTER FIVE

5 EFFECT OF MICROWAVE TREATMENT ON MINERAL SEPARATION PROCESSES

5.1 Introduction

A significant amount of valuable minerals are lost through tailings mainly because they cannot be liberated from the host rock or cannot be separated from the gangue material. During mineral processing, the Process Engineer is faced with a challenge of selecting the most efficient and economic grind size. High grade concentrates with little contamination are produced if the ore is ground finely enough to liberate the associated minerals. Fine grinding however increases energy costs and processing times and can lead to the production of very fine untreatable slime particles which may be lost into the waste (Wills, 2006). There are also other associated problems with fine grinding such as particle agglomeration, handling requirements and disposal. Obviously if the grind size is too large, the degree of liberation is low and this also lowers the efficiency of the separation processes and hence more valuable minerals are lost through tailings. The desired situation from a mineral processing point of view would be to achieve a higher liberation at coarse grinding but this is not normally possible. For example, if the ore is of low grade and the targeted minerals are of a very small grain size and are disseminated throughout the host rock, then fine grinding may be unavoidable unless a property between the minerals and the gangue is available to enhance liberation.

In Chapter Four, it was demonstrated that microwave pre-treatment of ores induces fracture in certain ore types. The magnitude of fracture was shown to be a function of among others the mechanical, mineralogical and electrical properties of the ore. The mineralogical properties that influence microwave induced fracture were shown to include both the nature of the minerals and texture (grain size, dissemination and association). It was shown that the initiated damage results in a reduction in strength which renders the ore more amenable to comminution. Microwave induced fractures were observed to originate from heating semi conducting mineral grains or hydrated mineral phases and they propagated predominantly via cracked grain boundaries between the heated and non-heating mineral phases which become the lines of weakness. Inter-granular fracture benefits mineral processing via increase in mineral liberation and recovery. The prospects of comminution energy savings and increased mineral recovery are the major drivers for inclusion of a microwave pre-treatment stage in the conventional process flow-sheet. Obviously this can only make economic sense if the benefits of including a microwave pre-treatment step outweigh the required capital and operating costs for inclusion of a microwave pre-treatment step. This therefore requires a thorough investigation of the anticipated benefits in economic terms, the so called value proposition, before the technology can be developed further to industrial scale.

The importance of the microwave treatment system on ore treatment efficiency was discussed in the last chapters. It was stated that careful design of the microwave system is required to ensure delivery of microwave power to the optimal applicator geometry based on throughput and processing requirements. The importance of the electric field strength (and therefore

power density) was also discussed. It was stated that overall, less energy is used to treat the ores if higher power levels are used over a short treatment time. Pulsed systems where very high power levels are created for short periods of time (ideally 1 MW for about 0.001 s) were said to offer a more economic method for microwave treatment of ores. Such systems have been shown to benefit ores where selective heating is desirable by maximizing the temperature gradient between the heated and non heating phases.

All previous work (which was reported in Chapter Three and also the work carried out as part of this study, which was discussed in Chapter Four) was conducted using batch treatment processes in either multimode or single mode microwave heating cavities. Any realistic industrial microwave treatment process necessitates development of a continuous treatment process. A specially designed novel continuous microwave treatment system was utilised for the work reported in this chapter. The basis for design and the treatment process is described later. This chapter investigates the effectiveness of the microwave treatment system developed with respect to quality of the grind product, mineral liberation and overall recovery. Two different copper ores were treated using a batch single mode applicator and a continuous process using a conveyor tunnel applicator. The specific aims and objectives of this work were to determine the effect of microwave pre-treatment on the following:

- Particle size distribution after grinding
- Mineral liberation by particle size
- Overall grade/recovery and recovery by particle size.
- Recovery kinetics

- Elucidate the implications of microwave pre-treatment in ore processing with respect to value proposition

5.2 Ores Used for Study

5.2.1 Introduction

The processing of low grade ores becomes more attractive if the amount of recoverable mineral can be increased using affordable processing techniques. Research developments in microwave assisted ore processing that were discussed in previous chapters have suggested that microwave pre-treatment of certain ore types has the potential to significantly increase beneficiation. Two ores that were provided by partners of this research work were selected for this study. A porphyry copper ore obtained from the Escondida deposit in the Antacama Desert, Northern Chile (copper ore I) and a low grade porphyritic monzonite copper ore obtained from USA (copper ore II) were used. The exact location of the copper II ore cannot be stated here for legal reasons.

5.2.2 Geology of Escondida Copper I Ore

The Escondida porphyry copper deposit, located in northern Chile, was one of the two largest known copper deposits in the world in the 1990s (Billiton, 2009). Porphyritic ores exhibit a texture of noticeably large crystals (or phenocrysts) which have formed in a finer grained matrix or ground mass (Guillou-Frottier and Burov, 2003). The ore body is characterized by vein-associated alteration-mineralization styles grouped in three main hydrothermal stages (Richards et al., 1999, Laurent and Evgenii, 2003). The early alteration contains magnetite, chalcopyrite, and bornite with less than

0.5% total sulphides and less than 0.2% copper grade (Richards et al., 1999). The second hydrothermal stage consists of vein associated chlorite-sericite quartz and quartz-sericite with chalcopyrite, pyrite, and molybdenite. In the chlorite-sericite and quartz-sericite zones, the content of sulphides ranges from less than 0.5-2% with a chalcopyrite to pyrite ratio of 3 to 1 and copper grades that range between 0.4 and 0.6% by weight. The late hydrothermal stage consists of an acid-sulphate mineral association that includes pyrophyllite, alunite and quartz as alteration minerals and a variety of sulphides that include bornite, chalcopyrite, pyrite, chalcocite, covellite, enargite, sphalerite, tennantite, and galena. The primary copper grades in this zone range from 0.6 to 1.0% (Richards et al., 1999).

5.2.3 Geology of the Copper II Ore Mine

The ore deposit is generally described as a porphyry copper ore. The geology of the mine area is mainly composed of monzonite, porphyritic quartz monzonite, latite porphyry, and quartz latite porphyry and consists of different zones with varying grades of sulphide mineralization. The low-grade core, which is generally less than 0.5% total sulphides, contains low concentrations of molybdenite, pyrite, chalcopyrite, and bornite. The high grade zone is dominated by bornite and chalcopyrite mineralization with lesser molybdenite and pyrite. The high grade zone may contain over 5% pyrite on the immediate margins and skarn deposits in limestone beds may contain as much as 90% sulphides. Sulphide mineralization changes from both disseminated and fracture-controlled within and on the margins of the ore body to almost exclusively fracture-controlled on the outer margins of the pyrite halo.

5.3 Ore Screening and Sampling

About 250 kg of each ore were received as crushed material with a top size of about 40 mm. The "as received" ore was then spread out on a concrete floor and left to dry at room temperature for two days. The ore was then screened using a Russell sieve and particles passing the 31.5 mm sieve but retained on the 10 mm sieves were retained. The screening was carried out to obtain particles of a size which was suitable for use in the microwave treatment. Particles larger than 31.5 mm would be too big for the microwave cavities available in the laboratory. The retained particles were then mixed to obtain a homogeneous mixture and then split into eight representative portions each weighing about 28 kg using the large Rotary Sample Divider (RSD) shown in Figure 4.2.

5.4 Ore Mineralogical and Textural Analysis

5.4.1 Introduction

Mineralogy and texture have been shown to influence the magnitude of microwave induced fracture. It was stated in previous chapters that fracture is induced in ores possessing a matrix of microwave absorbing and microwave transparent mineral phases and that higher thermal stresses are induced as the size of the microwave absorbent mineral grains increases, assuming all other factors constant. In addition, the mineralogy of an ore influences the choice of processing techniques used for separation and recovery of the valuable minerals. The grain size distribution is used to determine the grind size required to achieve the desired degree of liberation. Ore mineralogy and texture are therefore critical properties from the view point of microwave assisted comminution and generally in ore processing.

5.4.2 Method for Ore Mineralogical and Textural Analysis

Polished samples of ore specimens which were representative of each ore type were prepared for MLA examination and analysis. The same procedure described earlier in Section 4.3.2 was used to prepare polished samples suitable for MLA examination while ensuring that they were representative of the mineralogy and texture of the bulk ore. Fourteen specimens were examined for each ore type and the following data was processed and analysed:

- The modal mineralogy by weight composition
- The spatial distribution of each mineral phase
- The grain size distribution of the copper bearing minerals

5.4.3 Results of MLA Mineralogical and Textural Analysis

The complete results of all minerals identified in each measured section including the abundance of each mineral by weight and classified MLA images of all measured sections showing the mineral distributions are given in Appendix I. Tables 5.1 and 5.2 show the combined weight percentages of only the most abundant microwave absorbing and non microwave absorbing minerals in the ore specimen sections examined. The "responsiveness" to microwave heating is based on literature from previous work such as microwave heating studies carried out by (Chen et al., 1984).

Mineral	Formula	Microwave Heating	Weight %
Pyrite	FeS_2	readily heated	6.3
Hematite	Fe_2O_3	readily heated	2.1
Chalcocite group	Cu_2S	readily heated	1.5
Chalcopyrite	$CuFeS_2$	readily heated	0.5
Covellite	CuS	readily heated	0.4
Bornite	Cu_5FeS_4	readily heated	0.2
Quartz	SiO_2	does not heat	42.1
Illite	$K_{0.65}A_{2.0}[Al_{0.65}Si_{3.35}O_{10}](OH)_2$	does not heat	26.5
Pyrophyllite	$Al_2Si_4O_{10}(OH)_2$	does not heat	4.4

Table 5.1 Most abundant microwave absorbing and transparent minerals in Escondida copper I ore samples

Mineral	Formula	Microwave Heating	Weight %
Chalcopyrite	$CuFeS_2$	readily heated	0.8
Pyrite	FeS_2	readily heated	0.2
Orthoclase	$K[AlSi_3O_8]$	does not heat	42.1
Biotite	$K(Mg,Fe)_3AlSi_3O_{10}(OH,F)_2$	does not heat	22.6
Quartz	SiO_2	does not heat	13.8
Albite	$Na[AlSi_3O_8]$	does not heat	8.6

Table 5.2 Most abundant microwave absorbing and transparent minerals in copper II ore samples

The results of the ore modal mineralogy summarised in Tables 5.1 and 5.2 show that the Escondida copper I ore contains significant amounts of semi conducting minerals such as pyrite, hematite and chalcocite which are good absorbers of microwave energy. The combined weight percentage of minerals considered to be good microwave heaters is approximately 11%. The major gangue minerals which are transparent to microwave energy are quartz and

illite with a combined weight percentage of approximately 69%. The low grade copper II ore consists of just over 1% weight of minerals which can be classified as good microwave absorbers. These are chalcopyrite (0.8%) and pyrite (0.2%). The major transparent gangue minerals are orthoclase, biotite, quartz and albite which together account for approximately 87% by weight composition.

An example of a classified MLA specimen image of each ore sample is shown in Figure 5.1. The images on the right hand side have been modified to show the spatial distribution of microwave absorbing minerals within each particle. This was carried out by grouping all minerals into only three categories according to their microwave responsiveness. It can be seen that the microwave absorbing minerals are randomly distributed throughout the entire specimen sections. Similar observations were made in all the measured sections shown in Appendix I.

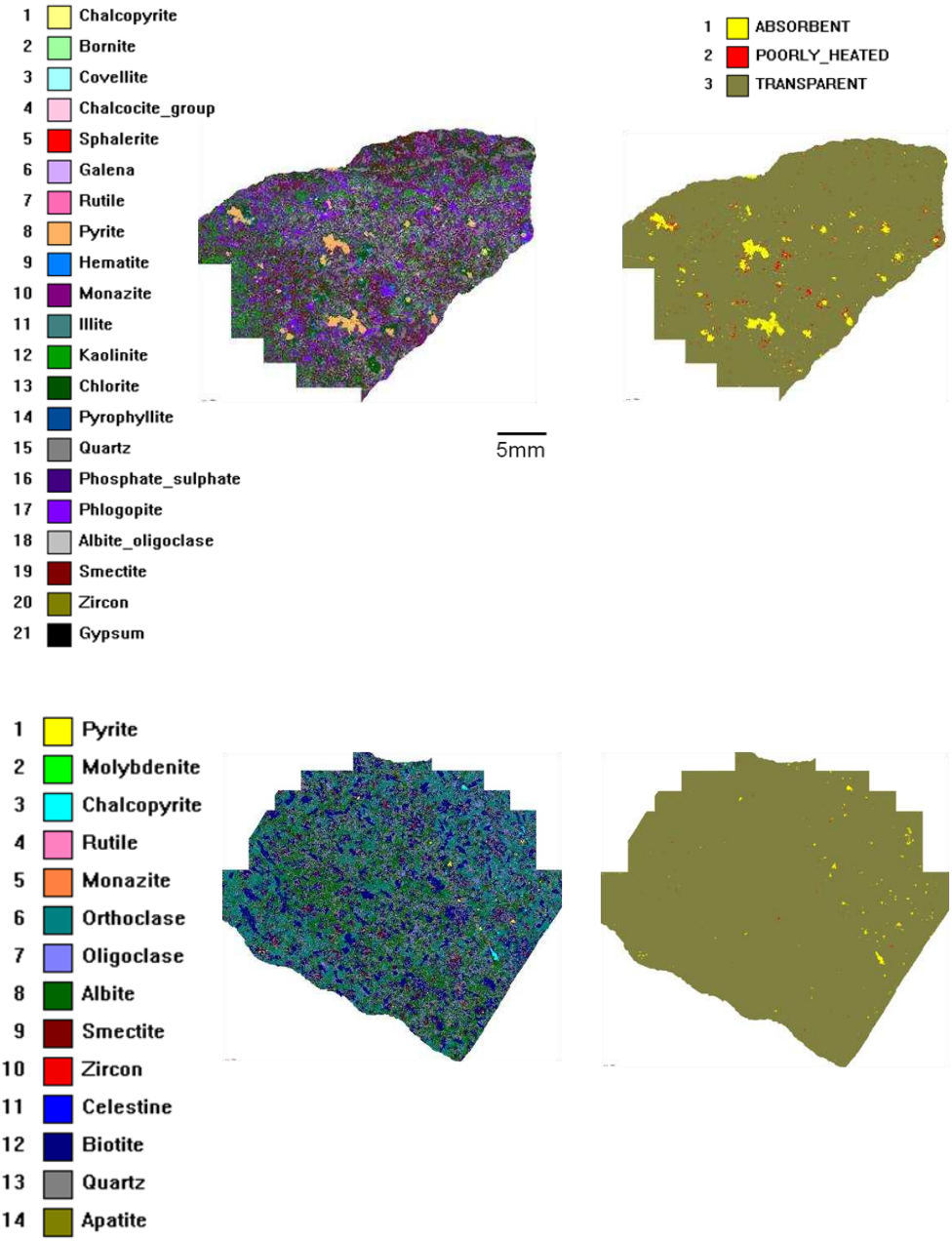

Figure 5.1 Classified MLA specimen images of Escondida (top) and Copper II copper ores (bottom)

The grain size distributions of microwave absorbing minerals (i.e. microwave heaters) in Escondida copper I ore based on the statistics in Table 5.3 are shown in Figure 5.2. The results show that the major sulphide mineral phases (pyrite and hematite) are coarse grained. For example, the results show that

about 40% of the pyrite grains are larger than 1 mm while more than half of hematite grains are larger than 0.1 mm. The d_{80} of pyrite is approximately 200 µm and that of the other microwave absorbing minerals ranges between 30-60 µm. The texture of Escondida copper I ore is, therefore, composed of a mixture of large and small pyrite and hematite mineral grains and finely disseminated copper sulphide minerals.

Mineral	Formula	Grain density grains/cm^2	Total grain count	Weight %
Pyrite	FeS_2	18	657	6.5
Hematite	Fe_2O_3	37	1350	2.1
Chalcocite	Cu_2S	57	2071	1.5
Chalcopyrite	$CuFeS_2$	26	937	0.5
Covellite	CuS	6	204	0.4
Bornite	Cu_5FeS_4	27	1005	0.2

Table 5.3 Statistics of Escondida copper I ore mineral grains used for textural analysis

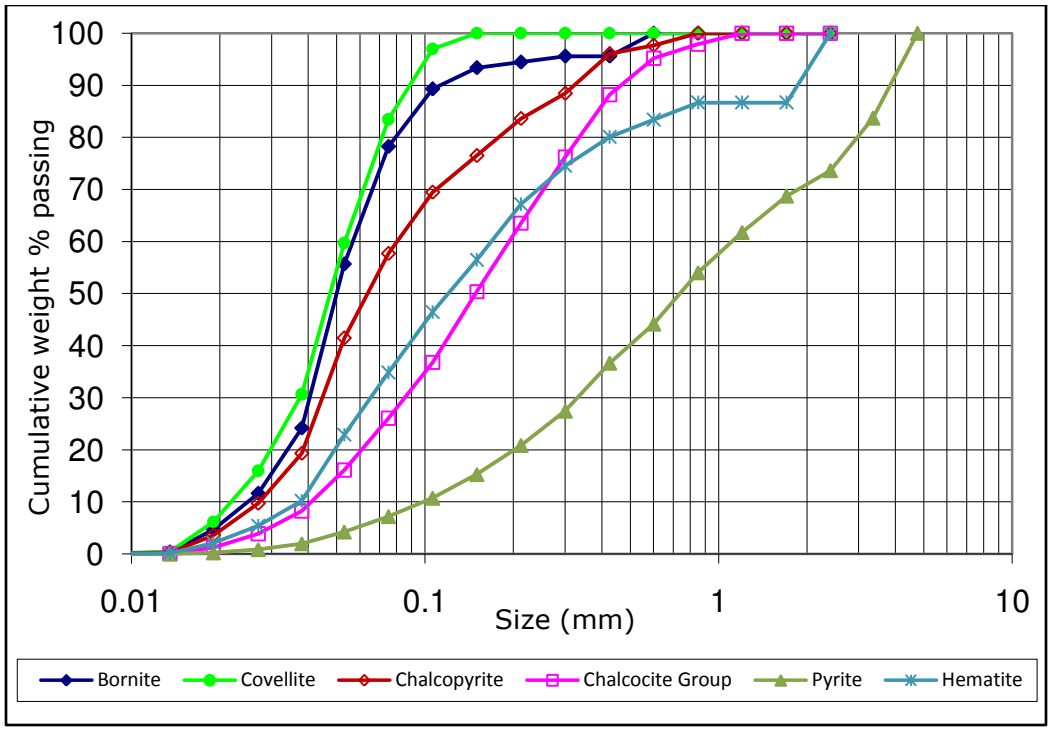

Figure 5.2 Grain size distribution of microwave heaters in Escondida copper I ore

The grain size distributions of chalcopyrite and pyrite which are the only major microwave heaters in the copper II ore are shown in Figure 5.3. The results are based on a total grain count of more than 5000 grains, equivalent to an average of approximately 110 grains per square centimetre. The results show a finer grain size distribution compared to the sulphide grains in Escondida copper I ore. The d_{80} of chalcopyrite grains is approximately 100 μm and only about half of the chalcopyrite grains are larger than 200 μm. The pyrite grains in copper II ore are even finer than chalcopyrite. The texture of the copper II ore therefore consists of mainly finely disseminated mineral grains.

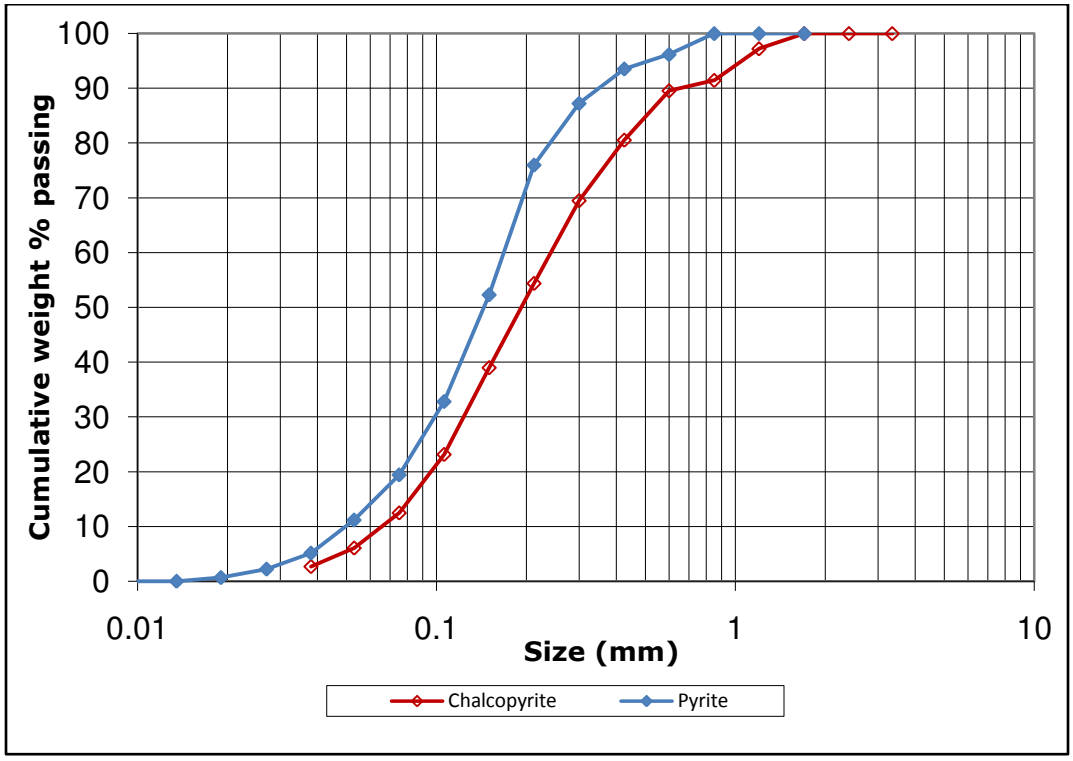

Figure 5.3 Grain size distribution of microwave heaters in Copper II ore

In summary, the two ores present two contrasting textures. The Escondida copper I ore contains a mixture of coarse and fine semiconducting mineral

grains whereas the copper II ore consists of mainly finely disseminated mineral grains.

5.5 Microwave Treatment of Ore Samples

5.5.1 Introduction

This section presents the methods used for treating ore samples with microwave energy. The influence of microwave treatment on mineral liberation and recovery was investigated by analysing samples of untreated ore and ore samples that were treated with microwave energy. The major microwave treatment method used was a conveyor based continuous process using a travelling wave applicator (discussed later). However, some treatments were also carried out in a single mode cavity batch process and also using pulse microwaves in order to investigate the influence of microwave power delivery method. However, it is emphasised that the work carried out using the pulse microwave system was limited by the fact that most of the work was carried out when the system was still being tested and not fully commissioned. Also the author lacked a permit to access the premises at e2v technologies laboratory in Chelmsford where the system was located and so relied on staff at Nottingham University and Chelmsford to carry out the treatments.

5.5.2 Method for Conveyor Continuous Process Treatment

The major technical requirement for the system required to carry out this work was the ability to induce high and uniform power density of at least 10^8 W/m^3 within the microwave absorbing mineral phases of the ore samples. A tunnel applicator to meet this requirement was developed by research teams

based at University of Nottingham and Stellenbosch University. The applicator design allows formation of multiple standing waves inside the heating cavity as shown in Figure 5.4.

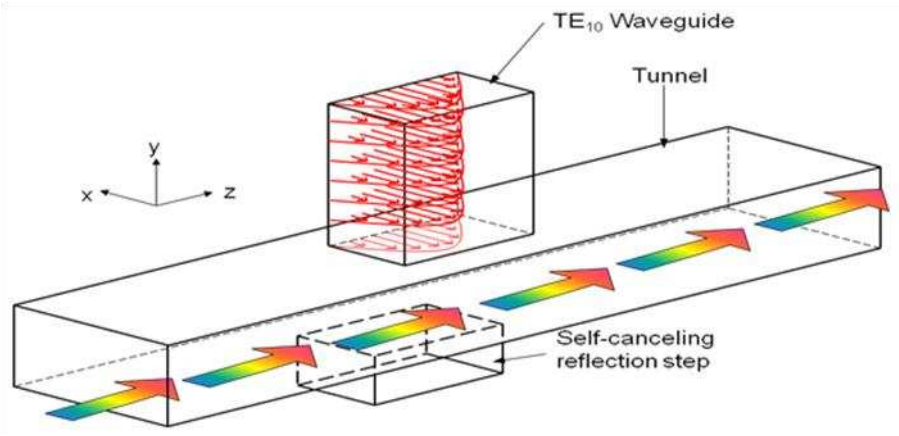

Figure 5.4 Schematic of geometry of applicator for continuous microwave treatment of ores (Wendy, 2005)

The main features of the applicator are described as follows (Wendy, 2005):

- It is fed orthogonally with a TE_{10} waveguide such that polarization in the waveguide is perpendicular to the direction of material movement.

- Variation in the electric field in the x-direction is eliminated by making the tunnel just the right width to minimize the E-field variation.

- Variation in the direction of material movement (z-direction) is not a major issue, since each particle should at some point encounter the same electric field strength.

- The only electric field variation of concern is that perpendicular to the direction of travel (y-direction). Variation in this direction leads to non-

uniform treatment of the sample as a result of the sample travelling through a hot spot.

The field strength variations in the y-direction were improved by the addition of a reflection step, a quarter of the effective wavelength deep, resulting in a total of half a wavelength being cancelled out in the step as shown in Figure 5.5. Due to the reflection of the microwaves, multiple hot spots are generated throughout the y-direction.

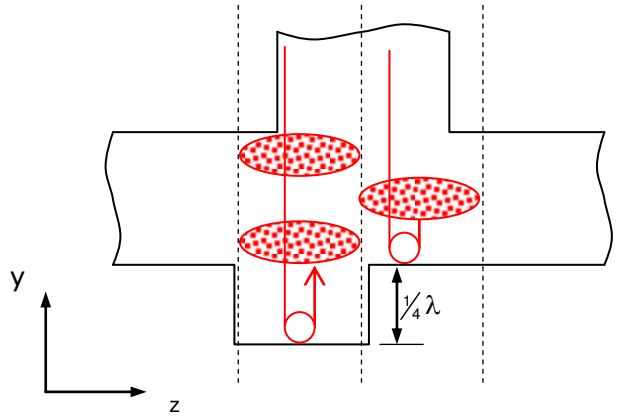

Figure 5.5 Cross sectional view of applicator showing hot spots as a result of introduction of a self cancelling step (Wendy, 2005)

The applicator also incorporated cascaded block structures (chokes) to prevent microwave radiation from escaping via either end of the tunnel. A schematic of the assembled applicator is shown in Figure 5.6.

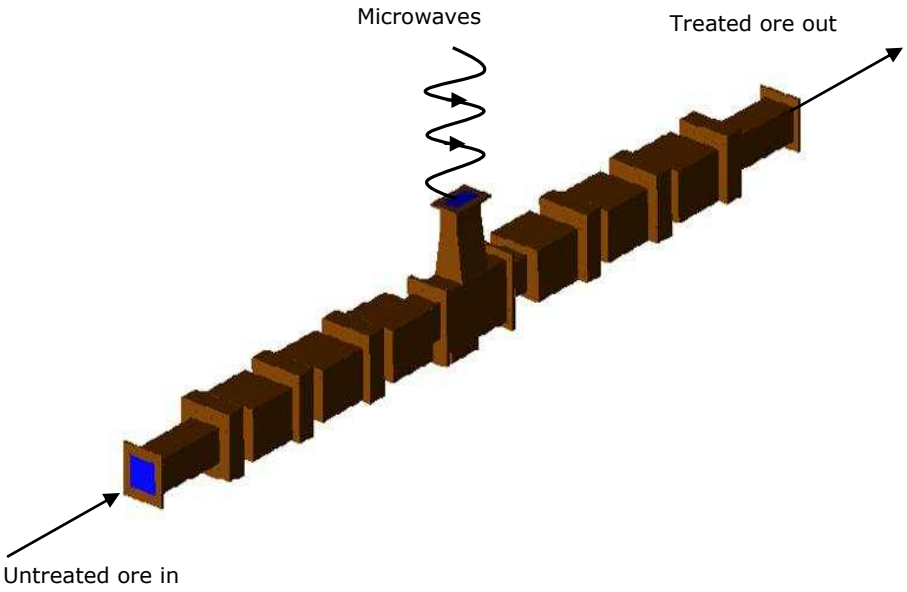

Figure 5.6 Configuration of applicator design for continuous microwave treatment of ores

The applicator was connected to a 30 kW variable power microwave generator. Microwaves were directed from the magnetron to the applicator by waveguides. The reflected power was redirected to the circulator and absorbed by a re-circulating water load. An automatic E-H tuner connected to the system ensured minimum amount of reflected power. Figure 5.7 shows an aerial view of the assembly of the major system components.

The material was fed through one end of the tunnel and carried by the conveyor belt through the applicator and to the exit at the other end of the tunnel. The throughput was determined by the belt speed which could be varied using a digital adjuster. The required power was set by control buttons attached to the Power Control Unit.

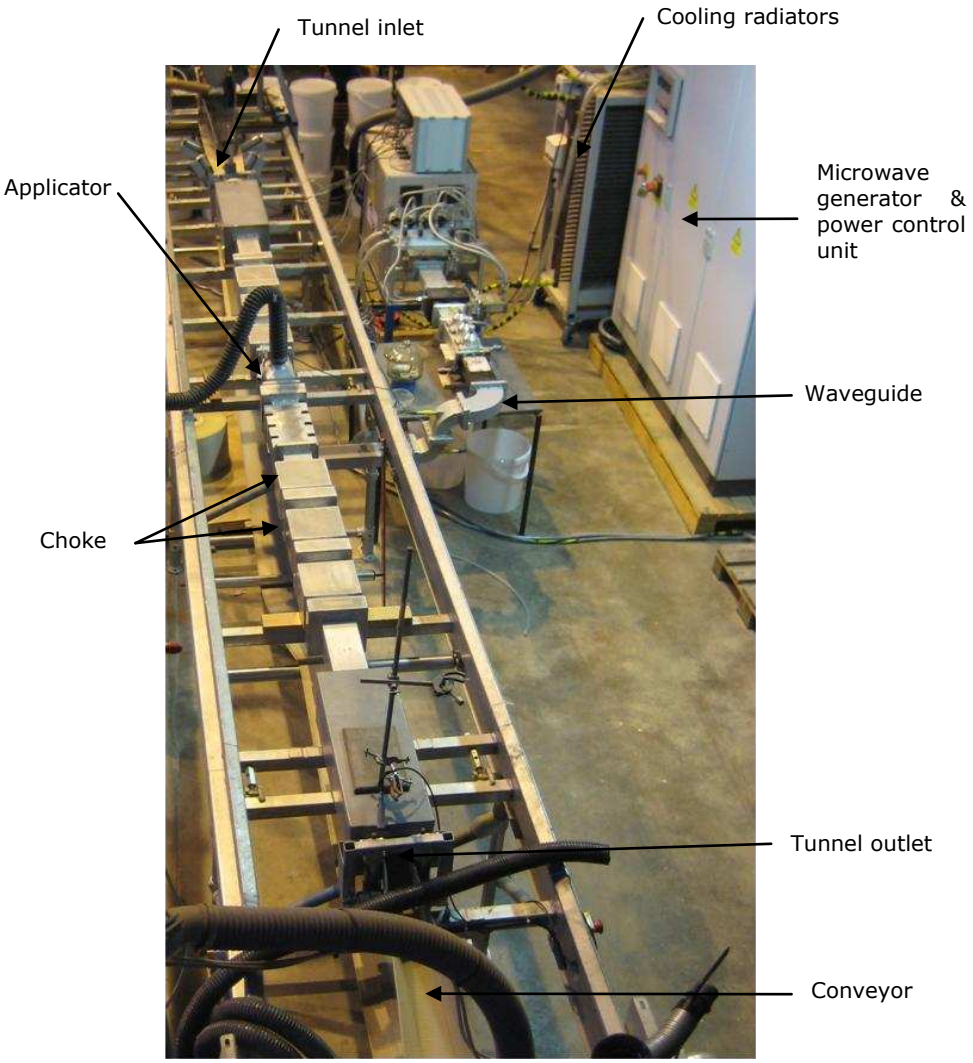

Figure 5.7 Microwave system used for continuous process ore treatment

During initial ore treatment trials, it was observed that there was a tendency for arcing to occur as a result of dielectric breakdown of air. Bright flashes were observed as the ore passed through the conveyor tunnel. If an arc occurred near the generator, a short circuit could occur and this could destroy the magnetron. A solution to the arcing problem was obtained when the material to be treated was confined within a rigid microwave-transparent material with a higher breakdown potential than air. This ensured that the

arcs would, in effect be quenched, before travelling back along the waveguides towards the generator. At the industrial scale, the sandwich belt and Japan pipe conveyors would most certainly provide a solution to the arcing problem. According to one of the world's leading conveyor manufacturers, *Dos Santos International*, sandwich belts are useful for movement of bulk materials which are sensitive to dust, air or water and are widely employed in the mining and industrial minerals industries (DSI, 2009). A sandwich belt conveyor consists of two belts which are pressed down on top of each other. In this way the material is essentially trapped and the particles do not move relative to each other. The fill factor is very high and voids are minimised which means that the likelihood of arcing is reduced significantly. A Japan pipe conveyor is essentially a conventional troughed belt conveyor which then employs transition idlers to form the belt into a pipe which acts as a dielectric barrier. On the discharge end, the pipe is unrolled and the belt returns to a conventional shape (Bateman, 2010).

In this study, uPVC ducts were used to provide a dielectric barrier and minimize arcing. All material to be treated was carefully packed into uPVC ducts of cross sectional area of 40×88 mm while ensuring a uniform packing density inside. The mass and length of the ducts were taken and these were used to calculate the packing density. The power level was adjusted to the maximum of 30 kW first by using a sacrificial material until the forward and reflected power gave steady readings. The material to be treated was then run through. Table 5.3 below shows a summary of the treatment conditions of each ore.

Control Parameter	Escondida Copper I Ore	Low Grade Copper II Ore
Sample mass (kg)	29.00	27.12
Duct length (m)	6.7	6.29
Packing density (kg/m)	4.33	4.31
Belt speed (m/s)	0.8	0.84
Forward Power (kW)	29.0	29.0
Reflected Power (kW)	5.5	4.0
Net Power (kW)	23.5	25.0
Energy Input (kWh/t)	**1.88**	**1.92**

Table 5.4 Treatment conditions for continuous process microwave treatment

The treated ore samples were then carefully removed from the ducts then bagged and labelled to be used for subsequent liberation and flotation tests described in later sections of this chapter.

5.5.3 Method for Single Mode Cavity Batch Treatment

The same microwave system and method described earlier in section 4.8.2 was used for single mode cavity batch process treatment. It was desirable that the samples are treated using similar energy inputs to those used in the conveyor continuous process. The sample mass and treatment times required were determined. However, due to the difficulty in setting the exact stroke speed and also in controlling the forward and reflected power, it was not possible to have exactly the same energy inputs. Table 5.4 shows a summary of the treatment conditions.

Control Parameter	Escondida copper I Ore	Copper II Ore
Sample mass (kg)	1.25	0.91
Treatment time (s)	0.37	0.44
Forward Power (kW)	14.1	15.0
Reflected Power (kW)	1.5	2.0
Net Power (kW)	12.6	13.0
Energy Input (kWh/t)	**0.80**	**1.76**

Table 5.5 Treatment conditions for single mode batch process treatment

5.5.4 Method for Pulse Microwave Treatment

Pulse microwave treatment of ores was carried out using a specially designed microwave system developed by e2v technologies as part of the wider ongoing partnership projects between University of Nottingham and AMIRA International. The unique capabilities of the rig used for pulsed microwave treatment was the ability to provide pulses of microwave energy variable in both pulse length (from 70 μs to 2 ms) and a peak power of up to 100 kW. The operating conditions of the test rig satisfied the claims put forward by Jones et al (2005) who suggested that future microwave assisted comminution equipment should be capable of generating power densities of between 1 x 10^{10} W/m^3 and 1 x 10^{12} W/m^3 with exposure times of between 0.2 and 0.002 s. The major system components of the pulse microwave test rig used are shown in Figure 5.8.

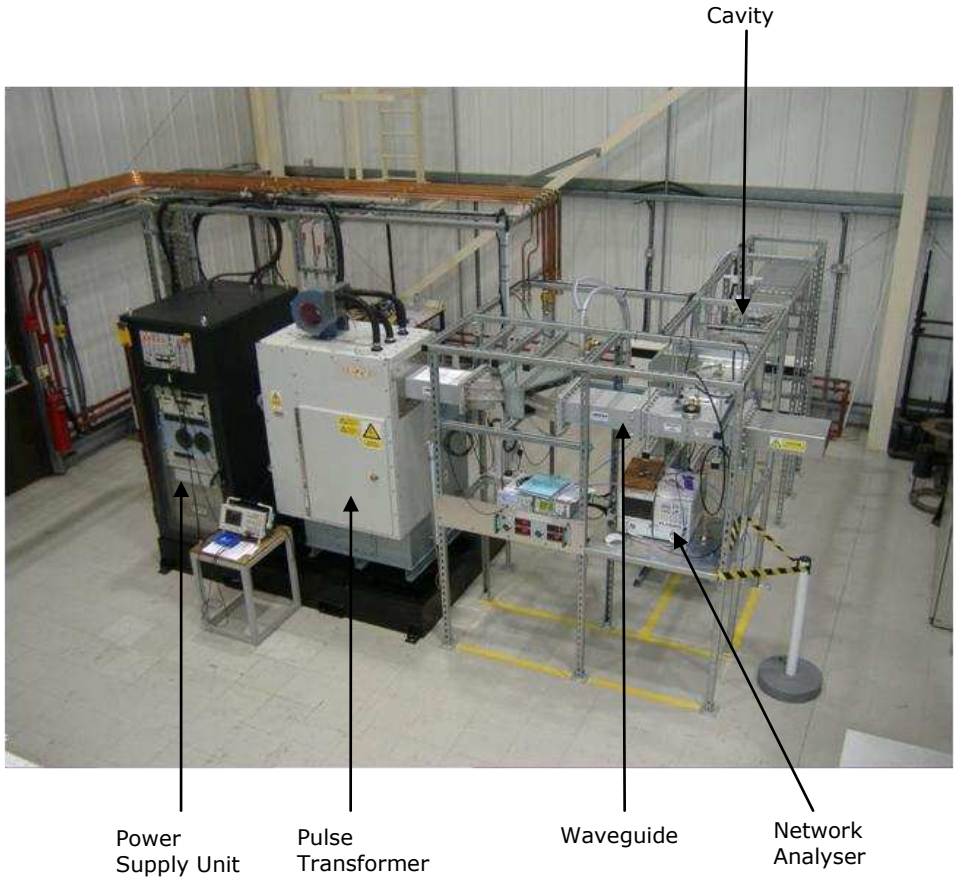

Figure 5.8 Microwave system used for continuous process ore treatment

Trial tests were first conducted to determine the mass of sample that ensured that the maximum amount of energy per pulse was being delivered. There was a tendency for arcing to occur when a small mass of sample was used. A higher proportion of the forward power was also reflected back when small samples were used. A compromise therefore had to be made between peak forward power and/or sample mass to determine optimum treatment parameters. A single pulse at maximum power was then fired into the sample and the peak and average forward and reflected powers were noted. Table 5.5 shows a summary of the treatment conditions.

Control Parameter	Escondida copper I Ore	Copper II Ore
Sample mass (kg)	0.255	0.224
Number of pulses	1	1
Pulse Repetition Frequency (Hz)	-	-
Pulse width (ms)	2	2
Foward Power (kW)	82.3	75.6
Reflected Power (kW)	27.8	16.6
Net Power (kW)	54.5	59.0
Energy Input (kWh/t)	**0.12**	**0.15**

Table 5.6 Treatment conditions for pulse microwave batch process treatment

5.6 Effect of Microwave Treatment on Particle Size Distribution after Grinding

5.6.1 Introduction

The quality of grinding in industrial processes is characterised by analysis of the product particle size distribution. Computer aided online product size analysis techniques have been developed to provide quick and accurate methods of measuring and characterising control parameters in industrial grinding processes. Despite this, grinding batch samples at different times is still by far the most familiar method used to determine the grind time required to achieve the desired grind size. The effect of microwave treatment on particle size distribution after grinding was investigated by conducting grinding tests on treated (by conveyor tunnel applicator) and untreated samples of ore. The particle size distributions of microwave treated and untreated material were analysed and compared.

5.6.2 Method for Grinding Tests

Each batch of untreated and treated ore particles was first crushed using a *Retsch BB2-67206* laboratory jaw crusher in order to obtain a product of top size of approximately 3.5 mm which is the typical size of feed material into a mineral processing ball mill. Crushing was carried out in two stages with a Closed Side Setting (CSS), i.e. the minimum gap between jaws at product discharge outlet, of 6.85 mm and 1.17 mm. The jaw crusher product was then mixed thoroughly using a rotary sample divider and then split into 1 kg test samples, which were then bagged and stored in a freezer to minimize surface oxidation of liberated mineral grains. The particle size distribution of the jaw crusher products was analysed by dry sieving using standard laboratory test sieves.

For each ore and treatment type, grinding tests were then carried out on samples of the jaw crusher product. A 1 kg test bag of the jaw crusher product was emptied into a *Legend Inc. SS 8×10 PN 24624* laboratory rod mill shown in Figure 5.9 and one litre of tap water was added. Grinding was carried out at 70% critical speed (69 rpm) for 2.5 min, 5 min, 10 min and 15 min. Wet sieving using a vibrating cascade sieve shaker was used to separate the ground mill product into two size fractions, one finer than 38 μm and the other coarser than 38 μm. The separated ground mill product was then filtered using pressure filters and then dried overnight in an oven at 70^0C. Each grinding test was repeated to check the reproducibility of the results.

Figure 5.9 Laboratory rod mill used for grinding calibration tests and prior to liberation and flotation testing

The particle size distribution of the fraction coarser than 38 μm was determined by dry sieving using standard √2 series sieves. The mass retained on each sieve was recorded on a data sheet shown in Appendix IV. The cumulative weight percentage passing each sieve size was then plotted on a logarithmic scale graph.

5.6.3 Results from Grinding Tests

Figure 5.10 shows the particle size distribution of the Escondida jaw crusher and grind mill products of untreated and conveyor microwave treated ore samples. The results obtained show a similar particle size distribution of untreated and treated jaw crusher products before grinding. However, there is a significant difference in particle size distribution between untreated and treated grind products after grinding for 2.5 minutes. The microwave treated product is finer than the untreated material. For example the d_{80} and d_{50} of

the microwave treated grind product is approximately 700 and 110 µm respectively whereas the corresponding sizes for the untreated products are 850 and 180 µm respectively. The difference in grind size distribution between the treated and untreated material reduces with increase in grind time. For example, only a slight difference is observed after grinding for 5 minutes and the 10 minutes grind products exhibit an almost similar size distribution curve. Microwave pre-treatment induces micro cracks which render the ore samples more amenable to grinding. As the ores are ground further, the induced cracks are consumed and the effects of microwave pre-treatment on grinding "diminish".

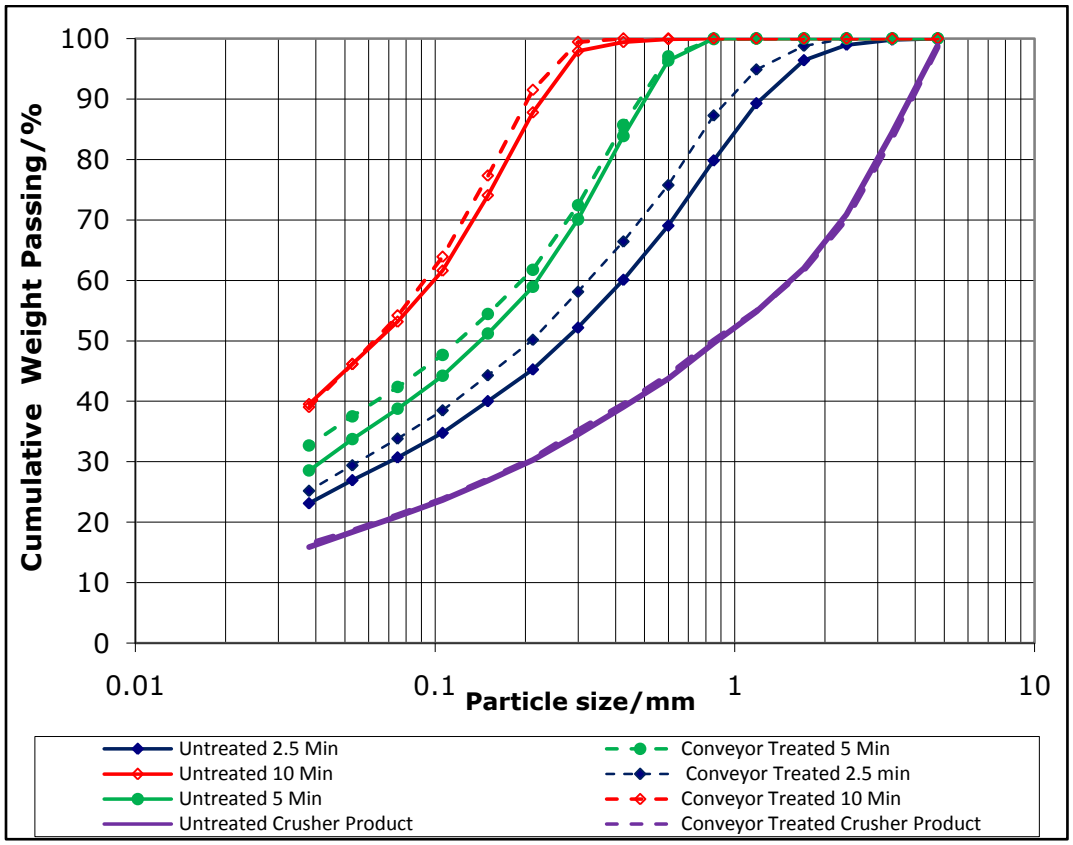

Figure 5.10 Particle size distribution of untreated and conveyor treated Escondida copper I ore samples after grinding for different durations

Figure 5.11 shows the particle size distribution of the copper II jaw crusher and grind mill products of untreated and conveyor microwave treated ore samples. The results are similar to those obtained for the Escondida copper I ore samples. Again, there is a slight difference in size distribution between untreated and treated ore samples after 2.5 and 5 minutes grinding but no noticeable difference after 10 and 15 minutes of grinding.

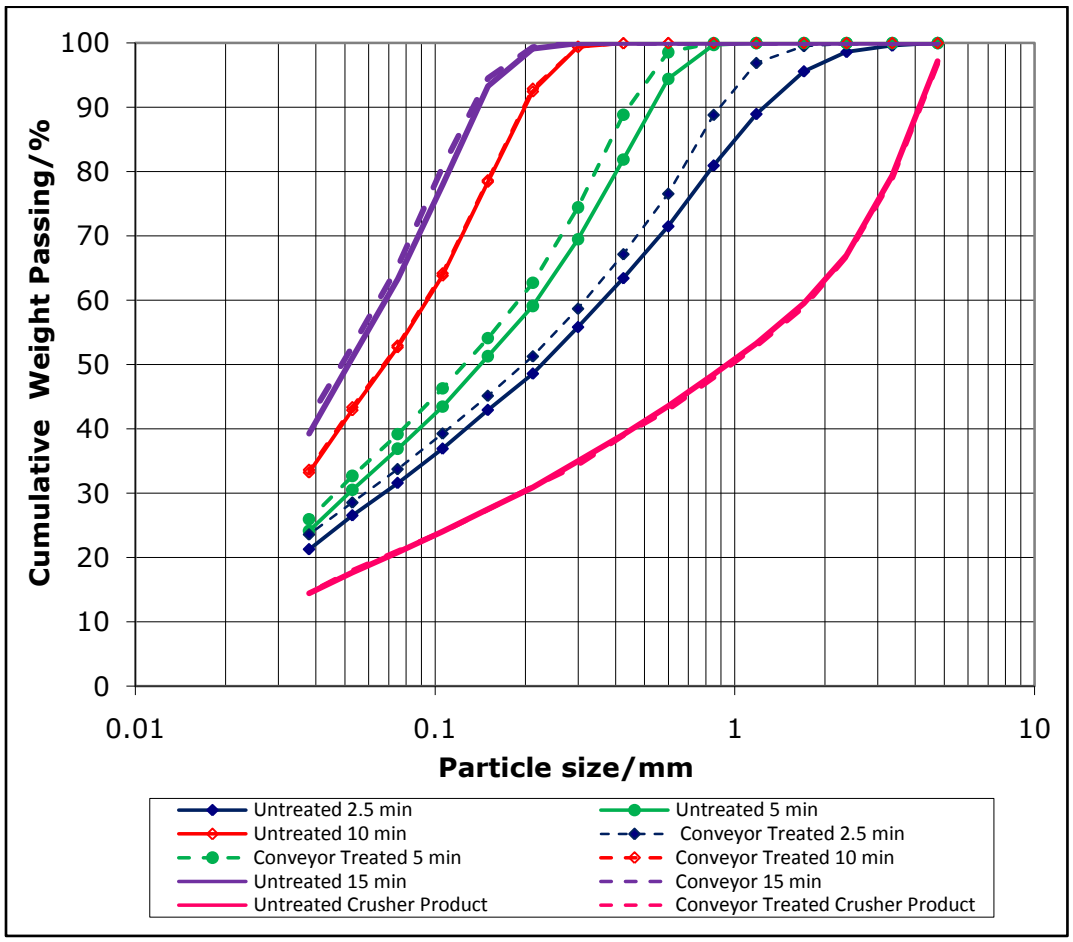

Figure 5.11 Particle size distribution of untreated and conveyor treated Copper II ore samples after grinding for different durations

Both results in Figures 5.10 and 5.11 show that as the grind time is increased, the particle size range becomes narrower and any effects that microwave treatment may have on the quality of grinding diminish. From the view point

of mineral processing, these results suggest that microwave treatment of copper ores is unlikely to have any significant effects on grind product particle size distribution so as to benefit froth flotation because the latter requires a grind quality equivalent to a d_{80} of less than 300 μm for efficient separation.

5.7 Effect of Microwave Treatment on Mineral Liberation

5.7.1 Introduction

It was shown in Chapter Four that microwave treatment of ores enhances inter-granular fracture and that this is likely to result into increased mineral liberation. This claim was investigated by subjecting microwave treated and untreated ore samples to mineral liberation tests. Any improvements in mineral liberation after microwave treatment were determined using the MLA. For the Escondida copper I ore, liberation tests were conducted on two different grind mill products in order to evaluate the effect on microwave treatment on coarse and fine grinding liberation. For the copper II ore, tests were carried out on same grind product but the analysis was carried out on three different particle size classes in order to evaluate liberation by particle size after microwave treatment.

5.7.2 Methodology for MLA Mineral Liberation Analysis

For each treatment type, a 1 kg test bag prepared in Section 5.6.2 was mixed with 1 litre of tap water and ground in a rod mill for a pre-set time. Wet sieving using a vibrating cascade sieve shaker was used to separate the ground mill into two size fractions, one finer than 38 μm and the other coarser than 38 μm. The separated ground mill was then filtered using pressure filters and then dried overnight in an oven at 70^0C. The fraction coarser than 38 μm

was split into four representative fractions using a riffle. One portion was then split into its respective size classes using standard √2 series sieves. Approximately 1-2 g of representative sample portions were obtained from each size class using a rotary sample divider and mounted into MLA sample blocks using epoxy resin. Samples were first thoroughly mixed using a small rotary sample divider and carefully placed into the MLA moulds to avoid particle segregation. The same procedure described in section 2.4.2 for preparation of polished sample sections suitable for MLA examination was followed only that in this case ground particles were mounted instead of thin solid sections.

The valuable copper bearing minerals (chalcopyrite, bornite, chalococite and covellite were all classified as "copper sulphide minerals" for purposes of liberation analysis. All the other minerals were classified as gangue. Each individual measured particle incorporating a copper sulphide mineral was binned within incremental composition ranges according to the weight percentage of copper sulphide minerals in that particle. For example, a particle containing 86% weight of $CuFeS_2$ would be apportioned to an incremental composition range of $80 \leq x < 90\%$ and that containing 12% CuS to $10 \leq X < 20\%$. The overall weight of copper sulphide minerals in each percentage range was presented on a cumulative distribution curve for different particle size classes between 4.75 mm and 38 μm. Particles finer than 38 μm were not analysed. This was because any particles below that size were expected to be fully liberated and their inclusion could be misleading. For the Escondida copper I ore, two grind times of 9 and 6.2 minutes were used to represent fine and coarse grinding respectively. For the copper II ore, a less grinding time of 4 minutes was used so as to give a wider particle size

distribution and enable classification of different size classes. Tests were carried out on untreated, conveyor treated, single mode and pulse treated samples.

5.7.3 Results of MLA Mineral Liberation Analysis

Figure 5.12 shows the liberation classes of the Escondida ore samples (all sizes from -1.18 mm+38 μm) after grinding for 9 minutes at different treatment conditions.

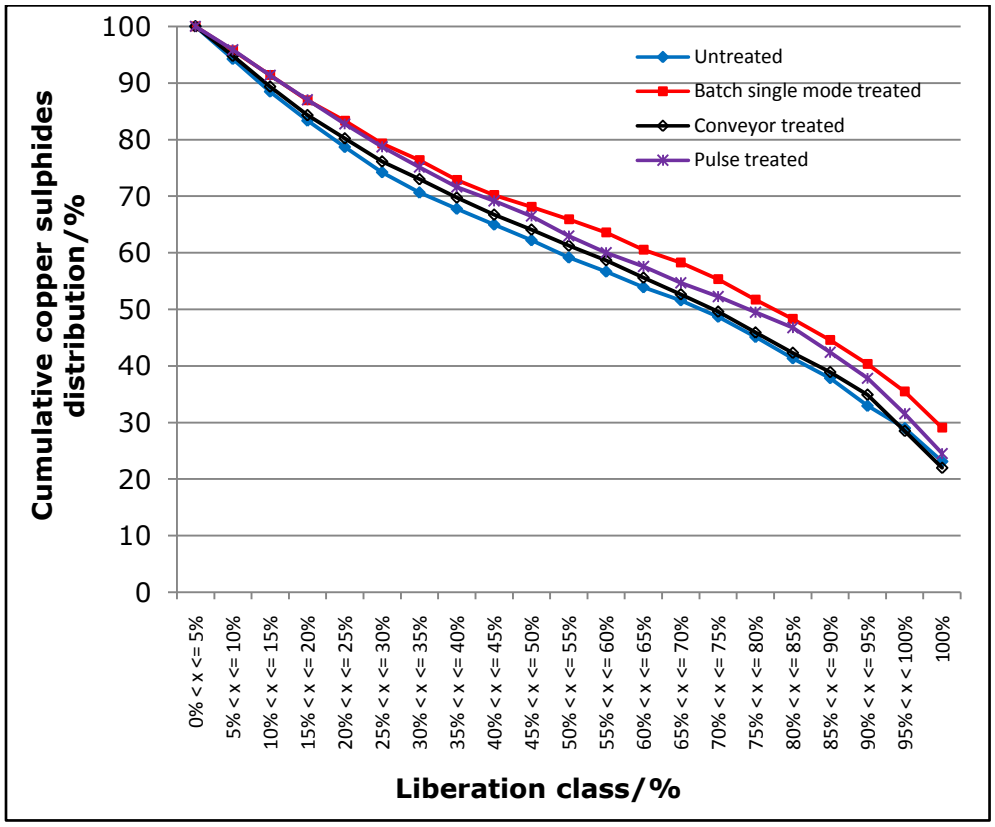

Figure 5.12 Copper sulphide liberation classifications for Escondida copper I ore samples after 9 mins grinding (d_{80}≈190 μm)

The results show that there is no significant change in liberation between the treated and conveyor treated ore samples. However a slight change is

observed in samples treated using the single mode cavity and pulse treated samples. For example, approximately 23% of untreated ore samples are fully liberated whereas about 30% of the single mode cavity treated particles are fully liberated representing a percentage increase in liberation of 7%. The percentage of partially liberated particles is also significantly higher in all liberation classes above 50% for single mode and pulse treated particles.

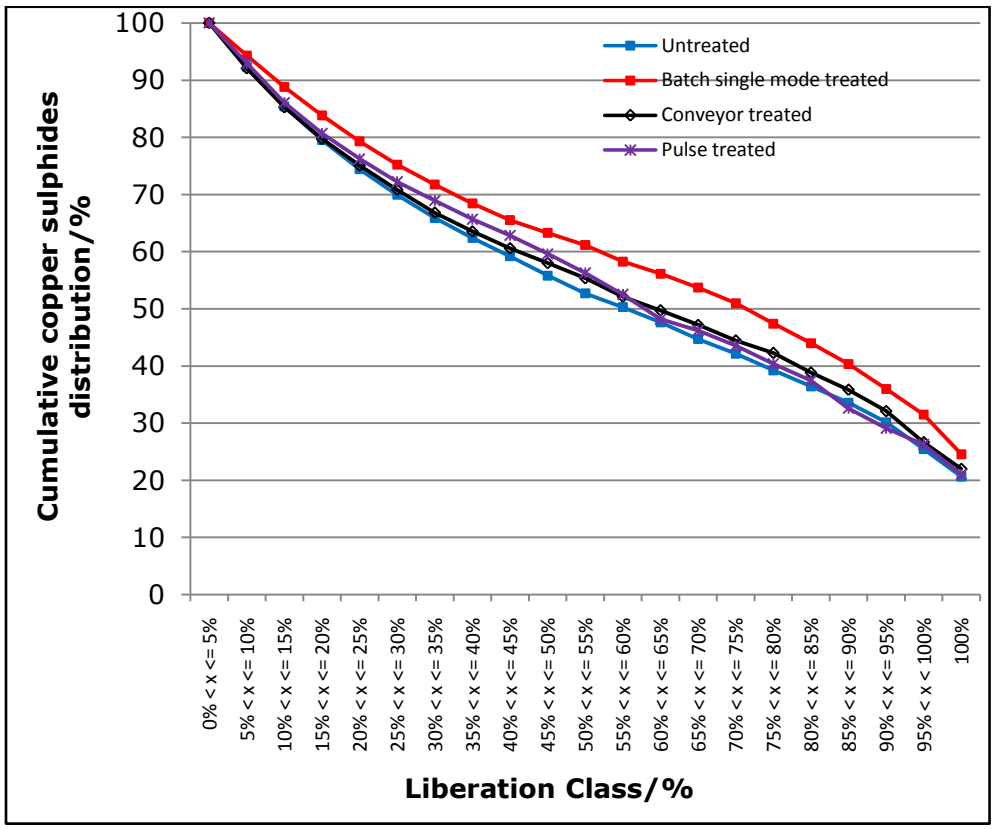

Figure 5.13 Copper sulphide liberation classifications for Escondida copper I ore samples after 6.2 mins grinding (d_{80}≈320 µm)

Figure 5.13 above shows the liberation analysis results of the coarse grind (6.2 mins). As with the fine grind, the results show virtually no difference in liberation between the untreated and conveyor treated samples. In this case however, no change in liberation is observed for pulse treated samples.

However, there is still a significant improvement in liberation for particles treated using the single mode cavity.

Figures 5.14 to 5.16 show the liberation analysis results of the Copper II ore samples after 4 minutes of grinding. An analysis of the degree of liberation by size class was carried out to investigate the effect of microwave treatment on liberation within different particle size classes. Three classes of -1.18 mm+425 µm, -425+212 µm and -212 µm were used to represent coarse, medium and fine particle sizes. It can be seen that for all treatment types, there is no change in liberation of coarse grained particles (-1.18 mm+424 µm). This is expected as the particles are still too coarse for the mineral grains to be liberated. Less than 3% of particles in this size class are liberated for all treatment types. However, significant improvements in liberation are observed in both the medium and fine particle sizes for conveyor treated and single mode treated particles. For example only approximately 22% of untreated particles in the -425+212 µm are fully liberated compared to about 43% of conveyor treated particles which are fully liberated. This represents a 21% increase in liberation. Likewise approximately 38% of particles less than 212 µm are fully liberated compared to 60% of conveyor treated material which represents a 22% increase in liberation.

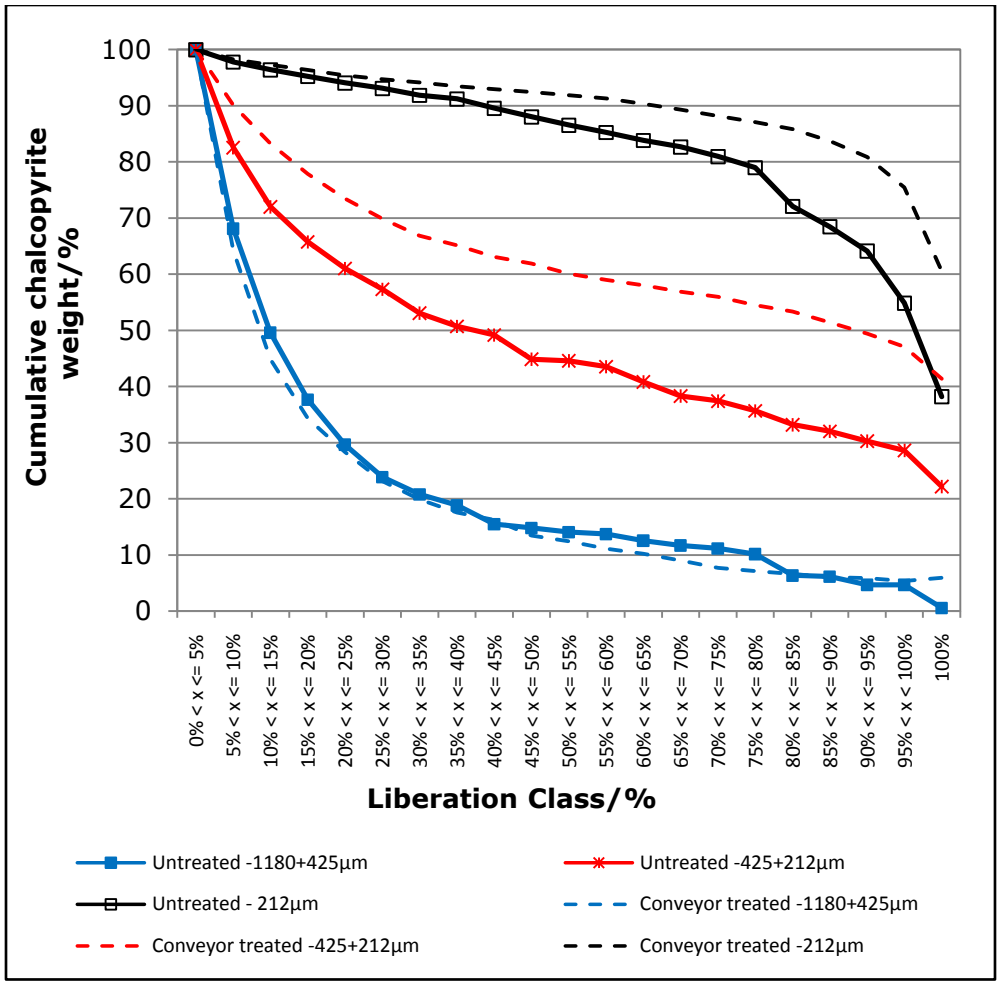

Figure 5.14 Chalcopyrite liberation classifications of untreated and conveyor treated Copper II ore samples after 4 mins grinding (d_{80}≈430 µm)

For the single mode treated particles, significant change in liberation was observed mostly in the partially liberated medium and fine size particles. For example, from Figure 5.15, an increase of at least 10% is observed in liberation classes between $25 \leq x \leq 95$ in the -425+212 µm size class. Single mode treated particles less than 212 µm show an increase in both partial and full liberation.

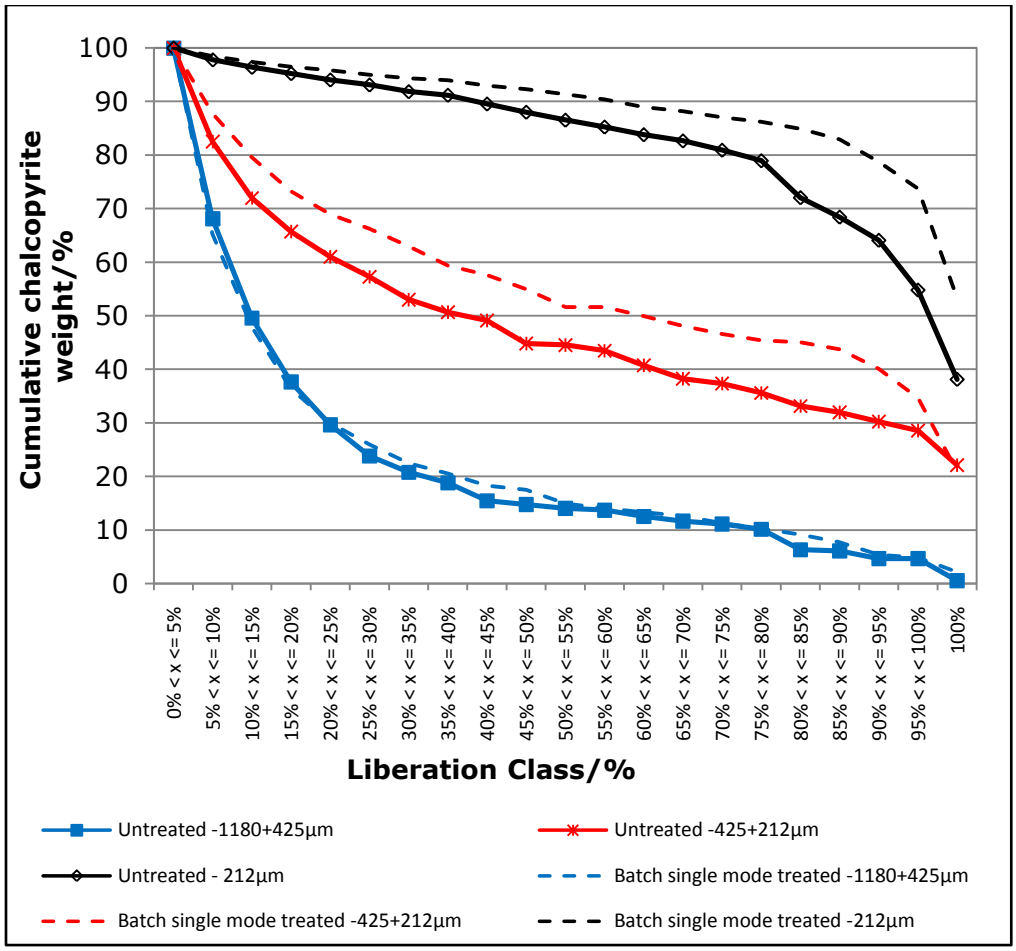

Figure 5.15 Chalcopyrite liberation classifications of untreated and single mode treated Copper II ore samples after 4mins grinding (d_{80}≈430µm)

The results obtained from pulse treated particles do not show significant increases in liberation in all particle size classes. There is an indication of a slight increase in liberation of the fine particles less than 212 µm although this could be have been influenced by the presence of very fine particles less than 100 µm which are expected to be liberated whether treated or untreated. The coarse fraction also shows an increase in liberation although the degree of liberation is low (less than 85%) As stated previously, the work involving the pulse test rig was carried out when the rig was still being tested prior to its commissioning. Some development work was still being conducted on the test

rig at the time this work was carried out and for this reason these results will not be included in the major discussions and conclusions that follow. Furthermore, subsequent test work involving grade–recovery analysis was not carried out on pulse treated samples.

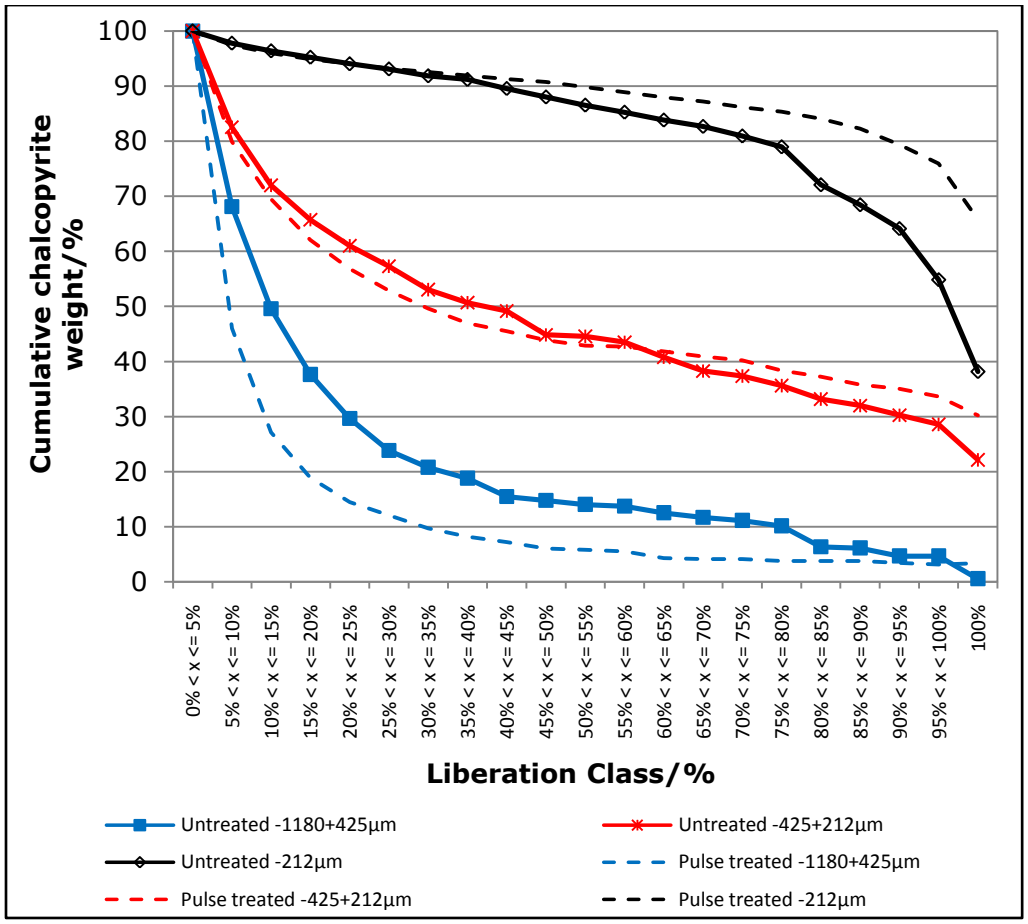

Figure 5.16 Chalcopyrite liberation classifications of untreated and pulse treated copper II ore samples after 4 mins grinding (d_{80}≈430 µm)

The liberation results from both the Escondida copper I and the copper II ore samples suggest that microwave pre-treatment of the two ores achieved significant improvements in mineral liberation. The influence of microwave treatment on liberation is more significant in medium grind size particles between 212 and 425 µm. The results obtained also show that the single

mode cavity achieves better results in terms of increased partial and full liberation. From the view point of mineral processing, this is a positive result because the size range of 212-425 μm which shows the highest percentage increases in liberation overlaps the flotation particle size of between 150 and 300 μm.

5.8 Effect of Microwave Treatment on Mineral Recovery

5.8.1 Introduction

In order to assess the economic benefits of microwave treatment in terms of value of mineral recovered, flotation tests were conducted on untreated and treated ore samples. An assay was then carried out on the collected concentrates to determine any increases in mineral recovery after microwave treatment. The standard flotation procedures currently used at the respective mines (Appendix IV) were adopted as much as possible. However, due to restrictions of chemicals available, some slight modifications to the standard procedure were made. The modifications made are discussed in the next section.

5.8.2 Materials and Method for Grade-Recovery Analysis

For each ore and microwave treatment type, a 1 kg test sample prepared in Section 5.6.2 was ground in a laboratory rod mill for a pre-determined period. The grind times required to give a d_{80} of 190 and 300 μm were estimated from the grinding curves shown in Figures 5.10 and 5.11. This was approximately 9 and 6 minutes respectively. The same grind times were used for both ores and treatment types although the grinding calibration curves show a slight difference between treated and untreated ores and also between the two

different ores. The grind sizes of d_{80} = 190 µm and d_{80} = 300 µm were selected to represent fine and coarse grind sizes in order to compare the effect of microwave treatment on coarse and fine grinding recovery. Grinding was conducted at approximately 60% solids weight by adding a litre of tap water. The ground mill was then carefully poured into a 4-litre stainless steel flotation tank. The use of a 4 litre tank, which was the smallest size available in laboratory, instead of the recommended 3.1 litre tank, lowered the pulp density from the recommended 26.5% to 21.4% solids by weight. A 62 g/t dose of Cytec Aero Promoter (AP) -3758 (MIBC) was used as the primary collector instead of the recommended dithiocarbamate. 18 g/t of AX-317 (SIBX) was used as a secondary collector. Oreprep X-133 (16 g/t dose) and Pine Oil (9 g/t dose) were used as frothers. Lime was added to adjust the mixture to the recommended pH of 10

A laboratory flotation cell (type Denver D12) was used to agitate the mill mixture for 5 min at an air flow rate of 0.5 l/min. Five concentrates were then collected after 30 s, 1 min, 2 mins, 5 mins and 12 mins to enable an assessment of the flotation kinetics to be made. The froth was scrapped every 10 s. A minimum of five flotation tests were conducted for each grind time to assess the repeatability of the results. For each grind time, three different sets of tests were carried out to assess grade-recovery, recovery kinetics and recovery by size. The collected concentrates were then filtered and dried in an oven overnight at 80ºC. The dried concentrates and tailings were sieved into their respective size classes using √2 sieve series, then pulverised, bagged and labelled and submitted to the ALS laboratory in Brisbane, Australia for assay. Atomic Emission Spectroscopy (ICP-AES) technique was used to determine the weight percentages of Cu and Fe while the LECO CNS-2000

analyzer was used to determine the sulphur content. The grade and recovery of copper sulphides (CuS), iron sulphides (FeS) and non sulphide gangue (NSG) were then determined.

Metallurgical efficiency of any concentration operation can be expressed by a curve showing the recovery attainable for any value of concentrate grade (Wills, 2006). There exists an inverse relationship between concentrate grade and overall recovery as shown in Figure 5.17. If the concentrate grade is very high, it implies that it has minimal contamination with unwanted material and inevitably some of the wanted material will be lost to the tailings and the overall recovery will be low. Therefore there is always a trade-off between grade and recovery during mineral processing. Overall metallurgical efficiency increases in the direction shown by the arrow in Figure 5.17 (i.e. by moving the whole curve to higher point so that both grade and recovery is maximized). For example, process B shows higher efficiency than process A assuming all other factors are constant.

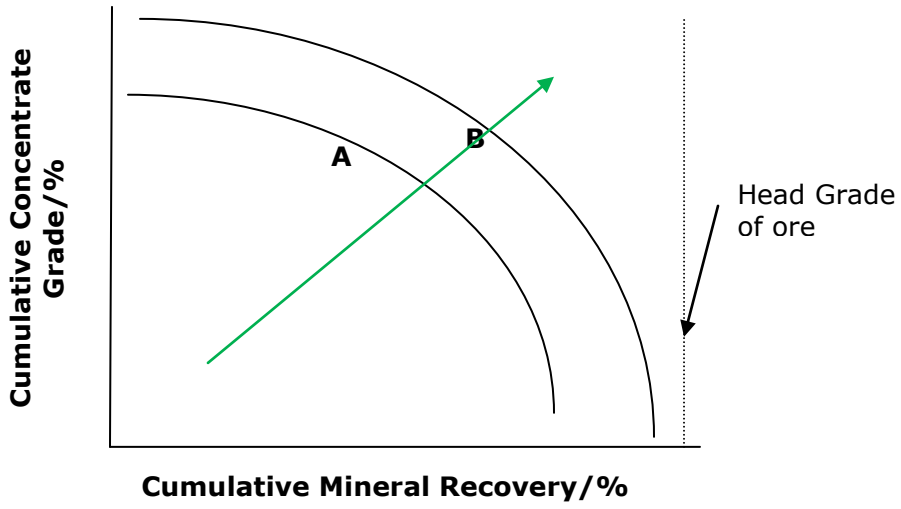

Figure 5.17 A Typical Grade-Recovery curve

5.8.3 Results of Mineral Grade-Recovery Analysis

Figures 5.18 and 5.19 show the cumulative grade – recovery curves of the Escondida copper I and the copper II fine grinds respectively. The results show that there is no noticeable difference in cumulative recovery of both Cu and CuS between treated and untreated samples. The Escondida conveyor treated samples however exhibit a 1.5-3% increase in Cu and CuS grade. The copper II samples do not show any increase in grade or recovery and in fact the results show a slight grade reduction of less than 1% after treatment but this is thought to be as a result of difficulty in experimental repeatability, especially during froth scrapping because the sulphide concentration of copper II ores is very low compared to the Escondida ores and therefore a small difference in measured Cu and CuS concentrations results in a more significant error.

A 3-6% decrease in both grade and recovery of FeS is observed in Escondida treated samples. Samples treated with a single mode cavity exhibit a higher reduction than those treated with the conveyor tunnel applicator. For example at 80% recovery, the grade of FeS in untreated samples is 48% while that in single mode and conveyor treated samples is 42% and 44% respectively. The copper II ore samples do not show a reduction in FeS grade after treatment but show an overall reduction in FeS recovery of about 5% after microwave treatment using the conveyor tunnel applicator. However, it should be noted that the overall grade of FeS in the copper II ore samples is very low (maximum 4%) compared to the Escondida samples (maximum 51%)

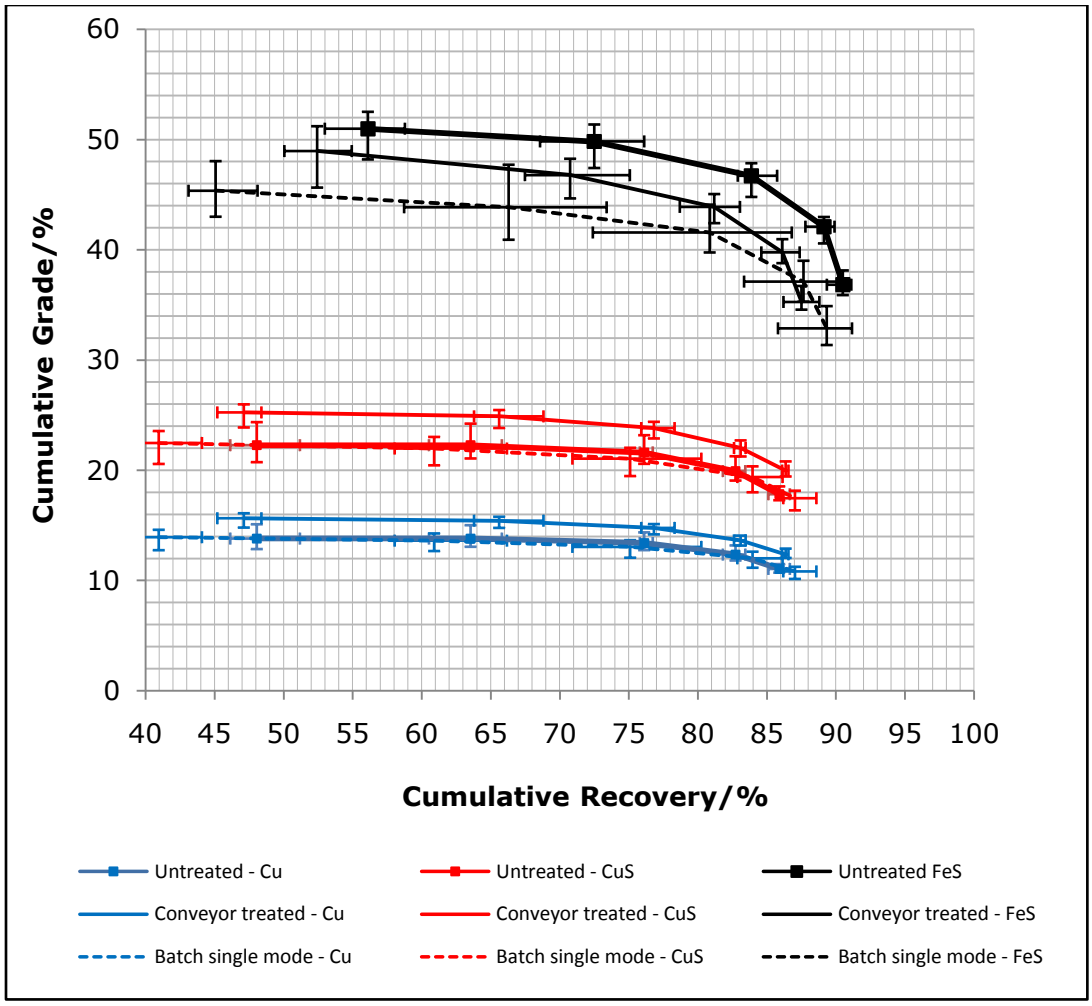

Figure 5.18 Cumulative grade-recovery of Escondida ore fine grind (9 mins) ore samples

Figures 5.20 and 5.21 show the cumulative grade – recovery curves of the Escondida and copper II coarse grinds respectively. A 1.4% increase in copper sulphide recovery is obtained for the conveyor treated Escondida samples whereas a 2% recovery increase is shown by samples treated using a single mode cavity. The conveyor treated samples showed no change in copper sulphide grade but the single mode treated samples showed a 1% increase in grade, mostly contributed by the first two concentrates. As with the fine grind, a 2-5% reduction in iron sulphide grade and recovery is obtained from Escondida samples. It appears therefore that microwave pre-treatment has a

positive effect on both grade and recovery at coarse grinding. It is most likely that this is due to the increase in liberation observed in medium grained particles (-425+212 μm) after microwave treatment (see Figures 5.14 and 5.15). The samples ground for 6 mins (coarse grind) possess more particles in this size range and hence the increase in overall grade and recovery. The fine grinds do not show any increase in grade or recovery perhaps, because most grains are already liberated and hence no noticeable different in liberation after microwave treatment.

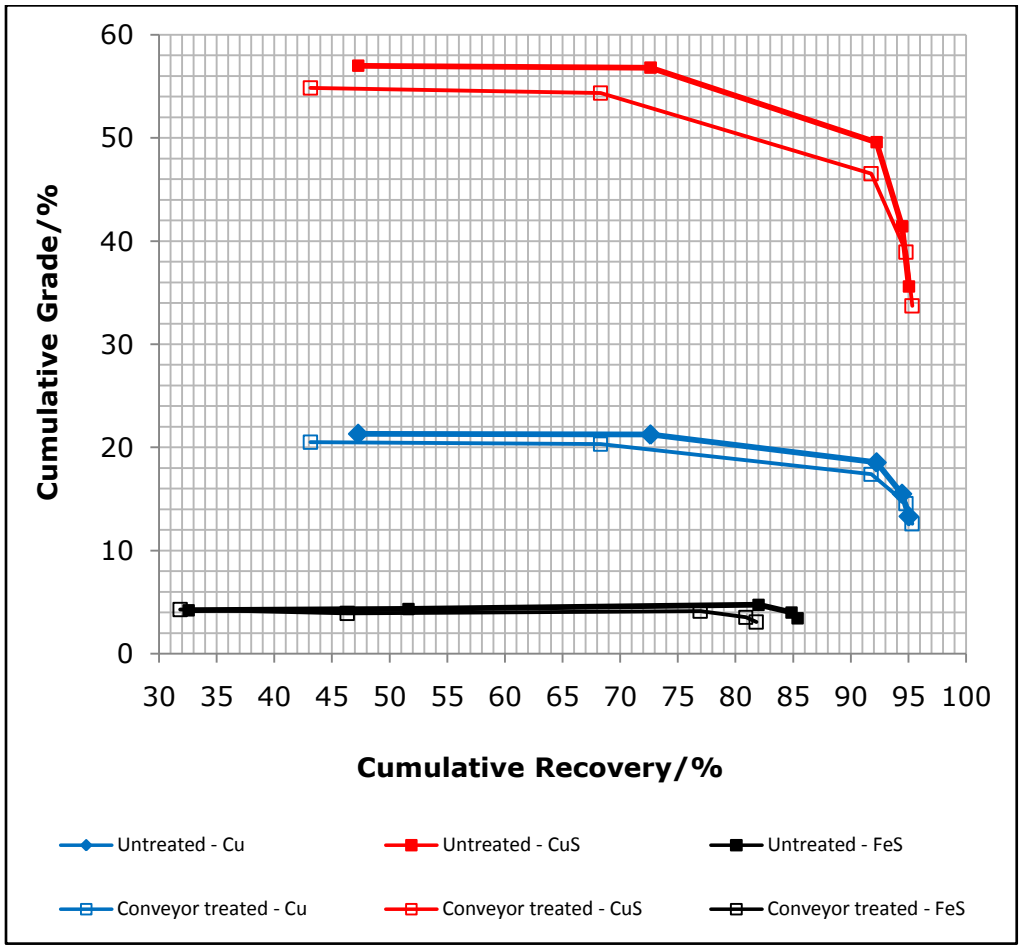

Figure 5.19 Cumulative grade-recovery of Copper II fine grind (9 mins) ore samples

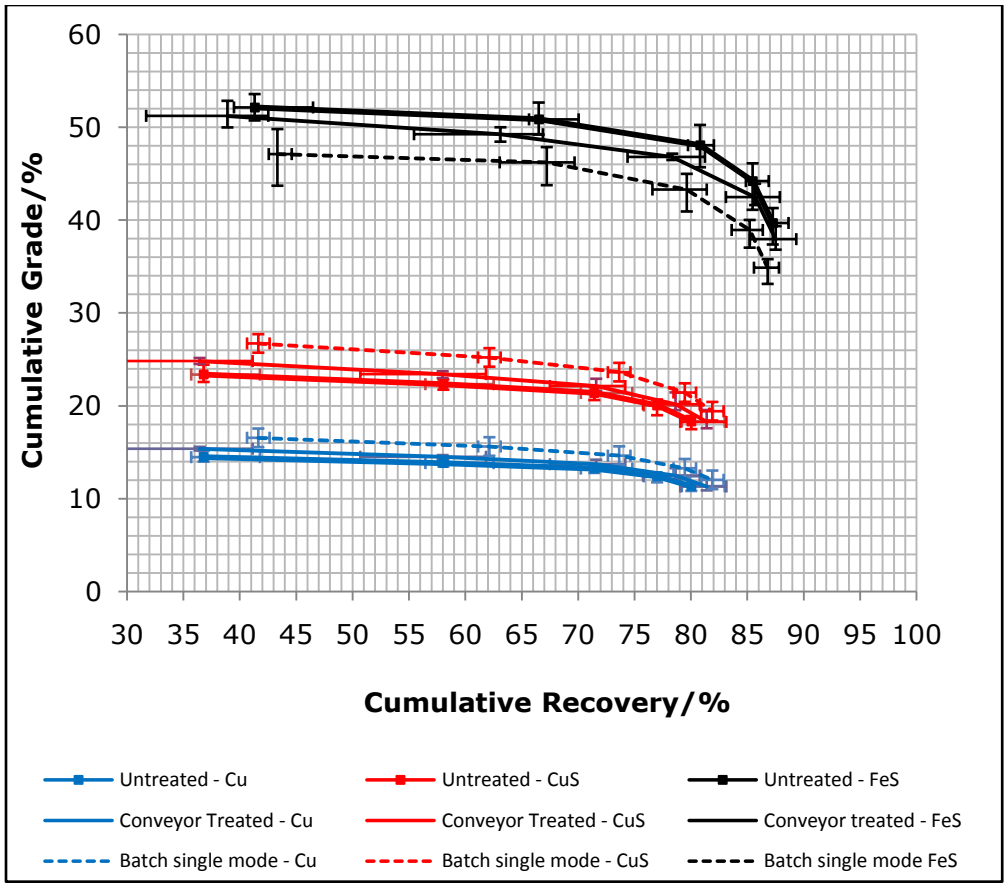

Figure 5.20 Cumulative grade-recovery of Escondida coarse grind (6 mins) ore samples

The conveyor treated copper II coarse grind results (Figure 5.21) showed a very low copper content in the first two concentrates. However, the overall copper grade was similar as the copper was recovered in later concentrates resulting into a 1% increase in copper recovery. The sulphur content of the tailings was very low for both untreated (0.07%) and treated samples (0.05%) and this resulted in the extra 20% iron sulphide recovery, as shown in Figure 5.21.

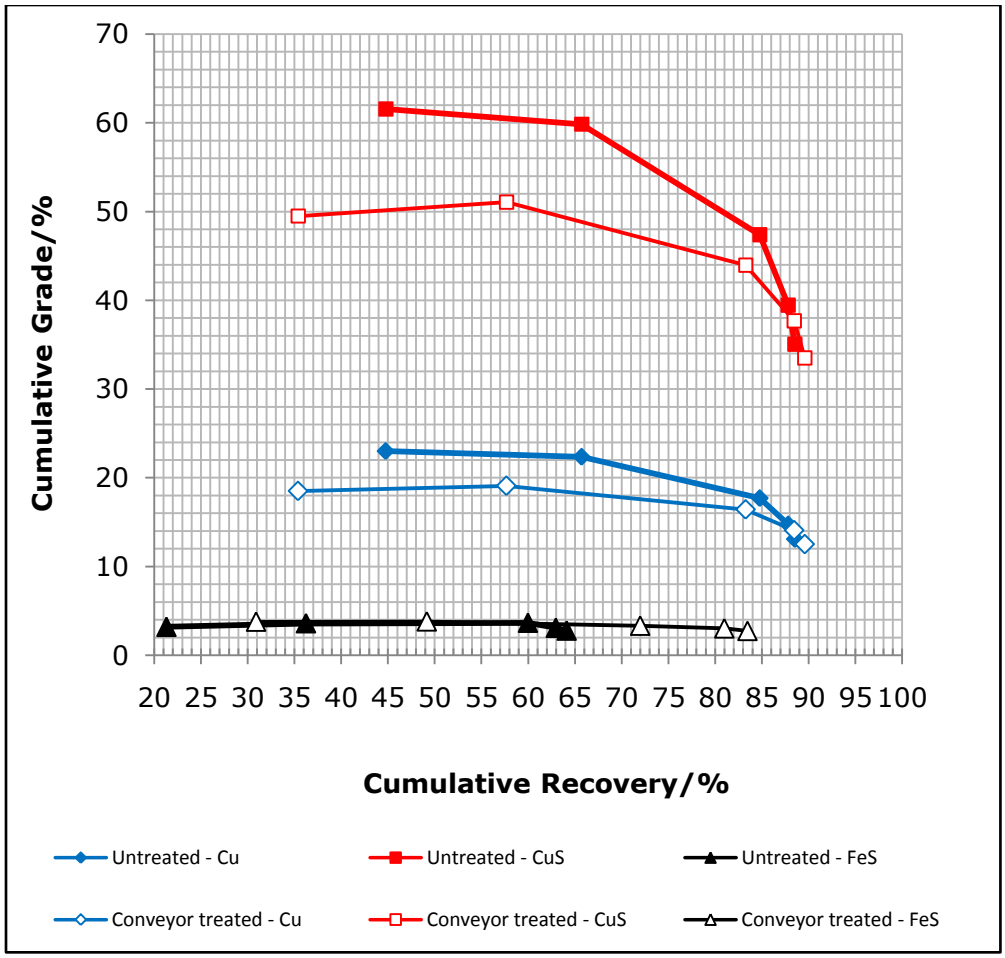

Figure 5.21 Cumulative grade-recovery of copper II coarse grind (6 mins) ore samples

Figures 5.22 and 5.23 show the rate of copper and iron sulphides recovery from the fine grinds. The results show virtually no difference in recovery kinetics. Over 80% of Escondida copper and iron sulphide is recovered after 5 minutes of flotation for both untreated and treated samples. The recovery kinetics of the coarse grinds are shown in Figures 5.24 and 5.25. Again, the results show no difference in rate of copper sulphides recovery. The results suggest that microwave treatment neither speeds nor slows the flotation kinetics. From the view point of microwave assisted processing, this is still a good result because it shows that microwave treatment does not alter the

physico-chemical properties of minerals, e.g. surface oxidation, to an extent that would inhibit the flotability of the minerals.

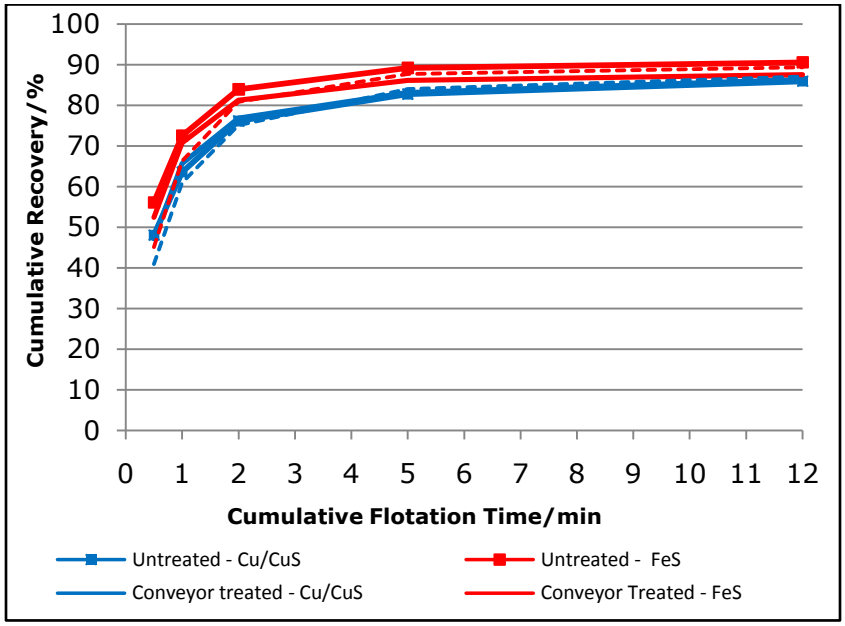

Figure 5.22 Recovery kinetics of Escondida fine grind (9 mins)

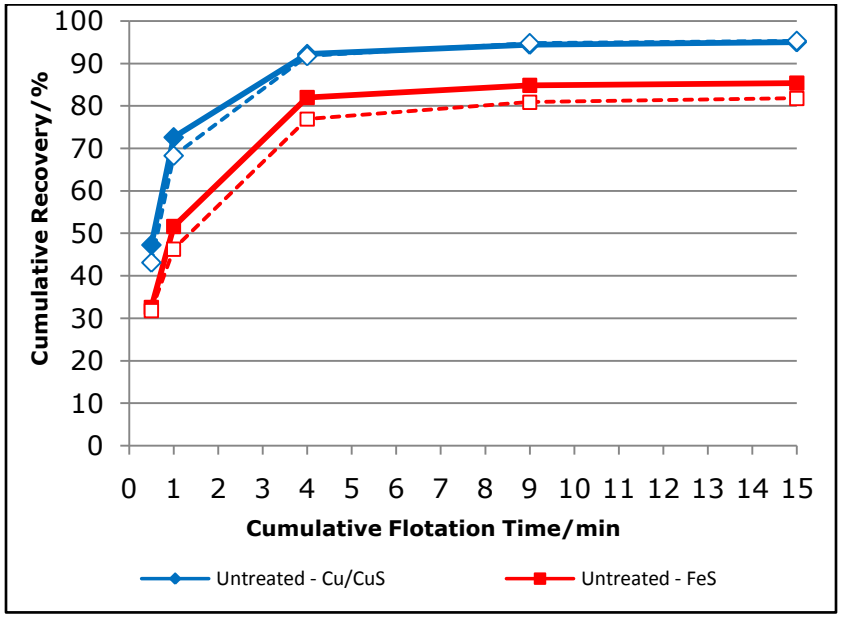

Figure 5.23 Recovery kinetics of Copper II fine grind (9 mins)

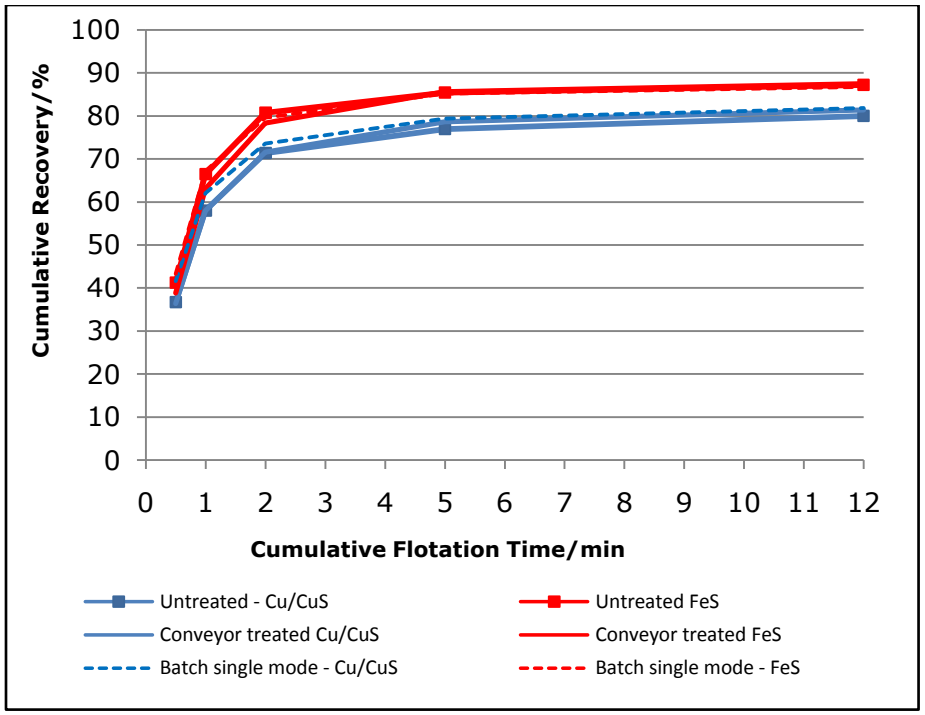

Figure 5.24 Recovery kinetics of Escondida coarse grind (6 mins)

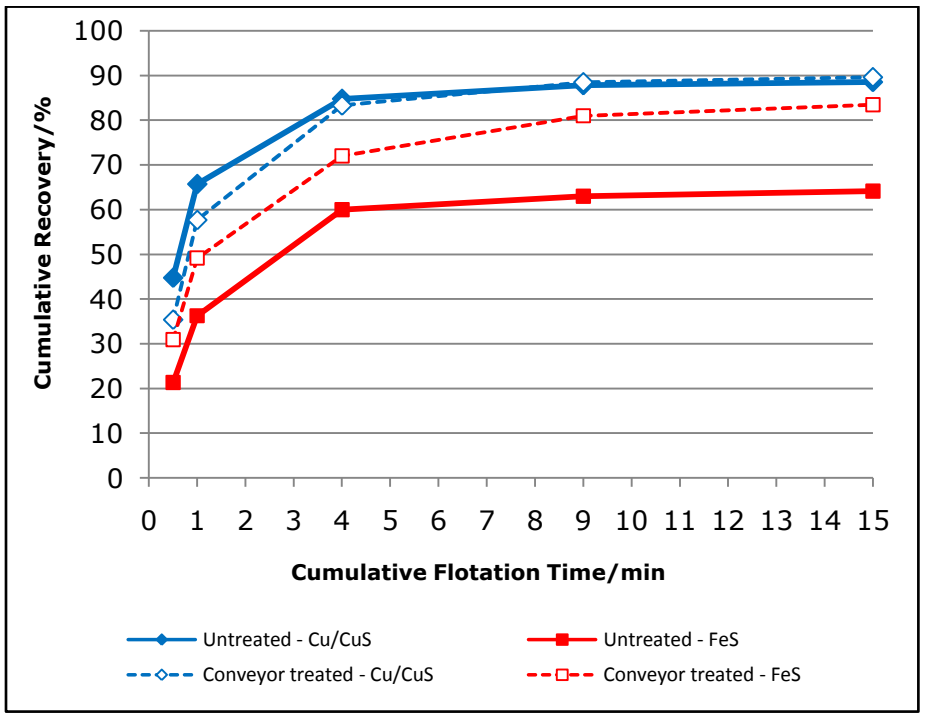

Figure 5.25 Recovery kinetics of Copper II coarse grind (6 mins)

The overall recovery of CuS and FeS from the different particle size classes between 0 and 425 μm (i.e. -425+300, -300+212, -212+150, -150+106, -106+75, -75+53, -53+38 and -38 μm) was determined by analysing the material retained on the respective sieve. Figures 5.26-5.28 show the results of the overall recovery as a function of the particle size. The results show variations in overall recovery between treated and untreated samples depending on the size range. For the fine grind, there is virtually no difference in copper sulphides recovery between the untreated and conveyor treated Escondida samples (Figure 5.26). The single mode treated samples show a slight decrease in copper sulphide recovery above 150 μm but it is believed that this is as a result of difficulty in reproducibility during flotation testing and size classification. The copper II conveyor treated fine grinds show a slight increase in recovery of copper sulphides between 100 and 200 μm (Figure 5.27) but again this could be due to testing reproducibility. Fine grinding diminishes the effects of microwave treatment on liberation as most minerals are already liberated and hence no significant changes in recovery were observed after microwave treatment.

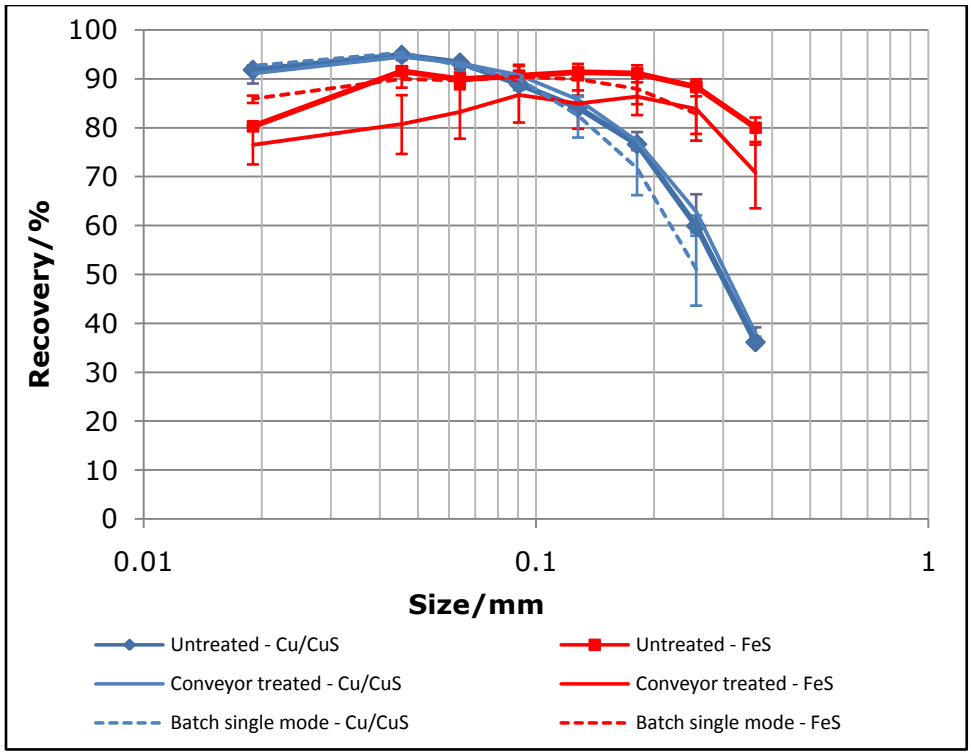

Figure 5.26 Sulphides recovery by size from Escondida fine grind

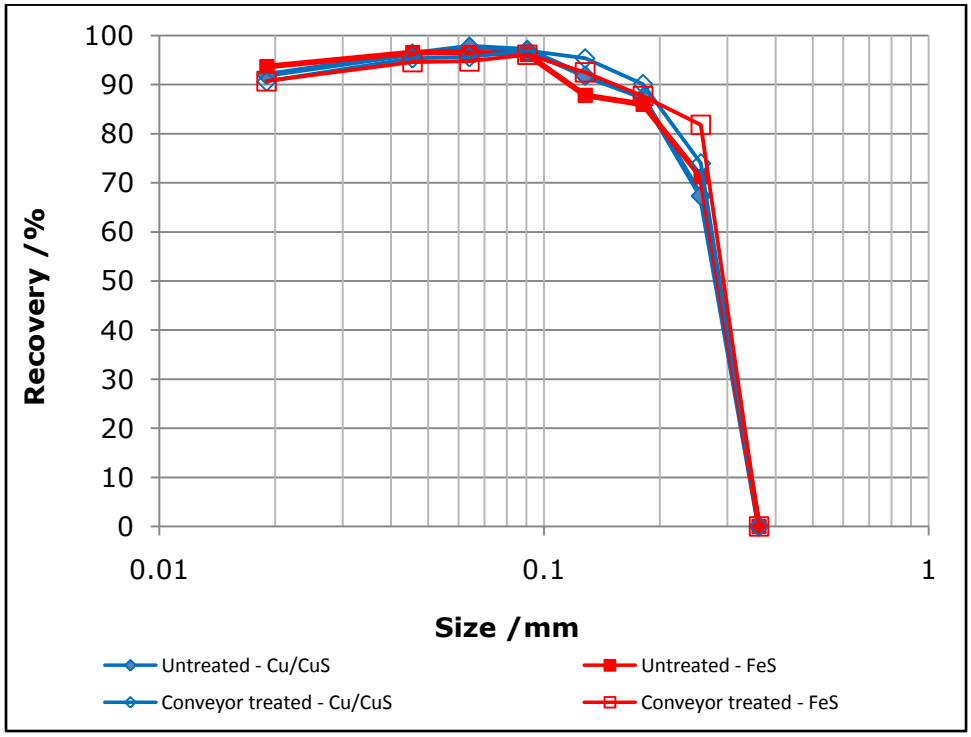

Figure 5.27 Sulphides recovery by size from Copper II fine grind

The liberation results shown in Figures 5.12 to 5.16 showed a significant increase in copper sulphides liberation in all single mode treated samples. The degree of liberation was more significant in the -425+212 µm size class of the coarse grinds. Figures 5.28 and 5.29 show the results of the recovery by size from the coarse grinds. The scale of the graphs in Figures 5.28 and 5.29, which show the recovery over the whole size range from 10 to 500 µm, does not enable a detailed comparison between recovery from untreated and treated samples. It should be noted that flotation processes are highly efficient and typical recoveries are often above 90%. However even an increase of a fraction percentage in recovery can be very significant if achieved at industrial scale.

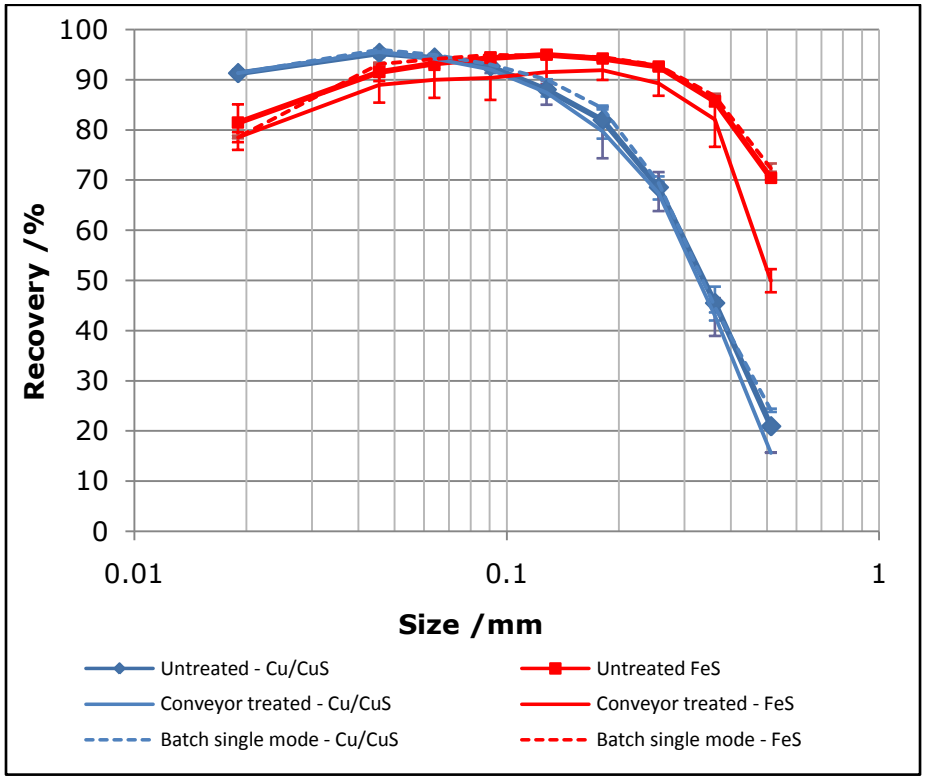

Figure 5.28 Sulphides recovery by size from Escondida coarse grind

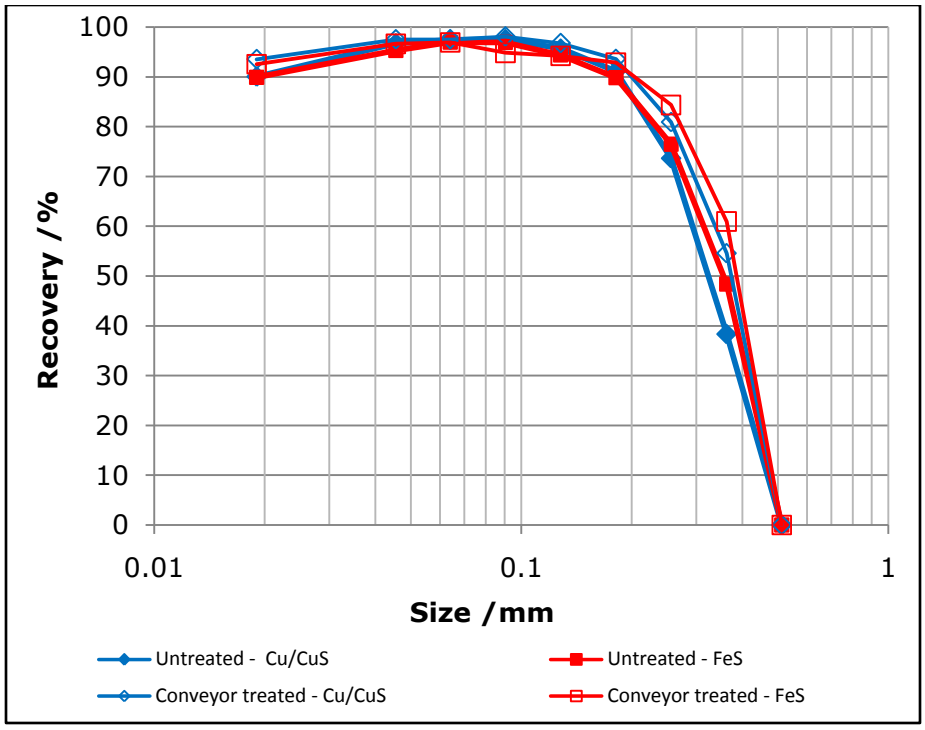

Figure 5.29 Sulphides recovery by size from copper II coarse grind

The recovery by size results were therefore analysed in more detail within the size range for which it was anticipated that a significant increase in sulphides recovery would be obtained based on the liberation results (Figures 5.30 and 5.31). The results reveal an increase of about 2% in copper sulphides recovery from Escondida single mode treated samples in the size range of 150-250 µm and a further increase of about 2% between 450 and 500 µm (Figure 5.30). The copper II conveyor treated samples show a higher increase in copper sulphides recovery of between 8-10% in the -400+200 µm size class. These results are very significant if considered at industrial scale operations of, say, 250,000 tons per day. For example, for a low grade copper ore with an average copper content of 0.5%, an increase of 10% in recovery could potentially result to about 112 tons of additional metal value per day (assuming 90% recovery). At the current copper price from the London Metal

Exchange, which is about $6,500/t, this is equivalent to over $700,000/day in real monetary value.

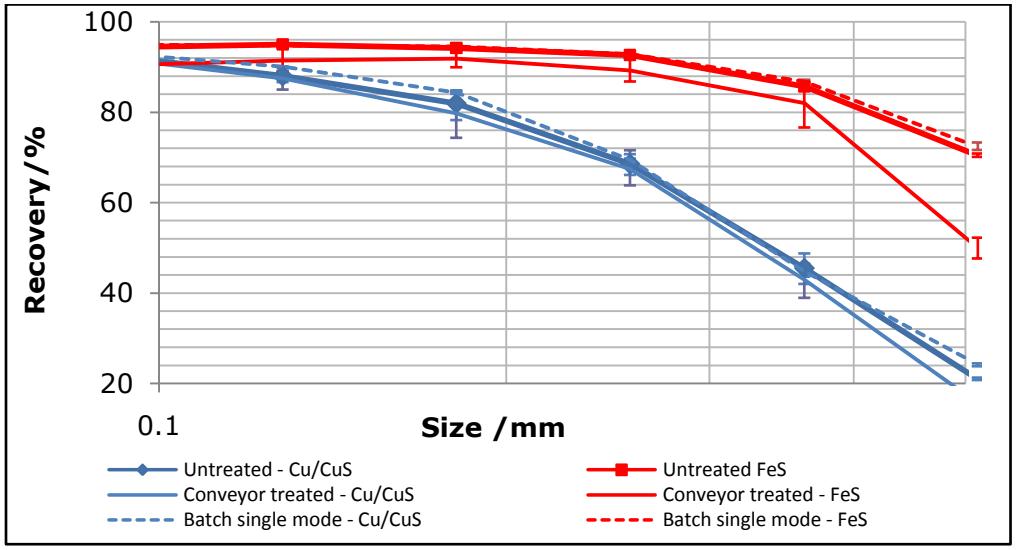

Figure 5.30 Escondida coarse grind sulphides recovery (-500+100 µm size class only)

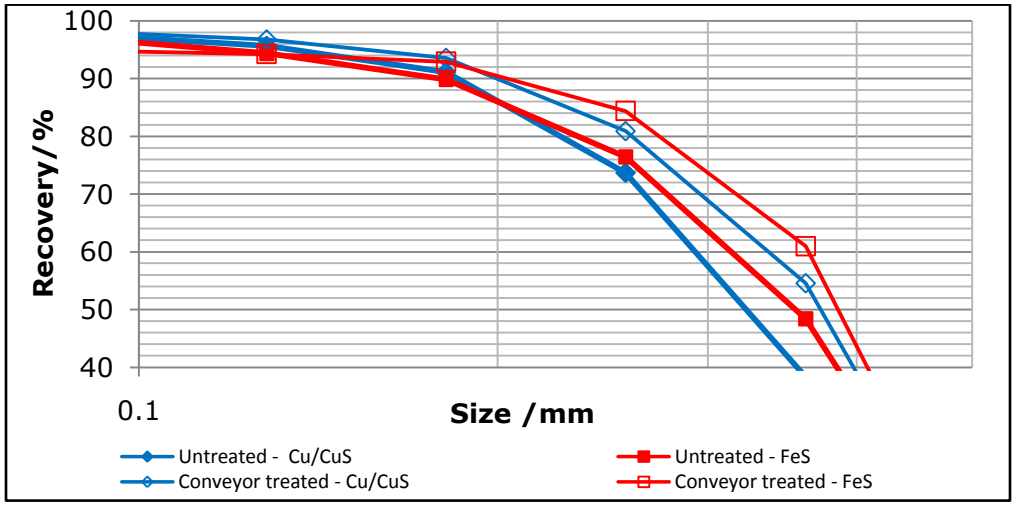

Figure 5.31 Copper II coarse grind sulphides recovery (-500+100 µm size class only)

These results clearly show that microwave pre-treatment of ores has potential for real economic benefits in terms of value proposition in addition to efficient resource utilization. The results suggest that microwave pre-treatment is

effective on low grade ores with finely disseminated mineral grains, which are particularly unattractive to process due to the costs involved. Microwave pre-treatment could therefore potentially provide the solution to some of the barriers in processing low grade ores.

It should also be noted that there is potential for higher recoveries if the performance of the microwave treatment systems is improved further. It was observed that the treatment process used in this study was not optimised due to applicator deficiencies, as will be discussed in the next section.

5.9 Evaluation of Design Performance of Single Mode and Tunnel Applicators

5.9.1 Introduction

The results from point load and pundit testing in the last chapter and also the liberation and flotation results discussed in this chapter suggest that there was a non uniform heating pattern inside the single mode and conveyor tunnel applicators contrary to the design specifications stated in Section 5.5.2. For particles treated using the single mode cavity, it appeared as though a significant proportion of the particles received sufficient thermal energy and experienced significant fracture resulting in the observed increases in liberation. The Escondida ore samples treated using the conveyor tunnel applicator seem not to have been adequately treated as there were no significant changes in liberation. Therefore, in order to confirm that the applicators were performing according to the design, an investigation aimed at establishing the electric field distributions (and therefore power density) inside the single mode cavity and the conveyor tunnel applicator was carried out.

5.9.2 Method for Evaluation of Single Mode Applicator Design

Small blocks (1 to 3 cm) of sawn Escondida copper I ore were carefully positioned inside a cylindrical PVC tube. Eleven vertical zones of six particles with a total weight of 1.65 kg were used. The tube was 285 mm in length and therefore each zone was approximately 26 mm thick. The zone and radial position (as the nearest time on a clock face) were carefully noted although some overlap between zones and radial positions was inevitable due to different particles sizes and shapes leading to uneven packing. The tube was then placed in the centre of the cavity as illustrated in Figure 5.32.

The particles were irradiated with microwave energy at 13 kW for 1.5 s (total energy input 2.73 kWh/t). The PUNDIT test (which was described in the last chapter) was then used to quantify damage to particles after irradiation with microwave energy. The results from PUNDIT testing were then used to infer the electric field distribution pattern within the cavity.

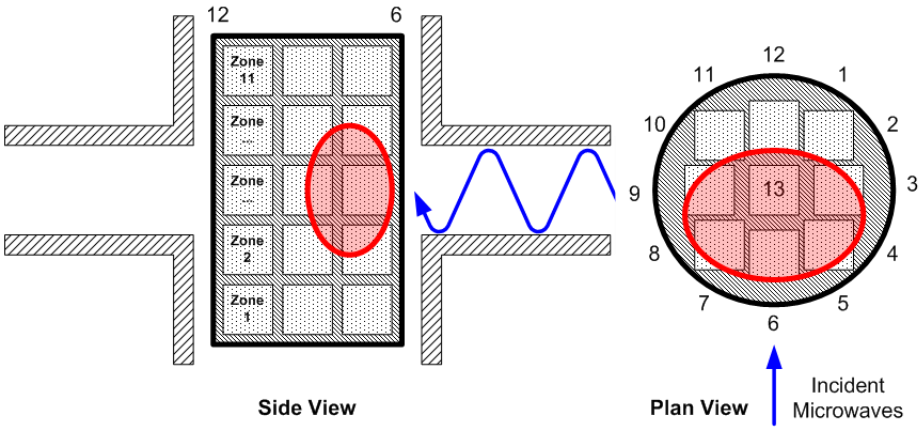

Figure 5.32 Arrangement of particles in the single mode cavity for determination of hot spots within the cavity

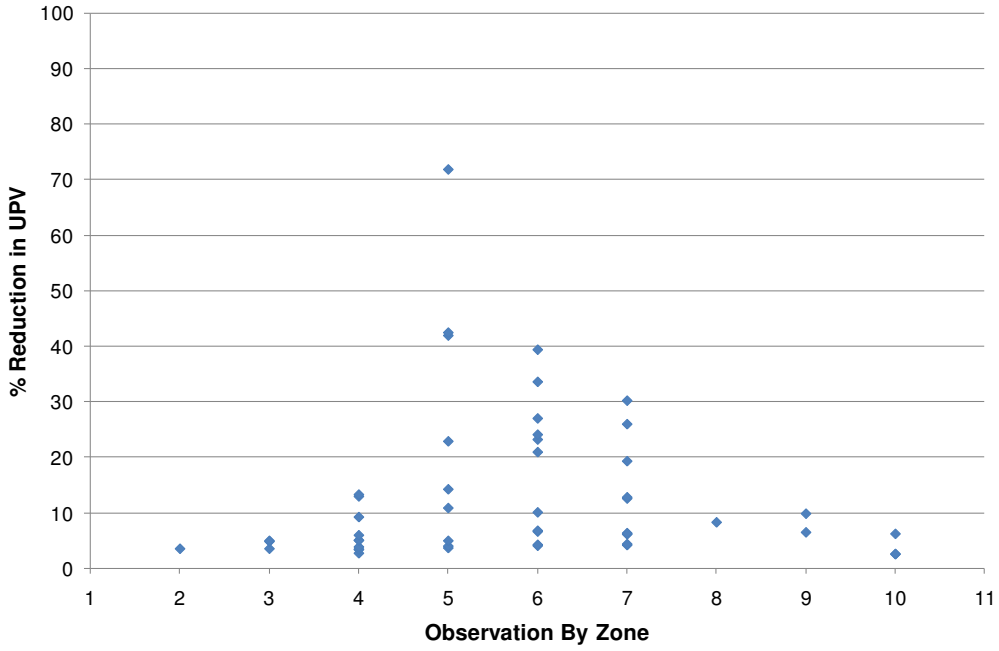

Figure 5.33 Reduction in UPV of particles in different zones in a single mode cavity

Figure 5.33 shows that the largest reduction in UPV occurs between zones 5 to 7, corresponding to the zones in line with the waveguide and extending about 10 mm either side. Some damage was also noted in zones 4, 8 and 9 demonstrating that the electric field and hence hot spot is not entirely confined to the waveguide area. Some particles in the above zones, however did not exhibit a change in UPV. This can be explained by considering the radial positions with respect to the direction of incident microwave energy. Figure 5.34 shows that the largest reductions in UPV occur in the front half facing incident microwaves (i.e. 5 to 9) and the central position 13. Only marginal reductions are recorded in particles in radial positions 1-3 and 10-12 which lie in the back half to incident microwaves.

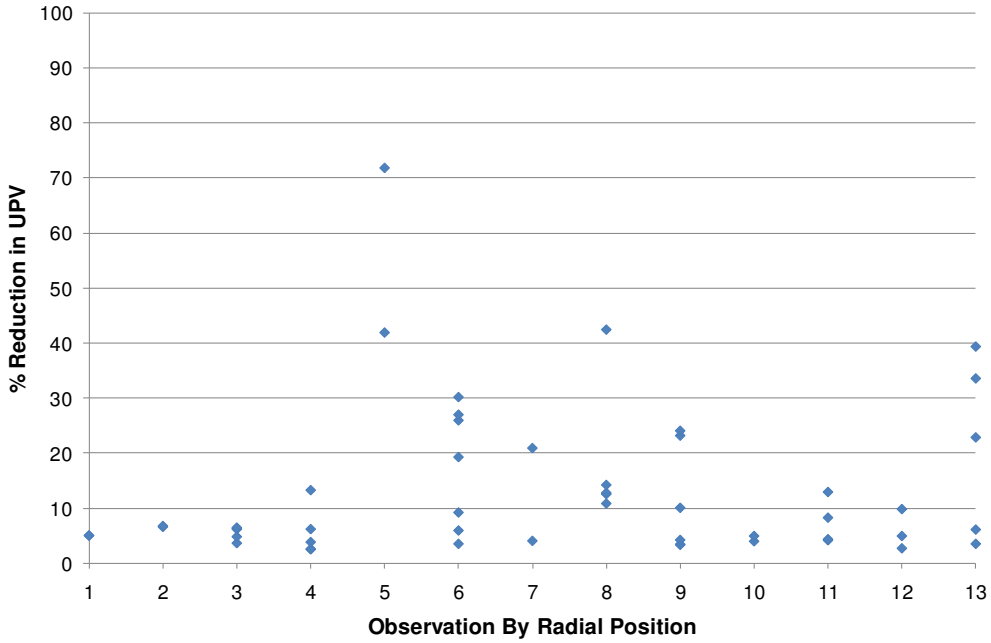

Figure 5.34 Reduction in UPV of particles in different radial positions in a single mode cavity

These results demonstrate that the majority of the power is absorbed in the front section of the sample incident to incoming microwave energy. Therefore, the "hot zone" where the electric field is concentrated is believed to be the region highlighted in red on Figure 5.33.

5.9.3 Evaluation of Conveyor Tunnel Applicator Design

Tests were carried out to investigate the electric field distribution inside the empty tunnel applicator and to evaluate the hot zone(s) when the applicator was loaded with ore. This work was carried out in conjunction with Dr. Georgios Dimitrakis, a Research Fellow at the University of Nottingham. The method that was used to establish the electric field in the empty cavity is described in detail by other authors (Chow and Reader, 2000). Essentially holes were drilled through the wall of the centre section of the applicator as shown in Figure 5.35. Sixteen rows and twelve columns of holes were drilled

and each of the holes was sized to allow a tight fit for the inserted probe. A coaxial probe was made by allowing a length of the inner conductor of the semi-rigid cable to protrude the drilled holes. A copper disc was soldered to the outer conductor in order to prevent common-mode current flow and possible damage to the measurement equipment.

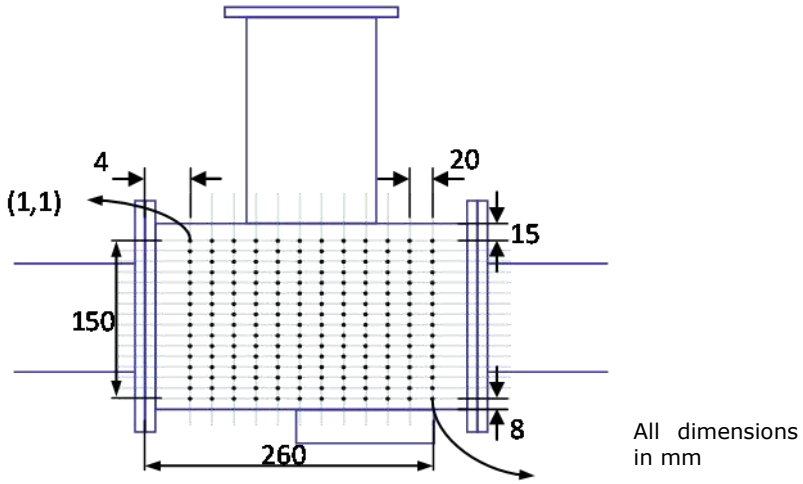

Figure 5.35 Applicator centre section with grid of holes for probe measurement

An HP8510 vector network analyser (VNA) was used to measure the magnitude of S_{11} from each of the drilled holes. S_{11} values give an indication of the relative normal field strengths and can therefore be normalised and plotted to provide field patterns. A schematic of the complete system used is shown in Figure 5.36.

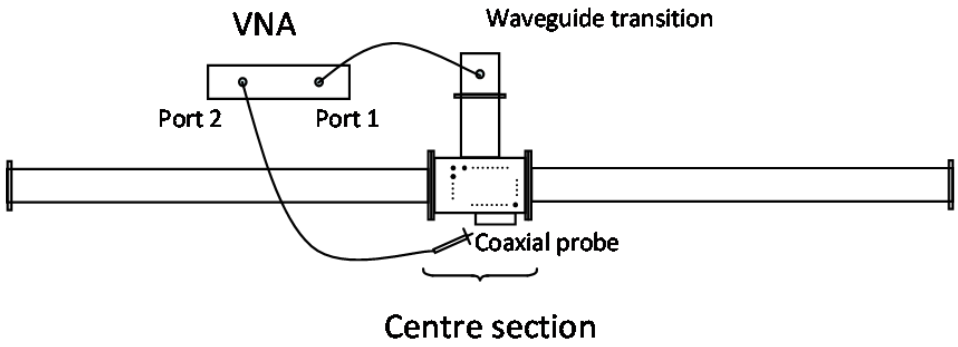

Figure 5.36 Conveyor tunnel applicator electric field probe measurement setup

Figure 5.37 shows the pattern obtained when the normalized data was processed using *Matlab Surface* software. A colour bar on the right provides the scale, which gives the relative magnitude of the measured S_{11} values. The probing hole labelled $(1,1)$ in Figure 5.31 corresponds to $(x, y) = (4,1)$ in Figure 5.37. Furthermore the scales in the two figures correspond and therefore the holes (and the measured field pattern points) in the horizontal direction are 20 mm apart, while those in the vertical direction are 10 mm apart. This arrangement of the holes was specifically determined since greater variation of the field pattern was expected in the vertical direction than the horizontal direction after investigating the results of preliminary simulations of the empty applicator.

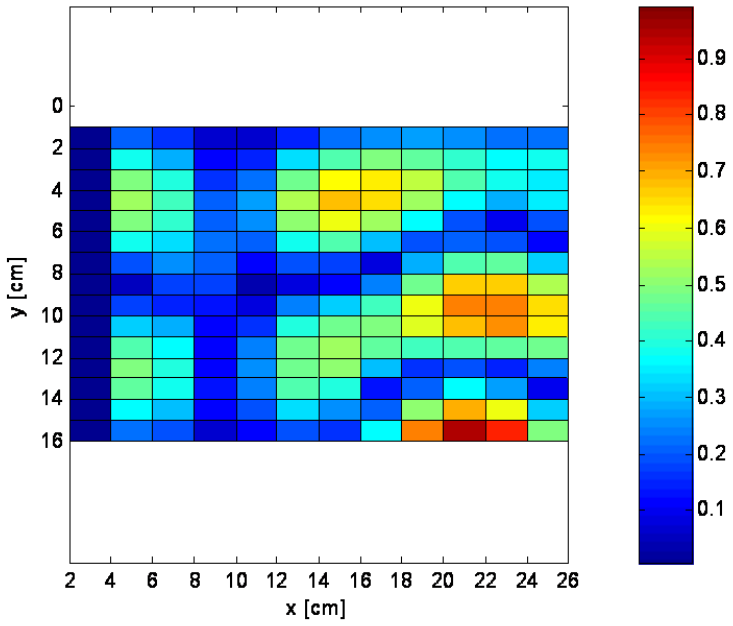

Figure 5.37 Un-interpolated electric field pattern of the empty tunnel applicator measured at 2.45 GHz

To improve visual resolution, a two-dimensional interpolation of the data was performed. This produces a 32×26 matrix of data points from the measured 13×16 matrix. When Figure 5.37 is interpolated, the field pattern shown in Figure 5.38 is produced.

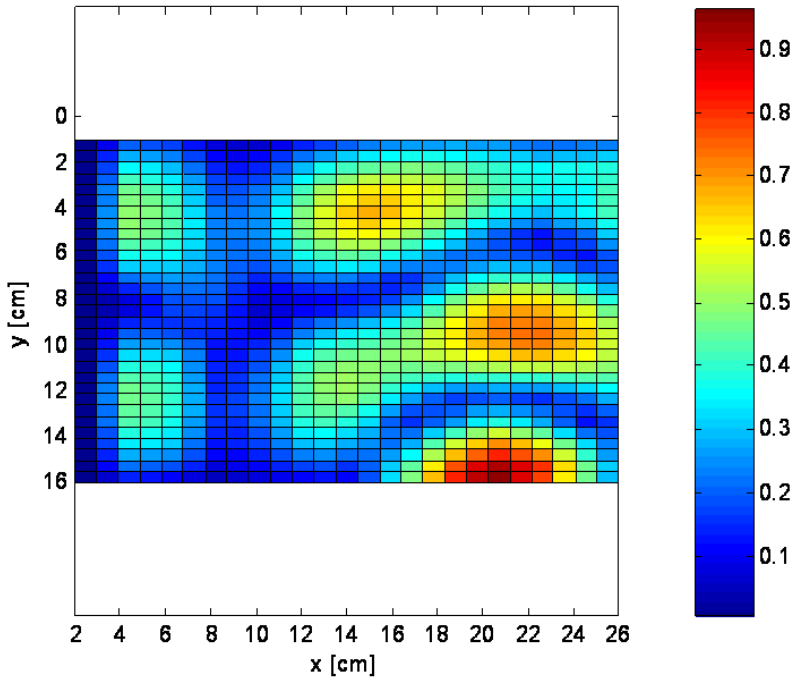

Figure 5.38 Interpolated electric field pattern of the empty tunnel applicator measured at 2.45 GHz

Figure 5.38 shows that the pattern of the electric field inside the empty cavity of the tunnel applicator is similar to original design (see Figure 5.5). This implies that every point along the y-axis on the conveyor moves through a hot region inside the applicator. However, it is also important that the "hot region" is confined and does not spread axially in the direction of ore movement. Treatment is maximized if the ore moves into a hot zone instantaneously so that there is a rapid change of temperature. The temperature gradient between heated semi conducting valuable minerals and non-heated microwave transparent gangue must be maximized for effective treatment to take place. For this to happen, the power must be confined to a specific region inside the applicator.

The temperature profile of a material placed inside a microwave cavity can be used to infer the power density induced within the material. Thermo-graphic analysis was used to determine the temperature profile of ore treated by the conveyor tunnel applicator. Tests were carried out on two different particle size classes of the same ore packed in a 3 m long PVC tube. The first size class consisted of fine material less than 10 mm while the second size class consisted of coarse material between 26.5 to 53 mm. The ores were irradiated with microwaves at 15 kW for 1 s and the temperature profile of each ore was determined using an infra-red thermo-graphic analyser. Figure 5.38 shows the thermographs obtained.

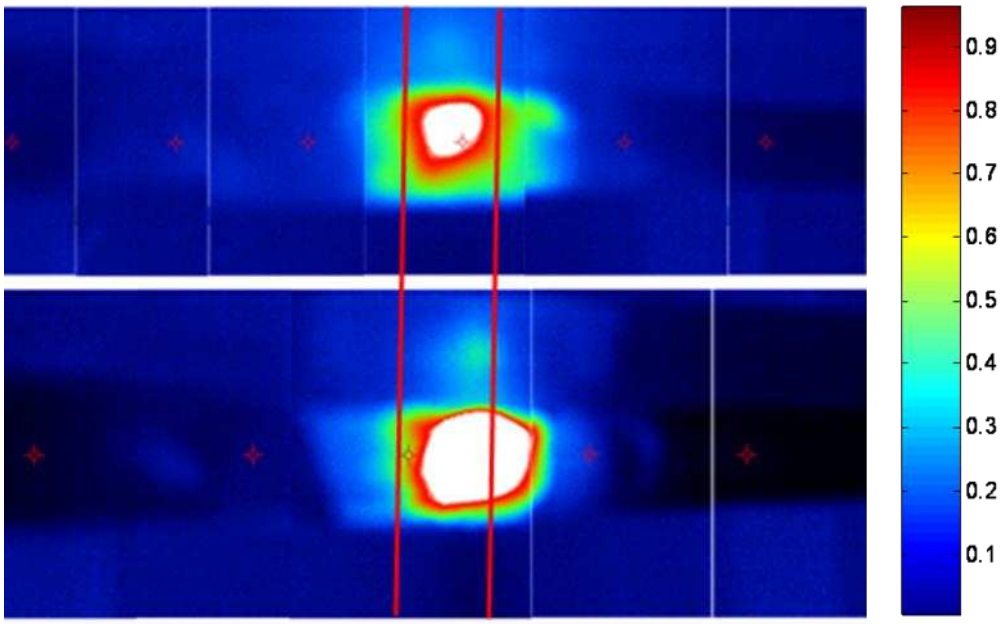

Figure 5.39 Thermographs of similar ore but different size classes after microwave treatment (top) fine material less than 10 mm and (bottom) coarse material between 26.5 and 53 mm

It can be seen that different size fractions of the same ore give different thermographs. The colour bars at the top show the temperature profile, red being hottest and dark blue the coldest. It can be seen that the hot zone of

fine material is confined to a smaller region compared to the coarse material. The warm zone (light blue) of the coarse material extends out to a large area suggesting that power is spread out more in coarse material than fine material. It is most likely that as the particle size becomes larger; the voidage is increased causing a power spread. This results into a deviation from the ideal scenario of a localised hot spot required for more efficient treatment. When power spreads into the material before it gets to the cavity, the material gets warm and the thermal gradient is not maximized when the material enters the hot zone. This shows that the rate of power density increase is as important as ultimate power density and the current design of the applicator does not take this into account. Any future continuous process applicator designs must be able to ensure localised hot spots and confinement of all the microwave energy.

5.10 Conclusions

Microwave pre-treatment of two copper ores has been shown to achieve improved mineral liberation in the particle size range suitable for flotation. Significant improvements in liberation of up to 20% were observed in single mode treated particles using modest energy inputs of less than 2 kWh/t. It was observed that higher improvements in degree of liberation are attained in coarser particle sizes between 212 and 425 μm. The increase in liberation is attributed to increased intergranular fracture after microwave treatment. As the size of the heated mineral grains increases, less energy is required to sufficiently raise the temperature such that thermal stresses of a sufficient magnitude are induced around the mineral grains. It was stated in Chapter Three that for very small grains, say below 100 μm, thermal conduction

between the heated grains and transparent gangue makes it unlikely that a high temperature gradient required to induce cracks is possible.

Flotation testing results showed improved copper sulphides recovery at larger particle sizes for both coarse and fine grinds of both ores. Approximately 2% increase in total copper sulphide recovery and up to 4% increases in copper sulphide grade in the first two concentrates were observed in Escondida copper I ore. The copper II ore samples showed a higher increase in copper sulphides recovery of 8-10% in the -400+200 μm size class. The results obtained also showed that microwave pre-treatment enhances selective mineral recovery as the grade-recovery of iron sulphides decreased in all but one microwave treated samples. This is a very significant result considering that heavy penalties are charged by smelters for impurities in concentrates.

The results from flotation testing clearly demonstrate that microwave pre-treatment of ores has potential for real economic benefits in terms of value proposition and also results into more efficient resource utilization. At the current copper price from the London Metal Exchange which is about $6,500/t, an increase of 8-10% in recovery is potentially equivalent to over $700,000 per day in real monetary value assuming large industrial scale operations processing about 250,000 tons per day. It is clear that the pay-back time for the additional microwave treatment step can be realised within a short period considering that the microwave treatment systems currently proposed are relatively inexpensive both in terms of capital cost and also running costs. The major running cost is the energy input and it has been demonstrated that effective treatments can be carried out using less than 1 kWh/t.

The major outstanding developments required to drive this technology to the next step towards industrial scale application is the lack of an effective continuous processing microwave applicator. It was shown that the conveyor tunnel applicator used in this study did not perform according to the design specifications. It was shown that power spreads in the transverse direction within the tunnel applicator. This causes a deviation from the ideal scenario of a localised hot spot required for more efficient treatment. It was shown that the power spread increases with increase in particle size (void space). It is concluded that rate of power density increase is as important as ultimate power density and the current design of the applicator did not take this into account. Any future applicator designs must be able to ensure localised hot spots and confinement of all the microwave energy.

CHAPTER SIX

6 CONCLUSIONS AND FURTHER WORK

6.1 Conclusions

Research developments in the last two decades have highlighted the potential for microwave heating to provide a step change in ore processing. Despite the presence of phyllosilicate minerals in most ore bodies, prior to this work, little or no information was available which examines the influence of hydrated minerals on microwave assisted comminution and liberation. This study found that interlayer absorbed water affects the dielectric properties of minerals. It was shown that there exists a direct relationship between the mineral dielectric properties and dehydration/dehydroxylation characteristics. Low temperature weight loss was found to be associated with minerals that exhibit higher values of both dielectric constant and loss and when dehydration takes place, this in turn leads to a drop in both ε' and ε''. It was concluded that loosely bound absorbed interlayer water, such as that present in some clay minerals such as montmorillonite, halloysite and hydrobiotite, behaves in a similar manner to the free water in an electromagnetic field. The hydroxyl groups within most phyllosilicate minerals do not impart high dielectric constant or dielectric loss, although there seems to be some increase in the dielectric constant on dehydration. This is in contrast to polar solvents incorporating OH groups such as alcohols, which heat rapidly in a microwave field. Most likely, the forces opposing dipole OH reorientation in the crystalline solid are profoundly higher than those in the liquid solvent and may not generate kinetic energy via rotation and molecular friction.

It was demonstrated that significant damage may be induced in ores containing hydrated minerals but devoid of semi conducting minerals after microwave treatment. SEM images showed that the presence of minerals containing interlayer absorbed water leads to increased likelihood of microwave-induced fracture in the localised area. Point load tests showed reductions in strength of up to 40% in some particles but the results showed a high degree of variability. However, it was found that the statistical dependency of the point load test may grossly affect the accuracy of the results and the method is particularly less effective for testing of "weak" ores, particularly clay minerals which exhibit some degree of plasticity. For the first time ever, microwave induced fracture was characterised by a non destructive ultrasonic based technique using a PUNDIT 7 tester. The results showed a reduction in Ultrasonic Pulse Velocity of between 2-14%. The results obtained from point load and PUNDIT tests both showed potential for comminution energy savings after microwave treatment, although no direct correlation between these tests and energy consumption by comminution machines currently exists.

It has been demonstrated that there is potential to significantly improve beneficiation at sizes suitable for flotation. Mineral liberation analysis tests conducted on two different porphyry copper ores showed significant improvements in liberation of up to 20% in particles treated using a single mode cavity at modest energy inputs of less than 2 kWh/t. It was observed that higher improvements in degree of liberation are attained in coarser particle sizes between 212 and 425 μm. The increase in liberation at coarser sizes is attributed to a shift from predominantly transgranular fracture to both transgranular and intergranular fracture after microwave treatment. As the

size of heated mineral grains increases, a higher temperature gradient exists between heated mineral grains and microwave transparent gangue and thermal stresses of a sufficient magnitude are induced and cracks are formed around the mineral grains. For very small grains, thermal conduction between the heated grains and transparent gangue makes it unlikely that a high temperature gradient required to induce cracks is possible.

The results from flotation testing demonstrated that microwave pre-treatment of ores has potential for real economic benefits in terms of value proposition, which potentially results into more efficient resource utilization. The results showed improved copper sulphides recovery at coarse grind sizes. Approximately 2% increase in total copper sulphide recovery and up to 4% increases in copper sulphide grade were observed in Escondida copper I ore. A higher increase in copper sulphide recovery of 8-10% in the -400+200 μm size class was obtained from the copper II ore samples. At the current copper price from the London Metal Exchange, which is about $6,500/t, an increase of 8-10% in recovery is potentially equivalent to over $700,000 per day in real monetary value assuming large industrial scale operations processing about 250,000 tons per day. This makes microwave assisted processing of ores attractive as the pay-back time for the additional microwave treatment step can be realised within a short period considering that the microwave treatment systems currently proposed are inexpensive both in terms of capital cost and also running costs. The major running cost, which is the required energy input, is potentially less than 1 kWh/t. The results obtained also showed that microwave pre-treatment may enhance selective mineral recovery by rejection of non targeted elements. The grade-recovery of iron sulphides was found to be significantly lower after microwave treatment. This

is very significant in terms of smelting costs where concentrate contamination leads to significant additional costs.

Prior to this work, there were claims that microwave pre-treatment could lead to surface oxidation of mineral grains, which would have detrimental effects on flotation. This study demonstrated that microwave treatment does not alter the physico-chemical properties of minerals in a manner that would inhibit the floatability of the minerals. The flotation kinetics after microwave treatment remained unchanged.

The major drawback to further developments towards industrial scale application was found to be the lack of an effective continuous processing microwave applicator. The batch single mode cavity was found to be effective in maximizing the power density required to induce significant damage to the ores. However, it was shown that the conveyor tunnel applicator used in this study did not perform according to the design specifications. Any realistic industrial microwave treatment process necessitates development of a continuous treatment process. It was shown that power spreads in the transverse direction within the tunnel applicator. This caused a deviation from the ideal scenario of a localised hot spot required for more efficient treatment. It is concluded that rate of power density increase is as important as the ultimate power density and the current design of the applicator did not take this into account. Any future applicator designs must be able to ensure localised hot spots and confinement of all the microwave energy.

6.2 Further Work

As stated in the last section, the major difficulty encountered during this work was the unreliability of microwave systems used for treatment. A careful design of a continuous process microwave applicator that delivers microwave power to the optimal applicator geometry based on throughput and processing requirements is required. It is recommended that research and development of microwave treatment systems that ensure optimal power delivery and homogeneity in a continuous process are fast tracked. The use of pulsed microwave energy was not largely tested in this work and also needs to be investigated further.

In order to determine the possible comminution energy savings after microwave treatment, there is need to develop a direct correlation between ore strength reduction and comminution energy savings. The correlation between point load test and comminution energy that was developed by (Bearman, 1997) may only be applied for single particle breakage and even then, the method has not been widely tested. The statistical dependency of the point load test also makes it less accurate and unreliable. It is recommended that non-destructive characterisation techniques, where measurements are conducted on the same sample before and after microwave treatment, be the major focus of further developments. This study has proposed a method for ultrasonic characterisation of microwave induced fracture using the PUNDIT tester. It is recommended that further developments on ultrasonic testing devices for rocks be carried out. There is also a need for further scientific research work in ultrasonic testing of rocks, especially to provide a thorough understanding of the influence of micro

cracks in a material on the dispersion and propagation of ultrasound pulse signals. The use of X-ray micro tomography in characterising microwave induced fracture should also be explored.

A thorough assessment of the economics of including a microwave pre-treatment step in the conventional process flow sheet needs to be carried out. This study has shown the anticipated benefits of microwave pre-treatment of ores in terms of increased value proposition. However, the capital and operational costs of the microwave pre-treatment step need to be evaluated against these benefits. the results from this study showed that pre-treatment of hydrated ores devoid of microwave absorbent semiconducting minerals is unlikely to be economically viable due to the high energy input. The higher energy requirement was attributed to the dehydration kinetics. Microwave induced dehydration kinetics should be investigated further with a view of lowering the overall energy requirement in treating hydrated minerals.

APPENDIX I

MLA Mineralogy and Textural Data

Modal Mineralogy (Weight %) of Ekati Kimberlite Diamond Ore (Type I)

Mineral	5207	52	52	52	52	52	52	52	52	52	52	52	52	52	52	51	Total
Olivine	40.76	41.7	27.0	41.5	49.9	42.2	42.2	38.9	35.9	43.7	39.0	22.9	42.9	38.3	29.1	45.0	39.05
Serpentine	26.64	23.2	27.8	21.6	19.4	23.9	20.9	23.3	26.9	24.4	30.7	30.3	26.6	23.7	19.2	23.4	24.24
Monticellite	18.67	16.0	11.3	10.9	16.9	18.2	18.4	13.6	13.8	17.9	12.8	6.41	11.3	14.2	11.0	11.7	13.92
Calcite	0.56	2.53	4.50	8.89	1.73	0.85	4.17	6.41	4.97	1.06	0.94	7.06	0.81	2.84	25.8	4.25	5.09
Barian_mica	5.14	4.42	3.81	3.01	4.19	4.78	5.16	4.28	3.96	5.42	4.24	3.35	4.67	5.01	5.12	4.69	4.48
Hydrobiotite	0.63	2.02	12.2	6.64	1.08	0.95	0.65	6.46	7.53	0.33	3.53	17.7	3.92	3.24	0.30	3.88	4.35
Humite_grou	3.51	3.52	2.02	2.02	3.22	3.85	2.29	3.09	2.96	2.94	4.15	1.38	3.77	2.97	0.78	3.41	2.83
Mica_group	0.67	1.90	6.62	2.62	1.03	0.56	2.06	1.56	1.83	0.77	1.08	7.62	2.63	2.69	2.08	0.75	2.25
Garnet_group	0.90	0.88	1.40	0.75	0.36	2.38	1.08	0.95	0.75	1.26	0.66	1.37	0.98	4.04	2.64	0.72	1.35
Spinel_group	0.99	0.93	0.47	0.37	1.10	1.15	1.10	0.45	0.61	1.15	0.67	0.29	0.52	0.73	0.38	0.87	0.75
Talc	0.19	1.93	0.43	0.60	0.16	0.15	0.43	0.01	0.01	0.08	0.58	0.20	0.40	1.11	0.10	0.31	0.43
Apatite	0.31	0.29	0.28	0.20	0.27	0.35	0.41	0.31	0.23	0.28	0.30	0.19	0.37	0.35	0.61	0.56	0.35
Brucite	0.35	0.31	0.37	0.28	0.31	0.40	0.36	0.44	0.33	0.38	0.55	0.29	0.60	0.37	0.15	0.16	0.34
Diopside	0.64	0.18	0.32	0.29	0.14	0.11	0.15	0.03	0.05	0.06	0.49	0.14	0.29	0.15	1.83	0.04	0.30
Larnite	0.03	0.08	1.42	0.16	0.09	0.05	0.42	0.17	0.10	0.05	0.09	0.62	0.03	0.12	0.49	0.08	0.25
Baryte	0.00	0.00	0.01	0.00	0.00	0.01	0.00	0.00	0.00	0.01	0.00	0.03	0.00	0.00	0.24	0.00	0.02
Strontianite	0.00	0.00	0.00	0.00	0.00	0.00	0.00	0.00	0.00	0.00	0.00	0.00	0.00	0.00	0.00	0.00	0.00
Total	**100**	**100**	**100**	**100**	**100**	**100**	**100**	**100**	**100**	**100**	**100**	**100**	**100**	**100**	**100**	**100**	**100**

Modal Mineralogy (Weight %) of Ekati Kimberlite Diamond ore (Type II)

Mineral	5210	52	52	52	52	52	52	52	52	52	52	52	52	52	52	52	52	Combined
Clavs	85.10	83.	4.4	60.	10.	31.	2.8	36.	28.	12.	75.	48.	87.	89.	86.	89.	87.	50.63
Feldspars	0.01	0.0	0.0	0.0	43.	0.4	0.0	0.8	32.	15.	0.0	1.0	1.5	0.9	1.8	0.9	1.9	7.83
Carbonat	1.45	1.2	0.0	0.7	0.2	3.0	0.0	3.5	3.2	1.3	0.1	4.1	0.3	1.6	2.0	0.3	0.2	1.55
Talc	2.20	3.6	0.0	27.	0.2	12.	0.0	8.7	1.9	0.0	19.	9.6	0.6	1.9	2.9	0.3	1.2	6.41
Biotite	2.51	2.4	0.0	0.4	16.	0.5	0.0	0.6	20.	24.	0.4	1.1	2.2	1.0	0.8	2.8	3.7	5.40
Chlorite	1.15	0.8	0.0	0.0	0.5	0.1	0.0	0.1	4.1	0.1	0.0	0.0	0.0	0.0	0.0	0.0	0.1	0.54
Hornblen	3.53	5.3	0.3	1.3	4.8	1.6	0.3	2.0	2.5	4.2	0.5	0.8	4.2	2.0	4.2	3.6	1.6	2.58
Allanite	0.48	0.4	0.1	0.1	0.4	0.2	0.1	0.3	0.2	0.7	0.0	0.3	0.5	0.6	0.5	0.4	0.3	0.36
Epidote	0.61	0.3	0.0	0.0	4.5	0.0	0.0	0.1	3.2	5.3	0.0	0.0	0.5	0.1	0.1	0.4	1.7	1.17
Hyalopha	0.00	0.0	0.0	0.0	4.8	0.0	0.0	0.0	1.5	0.3	0.0	0.0	0.0	0.1	0.0	0.0	0.0	0.61
Quartz	0.00	0.0	0.0	0.0	2.4	4.2	0.0	5.6	0.0	0.1	0.0	6.9	0.0	0.0	0.0	0.0	0.0	1.43
Thaumasi	1.52	1.2	92.	0.0	0.9	0.0	70.	0.0	0.1	1.1	0.0	0.0	0.2	1.7	0.5	0.3	0.2	7.56
Olivine	0.05	0.2	0.0	8.7	0.0	45.	0.0	40.	0.0	0.0	2.8	26.	0.0	0.0	0.0	0.0	0.0	9.20
Pyrite	0.02	0.0	0.0	0.3	0.0	0.2	0.0	0.4	0.0	0.0	0.9	0.4	0.1	0.2	0.1	0.0	0.0	0.19
Apatite	0.06	0.0	0.0	0.0	0.5	0.0	0.0	0.0	0.4	0.5	0.0	0.2	0.1	0.0	0.0	0.1	0.0	0.17
Apophylli	0.00	0.0	2.1	0.0	6.9	0.0	25.	0.0	0.0	3.0	0.0	0.0	0.4	0.0	0.0	0.1	0.0	1.97
Ilmenite	0.58	0.27	0.00	0.06	0.00	0.03	0.00	0.03	0.00	0.01	0.05	0.07	0.03	0.03	0.05	0.04	0.03	0.08
Pectolite	0.69	0.60	0.00	0.00	0.00	0.00	0.00	0.00	0.00	0.01	0.00	0.00	1.38	0.00	0.00	0.87	0.92	0.21
Tacharanite	0.02	0.02	0.12	0.00	0.28	0.00	0.20	0.00	0.07	14.62	0.00	0.00	0.05	0.15	0.06	0.02	0.03	0.88
Natrolite	0.00	0.00	0.00	0.00	3.25	0.00	0.00	0.00	1.42	14.73	0.00	0.00	0.00	0.00	0.00	0.00	0.00	1.23

Modal mineralogy (Weight %) of Nebo Babel Copper - Nickel ore

Particle	1	2	3	4	5	6	7	8	9	10	11	12	13	14	15	Overall (%)
Chalcopyrite	0.72	1.15	0.80	1.02	0.26	0.43	0.65	0.08	1.96	0.58	0.62	0.91	0.67	0.39	0.28	**0.71**
Ilmenite	0.38	0.11	1.33	0.81	0.16	0.43	0.09	0.40	1.86	0.61	0.07	0.14	0.85	0.10	0.59	**0.55**
Magnetite	0.30	0.12	0.78	0.83	0.10	0.18	0.35	0.43	1.51	0.57	0.10	0.28	1.02	0.04	0.48	**0.50**
Pentlandite	0.49	0.27	0.77	0.46	3.67	0.13	0.65	0.04	0.93	0.57	1.50	0.66	0.93	1.40	1.06	**0.92**
Pyrrhotite	2.63	1.83	5.25	2.32	21.06	0.60	4.45	0.16	5.15	2.89	6.99	3.41	5.11	9.10	4.77	**5.14**
Apatite	0.56	0.06	0.10	1.06	2.23	0.19	1.24	0.56	0.96	0.70	0.63	0.36	0.16	0.11	1.11	**0.69**
Biotite	1.74	1.71	2.90	3.10	0.74	1.28	2.01	1.20	1.71	2.39	2.31	1.71	1.90	4.15	2.10	**2.07**
Orthoclase	0.46	0.20	0.32	0.22	3.12	0.25	0.31	1.37	0.15	0.12	0.72	1.79	0.22	0.27	0.06	**0.65**
Plagioclase	37.23	44.24	55.08	45.20	55.72	63.11	52.48	76.78	28.46	37.78	61.81	54.51	59.16	54.35	25.92	**49.74**
Pyroxene	55.46	50.24	32.64	44.89	12.86	33.40	37.74	18.86	57.29	53.71	25.17	36.10	29.94	29.85	63.61	**38.95**
Quartz	0.04	0.09	0.04	0.09	0.10	0.01	0.04	0.11	0.01	0.07	0.07	0.13	0.04	0.26	0.03	**0.07**
Total	100	100	100	100	100	100	100	100	100	100	100	100	100	100	100	100

Modal Mineralogy (Weight %) of Los Bronces Copper Ore

MINERAL	52097	52098	52099	52100	52101	52102	52103	52104	52105	52106	52107	52140	52141	52142	52143	52144	Combined
Chalcopyrite	0.54	3.20	6.86	3.83	0.34	0.03	0.38	0.73	0.51	0.48	0.01	0.79	3.02	0.23	0.91	0.25	**1.37**
Bornite	0.06	0.50	0.10	0.33	0.03	0.09	0.03	0.10	0.09	0.04		0.09	0.56	0.02	0.30	0.08	**0.15**
Covellite	0.03	0.24	0.05	0.17	0.01	0.04	0.01	0.09	0.11	0.01	0.01	0.03	0.57	0.02	0.08	0.07	**0.09**
Digenite		0.01		0.02	0.01	0.02			0.20		0.02		0.01	0.06	0.04	0.05	**0.03**
Famatinite	0.02	0.23	1.02	0.14	0.02		0.03	0.04	0.04	0.02		0.04	0.10	0.02	0.02	0.03	**0.11**
Enargite		0.01	0.42	0.00									0.26				**0.04**
Pyrite	3.41	0.04	2.69	0.38	0.53		0.01	0.04	0.08	0.02		2.09	9.74	1.21			**1.15**
Molybdenite	0.02	0.00		0.11	0.01											0.01	**0.01**
Rutile	0.09	0.25	0.04	0.16	0.16	0.25	0.20	0.65	0.35	0.38	0.42	0.20	0.02	0.19	0.26	0.32	**0.25**
Hematite	2.39	0.02	20.41	0.03	0.09	0.34	0.03	0.04	0.79	0.17	0.19	0.06	35.89	0.40	0.19	0.59	**3.12**
Orthoclase	0.00	0.02	0.04		28.08	23.09		12.75	41.51	7.59	24.03			3.56	20.06	17.45	**10.36**
Plagioclase	0.12	7.81	0.08	0.02		35.92	0.19	26.09	0.00	35.43		0.11	0.04	32.28	0.04	0.96	**8.38**
Albite	0.43	23.36	0.20	0.19	40.08	4.65	1.03	16.17	25.92	13.81	15.99	0.67	0.46	6.67	16.98	1.00	**9.96**
Quartz	44.00	36.54	61.78	44.98	17.41	21.21	49.04	20.85	19.35	22.62	25.29	41.35	38.89	26.29	40.43	0.00	**32.39**
Apatite	0.07	0.12	0.42	0.13	0.02	0.19	0.16	0.26	0.12	0.19	0.28	0.27	0.02	0.18	0.02	0.01	**0.15**
Dravite	0.01	0.03	0.07	2.98	0.06	0.11	4.16	0.17	0.23	0.15	0.10	1.33	0.02	0.23	0.11	0.06	**0.64**
Chlorite	0.15	0.52	0.21	0.23	1.30	4.94	0.22	6.46	6.32	9.59	15.12	0.14	0.87	6.87	3.32	7.30	**3.99**
Muscovite	48.44	26.92	5.43	46.20	11.70	8.73	44.23	15.25	3.80	9.14	17.34	52.68	9.08	20.34	16.85	71.62	**27.44**
Clays	0.21	0.17	0.19	0.10	0.14	0.40	0.31	0.31	0.57	0.35	1.22	0.16	0.45	1.45	0.38	0.19	**0.41**
Total	99.99	100.00	100.00	100.00	100.00	99.99	100.00	99.99	100.00	100.00	100.00	100.00	100.00	100.00	99.99	100.00	**100.00**

Modal Mineralogy (Weight %) of Escondida Copper I Ore

Mineral	550	5	5	5	5	5	5	5	5	5	5	5	5	5	5	5	5	5	Total
Chalcopyrite	0.02	1.8	0.0	0.4	0.9	0.0	0.2	0.2	0.2	0.7	0.6	0.2	0.4	0.5	0.0	0.0	1.6	0.2	**0.49**
Bornite	0.00	0.0		0.0		0.0	0.4	0.3	0.6	0.0	0.0	0.1	0.2	0.7	0.0		0.0	0.1	**0.17**
Covellite	0.02	2.4	0.0	0.1	0.0		0.0	0.1	0.0			0.0	0.0	0.1	0.0		2.5	0.0	**0.35**
Chalcocite_grp	0.01	0.6	0.1	0.0	0.0	0.0	0.4	2.3	1.6			0.4	0.0	8.0	0.1		8.8	0.0	**1.46**
Galena	0.11		0.0	0.0	0.0		0.0	0.0	0.0	0.0		0.0	0.0		0.0		0.0	0.0	**0.01**
Rutile	0.11	0.4	0.0	0.1	0.3	0.1	0.1	0.0	0.0	0.3	0.3		0.2	0.0	0.4	0.2	0.0	0.5	**0.21**
Pyrite	48.34	5.8	0.0	8.1	0.4	7.0	0.0	2.3	0.6	4.1	0.0	8.0	0.2	1.9	0.3	0.5	6.0	0.4	**6.47**
Hematite	0.01	11.	0.0	3.3	0.0	0.0	23.	0.0	0.0	1.4	0.0		1.8	0.0	0.9	0.0	0.0	0.2	**2.13**
Illite	5.63	27.	14.	17.	18.	43.	7.5	29.	37.	2.9	20.	0.2	29.	43.	85.	30.	14.	56.	**26.51**
Kaolinite	0.60	0.0	0.1	0.0	0.0	0.1	1.2	0.0	0.0	18.	7.1	0.0	2.2	0.0	2.2	7.0	0.0	3.1	**2.12**
Chlorite		4.7	0.0	7.1	7.7	0.0	15.	0.0	0.0	12.	0.0	0.0	12.	0.0	0.9	0.0	0.0	0.2	**3.32**
Pyrophyllite	20.57	10.	31.	6.5	1.8	0.0	0.0	0.0	0.0	0.3	0.7	0.0	0.9	0.0	0.0	1.1	1.9	0.2	**4.37**
Quartz	4.91	19.	52.	52.	63.	46.	38.	62.	57.	13.	23.	90.	31.	44.	6.0	51.	64.	36.	**42.07**
Phosphate sulphate	19.55	0.1		0.0	0.0	2.2	0.0	0.5	0.1	0.2	0.3	0.2	0.0	0.1	0.2	0.0	0.0	0.7	**1.80**
Phlogopite		0.9		2.4	3.3	0.1	6.2	0.1	0.0	25.	0.2	0.0	15.	0.0	2.0	0.1		0.7	**3.11**
Albite_oligoclase	0.02	0.0	0.0	0.0	0.0	0.4	0.0	1.1	1.2	4.5	45.	0.0	1.4	0.3	0.6	8.1	0.0	0.6	**3.20**
Smectite	0.07	13.	0.0	0.3	0.0	0.0	5.8	0.3	0.0	14.	0.5	0.1	2.2	0.0	0.3	0.7	0.0	0.3	**1.98**
Zircon	0.00		0.0	0.0		0.0	0.0	0.0	0.0	0.0	0.0	0.0	0.0	0.0	0.0	0.0	0.0	0.0	**0.01**
Gypsum	0.02	0.0	0.0	0.4	2.7	0.0		0.0	0.0	0.0	0.0	0.0	0.9	0.0	0.0		0.0	0.0	**0.22**

Modal mineralogy (Weight %) of Copper II Ore

Mineral	1	2	3	4	5	6	7	8	9	10	11	12	13	14	15	Overall %*
Chalcopyrite	0.93	0.37	0.35	0.95	0.17	0.18	1.08	0.22	2.29	0.48	1.43	1.12	0.99	0.44	1.27	0.81
Molybdenite	0.02	0	0.00	0.01	0.00	0.00	0.05	0.00	0.00	0.00	0.02	0.01	0.00	0.00	0.01	0.01
Pyrite	0.10	0.05	0.01	0.58	0.01	0.64	0.08	0.16	0.32	0.04	0.40	0.22	0.17	0.05	0.14	0.20
Monazite	0.09	0.11	0.12	0.16	0.09	0.15	0.17	0.20	0.14	0.23	0.09	0.12	0.10	0.15	0.15	0.14
Rutile	0.15	0.12	0.12	0.24	0.12	0.19	0.13	0.11	0.15	0.14	0.10	0.23	0.18	0.18	0.15	0.15
Albite	4.52	18.66	15.14	1.85	10.72	4.18	3.76	25.94	5.65	9.02	0.90	2.90	4.29	8.87	11.19	8.62
Apatite	0.94	1.05	1.05	0.96	1.05	0.89	1.43	1.00	1.07	1.14	1.02	1.80	1.05	1.18	1.05	1.10
Biotite	19.99	20.89	23.42	22.28	22.21	23.01	26.36	22.60	23.92	22.35	25.11	23.25	21.85	20.52	22.01	22.64
Celestine	0.04	0.02	0.03	0.05	0.01	0.06	0.03	0.04	0.05	0.07	0.05	0.07	0.06	0.05	0.05	0.05
Oligoclase	5.59	7.54	6.48	0.15	13.19	1.90	4.05	9.41	6.13	5.27	0.23	1.42	5.38	8.47	5.56	5.41
Orthoclase	48.41	32.33	32.58	56.14	30.76	51.22	47.67	18.74	42.96	41.67	55.68	51.18	46.68	40.16	36.80	42.05
Quartz	13.01	12.98	13.54	15.46	14.59	13.68	10.58	16.26	13.03	14.02	13.92	15.10	12.97	13.32	15.36	13.82
Smectite	6.17	5.84	7.11	1.13	7.04	3.88	4.57	5.27	4.25	5.53	1.01	2.53	6.21	6.57	6.22	4.97
Zircon	0.03	0.03	0.04	0.04	0.03	0.03	0.05	0.05	0.05	0.04	0.04	0.04	0.04	0.04	0.03	0.04
Total	100.00	100.00	100.00	100.00	100.00	100.00	100.00	100.00	100.00	100.00	100.00	100.00	100.00	100.00	100.00	100

MLA Classified Images of Nebo Babel Nickel-Copper Ore

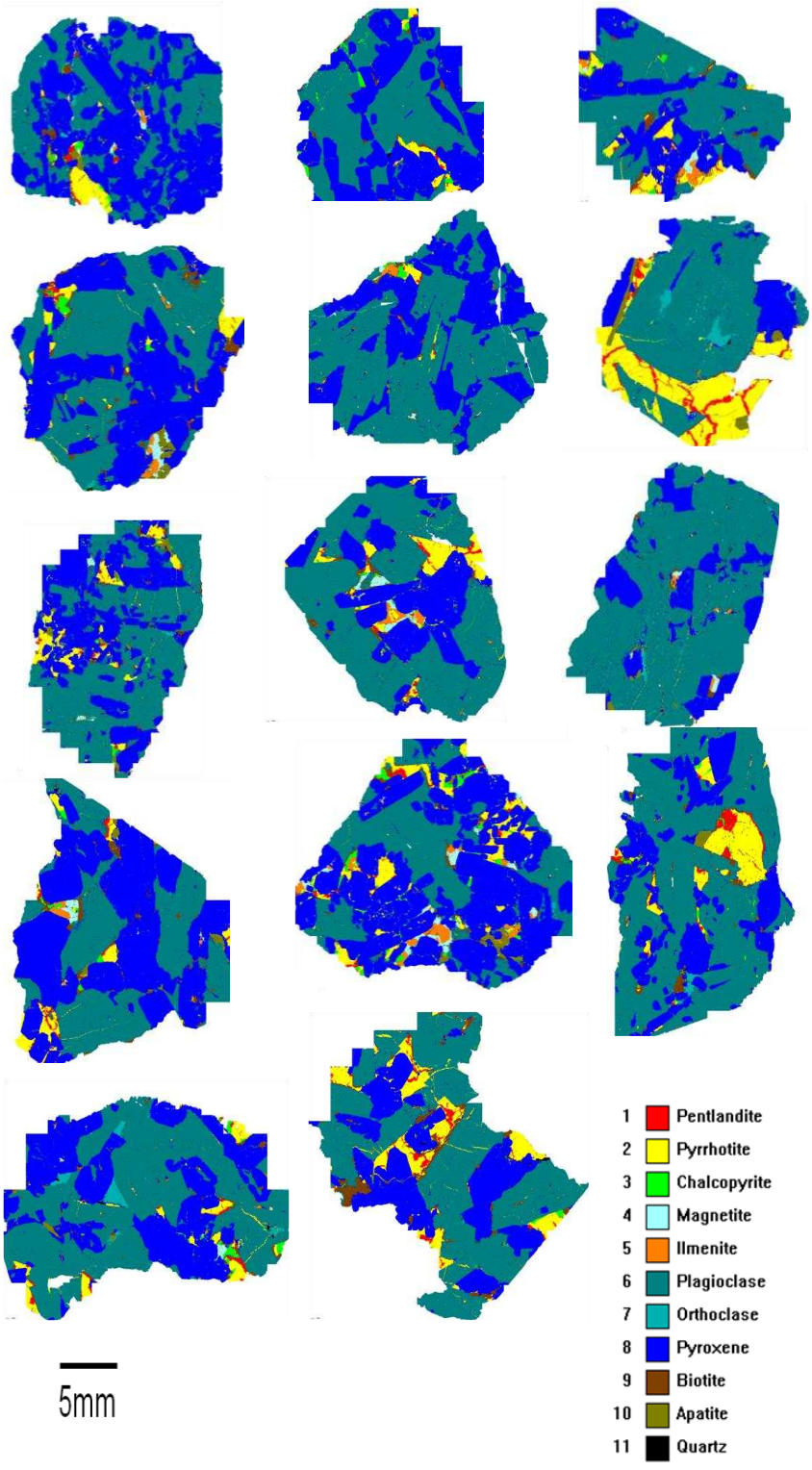

MLA Classified Images of Los Bronces Copper Ore

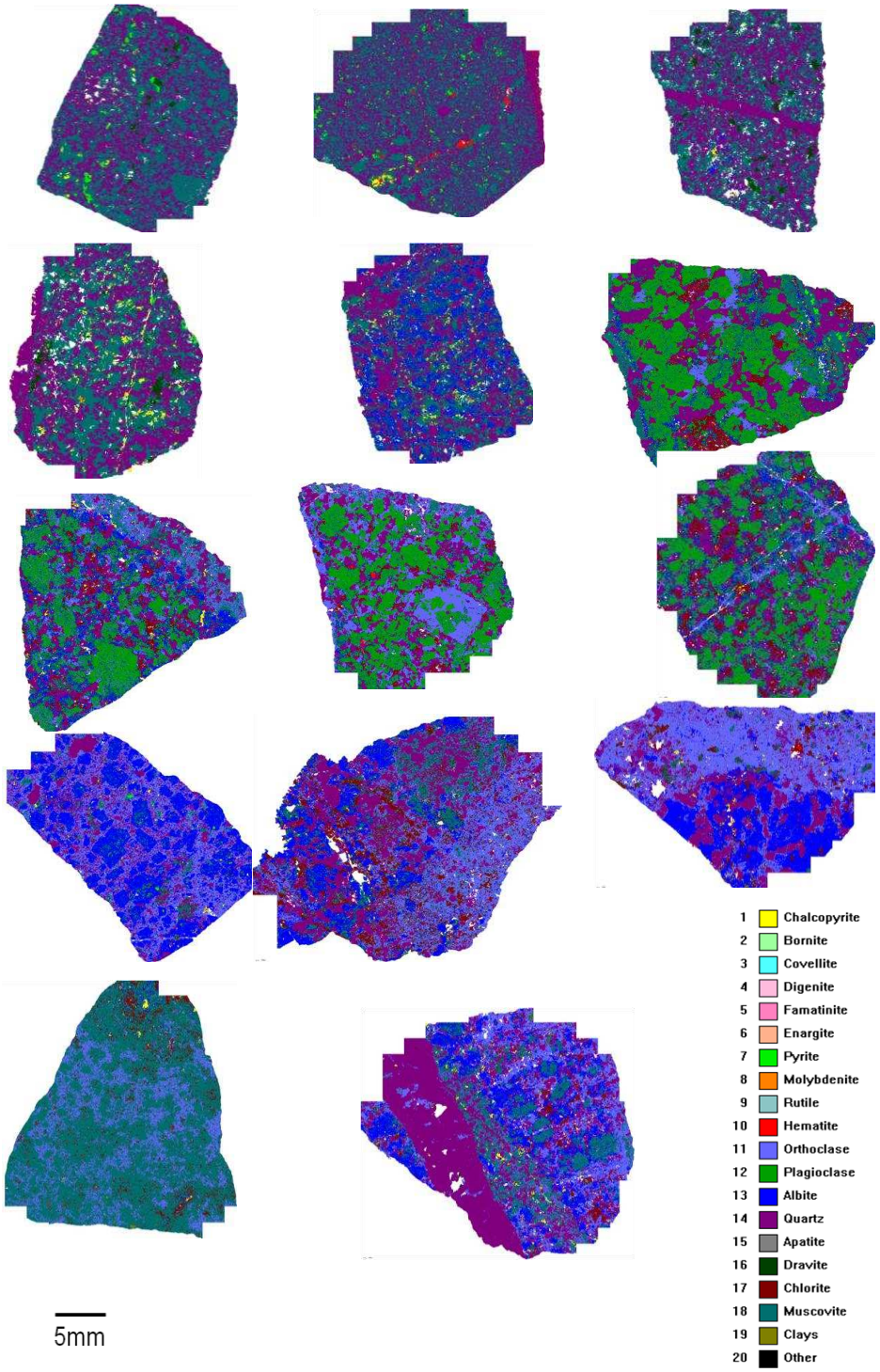

MLA Classified Images of Ekati Kimberilite Daimond (type I) Ore

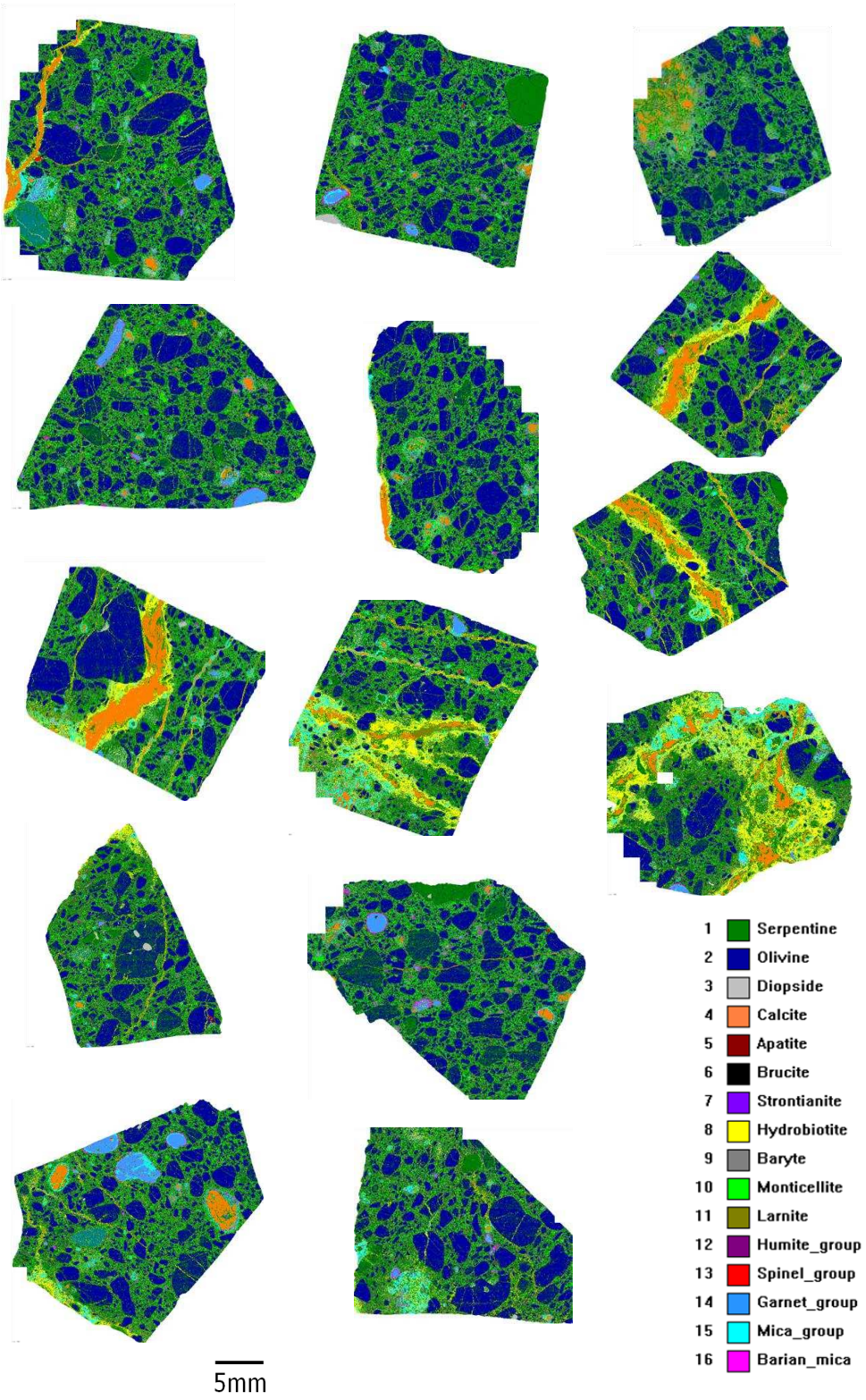

MLA Classified Images of Ekati Kimberilite Daimond (type II) Ore

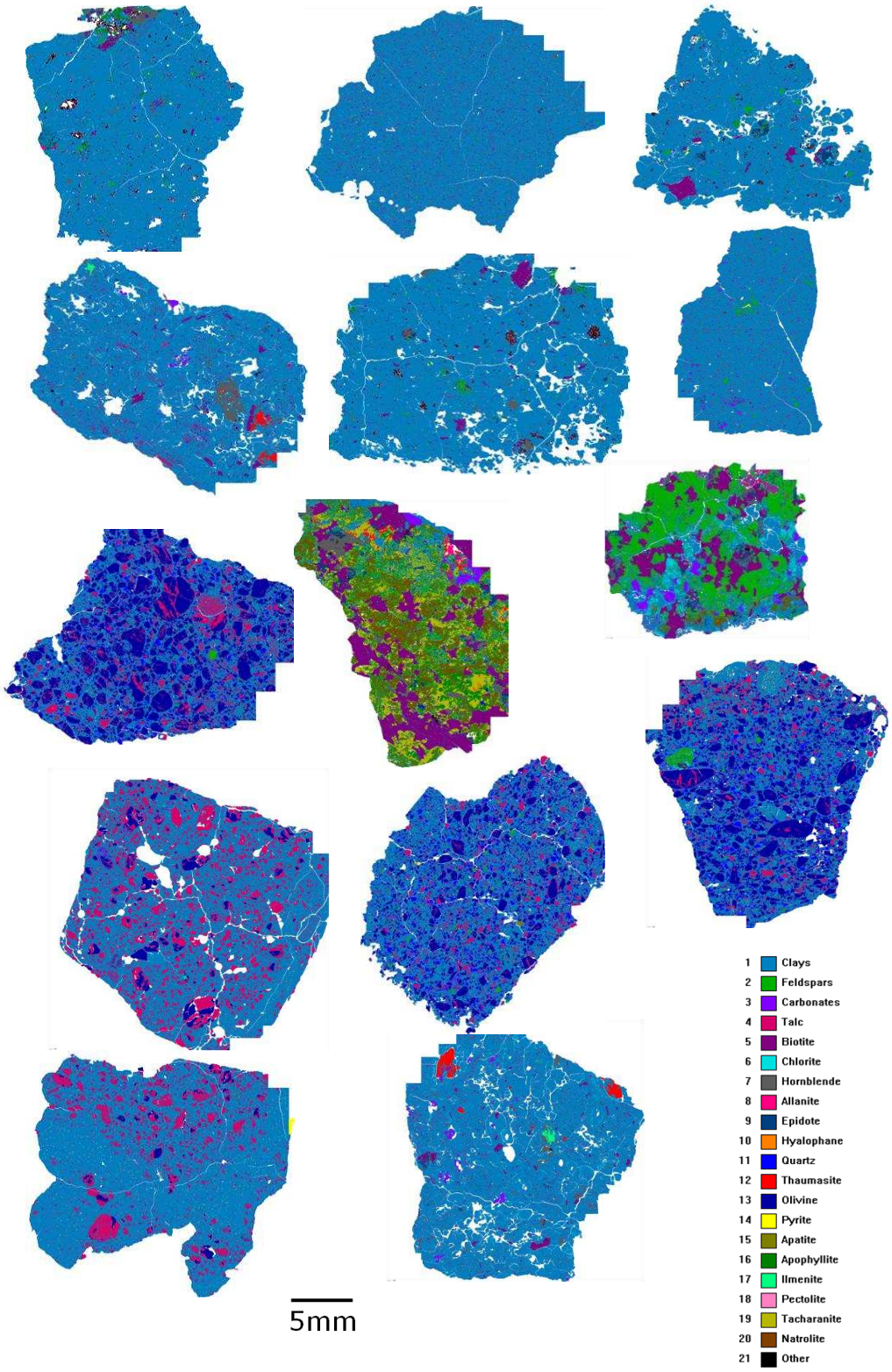

MLA Classified Images of Escondida Copper I Ore

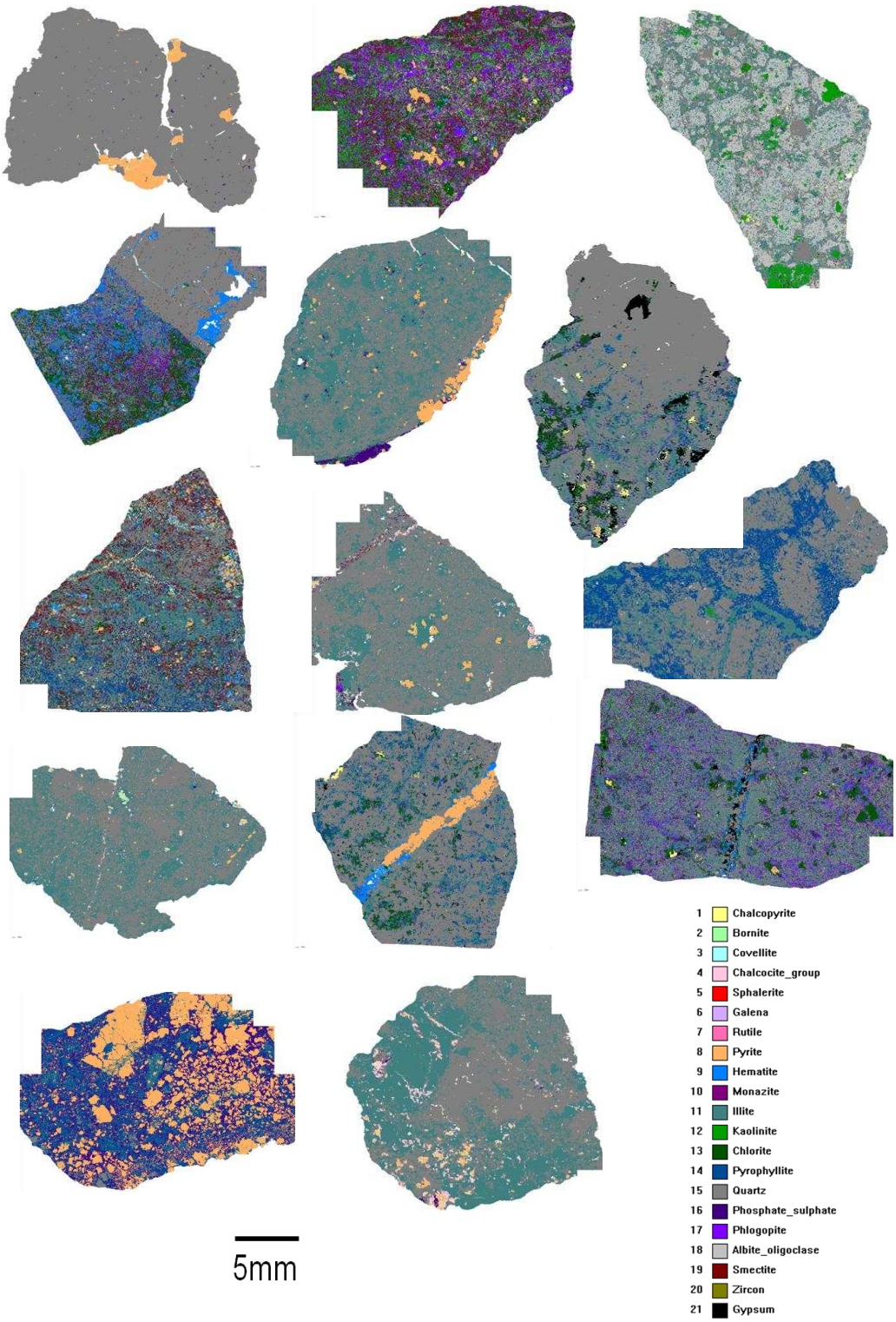

MLA Classified Images of Copper II Ore

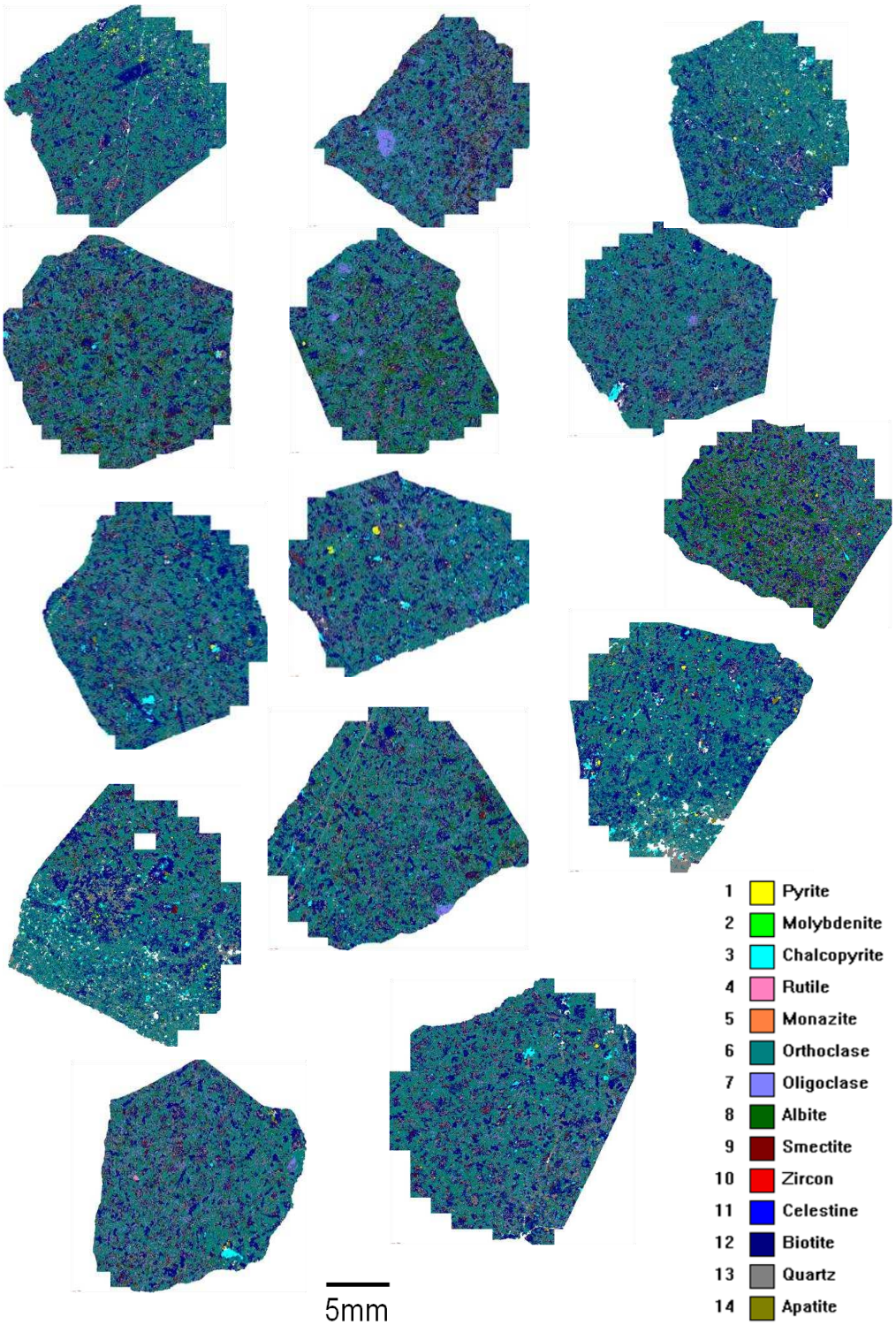

APPENDIX II

Mineral Dielectric Properties

Cavity Perturbation Dielectric Property Calculation Sheet

The University of Nottingham

DIELECTRIC PROPERTIES DATA SHEET

Sample ID

Description

				Bessel Function Values	@ 911 MHz	@ 2,450 MHz
Volume of Cavity (mm³)	15,190,473	TM010	0.5191	**J1**	-0.34026	0.2065
Volume of Sample (mm³)				**x1,m**	1	1
Mass of Tube (g)		TM030	0.2719	***OBV**	-0.30260	0.2066
Mass of Tube + Sample)		TM040		***SCV**	13,120,000	
Mass of Sample (g)		TM050				
Length of Sample (mm)		TM060				
Tube Diameter (mm)						
Sample Density (kg/m³)						
Particle Density (kg/m³)						
Void (%)						

	Freq	Q	B	@ 911 MHz		@ 2,450 MHz	
Temperature	9.12E+02						
	2.47E+03						
	9.12E+02						
	2.47E+03						
	9.12E+02						
	2.47E+03						
	9.12E+02						
	2.47E+03						
	9.12E+02						
	2.47E+03						
	9.12E+02						
	2.47E+03						
	9.12E+02						
	2.47E+03						
	9.12E+02						
	2.47E+03						
	2.47E+03						

OBV = Old Bessel Values

SCV = Staff Cavity Vol.

Mineral Dielectric Property Values at Different Temperatures

GYPSUM

Temp C	ε'	ε''
20	3.449	0.002
40	3.487	0.002
60	3.510	0.002
80	3.533	0.000
100	3.522	0.003
120	3.189	0.013
140	2.903	0.019
160	2.833	0.019
200	2.541	0.003
300	2.503	0.002
400	2.497	0.002
500	2.523	0.002
600	2.550	0.002
700	2.576	0.001
800	2.608	0.002

STICHTITE

Temp C	ε'	ε''
25	3.703	0.117
50	3.833	0.151
75	3.932	0.172
100	4.030	0.193
125	4.110	0.227
150	4.180	0.286
200	4.310	0.472
250	3.414	0.360
300	2.922	0.033
350	2.877	0.015
400	2.798	0.012
450	2.407	0.008
500	2.321	0.008
550	2.309	0.005
600	2.296	0.006
650	2.290	0.009
700	2.286	0.017
750	2.321	0.061
800	2.372	0.135
850	2.394	0.190

TALC

Temp C	ε'	ε''
30	1.595	0.009
100	1.570	0.001
125	1.577	0.002
150	1.580	0.001
200	1.593	0.001
250	1.606	0.002
300	1.606	0.002
400	1.635	0.001
500	1.653	0.001
600	1.677	0.002
700	1.706	0.003
850	1.752	0.004

MONTMORILLONITE

Temp C	ε'	ε''
20	4.490	1.110
100	4.531	1.131
140	3.810	1.125
180	2.771	0.486
220	2.036	0.048
260	1.948	0.010
300	1.948	0.011
340	1.948	0.011
380	1.954	0.013
420	1.959	0.016
460	1.000	0.000
500	1.000	0.000
540	1.000	0.001

HALLOYSITE

Temp C	ε'	ε''
20	4.100	0.309
40	4.170	0.318
60	4.202	0.350
80	4.164	0.412
100	3.329	0.269
120	3.071	0.146
160	2.778	0.047
200	2.719	0.026
250	2.665	0.020
300	2.620	0.013
350	2.622	0.013
400	2.571	0.016
450	2.526	0.015
500	2.504	0.016
550	2.048	0.009
600	1.959	0.013
650	1.972	0.009
700	1.967	0.011
800	1.983	0.014
850	1.997	0.012

KAOLINITE

Temp C	ε'	ε''
20	2.421	0.111
40	2.450	0.100
60	2.424	0.086
80	2.372	0.075
100	2.232	0.040
120	2.138	0.027
140	2.121	0.014
160	2.081	0.010
180	2.081	0.008
200	2.072	0.004
250	2.061	0.002
300	2.058	0.004
350	2.052	0.001
400	2.046	0.000
500	1.260	-0.001
600	1.283	0.000
700	1.540	-0.001
800	1.658	-0.001

APATITE

Temp C	ε'	ε''
40	3.315	0.060
50	3.315	0.056
100	3.314	0.048
150	3.335	0.056
200	3.365	0.066
225	3.388	0.072
250	3.411	0.077
300	3.439	0.088
350	3.484	0.100
375	3.515	0.109
400	3.533	0.113
425	3.564	0.119
450	3.599	0.126
475	3.633	0.136
500	3.681	0.145
525	3.706	0.151
550	3.736	0.156
575	3.772	0.163
600	3.846	0.175
625	3.887	0.183
650	3.918	0.188
675	3.951	0.193
700	3.970	0.193
725	4.013	0.197
750	4.066	0.205
775	4.106	0.208
800	4.097	0.200
855	4.171	0.209

ACTINOLITE

Temp C	ε'	ε''
20	2.489	0.032
50	1.561	0.004
100	1.561	0.004
150	1.899	0.003
200	1.917	0.004
250	1.915	0.004
300	1.916	0.003
350	1.918	0.003
400	2.208	0.004
450	2.259	0.006
500	2.303	0.008
550	2.331	0.011
600	2.344	0.015
650	2.371	0.019
700	2.393	0.022
750	2.411	0.019
800	2.417	0.018
850	2.440	0.021

APPENDIX III

Ore Strength Characterization Data

Microwave Treatment Conditions

Tube length (m) = 0.25
Sample length (m) = 0.195

Sample ID	Sample Mass	Packing Density	Treatment Time	Stroke Speed	Mass Flow Rate	Forward Power	Reflected Power	Input Power	Energy Expended
	g	g/m	s	m/s	t/h	kW	kW	kW	kWh/t
Nebo Babel Ni Cu T1	982	5036	0.25	1.000	18.1	15	1.7	13.3	0.73
Nebo Babel Ni Cu T2	974	4995	0.25	1.000	18.0	20	1.5	18.5	1.03
Nebo Babel Ni Cu T3	991	5082	1.1	0.227	4.2	23	3	20	4.81
Los Bronces Cu T1	850	4361	0.25	1.000	15.7	20	7	13	0.83
Los Bronces Cu T2	859	4403	1.1	0.227	3.6	21	10	11	3.05
Los Bronces Cu T3	852	4367	2.75	0.091	1.4	20	10	10	7.00
Ekati Kimberlite I T1	1196	21745	7.4	0.034	2.6	22	4	18	6.81
Ekati Kimberlite I T2	1100	20000	12.5	0.020	1.4	25	0.4	24.6	17.08
Ekati Kimberlite I T3	1338	24327	17	0.015	1.3	26	14	12	9.32
Ekati Kimberlite II T1	922	16769	3.5	0.071	4.3	27	4	23	5.33
Ekati Kimberlite II T2	1020	18553	7.86	0.032	2.1	26	4	22	10.36
Ekati Kimberlite II T3	957	17400	10	0.025	1.6	26	4	22	14.05

Point Load Tester Calibration Graph

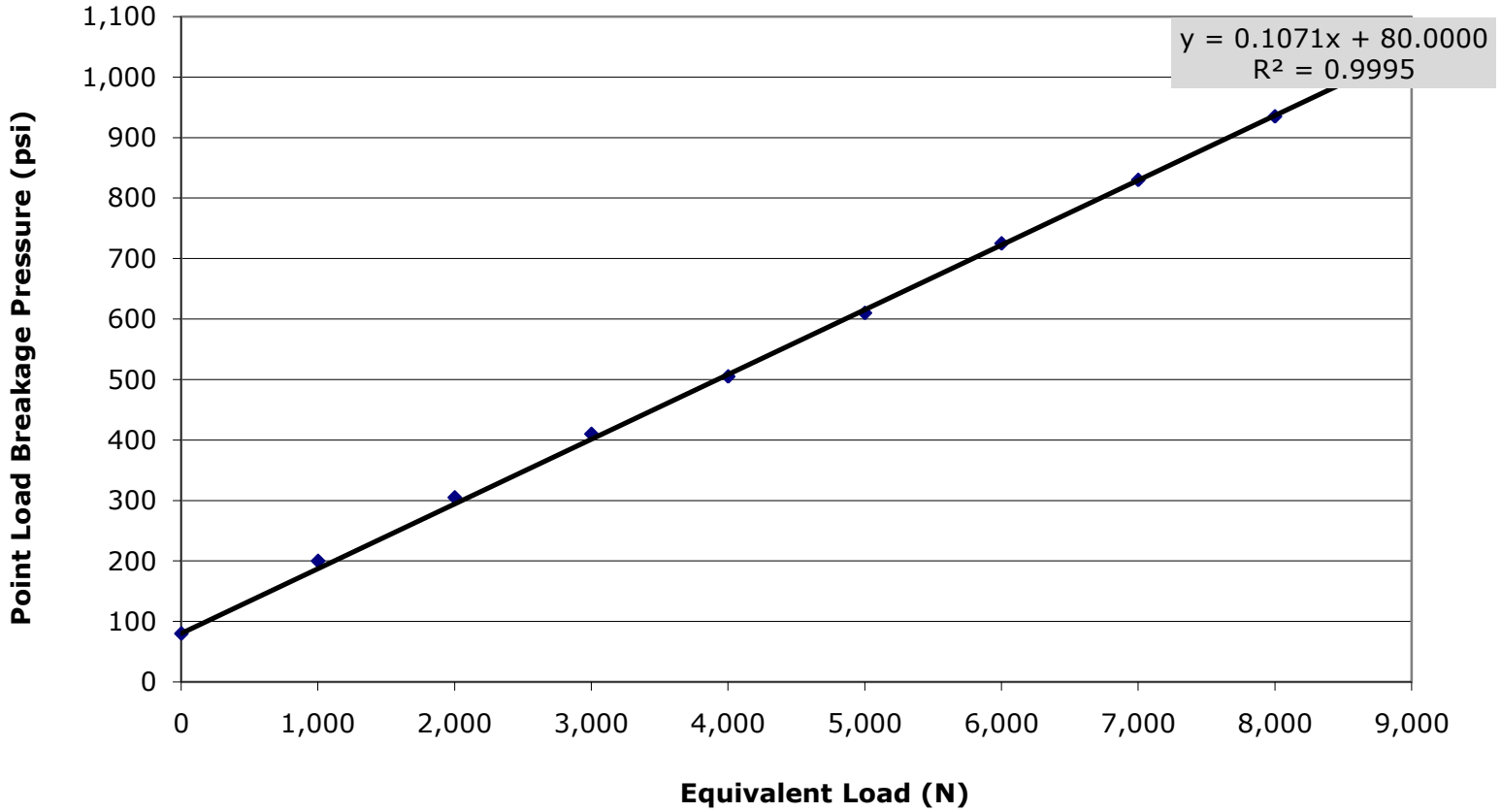

POINT LOAD TEST DATA SHEET						
Sample ID:			Nebo Babel Ni-Cu			
Description:			Untreated			
Count No.	**Spread (%)**	**Depth (mm)**	**Width (mm)**	**Breakage Load**		**Is(50)**
				Measured (lb/in²)	**Converted (N)**	
1	0.01	13.72	20.62	200	1121	1.74
2	0.02	17.54	20.07	310	2150	2.99
3	0.03	21.98	20.77	380	2804	3.33
4	0.04	23.37	18.58	370	2710	3.48
5	0.05	22.895	22.44	450	3458	3.72
6	0.06	23.405	20.14	420	3178	3.76
7	0.07	15.225	27.43	450	3458	3.81
8	0.08	24.015	21.29	450	3458	3.82
9	0.09	26.27	19.39	450	3458	3.99
10	0.11	22.12	20.04	430	3271	4.02
11	0.12	23.8267	20.23	450	3458	4.04
12	0.13	17.975	19.71	400	2991	4.18
13	0.14	14.515	24.69	450	3458	4.34
14	0.15	13.2425	23.52	430	3271	4.54
15	0.16	16.2733	23.3	470	3645	4.56
16	0.17	16.945	19.28	410	3084	4.56
17	0.18	20.905	20.64	480	3738	4.60
18	0.19	11.42	22.38	400	2991	4.73
19	0.20	23.63	21.71	550	4393	4.80
20	0.21	24.55	23.52	620	5047	4.98
21	0.22	12.46	15.76	330	2336	5.00
22	0.23	24.35	23.39	620	5047	5.03
23	0.24	22.8767	24.02	620	5047	5.07
24	0.25	15.22	18.19	410	3084	5.12
25	0.26	11.94	22.63	440	3364	5.13
26	0.27	15.38	19.07	430	3271	5.15
27	0.28	21.12	18.11	490	3832	5.34
28	0.29	23.815	18.42	530	4206	5.39
29	0.31	16.3075	23.7	570	4579	5.62
30	0.32	23.62	18.55	570	4579	5.86
31	0.33	14.6725	24.04	570	4579	5.87
32	0.34	16.59	24.18	610	4953	5.90
33	0.35	15.0475	24.01	580	4673	5.92
34	0.36	13.335	23.06	530	4206	5.93
35	0.37	14.015	23.37	550	4393	5.94
36	0.38	23.515	23.44	710	5888	5.97
37	0.39	16.98	14.98	430	3271	6.21
38	0.40	16.88	19.11	530	4206	6.28
39	0.41	14.05	23.92	590	4766	6.29
40	0.42	12.4525	22.65	540	4299	6.40
41	0.43	23.11	18.24	610	4953	6.52
42	0.44	24.2033	22.76	780	6542	6.73
43	0.45	19.495	19.58	630	5140	6.92
44	0.46	12.47	23.69	610	4953	7.05
45	0.47	14.66	23.91	670	5514	7.11
46	0.48	14.77	20.55	590	4766	7.12
47	0.49	19.81	24.2	800	6729	7.27
48	0.51	13.4275	23.62	650	5327	7.30

49	0.52	16.565	19.87	620	5047	7.33
50	0.53	14.26	23.09	660	5421	7.35
51	0.54	17.11	21.5	680	5607	7.39
52	0.55	23.87	16.2	640	5234	7.62
53	0.56	19.095	19.27	670	5514	7.63
54	0.57	14.705	23.88	720	5981	7.71
55	0.58	15.01	24	740	6168	7.83
56	0.59	17.265	18.21	630	5140	7.96
57	0.60	12.9875	23.99	700	5794	7.96
58	0.61	14.9075	23.27	730	6075	7.98
59	0.62	15.67	16.44	560	4486	8.11
60	0.63	14.4	17.69	580	4673	8.23
61	0.64	13.3725	20.2	630	5140	8.26
62	0.65	24.68667	23.95	1000	8598	8.31
63	0.66	23.135	16.53	700	5794	8.41
64	0.67	11.58	23.88	700	5794	8.52
65	0.68	22.47	17.02	720	5981	8.57
66	0.69	22.79667	19.77	830	7009	8.58
67	0.71	23.33667	19.95	860	7290	8.73
68	0.72	14.6525	20.79	710	5888	8.74
69	0.73	20.435	18.24	750	6262	8.82
70	0.74	13.7175	17.24	600	4860	9.02
71	0.75	13.3525	21.12	710	5888	9.05
72	0.76	12.985	22.87	760	6355	9.16
73	0.77	20.77	16.27	710	5888	9.22
74	0.78	13.19	13.24	480	3738	9.23
75	0.79	22.895	16.82	780	6542	9.39
76	0.80	20.775	16.15	720	5981	9.43
77	0.81	12.815	22.18	760	6355	9.52
78	0.82	13.105	23.98	830	7009	9.59
79	0.83	24.01	16.49	800	6729	9.60
80	0.84	22.31	16.69	780	6542	9.60
81	0.85	14.515	21.9	810	6822	9.66
82	0.86	16.255	16.32	660	5421	9.68
83	0.87	23.6	17.13	860	7290	10.10
84	0.88	23.47	16.49	830	7009	10.12
85	0.89	14.565	16.68	680	5607	10.41
86	0.91	24.51	18.35	960	8224	10.42
87	0.92	13.23	23.51	910	7757	10.77
88	0.93	17.61	13.31	630	5140	10.77
89	0.94	13.5275	22.83	900	7664	10.82
90	0.95	16.515	16.59	750	6262	10.90
91	0.96	14.065	20.86	860	7290	11.03
92	0.97	24.38	16.2	900	7664	11.03
93	0.98	24.76	14.24	840	7103	11.53
94	0.99	19.055	16.47	850	7196	11.67
95	1.00	12.335	18.71	1030	8879	16.10

Mean	7.2
St Deviation	2.50
Median	7.30

POINT LOAD TEST DATA SHEET

Sample ID:	Nebo Babel Ni-Cu
Description:	Treated (T1)15kW,0.25 s. Av RP =1.7kW

Count No.	Spread (%)	Depth (mm)	Width (mm)	Breakage Load		Is(50)
				Measured (lb/in²)	Converted (N)	
1	0.01	13.14	18.45	100	187	0.33
2	0.02	14.66	20.2	140	561	0.86
3	0.03	17.77	12.37	140	561	1.26
4	0.04	23.99	14.78	200	1121	1.79
5	0.05	22.05	15.46	200	1121	1.79
6	0.06	23.57	14.61	200	1121	1.82
7	0.07	22.91	18.35	280	1869	2.46
8	0.08	17.86	14.31	240	1495	2.89
9	0.09	13.76	24.58	320	2243	2.91
10	0.11	24.21	15.26	300	2056	3.15
11	0.12	17.37	16.5	280	1869	3.18
12	0.13	13.96	15.55	260	1682	3.43
13	0.14	23.03	19.23	380	2804	3.51
14	0.15	23.59	20	430	3271	3.88
15	0.16	16.26	22.38	400	2991	3.89
16	0.17	17.11	22.28	410	3084	3.92
17	0.18	24.5	18.84	420	3178	3.92
18	0.19	14.36	23.74	400	2991	3.93
19	0.20	20.2	21.12	440	3364	4.12
20	0.21	24.9	16.13	400	2991	4.27
21	0.22	14.02	21.97	400	2991	4.30
22	0.23	13.65	24.28	430	3271	4.32
23	0.24	21.93	17.92	420	3178	4.38
24	0.25	22.94	14.8	380	2804	4.57
25	0.26	23.53	15.55	400	2991	4.57
26	0.27	16.45	18.79	400	2991	4.61
27	0.28	24.2	14.82	400	2991	4.72
28	0.29	19.86	18.09	440	3364	4.85
29	0.31	14.63	23.71	480	3738	4.87
30	0.32	24.66	19.82	540	4299	5.03
31	0.33	22.82	18.65	500	3925	5.09
32	0.34	14.52	19.96	440	3364	5.23
33	0.35	19.78	16.36	430	3271	5.23
34	0.36	13.76	18	400	2991	5.31
35	0.37	22.97	17.61	500	3925	5.37
36	0.38	19.49	15.71	430	3271	5.49
37	0.39	16.4	15.6	400	2991	5.56
38	0.40	16.65	15.33	400	2991	5.61
39	0.41	14.55	16.73	420	3178	5.88
40	0.42	13.05	17.18	410	3084	5.90
41	0.43	17.9	18.34	510	4019	6.06
42	0.44	19.17	18.47	530	4206	6.06
43	0.45	23.87	15.21	500	3925	6.09
44	0.46	13.03	15.69	400	2991	6.27
45	0.47	13.37	15.46	400	2991	6.28
46	0.48	14.57	13.68	380	2804	6.34
47	0.49	14.99	17.79	480	3738	6.40
48	0.51	23.05	21.46	700	5794	6.49

49	0.52	13.6	23.97	600	4860	6.52
50	0.53	23.18	22.57	740	6168	6.55
51	0.54	17.88	17.22	520	4112	6.60
52	0.55	18.99	15.76	500	3925	6.66
53	0.56	25.42	17.21	620	5047	6.68
54	0.57	15.99	23.78	660	5421	6.70
55	0.58	23.65	12.56	460	3551	6.70
56	0.59	15.81	21.84	610	4953	6.71
57	0.60	23.35	17.12	600	4860	6.78
58	0.61	23.88	21.75	760	6355	6.89
59	0.62	23.77	18.42	660	5421	6.96
60	0.63	23.39	14.96	560	4486	7.15
61	0.64	15.21	15.68	480	3738	7.21
62	0.65	22.5	15.67	580	4673	7.27
63	0.66	16.55	20.48	640	5234	7.37
64	0.67	19.43	16.71	580	4673	7.39
65	0.68	24.05	19.92	760	6355	7.50
66	0.69	23.27	15.37	600	4860	7.56
67	0.71	17.4	15.23	520	4112	7.58
68	0.72	22.72	16.72	640	5234	7.59
69	0.73	18.59	14	500	3925	7.59
70	0.74	18.54	16.35	570	4579	7.59
71	0.75	16.23	19.98	640	5234	7.64
72	0.76	12.03	18.81	530	4206	7.69
73	0.77	23.9	12.3	510	4019	7.70
74	0.78	22.71	15.25	600	4860	7.73
75	0.79	23.02	14.08	580	4673	7.99
76	0.80	15.57	24.01	780	6542	8.13
77	0.81	24.03	15.98	680	5607	8.25
78	0.82	23.98	17.95	760	6355	8.33
79	0.83	19.03	17.3	660	5421	8.37
80	0.84	24.22	13.56	600	4860	8.39
81	0.85	22.84	13.7	600	4860	8.57
82	0.86	15.11	22.33	760	6355	8.63
83	0.87	23.31	21.91	940	8037	8.77
84	0.88	23.8	18.11	800	6729	8.78
85	0.89	16.16	19.53	710	5888	8.81
86	0.91	23.56	16.86	750	6262	8.82
87	0.92	16.59	18.21	680	5607	8.87
88	0.93	23.34	15.47	720	5981	9.23
89	0.94	22.79	16.58	770	6449	9.41
90	0.95	23.9	15.2	730	6075	9.42
91	0.96	18.42	15.27	670	5514	9.82
92	0.97	18.7	13.85	620	5047	9.83
93	0.98	22.44	14.95	740	6168	10.07
94	0.99	13.86	19.1	780	6542	10.90
95	1.00	23.77	13.3	750	6262	11.13

Mean	6.2
St	2.30
Median	6.49

The University of Nottingham

POINT LOAD TEST DATA SHEET

Sample ID:			Nebo Babel Ni-Cu			
Description:			Treated (T2) 20kW, 0.25s. Av. RP=1.5kW			
Count No.	**Spread (%)**	**Depth (mm)**	**Width (mm)**	**Breakage Load**		**Is(50)**
				Measured (lb/in²)	**Converted (N)**	
1	0.01	23.155	20.57	280	1869	2.18
2	0.02	22.3467	20.92	310	2150	2.51
3	0.03	23.67	25.12	380	2804	2.65
4	0.04	23.35	20.91	340	2430	2.77
5	0.05	12.1025	24.57	320	2243	3.13
6	0.06	14.59	20.8	310	2150	3.20
7	0.07	22.68	23.71	460	3551	3.63
8	0.08	21.375	24.08	460	3551	3.70
9	0.09	13.685	24.05	380	2804	3.73
10	0.11	16.81	20.05	370	2710	3.87
11	0.12	19.4533	24.06	470	3645	4.00
12	0.13	22.5	17.64	390	2897	4.00
13	0.14	18.69	20.72	420	3178	4.14
14	0.15	14.8625	21.63	400	2991	4.23
15	0.16	22.36	20.47	460	3551	4.24
16	0.17	12.3775	24.42	420	3178	4.41
17	0.18	13.0825	22.51	410	3084	4.50
18	0.19	12.19	21.2	390	2897	4.67
19	0.20	18.55	16.68	390	2897	4.71
20	0.21	13.32	15.12	320	2243	4.82
21	0.22	17.925	19.19	440	3364	4.84
22	0.23	13.5	19.74	400	2991	4.89
23	0.24	21.145	17.21	440	3364	4.93
24	0.25	19.355	18.03	440	3364	4.94
25	0.26	12.6325	23.73	460	3551	5.01
26	0.27	12.83	23.14	460	3551	5.09
27	0.28	23.25	20.48	550	4393	5.13
28	0.29	12.475	23.8	470	3645	5.16
29	0.31	24.6625	24.67	670	5514	5.18
30	0.32	13.18	23.88	500	3925	5.38
31	0.33	12.5125	20.63	440	3364	5.49
32	0.34	16.535	17.95	450	3458	5.56
33	0.35	14.1775	23.87	540	4299	5.66
34	0.36	15.4267	21.27	520	4112	5.80
35	0.37	23.2433	23.04	680	5607	5.83

36	0.38	13.38	22.82	520	4112	5.84
37	0.39	15.63	16.78	440	3364	5.97
38	0.40	17.795	16.79	470	3645	6.02
39	0.41	17.615	19	520	4112	6.03
40	0.42	14.5575	22.86	560	4486	6.08
41	0.43	14.0725	24.92	600	4860	6.15
42	0.44	16.93	18.9	520	4112	6.20
43	0.45	20.13	16	490	3832	6.20
44	0.46	25.7433	23.78	780	6542	6.23
45	0.47	16.985	22.68	620	5047	6.33
46	0.48	22.4667	23.04	720	5981	6.33
47	0.49	24.545	17	580	4673	6.39
48	0.51	22.725	17.02	560	4486	6.39
49	0.52	14.495	22.43	580	4673	6.47
50	0.53	23.82	20.82	690	5701	6.47
51	0.54	22.225	15.93	530	4206	6.48
52	0.55	17.52	16.91	500	3925	6.49
53	0.56	22.855	17.03	570	4579	6.50
54	0.57	17.515	18.27	550	4393	6.72
55	0.58	24.77	16.67	600	4860	6.74
56	0.59	21.54	15.6	540	4299	6.88
57	0.60	23.25	23.31	800	6729	6.91
58	0.61	15.5625	24.79	700	5794	6.98
59	0.62	23.715	17.9	660	5421	7.17
60	0.63	14.1225	22.57	630	5140	7.17
61	0.64	21.915	17.36	620	5047	7.19
62	0.65	14.97	17.43	520	4112	7.19
63	0.66	13.77	13.56	410	3084	7.26
64	0.67	21.435	18.56	660	5421	7.31
65	0.68	13.845	23.3	660	5421	7.41
66	0.69	16.95	17.61	570	4579	7.41
67	0.71	23.555	16.36	640	5234	7.60
68	0.72	14.525	22.94	700	5794	7.83
69	0.73	22.77667	19.42	760	6355	7.92
70	0.74	23.305	16.86	680	5607	7.95
71	0.75	17.845	15.44	560	4486	8.04
72	0.76	18.925	14.93	560	4486	8.05
73	0.77	18.15	17.08	620	5047	8.10
74	0.78	19.69	18.05	680	5607	8.15
75	0.79	14.86	18.87	630	5140	8.34
76	0.80	15.6975	22.48	760	6355	8.40

77	0.81	14.935	24.09	800	6729	8.53
78	0.82	15.0375	22.36	780	6542	8.90
79	0.83	22.68	21.32	920	7850	8.93
80	0.84	14.775	16.51	600	4860	9.04
81	0.85	16.63	16.57	640	5234	9.09
82	0.86	23.04	16.03	730	6075	9.12
83	0.87	20.27	17.64	750	6262	9.16
84	0.88	14.6	16.05	610	4953	9.54
85	0.89	11.615	22.72	750	6262	9.66
86	0.91	22.47667	23.8	1100	9533	9.77
87	0.92	15.7375	18.11	730	6075	9.95
88	0.93	15.18	17.82	710	5888	10.00
89	0.94	13.34	21.52	810	6822	10.30
90	0.95	13.695	23.78	900	7664	10.32
91	0.96	23.065	18.88	960	8224	10.47
92	0.97	22.22	16.36	840	7103	10.65
93	0.98	18.775	18.82	920	7850	11.23
94	0.99	13.7225	23.49	980	8411	11.45
95	1.00	17.675	16.12	840	7103	12.26

.

Mean	6.6
St Dev	2.20
Median	6.39

The University of Nottingham

POINT LOAD TEST DATA SHEET

Sample ID:	Nebo Babel Ni-Cu
Description:	Treated (T3) 23Kw, 1.1s. Av RP = 3kW

Count No.	Spread (%)	Depth (mm)	Width (mm)	Breakage Load		Is(50)
				Measured (lb/in²)	Converted (N)	
1	0.01	11.3575	24.17	80	0	0.00
2	0.02	11.26	22.07	160	748	1.21
3	0.03	23.82	18.68	210	1215	1.54
4	0.04	22.9	17.15	200	1121	1.58
5	0.05	15.56	15.58	170	841	1.61
6	0.06	17.08	16.46	190	1028	1.77
7	0.07	19.455	19.75	230	1402	1.87
8	0.08	12.04	17	180	935	1.89
9	0.09	14.695	15.57	190	1028	2.03
10	0.11	21.8867	19.29	250	1589	2.04
11	0.12	14.99	24.57	290	1963	2.43
12	0.13	16.46	18.35	270	1776	2.80
13	0.14	21.8333	20.36	330	2336	2.84
14	0.15	13.6125	23.53	310	2150	2.94
15	0.16	22.91	24.34	420	3178	3.15
16	0.17	13.855	22.49	330	2336	3.31
17	0.18	14.7525	23.93	370	2710	3.48
18	0.19	20.5	22.91	420	3178	3.56
19	0.20	22.835	18.4	370	2710	3.56
20	0.21	23.085	23.95	470	3645	3.66
21	0.22	23.615	24.04	490	3832	3.78
22	0.23	16.21	24.58	430	3271	3.88
23	0.24	22.73	24.03	500	3925	3.96
24	0.25	22.245	21.24	450	3458	3.99
25	0.26	23.4675	24.6	550	4393	4.25
26	0.27	25.24	19.71	480	3738	4.34
27	0.28	14.2725	23.55	430	3271	4.35
28	0.29	22.9075	25.27	580	4673	4.46
29	0.31	22.85	17.54	430	3271	4.51
30	0.32	23.62	14.52	380	2804	4.58
31	0.33	19.45	20.45	460	3551	4.59
32	0.34	15.77	18.06	380	2804	4.60
33	0.35	22.99	23.93	580	4673	4.70
34	0.36	12.3625	23.78	440	3364	4.79
35	0.37	16.7425	22.97	500	3925	4.90
36	0.38	11.07	10.92	240	1495	4.93
37	0.39	14.05	23.9	480	3738	4.94
38	0.40	18.3	19.05	450	3458	4.96
39	0.41	22.75	18.72	490	3832	4.96
40	0.42	16.385	23.39	510	4019	4.98
41	0.43	21.99	19.42	510	4019	5.11
42	0.44	22.26	17.21	470	3645	5.19
43	0.45	14.315	16.67	380	2804	5.26
44	0.46	21.9633	19.09	520	4112	5.32
45	0.47	18.925	19.6	500	3925	5.37
46	0.48	15.04	22.17	510	4019	5.51
47	0.49	18.65	20.6	530	4206	5.52
48	0.51	19.6567	21.33	560	4486	5.52

49	0.52	12.67	18.08	400	2991	5.53
50	0.53	18.865	19.33	510	4019	5.58
51	0.54	24.225	18.74	560	4486	5.60
52	0.55	22.365	17.48	510	4019	5.62
53	0.56	21.2967	21.32	600	4860	5.73
54	0.57	12.5625	24.01	530	4206	5.88
55	0.58	22.22	19.06	570	4579	5.90
56	0.59	14.33	24.22	590	4766	6.15
57	0.60	19.63	18.6	560	4486	6.34
58	0.61	23.655	16.38	560	4486	6.49
59	0.62	23.93333	20.76	700	5794	6.57
60	0.63	11.3675	21.55	510	4019	6.62
61	0.64	23.985	17.24	600	4860	6.63
62	0.65	23.39	16.09	560	4486	6.65
63	0.66	16.515	14.03	430	3271	6.74
64	0.67	23.37	16.74	590	4766	6.80
65	0.68	15.825	19.51	560	4486	6.80
66	0.69	19.245	18.85	600	4860	6.85
67	0.71	23.475	18.49	650	5327	6.86
68	0.72	13.765	24.29	640	5234	6.88
69	0.73	22.55333	19.78	680	5607	6.90
70	0.74	21.255	17.23	590	4766	6.96
71	0.75	23.7875	24.6	860	7290	7.00
72	0.76	13.205	23.1	610	4953	7.01
73	0.77	16.515	19.19	580	4673	7.03
74	0.78	14.0325	22.42	620	5047	7.11
75	0.79	21.365	16.64	590	4766	7.18
76	0.80	13.4925	22.44	620	5047	7.26
77	0.81	22.015	17.36	640	5234	7.44
78	0.82	22.015	19.31	710	5888	7.52
79	0.83	14.645	21.03	640	5234	7.68
80	0.84	21.255	17.32	660	5421	7.87
81	0.85	22.37	16.74	660	5421	7.92
82	0.86	19.76667	22	810	6822	8.12
83	0.87	22.38	15.55	640	5234	8.23
84	0.88	15.03	23.38	780	6542	8.51
85	0.89	12.8875	24.61	790	6636	8.93
86	0.91	13.7875	23.98	800	6729	8.95
87	0.92	23.245	23.71	1030	8879	8.96
88	0.93	14.985	24.01	840	7103	9.02
89	0.94	22.41	24.49	1060	9159	9.13
90	0.95	14.635	23.87	840	7103	9.19
91	0.96	13.5875	23.82	820	6916	9.34
92	0.97	16.24	18.6	740	6168	9.67
93	0.98	13.0325	24	840	7103	9.74
94	0.99	17.41	15.53	700	5794	10.47
95	1.00	19.6	13.3	680	5607	11.08

Comments

Mean	5.6
St Dev	2.31
Median	5.52

The University of Nottingham

POINT LOAD TEST ANALYSIS

Sample ID:	Los Bronces Cu
Description:	Untreated

Count No.	Spread (%)	Depth (mm)	Width (mm)	Breakage Load		Is(50)
				Measured (lb/in²)	Converted (N)	
1	0.01	23.6825	32.59	200	1121	0.82
2	0.02	24.29	28.45	230	1402	1.15
3	0.04	24.42	27.01	280	1869	1.61
4	0.05	24.35	26.8	300	2056	1.79
5	0.06	23.51	19.22	240	1495	1.85
6	0.07	23.51	16.71	220	1308	1.86
7	0.08	18.9125	22.54	250	1589	1.89
8	0.09	24.0267	20.7	270	1776	2.02
9	0.11	19.52	23.45	290	1963	2.21
10	0.12	18.9733	28.7	340	2430	2.27
11	0.13	16.01	25.78	310	2150	2.45
12	0.14	24.0975	26.76	380	2804	2.46
13	0.15	24.26	28.02	410	3084	2.57
14	0.16	24.0267	19.16	310	2150	2.64
15	0.18	21.0067	20.77	320	2243	2.73
16	0.19	24.63	33.42	510	4019	2.79
17	0.20	23.84	17.81	310	2150	2.85
18	0.21	20.4	18.86	310	2150	2.93
19	0.22	21.2675	27.74	440	3364	3.05
20	0.24	24.565	25.98	450	3458	3.09
21	0.25	16.195	25.38	370	2710	3.12
22	0.26	24.5	23.21	420	3178	3.18
23	0.27	24.31	23.83	430	3271	3.21
24	0.28	23.625	35.84	620	5047	3.34
25	0.29	15.5867	28.05	420	3178	3.38
26	0.31	14.465	19.45	310	2150	3.43
27	0.32	16.515	26.66	420	3178	3.44
28	0.33	14.9933	30.36	460	3551	3.56
29	0.34	18.605	24.58	430	3271	3.60
30	0.35	24.21	20.47	420	3178	3.63
31	0.36	18.015	25.25	440	3364	3.67
32	0.38	19.0675	29.57	520	4112	3.71
33	0.39	24.45	25.14	510	4019	3.72
34	0.40	24.445	23.9	490	3832	3.73
35	0.41	20.03	14.6	310	2150	3.82
36	0.42	23.64	20.55	440	3364	3.88
37	0.44	24.01	20.75	450	3458	3.92
38	0.45	23.8	27.9	580	4673	3.96
39	0.46	21.12	29.49	590	4766	4.08
40	0.47	24.39	23.13	520	4112	4.14
41	0.48	14.06	25.22	440	3364	4.21
42	0.49	24.065	13.4	340	2430	4.26
43	0.51	24.1067	14.18	360	2617	4.33
44	0.52	19.7	18.88	420	3178	4.41
45	0.53	24.96	16.5	420	3178	4.43
46	0.54	24.575	26.38	620	5047	4.44
47	0.55	19.965	20.71	460	3551	4.46
48	0.56	23.1	22.08	520	4112	4.47

49	0.58	24.11	25.15	600	4860	4.53
50	0.59	24.415	24.38	590	4766	4.56
51	0.60	18.185	21.36	460	3551	4.56
52	0.61	23.83	15.3	400	2991	4.62
53	0.62	24.13	16.97	440	3364	4.65
54	0.64	24.8	15.71	420	3178	4.67
55	0.65	24.46	25.68	640	5234	4.74
56	0.66	23.4567	12.6	350	2523	4.77
57	0.67	22.3	21.57	530	4206	4.77
58	0.68	24.315	18.02	480	3738	4.84
59	0.69	24.09333	16.23	450	3458	5.00
60	0.71	16.22	18.46	420	3178	5.02
61	0.72	24.7	27.03	710	5888	5.04
62	0.73	24.27	19.24	540	4299	5.22
63	0.74	24.35	27.63	750	6262	5.29
64	0.75	19.8225	27.05	670	5514	5.33
65	0.76	24.245	27.62	760	6355	5.38
66	0.78	22.13	20.82	570	4579	5.41
67	0.79	24.47333	23.37	680	5607	5.58
68	0.80	23.355	21.53	620	5047	5.60
69	0.81	19.87	23.27	630	5140	5.76
70	0.82	21.835	24.28	700	5794	5.91
71	0.84	24.105	32.04	950	8131	5.95
72	0.85	19.12333	17.96	510	4019	5.96
73	0.86	24.32333	33.17	1020	8785	6.18
74	0.87	20.32	23.96	700	5794	6.23
75	0.88	23.59	30.48	940	8037	6.26
76	0.89	23.66	18.6	610	4953	6.31
77	0.91	17.5625	31.86	870	7383	6.47
78	0.92	20.34	18.33	580	4673	6.57
79	0.93	24.18	17.92	620	5047	6.60
80	0.94	17.585	16.18	500	3925	6.77
81	0.95	24.375	19.96	710	5888	6.88
82	0.96	16.755	20.03	640	5234	7.49
83	0.98	20.74	19.91	730	6075	7.78
84	0.99	24.845	12.36	550	4393	8.20
85	1.00	19.185	27.9	1040	8972	8.55
					Mean	4.3
					St Dev	1.63
					Median	4.33
The University of Nottingham						

POINT LOAD TEST DATA SHEET						
Sample ID:			Los Bronces Cu			
Description:			Treated (T1) 0.25s, 20kW. Av RP=7kW			
Count No.	**Spread (%)**	**Depth (mm)**	**Width (mm)**	**Breakage Load**		**Is(50)**
				Measured (lb/in²)	**Converted (N)**	
1	0.01	16.77	37.09	80	0	0.00
2	0.02	24.57	19.67	100	187	0.22
3	0.04	24.42	30.77	100	187	0.14
4	0.05	24.24	32.25	100	187	0.14
5	0.06	22.09	33.65	100	187	0.14
6	0.07	20.44	26.5	120	374	0.36
7	0.08	24.06	19.09	120	374	0.46
8	0.09	17.34	17.03	120	374	0.62
9	0.11	23.16	14.13	120	374	0.63
10	0.12	18.53	20.59	140	561	0.74
11	0.13	24.29	26.32	160	748	0.66
12	0.14	16.75	20.98	160	748	1.02
13	0.15	21.49	27.53	200	1121	1.02
14	0.16	24.21	21.59	200	1121	1.22
15	0.18	19.34	19.12	200	1121	1.55
16	0.19	20.05	31.59	280	1869	1.54
17	0.20	18.96	31.72	340	2430	2.05
18	0.21	24.31	21.97	300	2056	2.19
19	0.22	22.28	30.78	380	2804	2.23
20	0.24	16.61	26.22	320	2243	2.46
21	0.25	19.88	20.19	300	2056	2.66
22	0.26	20.65	19.42	300	2056	2.70
23	0.27	24.95	26.06	400	2991	2.64
24	0.28	24.16	24.22	380	2804	2.71
25	0.29	19.54	18.86	300	2056	2.87
26	0.31	23.83	23.9	400	2991	2.95
27	0.32	24.75	27.62	460	3551	2.97
28	0.33	16.71	17.71	300	2056	3.33
29	0.34	24.48	17.07	340	2430	3.31
30	0.35	24.52	31.27	540	4299	3.20
31	0.36	24.35	29.36	520	4112	3.27
32	0.38	24.15	24.37	460	3551	3.42
33	0.39	14.95	20.42	340	2430	3.63
34	0.40	21.35	33.98	580	4673	3.45
35	0.41	24.72	24.59	480	3738	3.52
36	0.42	18.55	26.6	460	3551	3.62
37	0.44	24.31	25.13	500	3925	3.65
38	0.45	24.65	23.25	480	3738	3.73
39	0.46	25.05	19.1	420	3178	3.82
40	0.47	18.33	22.5	420	3178	3.85
41	0.48	20.7	26.48	520	4112	3.96
42	0.49	24.92	25.04	540	4299	3.96
43	0.51	17.95	18.68	380	2804	4.14
44	0.52	14.49	30.21	500	3925	4.03
45	0.53	23.83	16.82	400	2991	4.20
46	0.54	17.59	19.71	400	2991	4.23
47	0.55	13.22	25.26	440	3364	4.35
48	0.56	16.56	27.04	520	4112	4.39

49	0.58	14.17	19.49	400	2991	4.82
50	0.59	24.48	20.36	520	4112	4.70
51	0.60	25.16	21.91	560	4486	4.69
52	0.61	21.94	20.23	500	3925	4.79
53	0.62	24.77	16.78	460	3551	4.89
54	0.64	15.12	20.54	440	3364	4.97
55	0.65	20.49	23.4	560	4486	4.92
56	0.66	24.3	16.25	460	3551	5.11
57	0.67	25.11	23.09	620	5047	5.01
58	0.68	22.59	28.99	720	5981	5.02
59	0.69	16.62	28.5	620	5047	5.10
60	0.71	19.98	23.41	580	4673	5.19
61	0.72	21.55	14.72	420	3178	5.39
62	0.73	24.04	21.49	600	4860	5.31
63	0.74	22.85	19.18	540	4299	5.42
64	0.75	27.01	15.78	500	3925	5.48
65	0.76	22.83	32.54	840	7103	5.28
66	0.78	18.92	19.14	500	3925	5.50
67	0.79	24.28	16.22	500	3925	5.66
68	0.80	24.59	17.37	540	4299	5.74
69	0.81	24.53	24.95	740	6168	5.75
70	0.82	20.06	19.76	560	4486	5.89
71	0.84	17.88	31.37	820	6916	6.10
72	0.85	24.19	19.08	660	5421	6.65
73	0.86	16.04	24.52	680	5607	6.71
74	0.87	23.69	13.17	500	3925	7.06
75	0.88	24.42	21.63	760	6355	6.84
76	0.89	18.41	25.16	760	6355	6.87
77	0.91	24.36	26.51	920	7850	6.91
78	0.92	24.37	29.95	1060	9159	7.13
79	0.93	24.79	18.18	700	5794	7.36
80	0.94	15.18	20.9	640	5234	7.58
81	0.95	19.07	11.41	440	3364	7.87
82	0.96	16.49	17.3	580	4673	7.81
83	0.98	24.44	19.82	860	7290	8.56
84	0.99	24.24	16.48	740	6168	8.76
85	1.00	24.6	17.22	780	6542	8.81

.

Mean	4.0
St Dev	2.26
Median	4.03

The University of Nottingham

POINT LOAD TEST ANALYSIS

Sample ID:	Los Bronces Cu
Description:	Treated (T2) 1.1s, 21kW. Av RP=10kW

Count No.	Spread (%)	Depth (mm)	Width (mm)	Breakage Load		Is(50)
				Measured (lb/in²)	Converted (N)	
1	0.01	24.8	19.24	100	187	0.22
2	0.02	16.17	23.89	100	187	0.23
3	0.04	20.36	27.75	120	374	0.35
4	0.05	20.79	26.93	140	561	0.53
5	0.06	20.74	31.87	180	935	0.75
6	0.07	24.25	19.51	160	748	0.90
7	0.08	23.7	19.1	160	748	0.93
8	0.09	25.05	23.98	200	1121	1.07
9	0.11	24.06	22.64	200	1121	1.16
10	0.12	24.68	24.92	220	1308	1.22
11	0.13	18.57	12.09	140	561	1.26
12	0.14	17.81	22.39	200	1121	1.39
13	0.15	20.27	27.24	260	1682	1.59
14	0.16	24.66	15.86	200	1121	1.64
15	0.18	24.24	31.02	320	2243	1.69
16	0.19	23.86	28.22	300	2056	1.72
17	0.20	19.98	16.84	200	1121	1.73
18	0.21	24.42	24.45	300	2056	1.96
19	0.22	15.76	33.2	340	2430	2.17
20	0.24	24.1	21.84	300	2056	2.21
21	0.25	24.53	25.57	360	2617	2.38
22	0.26	24.45	24.07	360	2617	2.53
23	0.27	20.23	20.8	300	2056	2.55
24	0.28	18.88	17.22	260	1682	2.62
25	0.29	24.98	23.69	380	2804	2.72
26	0.31	24.64	26.75	420	3178	2.75
27	0.32	24.26	17.41	300	2056	2.76
28	0.33	16.55	20.36	300	2056	2.91
29	0.34	24.42	23.12	400	2991	3.01
30	0.35	18.57	24.84	400	2991	3.26
31	0.36	24.25	21.24	400	2991	3.29
32	0.38	24.28	16.65	340	2430	3.41
33	0.39	19.04	23.58	420	3178	3.60
34	0.40	24.67	22.85	460	3551	3.60
35	0.41	20.24	20.64	400	2991	3.74
36	0.42	21	20.16	400	2991	3.75
37	0.44	20.04	26.66	500	3925	3.82
38	0.45	23.92	27.12	560	4486	3.90
39	0.46	19.94	29.97	560	4486	3.90
40	0.47	17.62	30.04	540	4299	3.99
41	0.48	24.67	29.29	620	5047	3.99
42	0.49	19.96	27.83	540	4299	4.02
43	0.51	24.23	20.53	460	3551	4.05
44	0.52	16.66	26.55	480	3738	4.05
45	0.53	17.86	13.82	300	2056	4.12
46	0.54	15.89	20.36	400	2991	4.33
47	0.55	24.83	31.6	720	5981	4.37
48	0.56	17.8	23.01	480	3738	4.50

49	0.58	15.41	19.24	400	2991	4.66
50	0.59	24.1	25.32	620	5047	4.68
51	0.60	20.76	26.42	600	4860	4.69
52	0.61	25.65	18.85	500	3925	4.72
53	0.62	24.83	26.09	660	5421	4.80
54	0.64	24.59	25.09	640	5234	4.84
55	0.65	15.22	18.47	400	2991	4.89
56	0.66	16.49	29.79	620	5047	4.90
57	0.67	24.1	15.2	420	3178	4.91
58	0.68	24.52	29.16	760	6355	5.07
59	0.69	17.18	28.04	620	5047	5.09
60	0.71	18.76	20.71	500	3925	5.10
61	0.72	15.25	20.7	460	3551	5.18
62	0.73	15.88	26.47	580	4673	5.21
63	0.74	24.74	21.45	600	4860	5.24
64	0.75	24.27	21.66	600	4860	5.24
65	0.76	16.58	22.06	520	4112	5.37
66	0.78	19.08	19.42	500	3925	5.39
67	0.79	25.36	13.79	440	3364	5.57
68	0.80	24.22	26.63	760	6355	5.58
69	0.81	24.52	24.83	720	5981	5.60
70	0.82	24.57	24.71	720	5981	5.62
71	0.84	25.31	27.13	820	6916	5.82
72	0.85	16.18	23.2	580	4673	5.88
73	0.86	22.32	23.72	700	5794	5.98
74	0.87	24.8	20.11	640	5234	6.01
75	0.88	21.38	20.17	600	4860	6.04
76	0.89	20.01	22.44	640	5234	6.06
77	0.91	24.82	18.36	600	4860	6.11
78	0.92	25.37	15.12	520	4112	6.20
79	0.93	19.03	25.69	720	5981	6.22
80	0.94	26.07	23.19	840	7103	6.88
81	0.95	24.95	26.13	940	8037	7.08
82	0.96	18.17	16.78	560	4486	7.33
83	0.98	16.76	18.31	600	4860	7.61
84	0.99	25.2	21.41	860	7290	7.80
85	1.00	23.7	20.96	920	7850	8.87

.

Mean	3.9
St Dev	1.97
Median	4.05

The University of Nottingham

POINT LOAD TEST ANALYSIS						
Sample ID:			Los Bronces Cu			
Description:			Treated (T3) 2.75s, 20kW. Av RP= 10kW			
Count No.	**Spread (%)**	**Depth (mm)**	**Width (mm)**	**Breakage Load**		**Is(50)**
				Measured (lb/in²)	**Converted (N)**	
1	0.01	24.4	24.68	180	935	0.88
2	0.03	24.64	26.22	190	1028	0.91
3	0.04	24.77	24.77	200	1121	1.05
4	0.05	17.35	23.57	180	935	1.11
5	0.06	23.41	30.32	270	1776	1.40
6	0.08	23.87	33.06	300	2056	1.47
7	0.09	24.62	31.21	300	2056	1.53
8	0.10	23.95	31.25	320	2243	1.69
9	0.11	23.79	26.22	290	1963	1.77
10	0.13	23.89	28.46	310	2150	1.78
11	0.14	22.37	23.88	270	1776	1.82
12	0.15	24.52	17.91	250	1589	2.06
13	0.16	20.85	27.47	330	2336	2.16
14	0.18	18.16	30.62	340	2430	2.18
15	0.19	24.05	25.06	330	2336	2.19
16	0.20	24.58	21.14	300	2056	2.26
17	0.22	24.58	21.72	310	2150	2.30
18	0.23	18.37	23.84	300	2056	2.35
19	0.24	18.29	25.7	340	2430	2.58
20	0.25	18.18	20.23	300	2056	2.78
21	0.27	18.68	28.93	410	3084	2.88
22	0.28	23.06	21.67	360	2617	2.90
23	0.29	24.32	32.05	510	4019	2.93
24	0.30	24.53	15.36	290	1963	2.97
25	0.32	17.29	27.34	400	2991	3.08
26	0.33	25.09	22.15	400	2991	3.10
27	0.34	17.63	17.32	290	1963	3.16
28	0.35	23.75	26.6	460	3551	3.16
29	0.37	20.43	23.48	400	2991	3.27
30	0.38	24.45	19.17	370	2710	3.29
31	0.39	20.27	28.15	470	3645	3.34
32	0.41	19.58	24.35	420	3178	3.43
33	0.42	24.92	26.37	510	4019	3.51
34	0.43	24.36	18.96	390	2897	3.56
35	0.44	23.1	31.37	580	4673	3.58
36	0.46	24.49	23.97	480	3738	3.63
37	0.47	24.16	19.85	430	3271	3.86
38	0.48	17.97	23.87	440	3364	3.89
39	0.49	24.07	20.36	450	3458	3.99
40	0.51	19.02	31.06	590	4766	4.10
41	0.52	24.45	15.89	380	2804	4.11
42	0.53	24.37	26.49	580	4673	4.11
43	0.54	18.29	20.82	420	3178	4.17
44	0.56	23.1	26.14	580	4673	4.29
45	0.57	24.19	25.27	580	4673	4.33
46	0.58	17.54	20.76	440	3364	4.53
47	0.59	24.2	19.81	500	3925	4.64
48	0.61	23.62	27.24	650	5327	4.64

49	0.62	24.41	26.19	650	5327	4.74
50	0.63	24.74	24.91	630	5140	4.77
51	0.65	25.44	19.59	520	4112	4.78
52	0.66	19.69	21.29	500	3925	4.84
53	0.67	19.61	20.75	490	3832	4.85
54	0.68	19.82	21.69	520	4112	4.95
55	0.70	20.36	21.79	530	4206	4.97
56	0.71	24.71	19.45	540	4299	5.12
57	0.72	24.35	13.95	410	3084	5.16
58	0.73	24.05	31.92	830	7009	5.16
59	0.75	23.93	27.66	740	6168	5.25
60	0.76	15.49	22.05	500	3925	5.33
61	0.77	14.97	21.7	490	3832	5.38
62	0.78	24.73	13.1	410	3084	5.45
63	0.80	24.13	17.51	520	4112	5.51
64	0.81	24.41	27.77	800	6729	5.65
65	0.82	24.17	20.93	620	5047	5.65
66	0.84	14.95	26.8	620	5047	5.75
67	0.85	24.75	17.42	550	4393	5.83
68	0.86	19.75	29.61	800	6729	5.95
69	0.87	19.46	25.63	700	5794	5.97
70	0.89	24.61	20.31	670	5514	6.30
71	0.90	24.56	20.66	690	5701	6.41
72	0.91	24.39	24.41	830	7009	6.69
73	0.92	24.15	21.89	770	6449	6.91
74	0.94	24.61	20.81	750	6262	6.98
75	0.95	24.6	17.72	660	5421	7.10
76	0.96	14.2	15.6	460	3551	7.15
77	0.97	27.74	22.12	860	7290	7.16
78	0.99	22.27	14.7	540	4299	7.17
79	1.00	24.59	19.01	730	6075	7.42

.

Mean	4.0
St Dev	1.75
Median	4.10

The University of Nottingham

POINT LOAD TEST RECORD SHEET

Sample ID:	Ekati Kimberlite I
Description:	Untreated

Count No.	Spread (%)	Depth (mm)	Width (mm)	Breakage Load		Is(50)
				Measured (lb/in²)	Converted (N)	
1	0.02	13.85	15.87	80	0	0.00
2	0.04	16.85	17.14	100	187	0.31
3	0.06	13.77	16.86	100	187	0.35
4	0.07	17.58	16.06	120	374	0.65
5	0.09	14.21	16.84	140	561	1.04
6	0.11	13.27	14.46	160	748	1.68
7	0.13	16.55	17.46	320	2243	3.71
8	0.15	17.82	13.47	280	1869	3.84
9	0.17	14.02	14.86	280	1869	3.98
10	0.19	14.6	17.34	320	2243	4.00
11	0.20	18.31	18.57	380	2804	4.12
12	0.22	20.56	16.25	360	2617	4.12
13	0.24	13.97	15.08	300	2056	4.32
14	0.26	14.87	22.11	420	3178	4.40
15	0.28	17.36	15.16	340	2430	4.50
16	0.30	12.76	17.68	340	2430	4.58
17	0.31	29.02	17.75	500	3925	4.69
18	0.33	29.39	14.18	420	3178	4.71
19	0.35	13.02	19.31	380	2804	4.78
20	0.37	17.29	17.97	420	3178	4.98
21	0.39	12.76	18.67	380	2804	5.00
22	0.41	16.82	13.35	340	2430	5.21
23	0.43	18.07	14.55	380	2804	5.30
24	0.44	17.49	15.36	400	2991	5.45
25	0.46	18.4	14.9	400	2991	5.46
26	0.48	12.86	15.67	360	2617	5.54
27	0.50	17.88	18.38	480	3738	5.62
28	0.52	14.4	16.01	400	2991	5.82
29	0.54	13.88	16.29	400	2991	5.84
30	0.56	15.91	15.17	420	3178	6.18
31	0.57	17.77	16.65	480	3738	6.23
32	0.59	15.69	14.85	420	3178	6.36
33	0.61	15.75	13.07	380	2804	6.36
34	0.63	16.66	18.42	520	4112	6.42
35	0.65	16.99	13.18	400	2991	6.45
36	0.67	15.14	14.61	420	3178	6.59
37	0.69	15.19	17.96	500	3925	6.61
38	0.70	13.57	14.46	400	2991	6.66
39	0.72	15.64	13.23	400	2991	6.73
40	0.74	9.91	16.98	400	2991	6.74
41	0.76	14.42	21.54	580	4673	6.75
42	0.78	14.05	13.71	400	2991	6.89
43	0.80	23.83	10.08	400	2991	7.01
44	0.81	23.89	10.06	400	2991	7.01
45	0.83	18.7	14.49	520	4112	7.66
46	0.85	10.56	14.38	400	2991	7.68

47	0.87	13.25	15.77	480	3738	7.73
48	0.89	13.54	16.16	500	3925	7.83
49	0.91	16.74	14.58	520	4112	8.09
50	0.93	13.32	11.15	380	2804	8.18
51	0.94	19.35	14.48	560	4486	8.20
52	0.96	17.79	13.58	520	4112	8.40
53	0.98	11.63	17.77	540	4299	8.48
54	1.00	15.37	13.72	520	4112	9.01

	Mean	5.45
	Median	5.7
	St Dev	2.18

POINT LOAD TEST RECORD SHEET

Sample ID:	Ekati Kimberlite I
Description:	Treated (T1) 7.4s, 8kW

Count (No)	Spread (%)	Depth (mm)	Width (mm)	Breakage Load		Is(50)
				Measured (lb/in²)	Converted (N)	
1	0.02	13.65	20.35	80.00	0	0.00
2	0.03	13.35	14.37	80.00	0	0.00
3	0.05	13.43	16.76	80.00	0	0.00
4	0.07	16.64	20.77	80.00	0	0.00
5	0.08	17.50	20.02	80.00	0	0.00
6	0.10	19.10	14.90	80.00	0	0.00
7	0.12	10.17	11.99	80.00	0	0.00
8	0.14	14.53	14.75	100.00	187	0.39
9	0.15	17.56	13.10	100.00	187	0.40
10	0.17	14.17	16.33	140.00	561	1.08
11	0.19	15.05	14.53	140.00	561	1.17
12	0.20	17.38	13.22	140.00	561	1.19
13	0.22	15.29	14.45	160.00	748	1.56
14	0.24	17.15	13.33	200.00	1121	2.38
15	0.25	16.70	13.40	200.00	1121	2.40
16	0.27	25.32	15.08	260.00	1682	2.55
17	0.29	18.06	19.12	320.00	2243	3.23
18	0.31	19.01	16.50	300.00	2056	3.33
19	0.32	15.76	16.45	280.00	1869	3.37
20	0.34	15.02	18.23	300.00	2056	3.43
21	0.36	16.37	16.29	300.00	2056	3.66
22	0.37	35.35	16.04	420.00	3178	3.77
23	0.39	12.66	12.75	240.00	1495	3.92
24	0.41	26.96	16.36	400.00	2991	4.03
25	0.42	17.15	14.18	300.00	2056	4.10
26	0.44	11.99	18.44	320.00	2243	4.19
27	0.46	14.31	18.82	360.00	2617	4.35
28	0.47	13.27	14.51	300.00	2056	4.62
29	0.49	16.19	18.87	400.00	2991	4.63
30	0.51	14.09	15.22	320.00	2243	4.65
31	0.53	17.08	17.94	400.00	2991	4.73
32	0.54	18.24	16.89	400.00	2991	4.84
33	0.56	15.51	14.84	340.00	2430	4.90
34	0.58	7.73	16.70	280.00	1869	4.91
35	0.59	16.20	13.02	320.00	2243	5.03
36	0.61	11.52	18.30	360.00	2617	5.04
37	0.63	14.43	17.11	380.00	2804	5.10
38	0.64	15.10	17.38	400.00	2991	5.22
39	0.66	14.36	13.81	340.00	2430	5.49
40	0.68	14.30	16.90	400.00	2991	5.53
41	0.69	18.62	14.30	400.00	2991	5.66
42	0.71	16.40	16.05	420.00	3178	5.74
43	0.73	15.19	14.45	380.00	2804	5.87
44	0.75	13.99	13.94	360.00	2617	5.94
45	0.76	14.40	15.67	400.00	2991	5.94
46	0.78	14.90	16.02	420.00	3178	6.06
47	0.80	24.02	15.28	520.00	4112	6.33
48	0.81	13.53	16.00	420.00	3178	6.40

49	0.83	14.49	14.15	400.00	2991	6.56
50	0.85	16.45	18.03	540.00	4299	6.90
51	0.86	26.77	14.17	560.00	4486	7.01
52	0.88	14.99	15.18	460.00	3551	7.13
53	0.90	15.33	14.89	460.00	3551	7.18
54	0.92	15.00	16.37	500.00	3925	7.30
56	0.93	6.96	16.62	360.00	2617	7.32
57	0.95	15.06	13.18	420.00	3178	7.33
58	0.97	18.83	14.84	560.00	4486	8.12
59	0.98	17.12	13.21	500.00	3925	8.42
60	1.00	15.25	13.10	480.00	3738	8.61

Mean	4.22
Median	4.6
St Dev	2.29

The University of Nottingham

POINT LOAD TEST RECORD SHEET

Sample ID:	Ekati Kimberlite I
Description:	Treated (T2) 12.5s, 24.6kW

Count No.	Spread (%)	Depth (mm)	Width (mm)	Breakage Load		Is(50)
				Measured (lb/in²)	Converted (N)	
1	0.02	10.4	14.03	80	0	0.00
2	0.03	11.9	13.05	80	0	0.00
3	0.05	13	12.95	80	0	0.00
4	0.07	13.1	13	80	0	0.00
5	0.08	12.9	11.06	80	0	0.00
6	0.10	13.91	16.06	80	0	0.00
7	0.12	14.12	17.95	80	0	0.00
8	0.13	10.93	16.92	80	0	0.00
9	0.15	10.69	12.34	80	0	0.00
10	0.17	14.1	11.36	80	0	0.00
11	0.18	10.63	11.56	80	0	0.00
12	0.20	12.3	12.36	80	0	0.00
13	0.22	13.16	13.46	80	0	0.00
14	0.23	15.59	17.56	100	187	0.32
15	0.25	17.14	16.49	100	187	0.32
16	0.27	13.7	16.44	100	187	0.36
17	0.28	13.58	15.73	100	187	0.38
18	0.30	12.8	14.04	100	187	0.44
19	0.32	16.85	16.24	140	561	0.99
20	0.33	17.65	15.5	140	561	1.01
21	0.35	15.75	19.68	160	748	1.13
22	0.37	14.25	17.69	180	935	1.66
23	0.38	13.91	18.6	200	1121	1.91
24	0.40	15.82	19.8	300	2056	3.07
25	0.42	14.31	17.21	300	2056	3.73
26	0.43	15.87	20.28	360	2617	3.81
27	0.45	15.02	16.05	300	2056	3.90
28	0.47	13.6	17.55	340	2430	4.45
29	0.48	13.8	17.52	360	2617	4.76
30	0.50	15.41	18.74	400	2991	4.79
31	0.52	17.55	11.95	300	2056	4.81
32	0.53	16.26	14.59	340	2430	4.85
33	0.55	18.61	15.27	380	2804	4.97
34	0.57	17.14	16.92	400	2991	5.00
35	0.58	16.95	13.71	340	2430	5.05
36	0.60	14.86	18.02	400	2991	5.08
37	0.62	12.9	18.52	400	2991	5.34
38	0.63	15.37	18.51	440	3364	5.46
39	0.65	13.12	13.42	320	2243	5.48
40	0.67	15.55	19.33	460	3551	5.49
41	0.68	16.99	15.04	400	2991	5.66
42	0.70	19.95	19.23	540	4299	5.82
43	0.72	13.5	11.32	300	2056	5.86
44	0.73	14.23	17.01	440	3364	6.20
45	0.75	17.17	15.05	440	3364	6.32
46	0.77	19.13	15.05	480	3738	6.62
47	0.78	15.05	16.5	480	3738	6.89
48	0.80	18.37	19.92	620	5047	6.90

49	0.82	13.88	17.12	480	3738	6.94
50	0.83	16.31	15.11	480	3738	7.20
51	0.85	15.37	19.99	600	4860	7.31
52	0.87	12.5	17	480	3738	7.40
53	0.88	16.18	15.23	500	3925	7.53
54	0.90	17.7	13.4	480	3738	7.76
55	0.92	16.52	15.67	540	4299	7.92
56	0.93	13	19.34	580	4673	7.96
57	0.95	18.8	14.77	560	4486	8.17
58	0.97	15.36	15.15	560	4486	8.90
59	0.98	14.35	15.73	580	4673	9.27
60	1.00	19.29	15.89	740	6168	10.30
					Mean	3.92
					Median	4.8
					St Dev	3.13

The University of Nottingham

POINT LOAD TEST RECORD SHEET

Sample ID:			Ekati Kimberlite I			
Description:			Treated (T3) 17s, 12kW			
Count No.	**Spread (%)**	**Depth (mm)**	**Width (mm)**	**Breakage Load**		**Is(50)**
				Measured (lb/in²)	**Converted (N)**	
1	0.02	14.72	15.02	80	0	0.00
2	0.03	18.67	13.89	80	0	0.00
3	0.05	12.88	20.06	80	0	0.00
4	0.07	13.75	16.22	80	0	0.00
5	0.08	19.14	15.94	80	0	0.00
6	0.10	11.55	17.10	80	0	0.00
7	0.11	14.91	14.27	80	0	0.00
8	0.13	17.41	15.73	80	0	0.00
9	0.15	16.72	16.59	80	0	0.00
10	0.16	14.23	17.37	80	0	0.00
11	0.18	14.95	15.13	80	0	0.00
12	0.20	16.92	16.6	80	0	0.00
13	0.21	16.58	15.78	80	0	0.00
14	0.23	18.83	14.59	80	0	0.00
15	0.25	16.13	16.12	80	0	0.00
16	0.26	15.02	16.06	80	0	0.00
17	0.28	14.59	15.27	80	0	0.00
18	0.30	16.79	17.77	80	0	0.00
19	0.31	16.00	15.54	100	187	0.35
20	0.33	11.95	16.88	100	187	0.38
21	0.34	14.93	15.98	140	561	1.07
22	0.36	13.09	15.36	140	561	1.20
23	0.38	13.17	20.71	200	1121	1.77
24	0.39	16.80	14.29	200	1121	2.25
25	0.41	17.68	13.46	200	1121	2.32
26	0.43	16.33	13.99	200	1121	2.33
27	0.44	14.79	14.6	200	1121	2.36
28	0.46	14.50	20.99	320	2243	3.32
29	0.48	17.49	16.01	300	2056	3.59
30	0.49	17.34	18.33	340	2430	3.73
31	0.51	17.62	16.41	320	2243	3.81
32	0.52	15.37	15.12	300	2056	4.09
33	0.54	15.93	14.77	300	2056	4.10
34	0.56	18.46	12.35	280	1869	4.11
35	0.57	18.00	19.23	400	2991	4.28
36	0.59	12.22	16.91	320	2243	4.52
37	0.61	18.02	17.48	400	2991	4.71
38	0.62	13.92	13.82	300	2056	4.72
39	0.64	15.90	18.34	400	2991	4.81
40	0.66	14.64	16.92	380	2804	5.11
41	0.67	13.99	17.08	380	2804	5.20
42	0.69	13.18	18.79	400	2991	5.21
43	0.70	16.61	14.95	380	2804	5.40
44	0.72	16.32	15.60	400	2991	5.57
45	0.74	13.44	17.18	400	2991	5.63
46	0.75	14.30	16.52	400	2991	5.66
47	0.77	15.02	15.73	400	2991	5.79
48	0.79	15.87	15.04	400	2991	5.87

49	0.80	15.87	17.85	460	3551	5.87
50	0.82	14.56	17.42	460	3551	6.31
51	0.84	18.46	12.80	400	2991	6.35
52	0.85	12.04	17.10	420	3178	6.39
53	0.87	15.76	15.42	460	3551	6.83
54	0.89	13.99	15.55	440	3364	6.85
55	0.90	15.64	15.71	480	3738	7.08
56	0.92	18.22	12.14	420	3178	7.16
57	0.93	13.80	14.90	440	3364	7.20
58	0.95	14.63	14.74	460	3551	7.44
59	0.97	17.27	17.37	600	4860	7.89
60	0.98	14.62	14.89	500	3925	8.14
61	1.00	13.43	13.98	460	3551	8.22

Comments:

Mean	3.36
Median	3.8
St Dev	2.81

The University of Nottingham

POINT LOAD TEST ANALYSIS

Sample ID:	Ekati Kimberlite II
Description:	Untreated

Count No.	Spread (%)	Depth (mm)	Width (mm)	Breakage Load		Is(50)
				Measured (lb/in²)	Converted (N)	
1	0.03	13.5	21.3	100	187	0.28
2	0.05	10.5	23.1	120	374	0.60
3	0.08	17.7	24.9	140	561	0.63
4	0.11	9.9	22.2	120	374	0.64
5	0.13	14.5	25.7	140	561	0.68
6	0.16	17.8	20.1	140	561	0.77
7	0.18	17.4	20.8	150	654	0.88
8	0.21	17.7	23	160	748	0.90
9	0.24	10.7	22	140	561	0.93
10	0.26	17.8	18	150	654	1.01
11	0.29	16.2	18.1	150	654	1.06
12	0.32	15.6	22.6	170	841	1.11
13	0.34	19.8	21.4	180	935	1.14
14	0.37	15.7	21.1	170	841	1.18
15	0.39	15.1	23.1	180	935	1.23
16	0.42	19	19.2	180	935	1.30
17	0.45	10.6	23.7	170	841	1.31
18	0.47	14	19.9	170	841	1.34
19	0.50	15.4	22.1	190	1028	1.40
20	0.53	10.1	25.1	180	935	1.41
21	0.55	15.1	24.6	210	1215	1.50
22	0.58	14.6	26.5	220	1308	1.53
23	0.61	14.9	17.4	180	935	1.64
24	0.63	17.9	24.8	240	1495	1.67
25	0.66	12	28.8	230	1402	1.68
26	0.68	18	18.2	200	1121	1.70
27	0.71	18.6	22	230	1402	1.72
28	0.74	16.1	26.1	250	1589	1.78
29	0.76	11.8	24.9	220	1308	1.83
30	0.79	11	23.9	220	1308	1.98
31	0.82	12.8	19.8	210	1215	2.04
32	0.84	9.9	20.6	200	1121	2.08
33	0.87	16.2	25	280	1869	2.18
34	0.89	16.6	22	260	1682	2.20
35	0.92	17.7	17.4	240	1495	2.39
36	0.95	16.1	23.6	290	1963	2.44
37	0.97	16.4	21.1	280	1869	2.57
38	1.00	18.3	17	280	1869	3.00

Mean	1.5
Median	1.40
St Dev	0.62

The University of Nottingham

POINT LOAD TEST DATA SHEET

Sample ID:	Ekati Kimberlite II
Description:	Treated (T1) 3.5s, 23kW

Count No.	Spread (%)	Depth (mm)	Width (mm)	Breakage Load		Is(50)
				Measured (lb/in²)	Converted (N)	
1	0.03	16.1	23.4	110	280	0.35
2	0.05	15.1	25	120	374	0.45
3	0.08	17.8	20.2	120	374	0.51
4	0.11	12	22.6	120	374	0.57
5	0.13	16	22.4	140	561	0.74
6	0.16	17	24.6	160	748	0.86
7	0.18	15.9	26.6	170	841	0.93
8	0.21	13.9	22.1	150	654	0.94
9	0.24	17.8	20.9	160	748	0.99
10	0.26	15.2	20.7	160	748	1.09
11	0.29	10.3	21.8	150	654	1.12
12	0.32	12.1	27.3	180	935	1.17
13	0.34	17.6	23.6	190	1028	1.22
14	0.37	19.5	19.8	180	935	1.24
15	0.39	20.6	20.9	190	1028	1.26
16	0.42	16.7	23.1	190	1028	1.28
17	0.45	16.1	22.5	190	1028	1.34
18	0.47	20.3	18	180	935	1.34
19	0.50	13.2	22.2	180	935	1.38
20	0.53	15.4	22.2	190	1028	1.39
21	0.55	13.4	17.4	160	748	1.39
22	0.58	11.4	18.3	160	748	1.45
23	0.61	12.3	25.8	200	1121	1.48
24	0.63	13.9	22.1	190	1028	1.48
25	0.66	13.4	25.6	210	1215	1.54
26	0.68	14.5	20.4	190	1028	1.56
27	0.71	14.2	23.4	210	1215	1.63
28	0.74	12.3	20.6	190	1028	1.70
29	0.76	11.9	20.8	190	1028	1.71
30	0.79	13.6	22.6	210	1215	1.73
31	0.82	13.8	22.7	220	1308	1.84
32	0.84	21.1	21.5	250	1589	1.87
33	0.87	17.5	22.8	250	1589	1.95
34	0.89	14.7	20.2	220	1308	1.99
35	0.92	13	24.7	240	1495	1.99
36	0.95	15.9	20.5	230	1402	2.02
37	0.97	17.4	16.3	210	1215	2.09
38	1.00	15.4	22.2	250	1589	2.15

Comments:

Mean	1.36
Median	1.4
St Dev	0.47

The University of Nottingham

POINT LOAD TEST ANALYSIS

Sample ID:	Ekati Kimberlite II
Description:	Treated (T2) 7.86s, 22kW

Count No.	Spread (%)	Depth (mm)	Width (mm)	Breakage Load		Is(50)
				Measured (lb/in²)	Converted (N)	
1	0.03	16.1	15.8	110	280	0.52
2	0.05	13.8	24.8	140	561	0.72
3	0.08	13.0	20.6	140	561	0.90
4	0.11	15.0	20.3	150	654	0.98
5	0.13	12.1	22.8	150	654	0.98
6	0.16	17.5	21.6	160	748	0.97
7	0.18	16.7	20.5	160	748	1.05
8	0.21	17.4	23.3	170	841	1.01
9	0.24	20.4	24.7	180	935	0.97
10	0.26	15.0	23.2	170	841	1.10
11	0.29	17.9	18.9	170	841	1.23
12	0.32	17.3	21.5	180	935	1.22
13	0.34	11.1	18.3	160	748	1.47
14	0.37	14.2	22.7	180	935	1.29
15	0.39	13.2	23.5	180	935	1.30
16	0.42	10.5	21.6	170	841	1.44
17	0.45	20.5	21.3	200	1121	1.35
18	0.47	18.0	19.7	190	1028	1.44
19	0.50	14.7	18.7	180	935	1.54
20	0.53	12.0	27.1	200	1121	1.43
21	0.55	13.6	24.6	200	1121	1.47
22	0.58	12.1	21.5	190	1028	1.64
23	0.61	10.9	22.4	190	1028	1.67
24	0.63	9.2	20.3	180	935	1.83
25	0.66	13.9	25.7	220	1308	1.62
26	0.68	11.5	25.6	210	1215	1.67
27	0.71	15.4	21.6	210	1215	1.69
28	0.74	20.0	22.5	230	1402	1.62
29	0.76	12.8	21.1	200	1121	1.77
30	0.79	9.6	24.0	200	1121	1.82
31	0.82	11.4	21.4	220	1308	2.17
32	0.84	18.5	22.1	260	1682	2.07
33	0.87	12.3	15.8	200	1121	2.41
34	0.89	19.7	20.1	270	1776	2.32
35	0.92	15.4	19.3	250	1589	2.47
36	0.95	18.1	20.1	270	1776	2.43
37	0.97	16.3	25.8	310	2150	2.42
38	1.00	12.7	22.6	320	2243	3.31

Comments:

Mean	1.56
Median	0.6
St Dev	0.58

The University of Nottingham

POINT LOAD TEST ANALYSIS

Sample ID:	Kimberlite Type II
Description:	Treated (T3) 10s, 22kW

Count No.	Spread (%)	Depth (mm)	Width (mm)	Breakage Load		Is(50)
				Measured (lb/in²)	Converted (N)	
1	0.03	0	0	0	0	0.00
2	0.05	0	0	0	0	0.00
3	0.08	0	0	0	0	0.00
4	0.11	0	0	0	0	0.00
5	0.13	0	0	0	0	0.00
6	0.16	0	0	0	0	0.00
7	0.18	0	0	0	0	0.00
8	0.21	0	0	0	0	0.00
9	0.24	15.8	18.8	100	187	0.29
10	0.26	18.9	21.4	130	467	0.59
11	0.29	16.9	19.4	130	467	0.69
12	0.32	10.7	23.4	130	467	0.73
13	0.34	8.3	25.2	130	467	0.78
14	0.37	15.3	24.6	150	654	0.80
15	0.39	11.3	24.3	140	561	0.82
16	0.42	15.1	19.5	140	561	0.87
17	0.45	15.4	21.4	160	748	1.05
18	0.47	12.6	22.6	160	748	1.11
19	0.50	9.3	25.9	160	748	1.14
20	0.53	12.8	24	170	841	1.16
21	0.55	12.5	25.4	180	935	1.24
22	0.58	16.7	19.4	170	841	1.24
23	0.61	16.9	20.3	180	935	1.31
24	0.63	18.6	24.1	210	1215	1.36
25	0.66	9.7	15.9	140	561	1.37
26	0.68	15	19.1	180	935	1.49
27	0.71	16.7	26.4	230	1402	1.52
28	0.74	15.5	21.4	200	1121	1.57
29	0.76	15.7	18.4	190	1028	1.66
30	0.79	19	21.2	230	1402	1.77
31	0.82	13.2	22.7	220	1308	1.88
32	0.84	16.9	22.4	250	1589	2.02
33	0.87	10.2	27.3	240	1495	2.06
34	0.89	11.5	27.5	260	1682	2.16
35	0.92	15.1	23.3	280	1869	2.43
36	0.95	11.2	22.1	250	1589	2.57
37	0.97	13.4	24.1	300	2056	2.76
38	1.00	15.9	14.5	240	1495	3.04

Mean	1.15
Median	1.2
St Dev	0.85

The University of Nottingham

PUNDIT TEST RECORD SHEET							
Sample ID:		Nebo Babel Ni-Cu T1					
Description:		Treated 0.25s, 13.3kW					**Reduction in Relative UPV**
Particle ID	**Location ID**	**Depth (mm)**	**Transit Time (µs)**				
			Untreated	**Treated**	**Count**	**Spread (%)**	**%**
2	1	23.91	3.80	3.80	1	0.40	0.0
	2	23.84	4.00	4.00	2	0.80	0.0
	3	23.94	4.15	4.15	3	1.20	0.0
	4	23.82	3.90	3.90	4	1.61	0.0
3	1	18.28	2.70	2.70	5	2.01	0.0
	2	18.67	3.10	3.10	6	2.41	0.0
	3	18.83	2.85	2.85	7	2.81	0.0
5	1	22.84	3.95	3.95	8	3.21	0.0
	2	22.84	4.05	4.05	9	3.61	0.0
	3	24.03	3.85	3.85	10	4.02	0.0
7	1	14.80	2.40	2.40	11	4.42	0.0
	2	15.17	2.60	2.60	12	4.82	0.0
9	1	22.73	3.75	3.75	13	5.22	0.0
	2	22.82	3.70	3.70	14	5.62	0.0
	3	22.82	3.55	3.55	15	6.02	0.0
	4	14.91	2.65	2.65	16	6.43	0.0
	3	14.40	2.55	2.55	17	6.83	0.0
	4	13.81	2.45	2.45	18	7.23	0.0
	2	23.80	3.85	3.85	19	7.63	0.0
16	1	16.21	2.65	2.65	20	8.03	0.0
	2	16.28	2.65	2.65	21	8.43	0.0
	3	16.12	2.65	2.65	22	8.84	0.0
	4	16.02	2.70	2.70	23	9.24	0.0
17	1	18.66	3.15	3.15	24	9.64	0.0
	2	18.74	3.20	3.20	25	10.04	0.0
	2	16.20	3.05	3.05	26	10.44	0.0
19	1	18.50	3.20	3.20	27	10.84	0.0
	2	18.58	3.20	3.20	28	11.24	0.0
21	1	19.00	3.15	3.15	29	11.65	0.0
	2	23.25	3.80	3.80	30	12.05	0.0
25	1	13.35	2.15	2.15	31	12.45	0.0
	2	13.20	2.25	2.25	32	12.85	0.0
	3	14.10	2.20	2.20	33	13.25	0.0
28	1	19.36	4.10	4.10	34	13.65	0.0
	2	19.61	3.90	3.90	35	14.06	0.0
29	1	17.34	2.90	2.90	36	14.46	0.0
30	1	23.02	3.85	3.85	37	14.86	0.0
32	1	15.36	2.95	2.95	38	15.26	0.0
	2	15.80	3.00	3.00	39	15.66	0.0
	4	15.76	3.00	3.00	40	16.06	0.0
33	1	17.97	3.20	3.20	41	16.47	0.0
	2	14.49	3.00	3.00	42	16.87	0.0
	3	14.64	3.40	3.40	43	17.27	0.0
35	1	22.77	3.50	3.50	44	17.67	0.0
36	1	23.86	3.70	3.70	45	18.07	0.0
	2	23.94	3.75	3.75	46	18.47	0.0
38	1	18.06	3.20	3.20	47	18.88	0.0
	2	17.42	2.85	2.85	48	19.28	0.0

39	1	22.88	4.40	4.40	49	19.68	0.0
	2	23.05	4.30	4.30	50	20.08	0.0
	2	23.44	4.90	4.90	51	20.48	0.0
	3	23.78	4.75	4.75	52	20.88	0.0
41	1	16.50	2.60	2.60	53	21.29	0.0
	2	17.11	2.65	2.65	54	21.69	0.0
43	1	23.04	4.30	4.30	55	22.09	0.0
45	1	13.47	2.10	2.10	56	22.49	0.0
	2	13.68	2.10	2.10	57	22.89	0.0
	3	14.16	2.20	2.20	58	23.29	0.0
	3	19.50	4.00	4.00	59	23.69	0.0
49	1	23.42	3.80	3.80	60	24.10	0.0
	2	23.28	3.65	3.65	61	24.50	0.0
50	1	13.65	2.30	2.30	62	24.90	0.0
	2	13.40	2.30	2.30	63	25.30	0.0
	3	13.82	2.30	2.30	64	25.70	0.0
	4	13.51	2.25	2.25	65	26.10	0.0
51	1	23.12	4.20	4.20	66	26.51	0.0
	2	23.21	4.20	4.20	67	26.91	0.0
	3	23.28	4.25	4.25	68	27.31	0.0
	4	23.61	4.20	4.20	69	27.71	0.0
	2	18.02	3.00	3.00	70	28.11	0.0
	3	17.91	2.95	2.95	71	28.51	0.0
	2	19.09	3.55	3.55	72	28.92	0.0
55	1	15.30	2.75	2.75	73	29.32	0.0
	2	15.79	2.80	2.80	74	29.72	0.0
	3	15.50	2.60	2.60	75	30.12	0.0
	4	15.70	2.65	2.65	76	30.52	0.0
	3	20.13	4.80	4.80	77	30.92	0.0
62	1	14.55	2.50	2.50	78	31.33	0.0
	2	14.54	2.45	2.45	79	31.73	0.0
65	1	16.34	3.05	3.05	80	32.13	0.0
	2	16.71	3.00	3.00	81	32.53	0.0
	4	16.81	3.10	3.10	82	32.93	0.0
66	1	15.21	2.50	2.50	83	33.33	0.0
67	1	21.87	5.05	5.05	84	33.73	0.0
69	1	17.62	5.40	5.40	85	34.14	0.0
	2	17.12	5.15	5.15	86	34.54	0.0
	2	23.53	7.25	7.25	87	34.94	0.0
71	1	14.44	2.90	2.90	88	35.34	0.0
	2	14.22	2.75	2.75	89	35.74	0.0
	2	23.84	4.15	4.15	90	36.14	0.0
	2	24.65	5.85	5.85	91	36.55	0.0
	3	24.68	5.55	5.55	92	36.95	0.0
74	1	15.19	2.55	2.55	93	37.35	0.0
	2	15.39	2.75	2.75	94	37.75	0.0
	3	14.85	2.55	2.55	95	38.15	0.0
	4	15.02	2.65	2.65	96	38.55	0.0
79	1	19.88	3.60	3.60	97	38.96	0.0
	2	19.68	3.65	3.65	98	39.36	0.0
80	1	16.31	2.90	2.90	99	39.76	0.0
	2	15.94	3.00	3.00	100	40.16	0.0
	3	16.45	2.90	2.90	101	40.56	0.0
81	1	22.50	5.00	5.00	102	40.96	0.0
	2	22.38	3.80	3.80	103	41.37	0.0
82	1	13.13	2.55	2.55	104	41.77	0.0
	2	12.97	2.70	2.70	105	42.17	0.0

83	1	11.73	2.75	2.75	106	42.57	0.0
	2	12.30	2.75	2.75	107	42.97	0.0
	3	11.74	2.80	2.80	108	43.37	0.0
	4	12.34	2.85	2.85	109	43.78	0.0
84	1	23.71	3.75	3.75	110	44.18	0.0
	2	23.83	3.85	3.85	111	44.58	0.0
	3	16.48	3.00	3.00	112	44.98	0.0
	4	16.59	3.00	3.00	113	45.38	0.0
86	1	18.17	2.85	2.85	114	45.78	0.0
	2	18.67	3.10	3.10	115	46.18	0.0
87	1	23.89	3.95	3.95	116	46.59	0.0
	2	23.90	3.95	3.95	117	46.99	0.0
90	1	16.02	3.30	3.30	118	47.39	0.0
	2	16.02	3.15	3.15	119	47.79	0.0
	3	15.92	3.35	3.35	120	48.19	0.0
	4	16.01	3.35	3.35	121	48.59	0.0
93	1	19.43	3.30	3.30	122	49.00	0.0
	2	19.43	3.30	3.30	123	49.40	0.0
	2	23.50	3.95	3.95	124	49.80	0.0
	2	13.28	3.40	3.40	125	50.20	0.0
	3	13.28	3.60	3.60	126	50.60	0.0
	3	22.01	5.00	5.05	127	51.00	1.0
40	1	23.55	4.95	5.00	128	51.41	1.0
	2	25.79	4.50	4.55	129	51.81	1.1
	2	19.74	4.35	4.40	130	52.21	1.1
64	1	25.05	4.35	4.40	131	52.61	1.1
	3	23.13	4.35	4.40	132	53.01	1.1
57	1	20.18	4.15	4.20	133	53.41	1.2
	2	23.24	3.95	4.00	134	53.82	1.3
	2	23.73	3.95	4.00	135	54.22	1.3
47	1	23.79	3.90	3.95	136	54.62	1.3
23	1	23.42	3.85	3.90	137	55.02	1.3
61	1	24.03	3.85	3.90	138	55.42	1.3
4	1	23.13	3.65	3.70	139	55.82	1.4
1	1	22.95	3.55	3.60	140	56.22	1.4
	2	22.67	3.55	3.60	141	56.63	1.4
34	1	14.44	3.15	3.20	142	57.03	1.6
	2	17.79	3.05	3.10	143	57.43	1.6
	3	16.51	2.95	3.00	144	57.83	1.7
	3	14.45	2.95	3.00	145	58.23	1.7
	3	16.30	2.90	2.95	146	58.63	1.7
85	1	16.49	2.85	2.90	147	59.04	1.8
	2	16.64	2.85	2.90	148	59.44	1.8
58	1	15.10	2.75	2.80	149	59.84	1.8
26	1	17.77	8.20	8.35	150	60.24	1.8
	3	14.60	2.70	2.75	151	60.64	1.9
12	1	22.68	5.20	5.30	152	61.04	1.9
70	1	23.52	7.40	7.55	153	61.45	2.0
	2	22.51	4.85	4.95	154	61.85	2.1
77	1	17.91	4.60	4.70	155	62.25	2.2
	4	14.14	2.25	2.30	156	62.65	2.2
	4	13.94	2.20	2.25	157	63.05	2.3
	2	20.30	4.30	4.40	158	63.45	2.3
	2	23.97	4.30	4.40	159	63.86	2.3
	3	23.08	4.20	4.30	160	64.26	2.4
88	1	23.80	4.05	4.15	161	64.66	2.5
	2	24.10	4.00	4.10	162	65.06	2.5

	4	22.94	4.00	4.10	163	65.46	2.5
	2	17.81	4.00	4.10	164	65.86	2.5
6	1	24.03	3.90	4.00	165	66.27	2.6
73	1	24.66	5.85	6.00	166	66.67	2.6
95	1	23.62	3.90	4.00	167	67.07	2.6
	2	23.80	3.85	3.95	168	67.47	2.6
	2	22.93	3.60	3.70	169	67.87	2.8
8	1	16.42	3.60	3.70	170	68.27	2.8
68	1	22.75	3.55	3.65	171	68.67	2.8
54	1	19.25	3.45	3.55	172	69.08	2.9
	3	22.30	5.00	5.15	173	69.48	3.0
	2	19.06	3.20	3.30	174	69.88	3.1
	2	17.45	3.05	3.15	175	70.28	3.3
52	1	17.76	3.00	3.10	176	70.68	3.3
	2	22.99	4.20	4.35	177	71.08	3.6
	4	14.31	2.80	2.90	178	71.49	3.6
72	1	23.89	4.15	4.30	179	71.89	3.6
	2	21.92	5.45	5.65	180	72.29	3.7
	4	14.74	2.65	2.75	181	72.69	3.8
	2	23.17	3.95	4.10	182	73.09	3.8
44	1	24.19	6.55	6.80	183	73.49	3.8
	2	13.63	2.60	2.70	184	73.90	3.8
	2	13.52	2.60	2.70	185	74.30	3.8
	2	13.57	2.55	2.65	186	74.70	3.9
	3	23.20	3.75	3.90	187	75.10	4.0
	4	23.16	3.75	3.90	188	75.50	4.0
11	1	14.24	2.50	2.60	189	75.90	4.0
	2	22.67	3.65	3.80	190	76.31	4.1
75	1	13.03	2.30	2.40	191	76.71	4.3
46	1	20.33	4.50	4.70	192	77.11	4.4
37	1	13.37	2.20	2.30	193	77.51	4.5
98	1	12.87	3.30	3.45	194	77.91	4.5
96	1	13.96	3.25	3.40	195	78.31	4.6
24	1	24.72	7.55	7.90	196	78.71	4.6
60	1	23.83	4.10	4.30	197	79.12	4.9
91	1	23.51	6.95	7.30	198	79.52	5.0
	2	18.72	2.95	3.10	199	79.92	5.1
	3	24.08	3.80	4.00	200	80.32	5.3
	3	16.52	3.55	3.75	201	80.72	5.6
76	1	14.52	2.65	2.80	202	81.12	5.7
	2	14.65	2.65	2.80	203	81.53	5.7
	2	23.62	7.00	7.40	204	81.93	5.7
	2	14.03	2.55	2.70	205	82.33	5.9
	2	16.66	4.05	4.30	206	82.73	6.2
15	1	23.50	4.00	4.25	207	83.13	6.3
	4	16.51	3.20	3.40	208	83.53	6.3
94	1	16.64	3.95	4.20	209	83.94	6.3
	2	23.32	3.85	4.10	210	84.34	6.5
	2	23.97	3.80	4.05	211	84.74	6.6
	2	23.22	3.60	3.85	212	85.14	6.9
63	1	23.99	14.00	15.00	213	85.54	7.1
	2	24.23	6.80	7.30	214	85.94	7.4
	2	25.08	7.45	8.00	215	86.35	7.4
22	1	13.94	2.60	2.80	216	86.75	7.7
59	1	24.26	3.90	4.20	217	87.15	7.7
	3	16.25	3.15	3.40	218	87.55	7.9
56	1	23.89	3.70	4.00	219	87.95	8.1

31	1	23.31	3.60	3.90	220	88.35	8.3
	2	24.61	5.10	5.55	221	88.76	8.8
20	1	14.17	2.55	2.80	222	89.16	9.8
	2	16.40	3.55	3.90	223	89.56	9.9
53	1	23.45	3.75	4.15	224	89.96	10.7
	4	13.37	2.45	2.75	225	90.36	12.2
	2	23.03	4.45	5.05	226	90.76	13.5
18	1	16.06	2.95	3.35	227	91.16	13.6
27	1	24.39	5.05	5.75	228	91.57	13.9
	3	13.99	2.40	2.75	229	91.97	14.6
89	1	22.92	4.35	5.00	230	92.37	14.9
	3	13.92	2.45	2.85	231	92.77	16.3
	2	24.17	4.00	4.70	232	93.17	17.5
97	1	19.25	3.10	3.70	233	93.57	19.4
	3	16.49	2.75	3.30	234	93.98	20.0
	2	22.85	3.75	4.60	235	94.38	22.7
	2	22.10	4.20	5.25	236	94.78	25.0
42	1	17.72	2.90	3.65	237	95.18	25.9
	2	17.07	2.80	3.55	238	95.58	26.8
10	1	15.28	2.70	3.45	239	95.98	27.8
	3	22.82	3.75	4.85	240	96.39	29.3
	4	17.17	2.80	3.65	241	96.79	30.4
14	1	16.40	2.95	3.90	242	97.19	32.2
	2	24.26	3.85	5.20	243	97.59	35.1
13	1	24.13	3.85	5.30	244	97.99	37.7
92	1	22.77	3.80	5.45	245	98.39	43.4
	2	14.52	2.50	3.75	246	98.80	50.0
	2	23.05	3.90	6.00	247	99.20	53.8
48	1	22.00	4.25	6.65	248	99.60	56.5
78	1	22.79	3.80	6.45	249	100.00	69.7
Mean		19.14	3.62	3.78			4.41
Std Dev		4.03	1.25	1.36			9.78
Median		18.70	3.55	3.63			0.00
Minimum		11.73	2.10	2.10			0.00
Maximum		25.79	14.00	15.00			69.74
The University of Nottingham				School of Chemical & Environmental Engineering			

PUNDIT TEST RECORD SHEET							
Sample ID:		Nebo Babel Ni-Cu T2					
Description:		Treated 0.25s, 18.5kW					**Reduction in**
Particle ID	**Location ID**	**Depth (mm)**	**Transit Time (µs)**				**Relative UPV**
			Untreated	**Treated**	**Count**	**Spread**	**(%)**
2x	2	16.61	2.90	2.80	1	0.4	0.0
	2	14.04	2.55	2.55	2	0.8	0.0
	4	13.98	2.40	2.40	3	1.1	0.0
	2	15.28	2.65	2.65	4	1.5	0.0
	3	15.51	2.70	2.70	5	1.9	0.0
3	1	18.05	2.95	2.95	6	2.3	0.0
	2	23.19	3.65	3.65	7	2.7	0.0
5	1	22.91	3.75	3.75	8	3.0	0.0
6	1	21.07	5.05	5.05	9	3.4	0.0
7	1	16.65	3.00	3.00	10	3.8	0.0
8	1	18.15	3.05	3.05	11	4.2	0.0
9	1	21.41	3.55	3.55	12	4.5	0.0
	2	21.46	3.60	3.60	13	4.9	0.0
12	1	22.63	5.30	5.30	14	5.3	0.0
	2	20.52	3.35	3.35	15	5.7	0.0
18	1	17.19	3.65	3.65	16	6.1	0.0
20	1	14.99	2.65	2.65	17	6.4	0.0
	3	14.97	2.60	2.60	18	6.8	0.0
	2	23.38	4.95	4.95	19	7.2	0.0
	2	22.83	4.05	4.05	20	7.6	0.0
26	1	15.27	2.80	2.80	21	8.0	0.0
	2	15.22	2.85	2.85	22	8.3	0.0
	3	14.79	2.75	2.75	23	8.7	0.0
	4	14.87	2.75	2.75	24	9.1	0.0
	4	13.21	2.70	2.70	25	9.5	0.0
	2	13.63	2.30	2.30	26	9.8	0.0
30	1	13.58	2.40	2.40	27	10.2	0.0
	2	13.57	2.65	2.65	28	10.6	0.0
	3	13.33	2.50	2.50	29	11.0	0.0
	4	13.52	2.65	2.65	30	11.4	0.0
32	1	17.58	3.50	3.50	31	11.7	0.0
	3	14.02	2.35	2.35	32	12.1	0.0
	3	12.35	3.05	3.05	33	12.5	0.0
	4	12.76	3.05	3.05	34	12.9	0.0
35	1	24.72	4.00	4.00	35	13.3	0.0
36	1	17.78	2.80	2.80	36	13.6	0.0
	2	17.57	2.80	2.80	37	14.0	0.0
	2	22.90	3.65	3.65	38	14.4	0.0
	3	22.76	3.60	3.60	39	14.8	0.0
39	1	18.76	3.10	3.10	40	15.2	0.0
	2	18.90	3.20	3.20	41	15.5	0.0
40	1	19.19	3.65	3.65	42	15.9	0.0
	2	19.52	3.85	3.85	43	16.3	0.0
41	1	15.74	3.40	3.40	44	16.7	0.0
	3	15.78	3.45	3.45	45	17.0	0.0
	2	17.23	3.35	3.35	46	17.4	0.0
	3	23.40	3.85	3.85	47	17.8	0.0
48	1	14.21	2.55	2.55	48	18.2	0.0

	4	13.49	2.45	2.45	49	18.6	0.0
	2	14.56	2.45	2.45	50	18.9	0.0
50	1	13.73	2.35	2.35	51	19.3	0.0
	2	13.61	2.25	2.25	52	19.7	0.0
	3	13.85	2.35	2.35	53	20.1	0.0
	4	13.70	2.30	2.30	54	20.5	0.0
	4	13.25	3.10	3.10	55	20.8	0.0
	3	12.63	2.15	2.15	56	21.2	0.0
	4	12.81	2.25	2.25	57	21.6	0.0
53	1	14.59	2.40	2.40	58	22.0	0.0
	2	15.35	2.65	2.65	59	22.3	0.0
57	1	15.54	2.90	2.90	60	22.7	0.0
58	1	15.18	2.50	2.50	61	23.1	0.0
59	1	14.49	2.45	2.45	62	23.5	0.0
	3	13.76	2.30	2.30	63	23.9	0.0
	4	13.83	2.35	2.35	64	24.2	0.0
60	1	15.10	2.60	2.60	65	24.6	0.0
	2	14.71	2.50	2.50	66	25.0	0.0
	4	14.76	2.50	2.50	67	25.4	0.0
	2	24.41	5.80	5.80	68	25.8	0.0
63	1	22.30	5.35	5.35	69	26.1	0.0
66	1	22.49	3.85	3.85	70	26.5	0.0
	2	22.48	3.95	3.95	71	26.9	0.0
	3	22.43	3.95	3.95	72	27.3	0.0
67	1	22.27	3.45	3.45	73	27.7	0.0
	2	22.17	3.45	3.45	74	28.0	0.0
68	1	22.16	3.80	3.80	75	28.4	0.0
	2	22.29	3.75	3.75	76	28.8	0.0
69	1	22.44	4.45	4.45	77	29.2	0.0
	2	22.56	4.35	4.35	78	29.5	0.0
70	1	19.42	4.15	4.15	79	29.9	0.0
	2	15.91	2.70	2.70	80	30.3	0.0
	4	15.68	2.70	2.70	81	30.7	0.0
72	1	22.34	3.45	3.45	82	31.1	0.0
	2	22.44	3.40	3.40	83	31.4	0.0
	3	22.65	3.45	3.45	84	31.8	0.0
73	1	14.38	3.00	3.00	85	32.2	0.0
	2	14.49	2.95	2.95	86	32.6	0.0
	3	14.43	2.90	2.90	87	33.0	0.0
	2	13.40	2.25	2.25	88	33.3	0.0
76	1	18.93	3.35	3.35	89	33.7	0.0
	2	18.92	3.25	3.25	90	34.1	0.0
	2	17.10	2.95	2.95	91	34.5	0.0
	4	16.75	2.95	2.95	92	34.8	0.0
83	1	11.57	2.00	2.00	93	35.2	0.0
	2	11.56	2.05	2.05	94	35.6	0.0
	3	11.72	2.00	2.00	95	36.0	0.0
	4	11.61	2.05	2.05	96	36.4	0.0
84	1	11.98	2.05	2.05	97	36.7	0.0
85	1	12.35	2.15	2.15	98	37.1	0.0
	2	23.90	4.10	4.10	99	37.5	0.0
	2	18.00	3.00	3.00	100	37.9	0.0
90	1	19.77	3.30	3.30	101	38.3	0.0
	2	19.61	3.25	3.25	102	38.6	0.0
91	1	13.00	2.85	2.85	103	39.0	0.0
	2	12.91	2.95	2.95	104	39.4	0.0
	3	13.54	2.25	2.25	105	39.8	0.0

	4	13.69	2.40	2.40	106	40.2	0.0
	4	13.15	2.50	2.50	107	40.5	0.0
94	1	14.53	2.40	2.40	108	40.9	0.0
	2	15.02	2.50	2.50	109	41.3	0.0
96	1	18.83	3.05	3.05	110	41.7	0.0
	2	18.72	3.00	3.00	111	42.0	0.0
61	1	24.68	6.15	6.20	112	42.4	0.8
	2	14.73	4.50	4.55	113	42.8	1.1
	2	18.58	4.45	4.50	114	43.2	1.1
	2	21.41	4.20	4.25	115	43.6	1.2
	2	19.41	4.20	4.25	116	43.9	1.2
	2	24.82	4.05	4.10	117	44.3	1.2
86	1	23.74	4.00	4.05	118	44.7	1.3
	2	22.36	3.80	3.85	119	45.1	1.3
	2	23.19	3.80	3.85	120	45.5	1.3
	3	22.62	3.75	3.80	121	45.8	1.3
	2	16.71	3.75	3.80	122	46.2	1.3
4	1	22.94	3.65	3.70	123	46.6	1.4
25	1	23.03	3.55	3.60	124	47.0	1.4
	2	23.05	3.55	3.60	125	47.3	1.4
	2	15.68	3.50	3.55	126	47.7	1.4
	4	15.59	3.45	3.50	127	48.1	1.4
44	1	16.63	3.15	3.20	128	48.5	1.6
	3	13.73	3.15	3.20	129	48.9	1.6
65	1	14.60	3.10	3.15	130	49.2	1.6
51	1	13.48	3.05	3.10	131	49.6	1.6
	2	13.06	3.05	3.10	132	50.0	1.6
	4	14.68	3.05	3.10	133	50.4	1.6
	2	15.68	3.00	3.05	134	50.8	1.7
	4	15.65	3.00	3.05	135	51.1	1.7
	2	17.56	3.00	3.05	136	51.5	1.7
	4	12.71	3.00	3.05	137	51.9	1.7
	3	15.38	2.95	3.00	138	52.3	1.7
62	1	17.47	2.90	2.95	139	52.7	1.7
89	1	17.85	2.90	2.95	140	53.0	1.7
	3	15.54	2.85	2.90	141	53.4	1.8
	2	22.42	5.55	5.65	142	53.8	1.8
	2	21.22	5.50	5.60	143	54.2	1.8
81	1	12.19	2.75	2.80	144	54.5	1.8
2	1	15.49	2.70	2.75	145	54.9	1.9
	2	22.73	5.30	5.40	146	55.3	1.9
	2	14.83	2.65	2.70	147	55.7	1.9
	2	13.34	2.65	2.70	148	56.1	1.9
34	1	11.91	2.65	2.70	149	56.4	1.9
	3	15.17	2.65	2.70	150	56.8	1.9
	4	14.65	2.55	2.60	151	57.2	2.0
	3	14.49	2.55	2.60	152	57.6	2.0
11	1	14.85	2.50	2.55	153	58.0	2.0
	2	14.20	2.50	2.55	154	58.3	2.0
	4	14.33	2.50	2.55	155	58.7	2.0
	2	13.85	2.40	2.45	156	59.1	2.1
	2	14.41	2.40	2.45	157	59.5	2.1
	3	14.81	2.35	2.40	158	59.8	2.1
	4	13.93	2.35	2.40	159	60.2	2.1
92	1	13.64	2.35	2.40	160	60.6	2.1
29	1	13.93	2.25	2.30	161	61.0	2.2
	3	13.74	2.25	2.30	162	61.4	2.2

74	1	13.46	2.25	2.30	163	61.7	2.2
	3	13.25	2.25	2.30	164	62.1	2.2
80	1	18.80	4.50	4.60	165	62.5	2.2
	4	13.25	2.20	2.25	166	62.9	2.3
31	1	21.65	4.25	4.35	167	63.3	2.4
	3	21.35	4.25	4.35	168	63.6	2.4
	3	19.53	4.25	4.35	169	64.0	2.4
	3	12.12	2.00	2.05	170	64.4	2.5
	4	23.32	3.85	3.95	171	64.8	2.6
	2	22.51	3.75	3.85	172	65.2	2.7
55	1	23.61	3.75	3.85	173	65.5	2.7
	2	21.90	3.75	3.85	174	65.9	2.7
	2	17.65	3.55	3.65	175	66.3	2.8
22	1	23.12	4.95	5.10	176	66.7	3.0
13	1	20.13	3.25	3.35	177	67.0	3.1
15	1	20.02	3.10	3.20	178	67.4	3.2
82	1	14.45	4.65	4.80	179	67.8	3.2
77	1	17.20	3.00	3.10	180	68.2	3.3
	2	17.54	2.95	3.05	181	68.6	3.4
	2	12.49	2.95	3.05	182	68.9	3.4
	3	16.89	2.85	2.95	183	69.3	3.5
	3	14.32	2.70	2.80	184	69.7	3.7
71	1	15.82	2.70	2.80	185	70.1	3.7
88	1	21.93	3.95	4.10	186	70.5	3.8
17	1	23.10	7.80	8.10	187	70.8	3.8
28	1	23.63	3.90	4.05	188	71.2	3.8
	2	23.22	3.90	4.05	189	71.6	3.8
	3	13.83	2.50	2.60	190	72.0	4.0
47	1	23.09	3.70	3.85	191	72.3	4.1
	4	14.51	2.45	2.55	192	72.7	4.1
	2	12.94	2.35	2.45	193	73.1	4.3
14	1	13.41	2.30	2.40	194	73.5	4.3
33	1	14.14	2.30	2.40	195	73.9	4.3
	3	23.19	4.55	4.75	196	74.2	4.4
54	1	18.53	8.90	9.30	197	74.6	4.5
	4	13.48	2.20	2.30	198	75.0	4.5
	3	12.44	2.15	2.25	199	75.4	4.7
	2	23.41	6.25	6.55	200	75.8	4.8
	2	18.25	2.95	3.10	201	76.1	5.1
	3	22.55	3.80	4.00	202	76.5	5.3
	3	12.70	2.80	2.95	203	76.9	5.4
1	1	14.37	2.70	2.85	204	77.3	5.6
38	1	22.67	3.60	3.80	205	77.7	5.6
27	1	12.96	2.65	2.80	206	78.0	5.7
64	1	23.29	6.15	6.50	207	78.4	5.7
	3	24.82	4.15	4.40	208	78.8	6.0
	4	14.16	2.45	2.60	209	79.2	6.1
49	1	15.21	2.45	2.60	210	79.5	6.1
	2	17.84	3.25	3.45	211	79.9	6.2
	4	21.09	4.05	4.30	212	80.3	6.2
	2	16.78	3.20	3.40	213	80.7	6.3
	2	17.56	3.15	3.35	214	81.1	6.3
	2	23.30	4.55	4.85	215	81.4	6.6
45	1	17.48	3.00	3.20	216	81.8	6.7
	2	13.23	2.20	2.35	217	82.2	6.8
	2	23.21	7.95	8.50	218	82.6	6.9
	4	12.27	2.15	2.30	219	83.0	7.0

	2	12.86	2.10	2.25	220	83.3	7.1
52	1	12.10	2.05	2.20	221	83.7	7.3
24	1	22.88	3.90	4.20	222	84.1	7.7
	3	15.17	2.50	2.70	223	84.5	8.0
87	1	23.24	4.15	4.50	224	84.8	8.4
	3	13.53	2.30	2.50	225	85.2	8.7
	2	23.80	3.95	4.30	226	85.6	8.9
	2	12.40	2.15	2.35	227	86.0	9.3
	2	14.61	2.65	2.90	228	86.4	9.4
	3	25.72	4.15	4.55	229	86.7	9.6
	2	22.77	4.65	5.10	230	87.1	9.7
79	1	22.68	4.60	5.05	231	87.5	9.8
	3	23.68	3.95	4.35	232	87.9	10.1
	3	11.76	1.95	2.15	233	88.3	10.3
	2	12.36	1.90	2.10	234	88.6	10.5
93	1	13.18	2.30	2.55	235	89.0	10.9
46	1	12.85	2.25	2.50	236	89.4	11.1
	2	23.50	3.75	4.20	237	89.8	12.0
	2	14.28	2.45	2.75	238	90.2	12.2
19	1	13.77	2.45	2.75	239	90.5	12.2
10	1	23.63	3.95	4.45	240	90.9	12.7
	2	21.53	3.65	4.15	241	91.3	13.7
78	1	23.39	4.00	4.55	242	91.7	13.8
	2	24.58	4.20	4.80	243	92.0	14.3
	3	16.32	3.15	3.60	244	92.4	14.3
	2	25.53	4.15	4.80	245	92.8	15.7
21	1	16.81	2.85	3.30	246	93.2	15.8
	2	18.57	8.30	9.65	247	93.6	16.3
	2	13.87	2.45	2.85	248	93.9	16.3
	4	12.64	2.10	2.45	249	94.3	16.7
43	1	16.56	3.05	3.60	250	94.7	18.0
23	1	21.55	3.65	4.35	251	95.1	19.2
	4	16.48	3.20	3.85	252	95.5	20.3
	4	12.47	2.20	2.65	253	95.8	20.5
	3	12.82	2.75	3.35	254	96.2	21.8
56	1	24.53	4.10	5.00	255	96.6	22.0
95	1	15.50	2.45	3.00	256	97.0	22.4
37	1	14.80	2.60	3.20	257	97.3	23.1
	2	15.76	2.60	3.20	258	97.7	23.1
75	1	25.98	4.10	5.20	259	98.1	26.8
	2	23.70	4.00	5.10	260	98.5	27.5
	4	24.72	4.15	5.30	261	98.9	27.7
	2	12.77	2.25	2.90	262	99.2	28.9
16	1	17.75	3.15	4.20	263	99.6	33.3
42	1	22.13	3.85	5.40	264	100.0	40.3
Mean		17.47	3.25	3.39			4.0
Std Dev		4.12	1.05	1.15			6.5
Median		15.87	3.00	3.05			1.6
Minimum		11.56	1.90	2.00			0.0
Maximum		25.98	8.90	9.65			40.3

The University of Nottingham

PUNDIT TEST RECORD SHEET							
Sample ID:		Nebo Babel Ni-Cu T3					
Description:		Treated 1.1s, 20kW					**Reduction in Relative UPV**
Particle ID	**Location ID**	**Depth (mm)**	**Transit Time (µs)**				
			Untreated	**Treated**	**Count**	**Spread**	**(%)**
		13.11	2.30	2.30	1	0.39	0.0
1	1	12.74	2.25	2.25	2	0.77	0.0
	2	13.08	2.25	2.25	3	1.16	0.0
	3	12.62	2.15	2.15	4	1.54	0.0
	4	19.74	3.55	3.55	5	1.93	0.0
2	1	18.74	3.35	3.35	6	2.32	0.0
	2	22.47	3.75	3.75	7	2.70	0.0
3	1	19.63	3.35	3.35	8	3.09	0.0
	2	19.91	3.30	3.30	9	3.47	0.0
4	1	19.66	3.20	3.20	10	3.86	0.0
	2	13.11	2.30	2.30	11	4.25	0.0
5	1	12.98	2.15	2.15	12	4.63	0.0
	2	16.24	3.55	3.55	13	5.02	0.0
6	1	16.51	3.40	3.40	14	5.41	0.0
	2	13.90	2.30	2.30	15	5.79	0.0
	3	12.22	2.00	2.00	16	6.18	0.0
7	1	13.38	2.20	2.20	17	6.56	0.0
	2	23.96	4.65	4.70	18	6.95	1.1
	3	19.30	4.45	4.50	19	7.34	1.1
	4	22.52	3.85	3.90	20	7.72	1.3
8	1	19.08	3.80	3.85	21	8.11	1.3
	2	16.21	3.75	3.80	22	8.49	1.3
	3	23.81	3.75	3.80	23	8.88	1.3
	4	23.38	3.75	3.80	24	9.27	1.3
9	1	17.01	3.70	3.75	25	9.65	1.4
	2	22.35	3.70	3.75	26	10.04	1.4
	3	22.25	3.65	3.70	27	10.42	1.4
	4	23.36	3.65	3.70	28	10.81	1.4
10	1	16.85	3.60	3.65	29	11.20	1.4
	2	22.40	3.55	3.60	30	11.58	1.4
11	1	19.52	3.50	3.55	31	11.97	1.4
	2	18.60	3.45	3.50	32	12.36	1.4
12	1	21.34	3.45	3.50	33	12.74	1.4
	2	16.18	3.45	3.50	34	13.13	1.4
	3	15.25	3.45	3.50	35	13.51	1.4
	4	19.73	3.20	3.25	36	13.90	1.6
13	1	18.30	3.20	3.25	37	14.29	1.6
	2	18.56	3.15	3.20	38	14.67	1.6
14	1	14.80	3.05	3.10	39	15.06	1.6
	2	15.22	2.80	2.85	40	15.44	1.8
15	1	14.91	2.75	2.80	41	15.83	1.8
	2	17.25	2.65	2.70	42	16.22	1.9
16	1	16.72	2.65	2.70	43	16.60	1.9
	2	15.10	2.55	2.60	44	16.99	2.0
17	1	16.27	2.55	2.60	45	17.37	2.0
	2	14.81	2.40	2.45	46	17.76	2.1
	3	13.49	2.35	2.40	47	18.15	2.1
	4	13.20	2.35	2.40	48	18.53	2.1
18	1	14.37	2.35	2.40	49	18.92	2.1

	2	13.51	2.35	2.40	50	19.31	2.1
	3	13.90	2.30	2.35	51	19.69	2.2
	4	13.93	2.30	2.35	52	20.08	2.2
19	1	14.20	2.25	2.30	53	20.46	2.2
	2	13.86	2.25	2.30	54	20.85	2.2
	3	13.24	2.25	2.30	55	21.24	2.2
	4	23.03	6.65	6.80	56	21.62	2.3
20	1	12.84	2.20	2.25	57	22.01	2.3
	2	13.04	2.20	2.25	58	22.39	2.3
21	1	11.49	2.10	2.15	59	22.78	2.4
	2	23.37	3.95	4.05	60	23.17	2.5
	3	23.26	3.80	3.90	61	23.55	2.6
	4	23.41	3.80	3.90	62	23.94	2.6
22	1	23.97	3.75	3.85	63	24.32	2.7
	2	23.17	3.70	3.80	64	24.71	2.7
23	1	22.40	3.70	3.80	65	25.10	2.7
24	1	16.61	3.70	3.80	66	25.48	2.7
	2	23.57	3.70	3.80	67	25.87	2.7
	3	19.45	3.60	3.70	68	26.25	2.8
	4	23.57	3.60	3.70	69	26.64	2.8
25	1	22.21	5.35	5.50	70	27.03	2.8
	2	16.64	3.55	3.65	71	27.41	2.8
26	1	19.00	3.55	3.65	72	27.80	2.8
	2	18.78	3.55	3.65	73	28.19	2.8
27	1	21.98	3.55	3.65	74	28.57	2.8
	2	16.47	3.50	3.60	75	28.96	2.9
	3	22.28	5.20	5.35	76	29.34	2.9
28	1	21.17	3.40	3.50	77	29.73	2.9
	2	19.57	3.35	3.45	78	30.12	3.0
	3	19.31	3.20	3.30	79	30.50	3.1
	4	22.87	4.80	4.95	80	30.89	3.1
29	1	24.52	4.75	4.90	81	31.27	3.2
	2	16.16	4.60	4.75	82	31.66	3.3
30	1	14.79	2.85	2.95	83	32.05	3.5
	2	15.07	2.85	2.95	84	32.43	3.5
	3	22.25	4.10	4.25	85	32.82	3.7
31	1	17.15	2.70	2.80	86	33.20	3.7
	2	17.57	2.70	2.80	87	33.59	3.7
32	1	16.31	2.70	2.80	88	33.98	3.7
	2	23.14	6.70	6.95	89	34.36	3.7
33	1	12.41	2.65	2.75	90	34.75	3.8
34	1	12.45	2.60	2.70	91	35.14	3.8
	2	23.45	3.85	4.00	92	35.52	3.9
35	1	16.21	2.55	2.65	93	35.91	3.9
	2	15.25	2.55	2.65	94	36.29	3.9
36	1	23.38	3.75	3.90	95	36.68	4.0
	2	12.34	2.50	2.60	96	37.07	4.0
	3	23.11	4.95	5.15	97	37.45	4.0
	4	14.14	2.45	2.55	98	37.84	4.1
37	1	14.62	2.45	2.55	99	38.22	4.1
	2	14.62	2.45	2.55	100	38.61	4.1
	3	12.67	2.45	2.55	101	39.00	4.1
38	1	23.10	3.65	3.80	102	39.38	4.1
	2	21.96	3.65	3.80	103	39.77	4.1
	3	22.12	3.60	3.75	104	40.15	4.2
39	1	13.70	2.40	2.50	105	40.54	4.2
	2	21.91	3.55	3.70	106	40.93	4.2

	3	13.02	2.35	2.45	107	41.31	4.3
40	1	21.93	3.50	3.65	108	41.70	4.3
	2	23.89	4.65	4.85	109	42.08	4.3
41	1	14.31	2.30	2.40	110	42.47	4.3
	2	21.41	3.40	3.55	111	42.86	4.4
	3	21.32	3.40	3.55	112	43.24	4.4
	4	19.60	4.50	4.70	113	43.63	4.4
42	1	22.66	5.60	5.85	114	44.02	4.5
	2	19.18	3.35	3.50	115	44.40	4.5
	3	13.16	2.20	2.30	116	44.79	4.5
43	1	12.58	2.10	2.20	117	45.17	4.8
	2	12.58	2.05	2.15	118	45.56	4.9
	3	13.53	2.85	3.00	119	45.95	5.3
	4	15.02	2.85	3.00	120	46.33	5.3
44	1	11.33	1.85	1.95	121	46.72	5.4
	2	11.18	1.85	1.95	122	47.10	5.4
	3	22.38	3.70	3.90	123	47.49	5.4
	4	14.03	2.75	2.90	124	47.88	5.5
45	1	22.33	3.55	3.75	125	48.26	5.6
	2	12.25	2.65	2.80	126	48.65	5.7
46	1	23.69	5.20	5.50	127	49.03	5.8
	2	22.22	4.10	4.35	128	49.42	6.1
47	1	14.17	2.45	2.60	129	49.81	6.1
	2	22.86	4.05	4.30	130	50.19	6.2
	3	14.20	2.40	2.55	131	50.58	6.3
	4	19.14	3.15	3.35	132	50.97	6.3
48	1	13.75	2.35	2.50	133	51.35	6.4
	2	13.99	2.35	2.50	134	51.74	6.4
	3	13.61	2.35	2.50	135	52.12	6.4
	4	13.80	2.35	2.50	136	52.51	6.4
49	1	11.07	2.35	2.50	137	52.90	6.4
	2	13.66	2.35	2.50	138	53.28	6.4
50	1	14.85	2.30	2.45	139	53.67	6.5
	2	13.31	2.30	2.45	140	54.05	6.5
51	1	14.68	3.75	4.00	141	54.44	6.7
	2	13.49	2.25	2.40	142	54.83	6.7
52	1	22.08	3.55	3.80	143	55.21	7.0
	2	11.26	4.15	4.45	144	55.60	7.2
53	1	15.09	4.10	4.40	145	55.98	7.3
	3	15.80	2.70	2.90	146	56.37	7.4
54	1	23.95	4.70	5.05	147	56.76	7.4
	2	13.95	3.30	3.55	148	57.14	7.6
55	1	19.46	4.60	4.95	149	57.53	7.6
	2	16.52	3.20	3.45	150	57.92	7.8
	3	14.39	2.55	2.75	151	58.30	7.8
	4	23.54	5.55	6.00	152	58.69	8.1
56	1	21.07	4.30	4.65	153	59.07	8.1
	2	23.93	4.30	4.65	154	59.46	8.1
	3	23.67	3.60	3.90	155	59.85	8.3
	4	13.52	2.25	2.45	156	60.23	8.9
57	1	13.70	2.80	3.05	157	60.62	8.9
	2	22.67	4.45	4.85	158	61.00	9.0
	3	13.76	2.15	2.35	159	61.39	9.3
	4	23.74	3.75	4.10	160	61.78	9.3
58	1	22.38	3.70	4.05	161	62.16	9.5
	2	25.27	4.15	4.55	162	62.55	9.6
59	1	22.39	3.85	4.25	163	62.93	10.4

	2	14.72	2.40	2.65	164	63.32	10.4
60	1	15.90	2.80	3.10	165	63.71	10.7
	2	15.85	2.75	3.05	166	64.09	10.9
	3	16.51	3.20	3.55	167	64.48	10.9
61	1	14.63	3.20	3.55	168	64.86	10.9
	2	18.97	3.20	3.55	169	65.25	10.9
62	1	19.26	3.15	3.50	170	65.64	11.1
	2	22.19	4.30	4.80	171	66.02	11.6
63	1	14.19	2.55	2.85	172	66.41	11.8
	2	24.00	3.80	4.25	173	66.80	11.8
	3	21.88	3.70	4.15	174	67.18	12.2
	4	13.99	2.35	2.65	175	67.57	12.8
64	1	22.80	5.45	6.15	176	67.95	12.8
	2	22.10	3.50	3.95	177	68.34	12.9
65	1	21.94	5.05	5.70	178	68.73	12.9
	2	16.76	4.50	5.10	179	69.11	13.3
66	1	23.83	3.70	4.20	180	69.50	13.5
	2	13.51	2.20	2.50	181	69.88	13.6
67	1	13.90	2.20	2.50	182	70.27	13.6
	2	14.66	3.20	3.65	183	70.66	14.1
68	1	22.05	3.55	4.05	184	71.04	14.1
69	1	14.46	2.45	2.80	185	71.43	14.3
	2	19.71	3.45	3.95	186	71.81	14.5
70	1	19.53	3.45	3.95	187	72.20	14.5
71	1	14.04	2.35	2.70	188	72.59	14.9
	2	14.16	3.00	3.45	189	72.97	15.0
72	1	21.85	3.65	4.20	190	73.36	15.1
	2	22.84	4.25	4.90	191	73.75	15.3
	3	14.23	2.25	2.60	192	74.13	15.6
	4	22.63	3.65	4.25	193	74.52	16.4
73	1	15.56	7.55	8.80	194	74.90	16.6
	2	14.48	2.35	2.75	195	75.29	17.0
	3	18.88	3.15	3.70	196	75.68	17.5
	4	11.43	1.95	2.30	197	76.06	17.9
74	1	21.42	3.55	4.20	198	76.45	18.3
	2	14.29	2.40	2.85	199	76.83	18.8
	3	21.91	3.65	4.35	200	77.22	19.2
	4	22.45	4.55	5.45	201	77.61	19.8
75	1	14.89	4.25	5.10	202	77.99	20.0
	2	23.77	3.75	4.50	203	78.38	20.0
	3	11.69	2.25	2.70	204	78.76	20.0
76	1	21.06	3.70	4.45	205	79.15	20.3
	2	19.73	3.45	4.15	206	79.54	20.3
77	1	14.76	2.45	2.95	207	79.92	20.4
	2	22.94	4.15	5.00	208	80.31	20.5
78	1	12.87	2.10	2.55	209	80.69	21.4
	2	14.28	2.50	3.05	210	81.08	22.0
	3	25.21	4.25	5.20	211	81.47	22.4
	4	13.99	2.40	2.95	212	81.85	22.9
79	1	21.90	3.65	4.50	213	82.24	23.3
	2	15.21	2.50	3.10	214	82.63	24.0
	3	14.31	2.25	2.80	215	83.01	24.4
	4	22.54	4.40	5.50	216	83.40	25.0
80	1	13.81	2.75	3.45	217	83.78	25.5
	2	23.56	3.90	4.90	218	84.17	25.6
	3	21.44	4.20	5.30	219	84.56	26.2
	4	22.80	3.55	4.50	220	84.94	26.8

81	1	22.89	4.10	5.25	221	85.33	28.0
	2	21.71	4.95	6.40	222	85.71	29.3
82	1	13.57	2.55	3.30	223	86.10	29.4
	2	22.96	4.15	5.40	224	86.49	30.1
83	1	15.64	2.70	3.55	225	86.87	31.5
84	1	14.43	2.55	3.40	226	87.26	33.3
	2	21.85	5.20	6.95	227	87.64	33.7
	3	21.41	3.70	4.95	228	88.03	33.8
85	1	23.44	4.05	5.45	229	88.42	34.6
	2	23.46	3.85	5.20	230	88.80	35.1
86	1	23.50	3.85	5.20	231	89.19	35.1
	2	22.84	4.05	5.50	232	89.58	35.8
	3	23.03	4.15	5.65	233	89.96	36.1
	4	14.80	2.35	3.20	234	90.35	36.2
87	1	17.01	2.75	3.75	235	90.73	36.4
	2	23.75	3.90	5.35	236	91.12	37.2
88	1	23.47	3.95	5.45	237	91.51	38.0
	2	12.04	2.60	3.60	238	91.89	38.5
89	1	22.87	3.70	5.15	239	92.28	39.2
	2	11.53	1.90	2.65	240	92.66	39.5
90	1	23.89	3.70	5.20	241	93.05	40.5
	2	20.54	3.50	4.95	242	93.44	41.4
	3	21.91	3.55	5.10	243	93.82	43.7
	4	15.10	2.60	3.80	244	94.21	46.2
91	1	20.74	3.55	5.25	245	94.59	47.9
	2	22.20	3.40	5.10	246	94.98	50.0
	3	22.87	4.05	6.10	247	95.37	50.6
	4	13.91	2.35	3.65	248	95.75	55.3
92	1	22.87	3.85	6.00	249	96.14	55.8
	2	13.69	2.55	4.00	250	96.53	56.9
93	1	20.22	3.55	5.65	251	96.91	59.2
94	1	23.75	3.70	5.90	252	97.30	59.5
	2	22.32	3.45	5.80	253	97.68	68.1
	3	13.38	2.65	4.50	254	98.07	69.8
95	1	15.01	2.45	4.40	255	98.46	79.6
	2	22.85	3.75	7.20	256	98.84	92.0
96	1	22.79	3.95	7.80	257	99.23	97.5
	2	22.95	4.05	8.50	258	99.61	109.9
	3	22.95	3.80	8.90	259	100.00	134.2
Mean		18.23	3.31	3.78			13.6
Std Dev		4.18	0.91	1.26			18.9
Median		18.67	3.45	3.65			6.2
Minimum		11.07	1.85	1.95			0.0
Maximum		25.27	7.55	8.90			134.2

PUNDIT TEST RECORD SHEET							
Sample ID:		Los Bronces Cu - T1					
Description:		13kW, 0.25s UPV					Relative
Particle ID	**Location ID**	**Depth (mm)**	**Transit Time (µs)**				**Reduction**
			Untreated	**Treated**	**Count**	**Spread (%)**	**(%)**
4	1	18.01	4.80	4.80	1	0.5	0.0
	4	17.69	4.90	4.90	2	1.0	0.0
7	1	23.14	6.40	6.40	3	1.5	0.0
	2	22.62	6.15	6.15	4	2.0	0.0
	4	22.49	6.15	6.15	5	2.6	0.0
	2	22.00	5.85	5.85	6	3.1	0.0
	2	23.15	5.50	5.50	7	3.6	0.0
	3	20.50	4.85	4.85	8	4.1	0.0
13	1	19.88	6.35	6.35	9	4.6	0.0
	2	24.61	5.55	5.55	10	5.1	0.0
16	1	24.18	5.80	5.80	11	5.6	0.0
	2	24.53	5.65	5.65	12	6.1	0.0
23	1	19.24	6.05	6.05	13	6.6	0.0
	2	18.77	6.95	6.95	14	7.1	0.0
	3	19.11	6.55	6.55	15	7.7	0.0
	3	24.55	5.90	5.90	16	8.2	0.0
27	1	18.40	4.50	4.50	17	8.7	0.0
	2	18.69	4.55	4.55	18	9.2	0.0
29	1	16.75	4.50	4.50	19	9.7	0.0
30	1	16.32	3.80	3.80	20	10.2	0.0
32	1	24.10	5.60	5.60	21	10.7	0.0
	2	23.97	5.60	5.60	22	11.2	0.0
	2	25.18	6.05	6.05	23	11.7	0.0
34	1	24.48	5.50	5.50	24	12.2	0.0
35	1	24.14	6.00	6.00	25	12.8	0.0
36	1	22.24	5.15	5.15	26	13.3	0.0
	2	22.32	5.00	5.00	27	13.8	0.0
37	1	16.61	3.80	3.80	28	14.3	0.0
	2	16.98	3.70	3.70	29	14.8	0.0
	3	16.26	3.70	3.70	30	15.3	0.0
	4	16.64	3.70	3.70	31	15.8	0.0
38	1	17.59	4.45	4.45	32	16.3	0.0
	2	24.23	5.80	5.80	33	16.8	0.0
	3	24.51	5.60	5.60	34	17.3	0.0
	4	24.15	5.70	5.70	35	17.9	0.0
40	1	25.11	5.85	5.85	36	18.4	0.0
41	1	17.98	4.30	4.30	37	18.9	0.0
	2	17.91	4.10	4.10	38	19.4	0.0
42	1	24.98	7.85	7.85	39	19.9	0.0
	2	24.89	7.25	7.25	40	20.4	0.0
	3	24.89	6.50	6.50	41	20.9	0.0
43	1	18.58	5.65	5.65	42	21.4	0.0
	2	18.47	4.90	4.90	43	21.9	0.0
44	1	21.94	5.25	5.25	44	22.4	0.0
44	1	24.67	7.20	7.20	45	23.0	0.0
	4	24.81	7.40	7.40	46	23.5	0.0
	2	18.35	4.45	4.45	47	24.0	0.0
	3	18.33	4.45	4.45	48	24.5	0.0

46	1	24.29	5.80	5.80	49	25.0	0.0
	2	24.13	6.05	6.05	50	25.5	0.0
47	1	16.74	4.20	4.20	51	26.0	0.0
	2	16.67	4.10	4.10	52	26.5	0.0
48	1	24.37	8.25	8.25	53	27.0	0.0
	2	24.47	7.90	7.90	54	27.6	0.0
	2	16.67	4.80	4.80	55	28.1	0.0
	3	16.62	4.60	4.60	56	28.6	0.0
	4	16.84	4.65	4.65	57	29.1	0.0
51	1	13.45	3.30	3.30	58	29.6	0.0
	2	13.22	3.20	3.20	59	30.1	0.0
	3	13.18	3.20	3.20	60	30.6	0.0
52	1	24.37	7.50	7.50	61	31.1	0.0
	2	24.21	6.05	6.05	62	31.6	0.0
53	1	18.86	5.00	5.00	63	32.1	0.0
	2	18.97	5.10	5.10	64	32.7	0.0
	2	24.89	5.80	5.80	65	33.2	0.0
57	1	24.54	6.70	6.70	66	33.7	0.0
	3	24.59	6.60	6.60	67	34.2	0.0
58	1	23.94	6.35	6.35	68	34.7	0.0
59	1	16.70	3.80	3.80	69	35.2	0.0
	2	20.84	5.40	5.40	70	35.7	0.0
	3	20.58	5.30	5.30	71	36.2	0.0
	4	20.51	5.40	5.40	72	36.7	0.0
	2	19.06	4.25	4.25	73	37.2	0.0
67	1	24.52	5.80	5.80	74	37.8	0.0
	2	24.08	5.55	5.55	75	38.3	0.0
	3	24.53	5.80	5.80	76	38.8	0.0
	4	24.10	5.60	5.60	77	39.3	0.0
	2	20.32	5.00	5.00	78	39.8	0.0
	4	24.12	5.45	5.45	79	40.3	0.0
75	1	21.55	4.80	4.80	80	40.8	0.0
	2	14.83	3.60	3.60	81	41.3	0.0
	3	15.01	3.60	3.60	82	41.8	0.0
81	1	23.69	5.30	5.30	83	42.3	0.0
	3	24.65	7.15	7.20	84	42.9	0.7
2	1	24.77	6.95	7.00	85	43.4	0.7
	4	18.71	6.80	6.85	86	43.9	0.7
	2	24.63	6.65	6.70	87	44.4	0.8
	2	24.24	6.55	6.60	88	44.9	0.8
	3	24.28	6.55	6.60	89	45.4	0.8
	3	24.75	6.40	6.45	90	45.9	0.8
	3	21.45	6.35	6.40	91	46.4	0.8
33	1	25.13	6.25	6.30	92	46.9	0.8
	2	24.05	6.20	6.25	93	47.4	0.8
26	1	20.69	6.05	6.10	94	48.0	0.8
54	1	24.68	6.00	6.05	95	48.5	0.8
	2	24.56	5.95	6.00	96	49.0	0.8
49	1	24.28	5.90	5.95	97	49.5	0.8
85	1	25.05	5.90	5.95	98	50.0	0.8
21	1	24.60	5.85	5.90	99	50.5	0.9
14	1	24.35	5.65	5.70	100	51.0	0.9
	2	20.60	5.65	5.70	101	51.5	0.9
6	1	22.86	5.50	5.55	102	52.0	0.9
9	1	23.05	5.40	5.45	103	52.6	0.9
61	1	20.88	5.35	5.40	104	53.1	0.9
	2	22.84	5.30	5.35	105	53.6	0.9

10	1	19.41	4.65	4.70	106	54.1	1.1
	2	19.20	4.65	4.70	107	54.6	1.1
	2	19.67	4.55	4.60	108	55.1	1.1
79	1	19.48	4.55	4.60	109	55.6	1.1
	2	17.59	4.45	4.50	110	56.1	1.1
45	1	18.54	4.40	4.45	111	56.6	1.1
63	1	19.07	4.40	4.45	112	57.1	1.1
11	1	19.56	4.35	4.40	113	57.7	1.1
5	1	20.06	4.20	4.25	114	58.2	1.2
17	1	16.32	4.15	4.20	115	58.7	1.2
	4	16.76	4.00	4.05	116	59.2	1.3
	2	16.43	3.90	3.95	117	59.7	1.3
	2	16.27	3.90	3.95	118	60.2	1.3
31	1	15.12	3.80	3.85	119	60.7	1.3
	2	15.96	3.80	3.85	120	61.2	1.3
15	1	15.34	3.75	3.80	121	61.7	1.3
	2	15.17	3.75	3.80	122	62.2	1.3
	2	24.85	7.50	7.60	123	62.8	1.3
	3	15.03	3.70	3.75	124	63.3	1.4
	3	16.74	3.70	3.75	125	63.8	1.4
39	1	27.01	7.30	7.40	126	64.3	1.4
70	1	14.36	3.65	3.70	127	64.8	1.4
76	1	15.05	3.50	3.55	128	65.3	1.4
	4	21.30	6.40	6.50	129	65.8	1.6
	2	21.28	6.30	6.40	130	66.3	1.6
66	1	21.36	6.20	6.30	131	66.8	1.6
20	1	24.62	6.15	6.25	132	67.3	1.6
	4	13.04	3.05	3.10	133	67.9	1.6
	2	24.61	5.75	5.85	134	68.4	1.7
	3	24.51	5.65	5.75	135	68.9	1.8
38	1	24.60	5.60	5.70	136	69.4	1.8
	3	22.65	5.50	5.60	137	69.9	1.8
	3	20.74	5.25	5.35	138	70.4	1.9
	4	20.17	5.25	5.35	139	70.9	1.9
	2	20.19	5.10	5.20	140	71.4	2.0
64	1	18.33	4.65	4.75	141	71.9	2.2
	2	19.89	4.60	4.70	142	72.4	2.2
	2	16.89	4.50	4.60	143	73.0	2.2
73	1	17.34	4.50	4.60	144	73.5	2.2
	3	24.37	6.65	6.80	145	74.0	2.3
3	1	24.30	6.60	6.75	146	74.5	2.3
25	1	24.21	6.60	6.75	147	75.0	2.3
	2	24.17	6.45	6.60	148	75.5	2.3
	3	23.08	6.20	6.35	149	76.0	2.4
19	1	24.33	6.05	6.20	150	76.5	2.5
60	1	16.12	4.00	4.10	151	77.0	2.5
74	1	23.83	5.95	6.10	152	77.6	2.5
	2	24.44	5.85	6.00	153	78.1	2.6
68	1	24.44	5.85	6.00	154	78.6	2.6
24	1	24.64	5.75	5.90	155	79.1	2.6
84	1	24.19	5.60	5.75	156	79.6	2.7
	2	13.97	3.70	3.80	157	80.1	2.7
	3	22.12	5.45	5.60	158	80.6	2.8
	4	14.89	3.60	3.70	159	81.1	2.8
	3	21.39	5.10	5.25	160	81.6	2.9
72	1	20.74	5.10	5.25	161	82.1	2.9
22	1	21.77	5.05	5.20	162	82.7	3.0

48	1	16.94	4.90	5.05	163	83.2	3.1
	2	24.26	6.45	6.65	164	83.7	3.1
	2	24.43	6.15	6.35	165	84.2	3.3
65	1	24.72	6.05	6.25	166	84.7	3.3
	3	24.39	5.90	6.10	167	85.2	3.4
8	1	22.16	7.20	7.45	168	85.7	3.5
	4	14.65	4.10	4.25	169	86.2	3.7
78	1	22.53	5.40	5.60	170	86.7	3.7
	2	14.73	3.95	4.10	171	87.2	3.8
	3	14.27	3.95	4.10	172	87.8	3.8
	3	18.22	4.95	5.15	173	88.3	4.0
56	1	24.19	6.00	6.25	174	88.8	4.2
	2	22.58	5.40	5.65	175	89.3	4.6
18	1	24.95	6.45	6.75	176	89.8	4.7
67	1	23.93	6.30	6.60	177	90.3	4.8
	2	24.05	6.20	6.50	178	90.8	4.8
	2	24.19	6.15	6.45	179	91.3	4.9
	2	24.46	5.80	6.15	180	91.8	6.0
71	1	14.31	4.10	4.35	181	92.3	6.1
28	1	24.65	8.05	8.55	182	92.9	6.2
82	1	24.25	6.05	6.45	183	93.4	6.6
1	1	19.91	5.00	5.35	184	93.9	7.0
	3	23.27	5.50	5.95	185	94.4	8.2
62	1	24.57	5.90	6.40	186	94.9	8.5
72	1	24.41	5.30	6.15	187	95.4	16.0
	3	23.93	6.15	7.25	188	95.9	17.9
	3	24.25	5.45	6.55	189	96.4	20.2
50	1	23.65	6.40	7.70	190	96.9	20.3
	3	20.44	5.35	6.45	191	97.4	20.6
	2	21.30	4.90	6.25	192	98.0	27.6
	2	23.92	6.15	8.05	193	98.5	30.9
	2	24.19	5.35	7.05	194	99.0	31.8
	2	20.41	5.45	8.50	195	99.5	56.0
69	1	20.48	5.35	9.25	196	100.0	72.9
Mean		21.14	5.39	5.54			2.8
St Dev		3.54	1.07	1.18			7.9
Median		22.14	5.50	5.63			0.9
Minimum		13.04	3.05	3.10			0.0
Maximum		27.01	8.25	9.25			72.9

PUNDIT TEST RECORD SHEET							
Sample ID:		Los Bronces Cu - T2					
Description:		1.1s, 11Kw					**Relative UPV**
Particle ID	**Location ID**	**Depth (mm)**	**Transit Time (µs)**				**Reduction**
			Untreated	**Treated**	**Count**	**Spread (%)**	**(%)**
1	1	24.67	5.90	5.90	1	0.5	0.0
	2	24.21	5.95	5.95	2	1.0	0.0
	3	24.53	5.90	5.90	3	1.5	0.0
	4	24.65	6.05	6.05	4	2.0	0.0
2	1	16.17	4.20	4.20	5	2.5	0.0
3	1	24.96	6.00	6.00	6	3.0	0.0
	2	25.04	6.05	6.05	7	3.5	0.0
	3	24.74	5.85	5.85	8	4.0	0.0
	4	25.05	5.95	5.95	9	4.5	0.0
5	1	16.27	3.85	3.85	10	5.0	0.0
	2	15.96	3.75	3.75	11	5.5	0.0
	3	15.43	3.60	3.60	12	6.0	0.0
6	1	24.23	5.95	5.95	13	6.5	0.0
7	1	24.61	5.95	5.95	14	7.0	0.0
	2	24.87	6.05	6.05	15	7.5	0.0
8	1	20.36	7.60	7.60	16	8.0	0.0
	2	17.79	4.70	4.70	17	8.5	0.0
	3	17.97	4.70	4.70	18	9.0	0.0
10	1	16.76	3.60	3.60	19	9.5	0.0
11	1	24.66	5.75	5.75	20	10.1	0.0
	2	25.00	6.25	6.25	21	10.6	0.0
12	1	21.31	5.20	5.20	22	11.1	0.0
	2	21.45	5.25	5.25	23	11.6	0.0
12	1	15.41	3.95	3.95	24	12.1	0.0
13	1	25.65	7.70	7.70	25	12.6	0.0
14	1	17.50	4.50	4.50	26	13.1	0.0
	2	17.60	4.40	4.40	27	13.6	0.0
	3	17.54	4.40	4.40	28	14.1	0.0
	4	17.82	4.30	4.30	29	14.6	0.0
15	1	24.42	6.80	6.80	30	15.1	0.0
	3	24.71	6.80	6.80	31	15.6	0.0
	2	19.11	4.05	4.05	32	16.1	0.0
	4	19.26	4.20	4.20	33	16.6	0.0
18	1	25.31	5.55	5.55	34	17.1	0.0
19	1	24.67	6.85	6.85	35	17.6	0.0
21	1	18.33	4.70	4.70	36	18.1	0.0
	2	18.81	4.80	4.80	37	18.6	0.0
22	1	22.38	5.20	5.20	38	19.1	0.0
	2	22.21	4.95	4.95	39	19.6	0.0
	3	22.36	4.85	4.85	40	20.1	0.0
23	1	19.84	5.55	5.55	41	20.6	0.0
24	1	23.84	7.80	7.80	42	21.1	0.0
26	1	16.55	5.20	5.20	43	21.6	0.0
27	1	24.61	7.70	7.70	44	22.1	0.0
	2	24.29	7.60	7.60	45	22.6	0.0
28	1	25.05	5.65	5.65	46	23.1	0.0
	2	20.89	5.50	5.50	47	23.6	0.0
	3	20.58	5.20	5.20	48	24.1	0.0
	4	20.83	5.30	5.30	49	24.6	0.0

30	1	24.41	7.50	7.50	50	25.1	0.0
	2	24.23	7.35	7.35	51	25.6	0.0
	3	24.13	7.55	7.55	52	26.1	0.0
31	1	16.56	4.10	4.10	53	26.6	0.0
	2	16.60	4.10	4.10	54	27.1	0.0
32	1	16.66	3.70	3.70	55	27.6	0.0
	3	20.46	4.80	4.80	56	28.1	0.0
	3	24.00	5.50	5.50	57	28.6	0.0
35	1	19.96	4.80	4.80	58	29.1	0.0
36	1	21.39	5.35	5.35	59	29.6	0.0
	2	24.12	6.00	6.00	60	30.2	0.0
39	1	24.64	6.50	6.50	61	30.7	0.0
40	1	14.88	3.60	3.60	62	31.2	0.0
	2	15.21	3.80	3.80	63	31.7	0.0
	3	15.56	3.75	3.75	64	32.2	0.0
	2	24.81	6.05	6.05	65	32.7	0.0
	3	24.60	6.05	6.05	66	33.2	0.0
42	1	24.53	7.90	7.90	67	33.7	0.0
	2	24.58	7.90	7.90	68	34.2	0.0
	3	24.14	7.75	7.75	69	34.7	0.0
43	1	24.44	5.30	5.30	70	35.2	0.0
46	1	23.70	6.10	6.10	71	35.7	0.0
49	1	25.08	5.65	5.65	72	36.2	0.0
	2	25.20	5.70	5.70	73	36.7	0.0
	3	25.33	5.80	5.80	74	37.2	0.0
	3	24.63	5.40	5.40	75	37.7	0.0
	4	24.70	5.35	5.35	76	38.2	0.0
51	1	24.67	5.60	5.60	77	38.7	0.0
52	1	18.35	4.70	4.70	78	39.2	0.0
	2	18.57	4.85	4.85	79	39.7	0.0
	3	18.79	4.80	4.80	80	40.2	0.0
53	1	19.93	4.80	4.80	81	40.7	0.0
	2	19.48	5.05	5.05	82	41.2	0.0
	2	24.90	5.65	5.65	83	41.7	0.0
	3	24.86	5.70	5.70	84	42.2	0.0
55	1	25.37	6.30	6.30	85	42.7	0.0
55	1	17.86	6.10	6.10	86	43.2	0.0
56	1	16.02	4.45	4.45	87	43.7	0.0
	2	15.73	4.10	4.10	88	44.2	0.0
	2	23.65	5.15	5.15	89	44.7	0.0
	3	24.21	5.25	5.25	90	45.2	0.0
58	1	25.21	5.70	5.70	91	45.7	0.0
	2	25.50	5.45	5.45	92	46.2	0.0
59	1	18.23	5.00	5.00	93	46.7	0.0
60	1	24.67	6.20	6.20	94	47.2	0.0
	2	24.64	6.10	6.10	95	47.7	0.0
	2	19.11	4.70	4.70	96	48.2	0.0
	4	18.80	4.55	4.55	97	48.7	0.0
64	1	16.47	4.50	4.50	98	49.2	0.0
	3	16.64	4.65	4.65	99	49.7	0.0
	4	16.55	4.90	4.90	100	50.3	0.0
65	1	24.28	5.70	5.70	101	50.8	0.0
66	1	20.39	5.30	5.30	102	51.3	0.0
69	1	24.10	5.75	5.75	103	51.8	0.0
70	1	24.14	6.50	6.50	104	52.3	0.0
	2	24.25	6.40	6.40	105	52.8	0.0
	3	24.27	6.40	6.40	106	53.3	0.0

	2	17.82	4.45	4.45	107	53.8	0.0
77	1	24.43	5.80	5.80	108	54.3	0.0
	3	24.01	6.00	6.00	109	54.8	0.0
78	1	24.52	5.30	5.30	110	55.3	0.0
	2	24.43	5.55	5.55	111	55.8	0.0
80	1	20.55	5.50	5.50	112	56.3	0.0
	3	20.54	4.90	4.90	113	56.8	0.0
	4	19.95	5.00	5.00	114	57.3	0.0
	2	15.27	3.30	3.30	115	57.8	0.0
81	1	17.12	4.35	4.35	116	58.3	0.0
	2	17.17	4.45	4.45	117	58.8	0.0
	3	17.21	4.45	4.45	118	59.3	0.0
82	1	18.76	4.50	4.50	119	59.8	0.0
	2	24.35	5.40	5.40	120	60.3	0.0
83	1	18.88	4.90	4.90	121	60.8	0.0
	2	19.77	4.10	4.10	122	61.3	0.0
	3	20.38	4.75	4.75	123	61.8	0.0
	2	20.59	7.60	7.65	124	62.3	0.7
	2	24.75	7.05	7.10	125	62.8	0.7
16	1	24.93	6.90	6.95	126	63.3	0.7
62	1	24.07	6.75	6.80	127	63.8	0.7
	3	24.26	6.55	6.60	128	64.3	0.8
41	1	24.98	6.25	6.30	129	64.8	0.8
74	1	24.87	6.25	6.30	130	65.3	0.8
37	1	24.07	6.05	6.10	131	65.8	0.8
	2	23.80	5.85	5.90	132	66.3	0.9
4	1	24.97	5.65	5.70	133	66.8	0.9
	2	24.31	5.60	5.65	134	67.3	0.9
54	1	24.71	5.60	5.65	135	67.8	0.9
50	1	24.44	5.45	5.50	136	68.3	0.9
79	1	24.67	5.45	5.50	137	68.8	0.9
83	1	24.79	5.45	5.50	138	69.3	0.9
	2	20.96	5.30	5.35	139	69.8	0.9
	2	24.31	5.30	5.35	140	70.4	0.9
	2	24.57	5.20	5.25	141	70.9	1.0
29	1	20.67	5.10	5.15	142	71.4	1.0
	3	18.08	5.05	5.10	143	71.9	1.0
63	1	19.25	4.90	4.95	144	72.4	1.0
	4	20.91	4.80	4.85	145	72.9	1.0
33	1	20.73	4.75	4.80	146	73.4	1.1
	2	20.95	4.75	4.80	147	73.9	1.1
	3	18.95	4.60	4.65	148	74.4	1.1
	4	17.23	4.35	4.40	149	74.9	1.1
9	1	17.63	4.30	4.35	150	75.4	1.2
77	1	16.18	3.90	3.95	151	75.9	1.3
80	1	15.22	3.35	3.40	152	76.4	1.5
	4	24.48	6.20	6.30	153	76.9	1.6
	3	24.71	6.00	6.10	154	77.4	1.7
	2	24.25	5.80	5.90	155	77.9	1.7
	3	23.74	5.70	5.80	156	78.4	1.8
	2	24.22	5.40	5.50	157	78.9	1.9
20	1	20.98	8.10	8.25	158	79.4	1.9
	2	20.08	5.30	5.40	159	79.9	1.9
	3	23.99	5.20	5.30	160	80.4	1.9
	3	20.41	5.15	5.25	161	80.9	1.9
	3	20.64	5.10	5.20	162	81.4	2.0
	4	19.95	5.05	5.15	163	81.9	2.0

	2	16.29	5.05	5.15	164	82.4	2.0
	2	20.61	5.00	5.10	165	82.9	2.0
47	1	20.24	5.00	5.10	166	83.4	2.0
	2	24.27	9.70	9.90	167	83.9	2.1
75	1	20.01	4.80	4.90	168	84.4	2.1
68	1	19.08	4.50	4.60	169	84.9	2.2
	3	17.81	4.45	4.55	170	85.4	2.2
	2	24.99	6.60	6.75	171	85.9	2.3
	3	18.90	4.10	4.20	172	86.4	2.4
	2	24.90	6.15	6.30	173	86.9	2.4
85	1	24.04	6.15	6.30	174	87.4	2.4
17	1	18.88	4.00	4.10	175	87.9	2.5
	3	24.54	5.80	5.95	176	88.4	2.6
	2	20.02	5.40	5.55	177	88.9	2.8
	2	18.20	5.15	5.30	178	89.4	2.9
76	1	25.92	6.40	6.60	179	89.9	3.1
	2	24.28	6.35	6.55	180	90.5	3.1
84	1	19.99	4.60	4.75	181	91.0	3.3
73	1	17.79	4.20	4.35	182	91.5	3.6
25	1	24.21	5.60	5.80	183	92.0	3.6
	3	19.87	5.40	5.60	184	92.5	3.7
	2	23.94	5.30	5.50	185	93.0	3.8
57	1	23.23	5.30	5.50	186	93.5	3.8
	4	19.56	5.30	5.50	187	94.0	3.8
	4	24.35	6.35	6.65	188	94.5	4.7
61	1	24.10	6.45	6.80	189	95.0	5.4
34	1	23.83	5.25	5.55	190	95.5	5.7
	4	20.03	4.20	4.45	191	96.0	6.0
	2	26.21	6.50	6.90	192	96.5	6.2
45	1	15.79	4.20	4.55	193	97.0	8.3
71	1	24.60	5.35	5.80	194	97.5	8.4
	3	24.33	5.20	5.65	195	98.0	8.7
	2	24.76	5.30	5.90	196	98.5	11.3
	3	15.94	4.05	4.70	197	99.0	16.0
	2	15.70	4.00	4.65	198	99.5	16.3
	4	15.62	4.00	4.90	199	100.0	22.5
Mean		21.55	5.41	5.47			1.2
StDev		3.31	1.04	1.04			2.8
Median		22.38	5.30	5.40			0.0
Minimum		14.88	3.30	3.30			0.0
Maximum		26.21	9.70	9.90			22.5

PUNDIT TEST RECORD SHEET							
Sample ID:		Los Bronces Cu - T3					
Description:		10kW, 2.75s					
Particle ID	**Location ID**	**Depth (mm)**	**Transit Time (µs)**				**Relative UPV Reduction**
			Untreated	**Treated**	**Count**	**Spread (%)**	**(%)**
2	1	24.00	5.80	5.80	1	0.5	0.0
	2	23.86	5.90	5.90	2	1.0	0.0
3	1	24.06	6.40	6.40	3	1.6	0.0
	2	24.08	7.00	7.00	4	2.1	0.0
5	1	12.51	3.50	3.50	5	2.6	0.0
	2	12.66	3.65	3.65	6	3.1	0.0
	3	12.80	3.65	3.65	7	3.6	0.0
	4	12.85	3.60	3.60	8	4.2	0.0
7	1	19.48	3.95	3.95	9	4.7	0.0
	2	19.54	4.20	4.20	10	5.2	0.0
	2	24.14	5.90	5.90	11	5.7	0.0
	3	22.88	5.35	5.35	12	6.3	0.0
12	1	24.78	5.85	5.85	13	6.8	0.0
	2	23.89	7.60	7.60	14	7.3	0.0
	4	23.87	7.30	7.30	15	7.8	0.0
33	1	23.89	5.80	5.80	16	8.3	0.0
34	1	19.47	4.85	4.85	17	8.9	0.0
	2	19.62	4.80	4.80	18	9.4	0.0
	2	24.13	6.65	6.65	19	9.9	0.0
	2	25.30	6.05	6.05	20	10.4	0.0
	3	23.49	6.40	6.40	21	10.9	0.0
44	1	19.09	5.20	5.20	22	11.5	0.0
	2	19.11	5.00	5.00	23	12.0	0.0
	3	18.86	4.80	4.80	24	12.5	0.0
50	1	24.60	6.10	6.10	25	13.0	0.0
51	1	24.48	5.60	5.60	26	13.5	0.0
52	1	24.01	6.15	6.15	27	14.1	0.0
54	1	24.25	6.10	6.10	28	14.6	0.0
	2	24.56	6.15	6.15	29	15.1	0.0
55	1	17.29	4.10	4.10	30	15.6	0.0
	2	17.33	4.00	4.00	31	16.1	0.0
	2	24.60	5.70	5.70	32	16.7	0.0
	3	24.62	5.65	5.65	33	17.2	0.0
61	1	24.30	5.70	5.70	34	17.7	0.0
62	1	17.39	5.80	5.80	35	18.2	0.0
65	1	24.42	5.30	5.30	36	18.8	0.0
	2	24.29	5.50	5.50	37	19.3	0.0
	3	24.45	5.50	5.50	38	19.8	0.0
66	1	24.44	5.70	5.70	39	20.3	0.0
	2	24.61	5.85	5.85	40	20.8	0.0
67	1	15.06	3.50	3.50	41	21.4	0.0
	2	14.98	3.55	3.55	42	21.9	0.0
68	1	12.98	3.10	3.10	43	22.4	0.0
	2	13.14	3.00	3.00	44	22.9	0.0
	3	12.70	2.95	2.95	45	23.4	0.0
	4	12.75	3.00	3.00	46	24.0	0.0
	2	20.26	4.50	4.50	47	24.5	0.0
70	1	18.14	4.50	4.50	48	25.0	0.0

	2	18.34	4.70	4.70	49	25.5	0.0
	3	18.38	4.70	4.70	50	26.0	0.0
71	1	19.82	4.85	4.85	51	26.6	0.0
73	1	18.30	4.80	4.80	52	27.1	0.0
	2	18.15	4.40	4.40	53	27.6	0.0
	3	18.33	4.80	4.80	54	28.1	0.0
	4	18.36	4.80	4.80	55	28.6	0.0
74	1	23.06	6.15	6.15	56	29.2	0.0
76	1	24.19	5.15	5.15	57	29.7	0.0
	2	24.13	6.10	6.10	58	30.2	0.0
78	1	19.78	4.80	4.80	59	30.7	0.0
	2	19.48	4.65	4.65	60	31.3	0.0
	3	19.56	4.60	4.60	61	31.8	0.0
	2	18.05	4.00	4.00	62	32.3	0.0
	3	18.46	4.05	4.05	63	32.8	0.0
80	1	23.58	6.35	6.35	64	33.3	0.0
83	1	22.20	5.30	5.30	65	33.9	0.0
	2	22.34	5.75	5.75	66	34.4	0.0
56	1	24.73	7.55	7.60	67	34.9	0.7
	2	24.81	6.90	6.95	68	35.4	0.7
38	1	24.21	6.70	6.75	69	35.9	0.7
60	1	24.13	6.70	6.75	70	36.5	0.7
	2	24.48	6.60	6.65	71	37.0	0.8
	3	24.10	6.30	6.35	72	37.5	0.8
13	1	24.73	6.25	6.30	73	38.0	0.8
59	1	24.51	6.15	6.20	74	38.5	0.8
	3	24.23	6.05	6.10	75	39.1	0.8
39	1	25.57	6.05	6.10	76	39.6	0.8
	2	23.64	6.05	6.10	77	40.1	0.8
19	1	24.36	5.95	6.00	78	40.6	0.8
64	1	23.75	5.95	6.00	79	41.1	0.8
32	1	24.66	5.85	5.90	80	41.7	0.9
	2	24.68	5.80	5.85	81	42.2	0.9
	3	23.76	5.80	5.85	82	42.7	0.9
	2	24.39	5.80	5.85	83	43.2	0.9
	2	17.31	5.80	5.85	84	43.8	0.9
	2	23.85	5.75	5.80	85	44.3	0.9
	2	24.26	5.75	5.80	86	44.8	0.9
47	1	24.41	5.70	5.75	87	45.3	0.9
	2	24.12	5.50	5.55	88	45.8	0.9
	3	24.02	5.40	5.45	89	46.4	0.9
36	1	17.71	4.85	4.90	90	46.9	1.0
	2	14.32	4.65	4.70	91	47.4	1.1
69	1	20.46	4.65	4.70	92	47.9	1.1
48	1	18.37	4.50	4.55	93	48.4	1.1
	3	17.26	4.30	4.35	94	49.0	1.2
	3	19.37	4.20	4.25	95	49.5	1.2
	2	15.68	4.15	4.20	96	50.0	1.2
	2	15.04	4.10	4.15	97	50.5	1.2
20	1	15.29	4.00	4.05	98	51.0	1.3
	2	23.89	7.40	7.50	99	51.6	1.4
14	1	23.89	7.30	7.40	100	52.1	1.4
	3	14.83	3.60	3.65	101	52.6	1.4
49	1	24.92	6.85	6.95	102	53.1	1.5
	3	14.86	3.40	3.45	103	53.6	1.5
	2	24.04	6.55	6.65	104	54.2	1.5
58	1	24.59	6.50	6.60	105	54.7	1.5

23	1	24.64	6.45	6.55	106	55.2	1.6
77	1	24.26	6.45	6.55	107	55.7	1.6
	2	24.52	6.25	6.35	108	56.3	1.6
8	1	24.23	6.15	6.25	109	56.8	1.6
	3	23.64	6.05	6.15	110	57.3	1.7
	2	24.69	5.95	6.05	111	57.8	1.7
	3	24.09	5.45	5.55	112	58.3	1.8
27	1	19.58	4.90	5.00	113	58.9	2.0
	3	20.15	4.80	4.90	114	59.4	2.1
	2	17.36	4.80	4.90	115	59.9	2.1
6	1	24.41	6.55	6.70	116	60.4	2.3
	3	23.96	6.35	6.50	117	60.9	2.4
45	1	15.06	4.00	4.10	118	61.5	2.5
	3	24.64	6.00	6.15	119	62.0	2.5
	2	24.83	5.95	6.10	120	62.5	2.5
	4	16.38	3.95	4.05	121	63.0	2.5
40	1	23.35	5.80	5.95	122	63.5	2.6
42	1	24.44	5.75	5.90	123	64.1	2.6
82	1	25.09	5.70	5.85	124	64.6	2.6
	3	15.21	3.80	3.90	125	65.1	2.6
31	1	24.66	5.65	5.80	126	65.6	2.7
30	1	24.16	7.50	7.70	127	66.1	2.7
	2	24.82	5.60	5.75	128	66.7	2.7
29	1	14.81	3.60	3.70	129	67.2	2.8
	2	23.25	5.35	5.50	130	67.7	2.8
53	1	24.61	6.90	7.10	131	68.2	2.9
	2	24.20	5.05	5.20	132	68.8	3.0
	2	23.38	6.40	6.60	133	69.3	3.1
25	1	14.66	4.70	4.85	134	69.8	3.2
	2	24.42	6.20	6.40	135	70.3	3.2
26	1	24.56	6.05	6.25	136	70.8	3.3
18	1	24.45	6.00	6.20	137	71.4	3.3
	3	24.06	5.90	6.10	138	71.9	3.4
	4	23.67	5.75	5.95	139	72.4	3.5
	2	16.93	4.15	4.30	140	72.9	3.6
	2	22.87	5.50	5.70	141	73.4	3.6
43	1	24.05	5.50	5.70	142	74.0	3.6
63	1	20.85	5.50	5.70	143	74.5	3.6
	4	14.56	4.10	4.25	144	75.0	3.7
24	1	19.69	5.35	5.55	145	75.5	3.7
	4	23.31	5.30	5.50	146	76.0	3.8
4	1	16.62	3.90	4.05	147	76.6	3.8
79	1	17.97	3.90	4.05	148	77.1	3.8
	3	15.99	3.85	4.00	149	77.6	3.9
	2	24.49	7.30	7.60	150	78.1	4.1
	3	24.50	5.95	6.20	151	78.6	4.2
	2	24.62	5.90	6.15	152	79.2	4.2
	3	28.11	6.40	6.70	153	79.7	4.7
72	1	24.28	6.40	6.70	154	80.2	4.7
35	1	23.33	5.25	5.50	155	80.7	4.8
10	1	24.49	7.15	7.50	156	81.3	4.9
	2	18.26	4.00	4.20	157	81.8	5.0
	4	24.25	5.95	6.25	158	82.3	5.0
16	1	24.09	6.75	7.10	159	82.8	5.2
	2	15.21	3.80	4.00	160	83.3	5.3
	2	24.77	5.65	5.95	161	83.9	5.3
	2	23.92	6.40	6.75	162	84.4	5.5

11	1	22.95	5.15	5.45	163	84.9	5.8
	3	24.88	6.50	6.90	164	85.4	6.2
	2	24.74	8.05	8.55	165	85.9	6.2
1	1	24.41	5.60	5.95	166	86.5	6.3
	3	24.81	7.95	8.45	167	87.0	6.3
84	1	20.77	4.75	5.05	168	87.5	6.3
41	1	18.10	3.95	4.20	169	88.0	6.3
	3	14.26	3.90	4.15	170	88.5	6.4
21	1	17.63	4.50	4.80	171	89.1	6.7
	2	27.83	6.45	6.90	172	89.6	7.0
	3	24.57	7.90	8.55	173	90.1	8.2
81	1	24.32	8.30	9.00	174	90.6	8.4
17	1	27.28	6.20	6.75	175	91.1	8.9
	2	18.93	5.25	5.85	176	91.7	11.4
	3	20.47	5.10	5.70	177	92.2	11.8
37	1	23.82	6.75	7.65	178	92.7	13.3
22	1	24.56	8.35	9.50	179	93.2	13.8
	2	24.56	5.75	6.60	180	93.8	14.8
	2	24.61	7.40	8.50	181	94.3	14.9
	3	18.18	4.20	5.00	182	94.8	19.0
75	1	18.42	5.70	6.80	183	95.3	19.3
	2	20.34	5.00	6.00	184	95.8	20.0
15	1	24.36	5.50	6.70	185	96.4	21.8
57	1	20.00	5.25	6.40	186	96.9	21.9
9	1	24.45	6.65	8.20	187	97.4	23.3
	2	20.08	4.40	5.60	188	97.9	27.3
46	1	22.37	5.60	7.45	189	98.4	33.0
	2	17.98	4.20	5.85	190	99.0	39.3
	2	24.58	6.85	11.00	191	99.5	60.6
28	1	17.74	4.10	7.70	192	100.0	87.8
Mean		21.53	5.46	5.68			4.0
St Dev		3.78	1.13	1.29			9.4
Median		23.84	5.65	5.80			1.2
Minimum		12.51	2.95	2.95			0.0
Maximum		28.11	8.35	11.00			87.8
School of Chemical & Environmental Engineering							

PUNDIT TEST RECORD SHEET							
Sample ID:	Kimberlite I T1						
Description:	7.4s, 18kW						**Relative UPV**
Particle ID	**Location ID**	**Depth (mm)**	**Transit Time (µs)**				**Reduction**
			Untreated	**Treated**	**Count**	**Spread (%)**	**(%)**
1	1	26.77	6.40	4.90	1	1.7	0.0
65	1	15.51	3.20	2.60	2	3.4	0.0
47	1	6.96	1.70	1.40	3	5.1	0.0
38	1	7.73	1.80	1.60	4	6.8	0.0
11	1	18.24	3.10	2.80	5	8.5	0.0
42	1	15.33	3.20	2.90	6	10.2	0.0
49	1	13.53	2.80	2.60	7	11.9	0.0
28	1	15.00	2.90	2.70	8	13.6	0.0
34	1	14.36	3.00	2.80	9	15.3	0.0
24	1	15.06	3.20	3.00	10	16.9	0.0
43	1	15.19	3.30	3.10	11	18.6	0.0
12	1	17.12	3.40	3.20	12	20.3	0.0
44	1	15.25	3.50	3.30	13	22.0	0.0
48	1	11.52	2.50	2.40	14	23.7	0.0
31	1	25.32	5.80	5.60	15	25.4	0.0
8	1	15.02	3.00	2.90	16	27.1	0.0
2	1	14.43	3.20	3.10	17	28.8	0.0
23	1	14.99	3.20	3.10	18	30.5	0.0
50	1	14.40	3.30	3.20	19	32.2	0.0
33	1	16.20	3.80	3.70	20	33.9	0.0
5	1	13.35	3.40	3.40	21	35.6	0.0
21	1	13.99	3.20	3.20	22	37.3	0.0
22	1	19.01	3.80	3.80	23	39.0	0.0
29	1	15.10	3.10	3.10	24	40.7	0.0
36	1	14.17	3.10	3.10	25	42.4	0.0
45	1	16.70	4.00	4.00	26	44.1	0.0
54	1	15.76	3.40	3.40	27	45.8	0.0
57	1	12.66	2.70	2.70	28	47.5	0.0
39	1	14.49	3.30	3.40	29	49.2	3.0
7	1	15.05	2.90	3.00	30	50.8	3.4
46	1	24.02	4.80	5.00	31	52.5	4.2
58	1	17.15	3.60	3.80	32	54.2	5.6
52	1	18.83	3.50	3.70	33	55.9	5.7
41	1	14.30	3.20	3.40	34	57.6	6.3
27	1	35.35	7.20	7.70	35	59.3	6.9
56	1	17.15	3.90	4.20	36	61.0	7.7
40	1	16.37	3.60	3.90	37	62.7	8.3
16	1	13.43	2.90	3.20	38	64.4	10.3
37	1	26.96	5.50	6.10	39	66.1	10.9
17	1	13.27	3.60	4.00	40	67.8	11.1
6	1	16.19	3.20	3.60	41	69.5	12.5
4	1	13.65	3.10	3.50	42	71.2	12.9
20	1	18.62	3.60	4.10	43	72.9	13.9
55	1	14.90	2.90	3.40	44	74.6	17.2
3	1	17.08	3.80	4.50	45	76.3	18.4
15	1	16.45	3.20	3.80	46	78.0	18.8
32	1	17.56	5.30	6.30	47	79.7	18.9
35	1	11.99	3.00	3.60	48	81.4	20.0

10	1	14.31	3.20	3.90	49	83.1	21.9
14	1	14.53	3.20	3.90	50	84.7	21.9
25	1	16.40	3.40	4.20	51	86.4	23.5
13	1	14.09	2.90	3.60	52	88.1	24.1
61	1	10.17	2.70	3.40	53	89.8	25.9
26	1	15.29	3.80	5.00	54	91.5	31.6
53	1	19.10	3.60	5.80	55	93.2	61.1
30	1	17.38	4.20	6.90	56	94.9	64.3
19	1	17.50	3.30	6.00	57	96.6	81.8
18	1	16.64	3.50	6.90	58	98.3	97.1
9	1	18.06	3.80	7.90	59	100.0	107.9
Mean		16.00	3.45	3.87			13.2
Std Dev		4.20	0.86	1.37			23.5
Median		15.22	3.25	3.45			3.4
Minimum		6.96	1.70	1.40			0.0
Maximum		35.35	7.20	7.90			107.9

PUNDIT TEST RECORD SHEET							
Sample ID:		Kimberlite I - T2					
Description:		12.5s, 24.6kW					**Relative UPV**
Particle ID	**Location ID**	**Depth (mm)**	**Transit Time (µs)**				**Reduction**
			Untreated	**Treated**	**Count**	**Spread (%)**	**(%)**
64	1	14.56	2.70	2.40	1	1.7	0.0
62	1	17.68	4.10	3.80	2	3.3	0.0
109	1	13.80	2.90	2.70	3	5.0	0.0
59	1	13.99	4.70	4.40	4	6.7	0.0
69	1	17.27	3.30	3.10	5	8.3	0.0
101	1	14.50	3.10	3.00	6	10.0	0.0
63	1	18.02	3.50	3.40	7	11.7	0.0
70	1	18.46	4.30	4.20	8	13.3	0.0
73	1	16.32	3.10	3.10	9	15.0	0.0
76	1	17.49	3.50	3.50	10	16.7	0.0
80	1	16.61	3.40	3.40	11	18.3	0.0
81	1	13.99	2.70	2.70	12	20.0	0.0
82	1	15.76	3.10	3.10	13	21.7	0.0
84	1	14.62	3.10	3.10	14	23.3	0.0
87	1	13.18	2.90	2.90	15	25.0	0.0
96	1	12.22	2.30	2.30	16	26.7	0.0
106	1	12.04	2.50	2.50	17	28.3	0.0
72	1	16.80	3.30	3.40	18	30.0	3.0
119	1	15.93	3.30	3.40	19	31.7	3.0
68	1	15.02	3.20	3.30	20	33.3	3.1
102	1	13.44	2.70	2.80	21	35.0	3.7
88	1	11.55	2.40	2.50	22	36.7	4.2
74	1	18.22	4.20	4.40	23	38.3	4.8
111	1	18.15	3.60	3.80	24	40.0	5.6
89	1	14.91	3.50	3.70	25	41.7	5.7
67	1	15.64	3.10	3.30	26	43.3	6.5
83	1	14.93	3.10	3.30	27	45.0	6.5
104	1	13.92	3.10	3.30	28	46.7	6.5
60	1	13.17	2.80	3.00	29	48.3	7.1
108	1	16.33	3.40	3.70	30	50.0	8.8
114	1	17.34	3.10	3.40	31	51.7	9.7
77	1	14.64	3.70	4.10	32	53.3	10.8
90	1	17.62	3.20	3.60	33	55.0	12.5
107	1	14.30	2.90	3.30	34	56.7	13.8
113	1	11.95	3.40	3.90	35	58.3	14.7
92	1	13.43	3.30	3.80	36	60.0	15.2
94	1	14.79	2.80	3.30	37	61.7	17.9
117	1	15.90	3.20	3.80	38	63.3	18.8
71	1	15.87	3.30	4.00	39	65.0	21.2
85	1	15.87	2.80	3.40	40	66.7	21.4
118	1	15.37	3.20	3.90	41	68.3	21.9
103	1	14.63	2.60	3.40	42	70.0	30.8
91	1	18.00	3.30	4.60	43	71.7	39.4
115	1	16.00	3.00	4.50	44	73.3	50.0
116	1	14.59	3.10	5.40	45	75.0	74.2
112	1	15.02	3.00	5.90	46	76.7	96.7
95	1	16.72	3.40	6.70	47	78.3	97.1
93	1	17.41	4.20	8.40	48	80.0	100.0

86	1	13.09	2.70	6.70	49	81.7	148.1
75	1	12.88	2.70	8.70	50	83.3	222.2
97	1	14.23	3.30	11.50	51	85.0	248.5
110	1	16.13	3.20	12.50	52	86.7	290.6
66	1	18.67	6.50	spalled	53	88.3	290.6
78	1	13.75	3.00	spalled	54	90.0	290.6
79	1	19.14	3.50	spalled	55	91.7	290.6
98	1	14.95	3.10	spalled	56	93.3	290.6
99	1	16.92	3.60	spalled	57	95.0	290.6
100	1	16.58	3.60	spalled	58	96.7	290.6
105	1	18.83	4.00	spalled	59	98.3	290.6
120	1	16.79	3.40	spalled	60	100.0	290.6
Mean		15.51	3.29	4.19			66.1
Std Dev		1.91	0.63	2.07			106.8
Median		15.64	3.20	3.40			9.3
Minimum		11.55	2.30	2.30			0.0
Maximum		19.14	6.50	12.50			290.6

APPENDIX IV

Mineral Liberation and Recovery Analysis Data

GRINDING CALIBRATION

Sample ID	ESCONDIDA UNTREATED - GRINDING CALIBRATION								ESCONDIDA CONVEYOR TREATED					
Description	2.5 min		5 min		10 min		15 min		2.5 min		5 min		10 min	
Size	Mass Retained		Mass Retained		Mass Retained		Mass Retained		Mass Retained		Mass Retained		Mass Retained	
(mm)	(g)	(%)	(g)	(%)	(g)	(%)	(g)	(%)	(g)	(%)	(g)	(%)	(g)	(%)
4.75		0.0		0.0		0.0		0.0		0.0		0.0		0.0
3.35	2.02	0.2		0.0		0.0		0.0		0.0		0.0		0.0
2.36	8.28	0.8		0.0		0.0		0.0		0.0		0.0		0.0
1.70	25.38	2.6		0.0		0.0		0.0	12.03	1.2		0.0		0.0
1.18	70.44	7.1		0.0		0.0		0.0	39.03	3.9		0.0		0.0
0.850	93.65	9.5	0.92	0.1	0.00	0.0		0.0	75.51	7.6		0.0		0.0
0.600	106.65	10.8	27.76	2.8	1.13	0.1		0.0	114.42	11.5	35.99	3.6		0.0
0.425	88.65	9.0	110.78	11.4	4.78	0.5		0.0	92.74	9.3	124.19	12.5		0.0
0.300	78.22	7.9	129.30	13.3	14.90	1.5		0.0	82.57	8.3	136.80	13.8	5.59	0.6
0.212	68.47	6.9	104.04	10.7	101.60	10.2	5.49	0.6	79.01	8.0	110.54	11.1	78.44	7.9
0.150	51.85	5.2	71.27	7.3	137.22	13.7	57.26	5.8	58.37	5.9	76.86	7.7	140.22	14.2
0.106	51.98	5.3	65.96	6.8	124.73	12.5	148.76	15.1	57.63	5.8	69.44	7.0	132.72	13.4
0.075	40.12	4.1	51.72	5.3	84.49	8.4	132.37	13.4	46.38	4.7	54.18	5.5	95.93	9.7
0.053	37.26	3.8	47.43	4.9	70.47	7.0	104.05	10.5	43.92	4.4	49.87	5.0	79.27	8.0
0.038	37.81	3.8	46.72	4.8	66.04	6.6	90.05	9.1	41.88	4.2	51.31	5.2	70.56	7.1
-0.038	228.75	23.1	318.75	32.7	395.41	39.5	448.36	45.5	250.09	25.2	283.39	28.6	385.79	39.0
Calc. Head	989.53	100.0	974.65	100.0	1,000.77	100.0	986.34	100.0	993.58	100.0	992.57	100.0	988.52	100.0

REPRODUCABILITY CHECK TESTS

Sample ID	ESCONDIDA UNTREATED - GRINDING TESTS											
Description	6 min (A)		6 min (B)		9 min (A)		9 min (B)		9 min (C)		9 min (D)	
Size	Mass Retained		Mass Retained				Mass Retained		Mass Retained		Mass Retained	
(mm)	(g)	(%)	(g)	(%)	(g)	(%)	(g)	(%)	(g)	(%)	(g)	(%)
4.75		0.0		0.0		0.0		0.0		0.0		0.0
3.35		0.0		0.0		0.0		0.0		0.0		0.0
2.36		0.0		0.0		0.0		0.0		0.0		0.0
1.70		0.0		0.0		0.0		0.0		0.0		0.0
1.18		0.0		0.0		0.0		0.0		0.0		0.0
0.850		0.0		0.0		0.0		0.0		0.0		0.0
0.600		0.0		0.0		0.0		0.0		0.0		0.0
0.425	36.40	3.7	65.67	6.6		0.0		0.0	0.46	0.0	0.49	0.0
0.300	125.62	12.6	137.24	13.8	20.83	2.1	13.31	1.3	20.05	2.0	24.10	2.5
0.212	132.69	13.4	119.60	12.0	115.70	11.7	98.06	9.9	117.16	11.8	128.53	13.1
0.150	92.68	9.3	83.80	8.4	135.05	13.6	136.49	13.8	134.69	13.6	141.05	14.4
0.106	73.54	7.4	66.68	6.7	111.14	11.2	115.61	11.7	110.70	11.1	116.84	11.9
0.075	59.31	6.0	55.19	5.6	83.80	8.5	88.01	8.9	78.81	7.9	81.98	8.3
0.053	50.32	5.1	47.04	4.7	66.63	6.7	71.41	7.2	65.10	6.6	69.54	7.1
0.038	47.46	4.8	45.29	4.6	61.46	6.2	65.50	6.6	59.91	6.0	67.60	6.9
-0.038	375.80	37.8	372.84	37.5	395.55	39.9	401.52	40.6	406.68	40.9	352.65	35.9
Calc. Head	993.82	100.0	993.36	100.0	990.16	100.0	989.91	100.0	993.56	100.0	982.78	100.0

REPRODUCABILITY CHECK TESTS

Sample ID	ESCONDIDA CONVEYOR TREATMENT						ESCONDIDA SINGLE MODE BATCH TREATMENT					
Description	6 min (C)		9 min (E)		9 min (F)		6 min (D)		9 min (G)		9 min (H)	
Size	Mass Retained		Mass Retained		Mass Retained		Mass Retained		Mass Retained		Mass Retained	
(mm)	(g)	(%)	(g)	(%)	(g)	(%)	(g)	(%)	(g)	(%)	(g)	(%)
4.75		0.0		0.0		0.0		0.0		0.0		0.0
3.35		0.0		0.0		0.0		0.0		0.0		0.0
2.36		0.0		0.0		0.0		0.0		0.0		0.0
1.70		0.0		0.0		0.0		0.0		0.0		0.0
1.18		0.0		0.0		0.0		0.0		0.0		0.0
0.850		0.0		0.0		0.0		0.0		0.0		0.0
0.600		0.0		0.0		0.0		0.0		0.0		0.0
0.425	35.41	3.6		0.0		0.0	13.01	1.3		0.0		0.0
0.300	125.08	12.6	19.67	2.0	16.95	1.7	108.69	11.1	5.89	0.6	9.62	1.0
0.212	132.61	13.3	114.84	11.6	111.25	11.2	134.69	13.7	76.16	7.8	73.84	7.5
0.150	92.62	9.3	138.65	14.0	139.31	14.0	106.43	10.8	143.53	14.6	136.17	13.8
0.106	72.84	7.3	112.59	11.4	114.73	11.6	98.50	10.0	127.18	13.0	142.59	14.5
0.075	59.71	6.0	82.30	8.3	82.54	8.3	73.36	7.5	104.45	10.6	98.75	10.0
0.053	50.62	5.1	67.33	6.8	68.27	6.9	61.48	6.3	90.55	9.2	82.26	8.4
0.038	47.28	4.7	65.05	6.6	64.22	6.5	60.33	6.1	52.85	5.4	71.23	7.2
-0.038	379.89	38.1	389.90	39.4	394.35	39.8	325.15	33.1	380.32	38.8	369.83	37.6
Calc. Head	996.07	100.0	990.35	100.0	991.63	100.0	981.64	100.0	980.93	100.0	984.29	100.0

GRINDING CALIBRATION AND TEST RESULTS

CONVEYOR TREATED COPPER II ORE GRINDING CALIBRATION AND GRINDING TESTS											
2.5 min		5 min		10 min		15 min		6 min (A+C)		9 min (B+D)	
Mass Retained		**Mass Retained**		**Mass Retained**		**Mass Retained**		**Mass Retained**		**Mass Retained**	
(g)	**(%)**	**(g)**	**(%)**	**(g)**	**(%)**	**(g)**	**(%)**	**(g)**	**(%)**	**(g)**	**(%)**
	0.0		0.0		0.0		0.0		0.0		0.0
0.65	0.1		0.0		0.0		0.0		0.0		0.0
0.67	0.1		0.0		0.0		0.0		0.0		0.0
3.42	0.3		0.0		0.0		0.0		0.0		0.0
26.04	2.6		0.0		0.0		0.0		0.0		0.0
79.98	8.1		0.0		0.0		0.0		0.0		0.0
121.45	12.3	13.86	1.4		0.0		0.0		0.0		0.0
93.25	9.4	95.86	9.7	0.24	0.0		0.0	49.14	2.5		0.0
83.89	8.5	141.57	14.4	5.53	0.6		0.0	235.15	11.8	4.60	0.2
73.47	7.4	115.44	11.7	64.03	6.5	6.33	0.6	276.56	13.9	77.16	3.9
60.74	6.1	84.74	8.6	140.19	14.3	47.02	4.8	205.48	10.4	250.28	12.7
58.17	5.9	76.86	7.8	142.36	14.5	135.48	13.9	171.83	8.7	296.07	15.0
54.82	5.5	69.81	7.1	110.53	11.2	151.01	15.5	151.45	7.6	236.97	12.0
51.50	5.2	63.91	6.5	94.35	9.6	121.39	12.4	138.19	7.0	198.49	10.1
49.22	5.0	66.27	6.7	95.83	9.7	110.45	11.3	137.84	6.9	188.37	9.5
233.57	23.6	255.23	25.9	330.57	33.6	405.52	41.5	618.93	31.2	722.40	36.6
990.84	100.0	983.55	100.0	983.63	100.0	977.20	100.0	1,984.57	100.0	1,974.33	100.0

GRINDING CALIBRATION AND TEST RESULTS

Sample ID	UNTREATED COPPER II ORE GRINDING CALIBRATION AND GRINDING TESTS											
Description	2.5 min		5 min		10 min		15 min		6 min (A+D)		9 min (C+E)	
Size	Mass Retained		Mass Retained		Mass Retained		Mass Retained		Mass Retained		Mass Retained	
(mm)	(g)	(%)	(g)	(%)	(g)	(%)	(g)	(%)	(g)	(%)	(g)	(%)
4.75	0.00	0.0		0.0		0.0		0.0		0.0		0.0
3.35	3.99	0.4		0.0		0.0		0.0		0.0		0.0
2.36	9.73	1.0		0.0		0.0		0.0		0.0		0.0
1.70	29.92	3.0		0.0		0.0		0.0		0.0		0.0
1.18	65.76	6.6		0.0		0.0		0.0		0.0		0.0
0.850	79.35	8.0	2.83	0.3		0.0		0.0		0.0		0.0
0.600	93.77	9.5	52.42	5.3	0.00	0.0		0.0		0.0		0.0
0.425	79.95	8.1	124.49	12.6	0.32	0.0	0.00	0.0	62.59	3.2		0.0
0.300	75.30	7.6	122.91	12.4	5.51	0.6	0.35	0.0	244.33	12.4	6.80	0.3
0.212	71.76	7.2	102.89	10.4	68.62	6.9	8.47	0.9	266.99	13.5	91.47	4.6
0.150	55.97	5.6	77.44	7.8	139.17	14.1	57.60	5.8	199.23	10.1	262.02	13.2
0.106	59.63	6.0	77.85	7.8	144.44	14.6	152.02	15.4	170.89	8.7	295.95	14.9
0.075	52.87	5.3	64.96	6.5	110.37	11.1	145.04	14.7	151.22	7.7	238.25	12.0
0.053	49.94	5.0	63.40	6.4	96.83	9.8	120.93	12.2	141.10	7.1	199.49	10.0
0.038	52.27	5.3	63.09	6.4	95.87	9.7	116.65	11.8	130.89	6.6	179.75	9.0
-0.038	210.77	21.3	239.55	24.2	329.15	33.2	388.89	39.3	607.55	30.8	717.75	36.0
Calc. Head	990.98	100.0	991.83	100.0	990.28	100.0	989.95	100.0	1,974.79	100.0	1,991.47	100.0

Appendix IV: Mineral Liberation and Recovery Analysis Data

FLOTATION TEST RECORD SHEET

Test ID								**Date**				
Description								**Technician**				
Stage	**Time / Mass**	**Air Flow**	**Float Time**		**NaHS**	**AP-3758 Collector**	**AX-317 Collector**	**X-133 Frother**	**Pine Oil (Dertol 90)**	**Lime (CaO)**	**pH**	**Eh**
			Conc.	**Cum.**	**10%**	**Neat**	**1%**	**Neat**	**Neat**	**Neat**		
	(min) / (g)	**(L/min)**	**(min)**	**(min)**	**(mL)**	**(µL)**	**(mL)**	**(µL)**	**(µL)**	**(g)**		
Grind					1.0	64.0	1.8	18.0	10.0			
Condition		0.5			1.0							
Rougher												
Concentrate 1		3.0	0.5	0.5	Froth scraping rate every 10s							
Concentrate 2		3.0	0.5	1.0	Froth scraping rate every 10s							
Concentrate 3		3.0	1.0	2.0	Froth scraping rate every 10s							
Concentrate 4		3.0	3.0	5.0	Froth scraping rate every 10s							
Concentrate 5		5.0	7.0	12.0	Froth scraping rate every 15s							
Tailings												
Total Reagent					200.0	62.4	18.0	16.2	9.3			

Sample Parameters:			Grind Conditions:			Flotation Conditions:		
Sample Mass	1,000	g	% Critical Speed	70	%	Cell Volume	4,000	mL
Solids Density	3.12	g/mL	Water Addition	1,000	mL	Water Addition	3,679	mL
Sample Volume	321	mL	Pulp % Solids	50	%	Pulp % Solids	21.4	%
Grind Size (P___)		µm	Pulp Density	1.51	g/mL	Pulp Density	1.17	g/mL

Jenway 370 pH/mV/°C Meter
Denver D-12 Flotation Machine & 4L Stainless Steel Cell
Legends Inc. Stainless Steel Rod Mill & Charge
Reagents Supplied By:
Cytec (AP-3758,X-133,AX-317)
Fisher (NaHS,CaO)
Marlin Chemicals (Pine Oil)

Comments

REFERENCES

AL-HARAHSHEH, M. & KINGMAN, S. W. (2004) Microwave assisted leaching - a review. *Hydrometallurgy,* 73**,** 189-203.

ALTSCHULER, H. M., SUCHER, M. & FOX, J. (1963) Handbook of microwave measurements, Vol. 2. *Polytechnic Press, Interscience Publishers*.

AMADEI, B. (1995) Importance of anisotropy when estimating and measuring in situ stresses in rock. University of Colorado. Department of Civil, Environmental, and Architectural Engineering.

AMANKWAH, R. K., PICKLES, C. A. & YEN, W. T. (2005) Gold recovery by microwave augmented ashing of waste activated carbon. *Minerals Engineering,* 18**,** 517-526.

AMIRA (2006) AMIRA Project P879 Microwave Processing Of Ores. Report on Investigations. Nottingham, The University of Nottingham.

ANTONUCCI, V. & CORREA, C. (1995) Sulphuric acid leaching of chalcopyrite concentrate assisted by application of microwave energy. *COPPER 95-COPRE 95 international conference.* Santiago, Chile, The Metallurgical Society of CIM.

APELT, T. A. & THORNHILL, N. F. (2009) Inferential measurement of sag mill parameters IV: Inferential model validation. *Minerals Engineering,* 22**,** 1032-1044.

ARAI, M. (1995) Open ended coaxial probes for high temperature dielectric measurements. *Electrical Engineering.* Nottingham, University of Nottingham.

ARAI, M., BINNER, J. G. P., CARR, G. E. & CROSS, T. E. (1993) High temperature dielectric property measurements of engineering ceramics. *American Ceramic Society,* 36**,** 483-492.

ATWATER, J. E. & WHEELER, R. R. J. (2003) Complex permittivities and dielectric relaxation of granular activated carbons at microwave frequencies between 0.2 and 26 GHz. *Carbon,* 41**,** 1801-1807.

ATWATER, J. E. & WHEELER, R. R. J. (2004) Microwave permittivity and dielectric relaxation of a high surface area activated carbon. *Applied Physics A - Materials science and processing,* 79**,** 125-129.

AUSTIN, L. G. & BAGGA, P. (1979) An analysis of fine dry grinding in ball mills. *Powder Technology,* 28**,** 83-90.

AYATOLLAHI, M. R. & ALIHA, M. R. M. (2007) Fracture toughness study for a brittle rock subjected to mixed mode I/II loading. *International Journal of Rock Mechanics and Mining Sciences,* 44**,** 617-624.

AYDOGAN, N. A., ERGÜN, L. & BENZER, H. (2006) High pressure grinding rolls (HPGR) applications in the cement industry. *Minerals Engineering,* 19**,** 130-139.

BATEMAN (2010) Bateman Engineered Technologies - Japan Pipe Conveyors. http://www.batemanengineering.com/BETJapanPipeConveyors.htm.

BATT, J., BINNER, J. G. P., CROSS, T. E., GREENACRE, N. R., HAMLYN, M. G., HUTCHEON, R. M., SUTTON, W. H. & WEIL, C. M. (1995) A parallel measurement programme in high temperature dielectric property measurements: An update. *Ceramic Transactions,* 59**,** 243-250.

BEARMAN, R. A. (1991) The application of rock mechanics parameters to the prediction of crusher performance. *Camborne school of mines.*

BEARMAN, R. A. (1999) The use of the point load test for the rapid estimation of Mode I fracture toughness. *International Journal of Rock Mechanics and Mining Sciences,* 36**,** 257-263.

BEARMAN, R. A., BRIGGS, C. A. & KOJOVIC, T. (1997) The applications of rock mechanics parameters to the prediction of comminution behaviour. *Minerals Engineering,* 10**,** 255-264.

BILLITON, B. (2009) BHP Billiton 2009 Annual Report. http://www.bhpbilliton.com/bbContentRepository/docs/annualReport2009.pdf.

BORGNAKKE, C. (2008) *Fundamentals of Thermodynamics*, John Wiley and sons.

BOTSCO, R. & MCMASTER, R. (1986) *Nondestructive Testing Handbook*, ASNT.

BOTTCHER, C. J. F. (1973) *Theory of electric polarization,* London, Elsevier.

BROCH, E. S. (1971) Point Load Testing of Rocks. London, Imperial College of Science and Technology.

CEZAIRLIYAN, A. (1981) Specific heat of solids. *Data Series on Material Properties.* Hemisphere Publishing Corporation.

CHAN, C. T. & READER, H. C. (2000) *Understanding Microwave Heating Cavities,* London, Artech House

CHEN, T. T., DUTRIZAC, J. E., HAQUE, K. E., WYSLOUZIL, W. & KASHYAP, S. (1984) The relative transparency of minerals to microwave radiation. *Canadian Metallurgical Quarterly,* 23**,** 349-351.

CHOW, T. C. V. & READER, C. H. (2000) *Understanding Microwave Heating Cavities,* London, Artech House.

CLARK, D. E., FOLZ, D. C. & WEST, J. K. (2000) Processing materials with microwave energy. *Materials Science and Engineering,* 287**,** 153-158.

CLARK, S. P. (1966) *Handbook of Physical constants,* New York, Geological Society of America.

CLARKE, A. J. & WILLS, B. A. (1989) Technical note Enhancement of cassiterite liberation by high pressure roller comminution. *Minerals Engineering,* 2**,** 259-262.

CLAUSER, E. & HUENGES, E. (1995) *Thermal conductivity of rocks and minerals*.

CONNOLLY, J. (2005) Introduction to X-ray powder diffraction. University of New Mexico

DAHLSTROM, D. A. (1986) Impact of Changing Energy Economics on Mineral Processing. *Mining Engineering,* 38**,** 45.

DINNEBIER, R. E. & BILLINGE, S. J. L. (2008) *Powder Diffraction: Theory and Practice,* Cambridge, The Royal Society of Chemistry.

DOE, U. S. (2004) Mining Industry of the Future: Mineral Processing Technology Roadmap. US Department of Energy.

DONOVAN, S., KLEIN, O., DRESSEL, M., HOLCZER, K. & GRUNER, G. (1993) Microwave cavity perturbation technique: Part II: Experimental scheme. *International journal of infrared and millimeter waves,* 14**,** 2459-2487.

DRESSEL, M., KLEIN, O., DONOVAN, S. & GRUNER, G. (1993) Microwave cavity perturbation technique: Part III: Applications. *International Journal of Infrared and Millimeter Waves,* 14**,** 2489-2517.

DSI (2009) Dos Santos International; Snake Sandwich Conveyor Profiles. http://www.dossantosintl.com.

DUTRIZAC (1978) The kinetics of dissolution of chalcopyrite in ferric ion media. *Met. Trans.,* b**,** 431-438.

DUTRIZAC, J. E., MACDONALD, R. J. C. & INGRAHAM, T. R. (1969) The kinetics of dissolution of synthetic chalcopyrite in aqueous acidic ferric sulphate solution. *Trans. Metall. Soc. AIME* 245**,** 955-959.

EBERHART, J. P. (1991) *Structural and Chemical analysis of Materials*, Wiley.

EC (1996) IPPC Direcetive (Directive 96/61/EC). Brussels, EU.

ELORANTA, J. W. (1997) Efficiency of Blasting vs. Crushing & Grinding. *Twenty-Third Conference of Explosives and Blasting Technique.* Las Vegas, Nevada, International Society of Explosives Engineers, Cleveland, Ohio.

FENG, D. & ALDRICH, C. (1999) Effect of particle size on flotation performance of complex sulphide ores. *Minerals Engineering,* 12**,** 721-731.

FETT, T. & MUNZ, D. (2003) 9.1 Fracture Mechanics. *Handbook of Advanced Ceramics.* Oxford, Academic Press.

FITZGIBBON, K. E. & VEASEY, T. J. (1990) Thermally assisted liberation - a review. *Minerals Engineering,* 3**,** 181-185.

FORD, J. D. & PEI, D. C. T. (1967) High temperature chemical processing via microwave absorption. *Journal of Microwave Power* 2**,** 61-64.

FORSMO, S. P. E. (2005) Oxidation of magnetite concentrate powders during storage and drying. *International Journal of Mineral Processing,* 75**,** 135-144.

FUERSTENAU, D. W. & ABOUZEID, A. Z. M. (2002) The energy efficiency of ball milling in comminution. *International Journal of Mineral Processing,* 67**,** 161-185.

FUERSTENAU, D. W. & KAPUR, P. C. (1995) Newer energy-efficient approach to particle production by comminution. *Powder Technology,* 82**,** 51-57.

FUERSTENAU, D. W., KAPUR, P. C., SCHOENERT, K. & MARKTSCHEFFEL, M. (1990) Comparison of energy consumption in the breakage of single particles in a rigidly mounted roll mill with ball mill grinding. *International Journal of Mineral Processing,* 28**,** 109-125.

FUERSTENAU, D. W., LUTCH, J. J. & DE, A. (1999) The effect of ball size on the energy efficiency of hybrid high-pressure roll mill/ball mill grinding. *Powder Technology,* 105**,** 199-204.

G8 (2009) Chair's Summary from The G8 Summit 2009 held in L'Aquila from 8 to 10 July 2009 http://www.g8italia2009.it/static/G8_Allegato/Chair_Summary,1.pdf.

GERRARD, M., COSTELLO, B. & MORLEY, C. (2004) Operational Experiences and Performance Assessment of HPGR Technology at Argyle Diamond Mine. *Rio Tinto Comminution Workshop 2004.* Perth.

GREENACRE, N. R. (1996a) Measurement of the high temperature dielectric properties of caramics at microwave frequencies. *Electrical engineering.* Nottingham, University of Nottingham.

GREENACRE, N. R. (1996b) Measurement of the high temperature dielectric properties of caramics at microwave frequencies. *Electrical Engineering.* Nottingham, University of Nottingham.

GRIM, R. E. (1968) *Clay Mineralogy,* London, McGraw-Hill.

GROVES, L. (2007) Selective Heating of minerals and Ores using Microwave Energy. *School of Chemical and Environmental Engineering.* Nottingham, University of Nottingham.

GUILLOU-FROTTIER, L. & BUROV, E. (2003) The development and fracturing of plutonic apexes: implications for porphyry ore deposits. *Earth and Planetary Science Letters,* 214**,** 341-356.

GUISEPI, R. A. (2000) An Overview of the Paleolithic-Prehistoric cultural stage, or level of human development, characterized by the creation and use of stone tools. http://history-world.org/stone_age1.htm

GUPTA, A. & YAN, D. S. (2006) Size Reduction and Energy Requirement. *Mineral Processing Design and Operation.* Amsterdam, Elsevier Science.

GUTSCHE, O. & FUERSTENAU, D. W. (2004) Influence of particle size and shape on the comminution of single particles in a rigidly mounted roll mill. *Powder Technology,* 143-144**,** 186-195.

HAIRETDINOV, E. F., UVAROV, N. F., REAU, J.-M. & HAGENMULLER, P. (1998) Dielectric relaxation of free charge carriers in some fluorite-type solid solutions. *Physica B,* 244**,** 201-6.

HALL, D. A., BEN-OMRAN, M. M. & STEVENSON, P. J. (1998) Field and temperature dependence of dielectric properties in BaTiO3-Based piezoceramics. *Journal of Physics: Condensed Matter,* 10**,** 461-476.

HAMON, B. V. M., R. J. (1952) Dielectric Absorption and D.C. Conductivity in n-Primary Alcohols. *Australian Journal of Scientific Research,* 5**,** 671-697.

HAN, K. N. (1996) A textbook of hydrometallurgy : F. Habashi. Metallurgy Extractive Quebec, Sainte Foy, Que., 1993, 689 pp. *International Journal of Mineral Processing,* 46**,** 293-294.

HARRISON, P. C. (1997) A fundamental study of the heating effect of 2.45 MHz microwave radiation of minerals. Birmingham, University of Birmingham.

HOLDERFIELD, S. P. & SALSMAN, J. B. (1992) Observed trends in the dielectric properties of minerals at elevated temperatures. *Microwave processing of materials III - Materials research society symposium proceedings,* 269**,** 589-594.

HOLMAN, B. W. (1926) Heat treatment as an agent in rock breaking. *Trans IMM* 26**,** 219.

HUTCHEON, R. M., JONG, M. D. & ADAMS, F. (1992a) A system for rapid measurements of RF and microwave properties up to 1400 C. *Journal of Microwave Power and Electromagnetic Energy,* 27**,** 87-92.

HUTCHEON, R. M., JONG, M. D., ADAMS, F., LUCUTA, P. G., MCGREGOR, J. E. & BAHEN, L. (1992b) RF and microwave dielectric measurements to 1400C and dielectric loss mechanisms. *Materials Research Society Symposium Proceedings,* 269**,** 541-551.

IEA (2009) International Energy Agency : World Energy Statistics 2009. http://www.iea.org.

IKEDA, M., FUKANANGA, T. & MIURA, T. (2003) Influence of sample insertion hole on resonant cavity perturbation measuring method. *IEEE MTT-S International microwave symposium digest,* 2**,** 1423-1426.

IPCC (2007) Intergovernmental Panel on Climate Change, Fourth Assessment Report: Mitigation of Climate Change. http://www.ipcc.ch/publications_and_data/ar4/wg3/en/ch12.html.

ISRM (1985) Standard Method for Determining Point Load Strength. *1985 [EUR 4].*

JACOBS, I. S. (1982) Tracking Pyrite Sulfur in the microwave desulfurization of coal. *Journal of Applied Physics* 153**,** 2730-32.

JKMRC (2004) MLA System User Operating Manual Module. Brisbane, Julius Kruttschnitt Mineral Research Centre.

JOHNSON, G., HUNTER, I. & HOLLE, H. (1993) Quantifying and improving the power efficiency of SAG milling circuits. *Minerals Engineering,* 7**,** 141-152.

JONES, D. A. (2005) Understanding microwave treatment of ores. *School of Chemical, Environmental and Mining Engineering.* Nottingham, University of Nottingham.

JONES, D. A., KINGMAN, S. W., WHITTLES, D. N. & LOWNDES, I. S. (2005) Understanding microwave assisted breakage. *Minerals Engineering,* 18**,** 659-669.

JONES, D. A., KINGMAN, S. W., WHITTLES, D. N. & LOWNDES, I. S. (2007) The influence of microwave energy delivery method on strength reduction in ore samples. *Chemical Engineering and Processing,* 46**,** 291-299.

KAPUR, P. C. & FUERSTENAU, D. W. (1987) Energy-size reduction "laws" revisited. *International Journal of Mineral Processing,* 20**,** 45-57.

KELLERWESSEL, H. (1993) High pressure particle bed comminution of mineral raw materials. *AUFBEREITUNGS-TECHNIK* 5**,** 243-249.

KELLY, E. G. & SPOTTISWOOD, D. J. (1982) *Introduction to mineral processing*, Wiley and sons.

KINGMAN, S. W., CORFIELD, G. M. & ROWSON, N. (1999) Effects of microwave radiation upon the mineralogy and magnetic processing of a massive norwegian ilemnite ore. *Magnetic and Electrical Separation,* 9**,** 131-148.

KINGMAN, S. W., JACKSON, K., CUMBANE, A., BRADSHAW, S. M., ROWSON, N. & GREENWOOD, R. (2004) Recent developments in microwave assisted comminution. *International Journal of Mineral Processing,* 74**,** 71-83.

KITTEL, C. (1986) *Introduction to solid state physics*, John Wiley and Sons.

KNACKE, K. & HESSELMANN (1991) *Thermochemical Properties of Inorganic Compounds*, Springer-Verlag.

KRUESI, P. R. & FRAHM, V. H. (1982) Process for the recovery of nickel, cobalt and manganese from their oxides and silicates.

LANDAU, L. D., LIFSHITZ, E. M. & PITAEVSKI, L. P. (1984) *Electrodynamics of Continuous Media,* Oxford, England, Pergamon Press

LAURENT, G. F. & EVGENII, B. (2003) The development and fracturing of plutonic apexes: implications for porphyry ore deposits. *Earth and Planetary Science Letters,* 214**,** 341-356.

LAWN, B. R. & WILSHAW, T. R. (1975) *Fracture of brittle solids,* Cambridge [Eng.] ; New York Cambridge University Press.

LESTER, E. & KINGMAN, S. W. (2004) The effect of microwave pre-heating on five different coals. *Fuel,* 83**,** 1941-1947.

LESTER, E., KINGMAN, S. W. & DODDS, C. (2005) Increased coal grindability as a result of microwave pretreatment at economic energy inputs. *Fuel,* 84**,** 423-427.

LINDQVIST, M. (2008) Energy considerations in compressive and impact crushing of rock. *Minerals Engineering,* 21**,** 631-641.

LOWRISON, G. C. (1974) The size reduction of solid materials. *Crushing and Grinding.* Butterworth, London

MCGILL, S. L. (1988) The Effects of Power Level on the Microwave Heating of Selected Chemicals and Minerals. *Materials Research Society Proceedings* 124**,** 247-252.

MEHDIZADEH, M. (2009a) Microwave Multimode Cavities for Material Heating. *Microwave/RF Applicators and Probes for Material Heating, Sensing, and Plasma Generation.* Boston, William Andrew Publishing.

MEHDIZADEH, M. (2009b) Single-mode Microwave Cavities for Material Processing and Sensing. *Microwave/RF Applicators and Probes for Material Heating, Sensing, and Plasma Generation.* Boston, William Andrew Publishing.

MEREDITH, R. (1998) Engineers' Handbook of Industrial Microwave Heating. *The Institution of Electrical Engineers, London*.

METAXAS, A. C. & MEREDITH, R. J. (1983) Industrial Microwave Heating. *The Institution of Electrical Engineers, London*.

MINGOS, D. M. P. & BAGHURST, D. R. (1991) Applications of microwave dielectric heating effects to synthetic problems in chemistry. *Chemical society reviews,* 20**,** 1-47.

MORRELL, S. (2003) Modelling of the Load-throughput Response of AG/SAG Mills. Final P9M Research Report. Melbourne.

MORRELL, S. (2008) A method for predicting the specific energy requirement of comminution circuits and assessing their energy utilisation efficiency. *Minerals Engineering,* 21**,** 224-233.

MORRISON, R. D. & CLEARY, P. W. (2008) Towards a virtual comminution machine *Minerals Engineering,* 21.

NAPIER-MUNN, T. J., MORRELL, S., MORRISON, R. D. & KOJOVIC, T. (1996) Mineral comminution circuits: their operation and optimisation. Julius Kruttschnitt Mineral Research Centre.

NELSON, S. A. (2008) Phyllosilicates (Micas, Chlorite, Talc, & Serpentine).

NELSON, S. O. (1988) Estimating the permittivity of solids from measurements on granular of pulverised materials. *Microwave Processing of Materials - Materials Research Society Symposium Proceedings.* Reno, Nevada, USA.

NELSON, S. O. & BARTLEY, P. G. (2002) Measuring frequency- and temperature-dependent permittivities of food materials. *IEEE Transactions on Instrumentation and Measurement,* 51**,** 589-592.

NORGATE, T. E. & WELLER, K. R. (1994) Selection and operation of high pressure grinding rolls circuits for minimum energy consumption. *Minerals Engineering,* 7**,** 1253-1267.

OCEPEC, D., SALATIC, D. & GRUJIC, M. (1986) Energy saving in the comminution processes. *World Congress Particle Technology, Part II. Comminution.* Nurnberg

OLUBAMBI, P. A., POTGIETER, J. H., HWANG, J. Y. & NDLOVU, S. (2007) Influence of microwave heating on the processing and dissolution behaviour of low-grade complex sulphide ores. *Hydrometallurgy,* 89**,** 127-135.

PARKER, A. J., PAUL, R. L. & POWER, G. P. (1981) Electrochemistry of the oxidative leaching of copper from chalcopyrite. *Journal of Electroanalytical Chemistry,* 118**,** 305-316.

PICKLES, C. A., MOURIS, J. & HUTCHEON, R. M. (2005) High temperature dielectric properties of geothite from 400 to 3000 MHz. *Journal of Materials Research,* 20**,** 18-29.

PLINT, S. M. (2006) Compositional design and fabrication of a perovskite anode for the integrated planar solid oxide fuel cell

Universty of St Andrews.

PORCH, A. & GOUGH, C. E. (1997) Microwave applications of high-temperature superconductors. *Current Opinion in Solid State and Materials Science,* 2**,** 11-17.

POWELL, M. S., MORRELL, S. & LATCHIREDDI, S. (2001) Developments in the understanding of South African style SAG mills. *Minerals Engineering,* 14**,** 1143-1153.

POWELL, M. S., WESTHUIZEN, V. A. P. & MAINZA, A. N. (2009) Applying grind curves to mill operation and optimisation. *Minerals Engineering,* 22**,** 625-632.

PRASSIANAKIS, I. N. (1977) Non-Destructive Testing of Materials-The Method of Ultrasounds. Athens, N.T.U.A.

PRASSIANAKIS, I. N. (1994) An experimental approach to damage evaluation using ultrasounds. *European Journal of NDT Insight* 93-96.

PROCEQ (2009) PUNDIT Plus - Ultrasonic instrument. http://www.proceq.com/en/products/concrete-testing/ultrasonic-testing/pundit-plus-cns-farnell-line.html.

RAJ, B., RAJENDRAN, V. & PALANICHAMY, P. (2004) Science and technology of ultrasonics.

REED, S. J. B. (1996) Electron Microprobe analysis and Scanning Electron Microscopy in Geology. Cambridge, Cambridge University Press.

RHODES, M. (1998) *Introduction to Particle Technolgy,* Chichester, Wiley & Sons.

RICHARDS, J. P., NOBLE, S. R. & PRINGLE, M. S. (1999) A revised Late Eocene age for porphyry magmatism in the Escondida area, Northern Chile. *Economic Geology,* 94**,** 1231-1248.

ROBERTS, S. & VON HIPPEL, A. (1946) A new method for measuring dielectric constant and loss in the range of centimeter waves *Journal of Applied Physics,* 17**,** 610.

RYYNÄNEN, S. (1995) The electromagnetic properties of food materials: A review of the basic principles. *Journal of Food Engineering,* 26**,** 409-429.

SACK, D. A. & OLSON, L. D. (1995) Advanced NDT methods for evaluating concrete bridges and other structures. *NDT&E International,* 28**,** 349-357.

SALSMAN, J. B. (1989a) Measurement of dielectric properties in the frequency range of 300 MHz to 3 GHz as a function of temperature and density. *Bureau of Mines Tuscaloosa Research Center Report*.

SALSMAN, J. B. (1989b) Measurement of dielectric properties in the frequency range of 300 MHz to 3 GHz as a function of temperature and density. *Microwaves*.

SALSMAN, J. B. (1991) Technique for measuring the dielectric properties of minerals as a function of temperature and density at microwave heating frequencies. *Materials Research Society Symposium Proceedings,* 189**,** 509-515.

SALSMAN, J. B., WILLIAMSON, R. L., TOLLEY, W. K. & RICE, D. A. (1996) Short-pulse microwave treatment of disseminated sulfide ores. *Minerals Engineering,* 9**,** 43-54.

SALTIEL, C., DATTA, A. K., JAMES P. HARTNETT, T. F. I. J. Y. I. C. & GEORGE, A. G. (1999) Heat and Mass Transfer in Microwave Processing. *Advances in Heat Transfer.* Elsevier.

SCAIFE, B. K. P. (1989) *Principles of dielectrics,* Oxford, Clarendon Publishers.

SCHOENERT, K. (1972) Role of fracture physics in understanding comminution Phenomena. *Trans. SME/AIME* 252**,** 21-26.

SCHOENERT, K. (1979) Aspects of the physics of breakage relevant to comminution. *Fourth Tewksbury Symposium.* University of Melbourne

SCHONERT, K. (1972) Role of fracture physics in understanding comminution Phenomena. *Trans. SME/AIME* 252**,** 21-26.

SCHWECHTEN, D. & MILBURN, G. H. (1990) Experiences in dry grinding with high compression roller mills for end product quality below 20 microns. *Minerals Engineering,* 3**,** 23-34.

SCOTT, G., BRADSHAW, S. M. & EKSTEEN, J. J. (2008) The effect of microwave pretreatment on the liberation of a copper carbonatite ore after milling. *International Journal of Mineral Processing,* 85**,** 121-128.

SEBASTIAN, M. T. (2008) Measurement of Microwave Dielectric Properties and Factors Affecting Them. *Dielectric Materials for Wireless Communication.* Amsterdam, Elsevier.

SHI, F. M., R., CERVELLIN, A., BURNS, F. & MUSA, F. (2009) Comparison of energy efficiency between ball mills and stirred mills in coarse grinding. *Minerals Engineering,* 22**,** 673-680.

SINKANKAS, J. (1964) *Mineralogy,* London, Van Nostrand Reinhold Company.

SIPPLE, E.-M., BRACCONI, P., DUFOUR, P. & MUTIN, J.-C. (2001) Microstructural modifications resulting from the dehydration of gypsum. *Solid State Ionics,* 141-142**,** 447-454.

SMITH, E. K. (1995) Propagation at Microwave Frequencies. *Handbook of Microwave Technology.* San Diego, Academic Press.

STUERGA, D. & GAILLARD, P. (1996) Microwave heating as a new way to induce localized enhancements of reaction rate. Non-isothermal and heterogeneous kinetics. *Tetrahedron,* 52**,** 5505-5510.

SUGIMOTO, H. & NORIMOTO, M. (2004) Dielectric relaxation due to interfacial polarization for heat-treated wood. *Carbon,* 42**,** 211-218.

SUKUMAR, N. & SROLOVITZ, D. J. (2004) Finite element-based model for crack propagation in polycrystalline materials. *Computational Applied Mathematics,* 23**,** 2-3.

SUMNU, G., SAHIN, S. & DA-WEN, S. (2005) Recent Developments in Microwave Heating. *Emerging Technologies for Food Processing.* London, Academic Press.

SUTTON, W. H. (1989) Microwave processing of ceramic materials. *American Ceramic Society Bulletin,* 68**,** 376-386.

TAVARES, L. M. (2005) Particle weakening in high-pressure roll grinding. *Minerals Engineering,* 18**,** 651-657.

TAVARES, L. M. & KING, R. P. (1998) Single-particle fracture under impact loading. *International Journal of Mineral Processing,* 54**,** 1-28.

THOSTENSON, E. T. & CHOU, T.-W. (1999) Microwave processing: fundamentals and applications. *Composites Part A,* 30**,** 1055-1071.

TINGA, W. R. (1992) Rapid high temperature measurement of microwave dielectric properties. *Materials research society symposium proceedings,* 269**,** 503-516.

TODOR, D. N. (1976) *Thermal Analysis of Minerals,* Kent, Abacus Press.

TOULOUKIAN, Y. S., ROY, R. F. & BECK, A. E. (1981) Thermophysical Properties of rocks. *Cindas data series on material properties,* II**,** 409-502.

TRABELSI, S., KRASZEWSKI, A. W. & NELSON, S. O. (1999) Density- and structure-independant calibration method for microwave moisture determination in granular materials. *IEEE Antennas and Propogation Society International Symposium.* Piscataway, NJ, USA.

TRABELSI, S., KRASZEWSKI, A. W. & NELSON, S. O. (2001) Micowave dielectric sensing of bulk density of granular materials. *Measurement Science and Technology,* 12**,** 2192-2197.

TROMANS, D. (2008) Mineral comminution: Energy efficiency considerations. *Minerals Engineering,* 21**,** 613-620.

UN (1998) Kyoto Protocol to the UN Framework Convention on Climate Change. Kyoto.

VAUGHAN, D. J. & PATTRICK, R. A. D. (1995) *Mineral Surfaces,* London, Chapman and Hall.

VEASEY, T. J. & FITZGIBBON, K. E. (1990) Thermally Assisted Liberation - A Review. *Minerals Engineering,* 13**,** 181-185.

VENKATESH, M. S. & RAGHAVAN, G. S. V. (1999a) Dielectric properties measurement using a cavity perturbation technique. *Workshop on Electromagnetic Wave Interaction with Water and Moist Substances.* Athens.

VENKATESH, M. S. & RAGHAVAN, G. S. V. (1999b) Dielectric properties measurement using a cavity perturbation technique. *Workshop on electromagnetic wave interaction with water and moist substances,* 3**,** 194-198.

VENUGOPAL, R. & RAJAMANI, R. K. (2001) 3D simulation of charge motion in tumbling mills by the discrete element method *Powder Technology,* 115**,** 157-166.

VON HIPPEL, A. (1954) Dielectric Materials and Applications. *Technology press of M.I.T., Wiley and Sons, New York*.

VORSTER, W., ROWSON, N. A. & KINGMAN, S. W. (2001) The effect of microwave radiation upon the processing of Neves Corvo copper ore. *International Journal of Mineral Processing,* 63**,** 29-44.

VUTUKURI, V. S., LAMA, R. D. & SALUJA, S. S. (1974) Handbook on mechanical properties of rocks. Testing techniques and results. Volume 1. Textbook : 200F, 30T, 260R. TRANS. TECH. PUBLICATIONS, V1, 1974, 300P. *International Journal of Rock Mechanics and Mining Sciences & Geomechanics Abstracts,* 11**,** A218-A218.

WALKIEWICZ, J. W., CLARK, A. E. & MCGILL, S. L. (1991) Microwave-assisted grinding. *IEEE Transactions on Industry Applications,* 27**,** 239-242.

WALKIEWICZ, J. W., KAZONICH, G. & MCGILL, S. L. (1988) Microwave Heating Characteristics of Selected Minerals and Compounds. *Mineral and Metallurgical Processing,* 5**,** 39-42.

WANG, Y. & FORSSBERG, E. (2007) Enhancement of energy efficiency for mechanical production of fine and ultra-fine particles in comminution. *China Particuology,* 5**,** 193-201.

WANG, Y., FORSSBERG, E. & SVENSSON, M. (2000) Microwave assisted comminution and liberation of minerals. *Mineral processing on the verge of the 21st century. Proceedings of the 8th International Mineral Processing Symposium* Balkema, Rotterdam.

WENDY, N. (2005) Report : Design of a Tunnel Applicator for the Microwave Treatment of Oil Contaminated Drill Cuttings. Stellenbosch, Stellenbosch University, Faculty of Engineering, Department of Process Engineering.

WHITTAKER, G. (1997) A Basic Introduction to Microwave Chemistry. web ref - http://homepages.ed.ac.uk/ah05/microwave.html.

WHITTLES, D. N., KINGMAN, S. W. & REDDISH, D. J. (2003) Application of numerical modelling for prediction of the influence of power density on microwave-assisted breakage. *International Journal of Mineral Processing,* 68**,** 71-91.

WILLS, B. A. (2006) *Mineral Processing Technology - An Introduction to the Practical Aspects of Ore Treatment and Mineral Recovery,* Oxford, Elsevier.

WITTKE, J. H. (2003) Electron Microprobe Techniques. University of Arizona.

WONG, T. F. & BRACE, W. F. (1979) Thermal expansion of rocks: some measurements at high pressure. *Tectonophysics,* 57**,** 95-117.

WORNER, H. K. (1990) Microwave irradiation of composites.

WU, M., YAO, X. & ZHANG, L. (2000) An improved coaxial probe technique for measuring microwave permittivity of thin dielectric materials. *Measurement science and technology,* 11**,** 1617-1622.

YAMAGUCHI (1970) Test pieces required to determine the strength of rock. *Int. J. Rock Mech. Min. Sci,* 7**,** 209-277.

YATES, A. (1919) Effect of Heating and Quenching Cornish Tin Ores before Crushing. *Trans I.M.M,* 28**,** 41.

YOUNG, C. A., TAYLOR, P. R., ANDERSON, C. G. & CHOI, Y. (Eds.) (2008) *Hydrometallurgy 2008.Proceedings of the sixth international symposium,* Phoenix, society for mining, metallurgy and exploration.

ZENG, Y. & FORSSBERG, E. (1991) Effects of mill feed size on product fineness and energy consumption in coarse grinding. *Minerals Engineering,* 4**,** 599-609.

ZENG, Y. & FORSSBERG, E. (1992) Effects of mill feed size and rod charges on grinding performance. *Powder Technology,* 69**,** 119-123.